Met. O. 864b

METEOROLOGICAL OFFICE

Geophysical Memoirs No. 120

(SECOND NUMBER, VOLUME XVII)

AVERAGE TEMPERATURES, CONTOUR HEIGHTS AND WINDS AT 30 MILLIBARS OVER THE NORTHERN HEMISPHERE

BY

R.A. EBDON

LONDON: HER MAJESTY'S STATIONERY OFFICE

£11.50 NET

Met. O. 864b

METEOROLOGICAL OFFICE

Geophysical Memoirs No. 120

(SECOND NUMBER, VOLUME XVII)

AVERAGE TEMPERATURES, CONTOUR HEIGHTS AND WINDS AT 30 MILLIBARS OVER THE NORTHERN HEMISPHERE

BY

R.A. EBDON

LONDON: HER MAJESTY'S STATIONERY OFFICE

U.D.C. 551.587(4/9)

Geophys. Mem., London

17, No. 120, 1977

TABLE OF CONTENTS

APPENDIX

LIST OF ILLUSTRATIONS

LIST OF ILLUSTRATIONS *(contd)*

AVERAGE TEMPERATURES, CONTOUR HEIGHTS AND WINDS AT 30 MILLIBARS OVER THE NORTHERN HEMISPHERE

SUMMARY

Geophysical Memoirs No. 112 (1970) included charts and diagrams describing average temperatures, contour heights and winds, and the variability of each, at the 50-mb level (approximately 20.5 km) over the northern hemisphere for the months of January, April, July and October and for areas north of 45°N for the months of February and March. The aim of this Memoir is to provide a comparable climatology of the 30-mb (approximately 24-km) level. Charts for August and September are included in this publication as it is during these months that the high-latitude stratosphere changes from the regime typical of summer to that typical of winter.

The Memoir is divided into three parts. Part I deals with average temperatures and includes a section on 'The final warming' when the high-latitude stratospheric-temperature patterns undergo large oscillations which result in a sudden warming (sometimes of 30 deg) during the late-winter or early-spring months. The average contour-height charts are described in Part II. The average winds are dealt with in Part III where sections are included describing the elliptical nature of the wind distributions, the quasi-biennial oscillation in tropical stratospheric winds and the spring and autumn reversals of 30-mb winds over Scotland.

The basic charts, i.e. those showing the average values and their variability for the months considered, are published together as Plates 1 to 48 (for ease of reference) whilst additional charts and diagrams are included in the relevant part of the text.

THE DATA

The charts are based upon observations by radiosonde and radar wind-finding equipment made chiefly within an eight-year period. For January, February, March and April the years used for most stations were 1958–65 and for July, August, September and October 1957–64. All available ascents, irrespective of hours of observation, were used in the computation of the averages and standard deviations. The individual values of 30-mb data were obtained from several different sources. The International Geophysical Year (IGY) and the International Geophysical Co-operation (IGC) microcards were used for months between July 1957 and October 1959. Apart from these IGY/IGC microcards the main source of the daily values was the Daily Series, Part II Data Tabulations (1955–64). In addition the publications for some individual countries were used and considerable help was obtained from data supplied on punched cards from the United States of America and Norway, microfilm from USSR and Denmark and manuscript data from Italy. Without the co-operation of these other meteorological services it would be impossible to undertake a project of this nature. Russian data for 1966 were used in place of 1960 for some of the months as 1960 appeared to be a year when fewer ascents reached 30 mb.

Data were available for about 300 stations on the hemispheric charts and about 180 in February, March, August and September when the charts were restricted to the area north of 45°N. The values of temperature, wind and contour height for each individual ascent were punched on to paper tape or cards, written to magnetic tape and processed in the Meteorological Office computer. The program calculated and printed out pentad (i.e. 5-day) mean values for the various elements, monthly means calculated from the pentad values and eight-year averages calculated from the monthly means. For every station the various pentad and monthly means and the eight-year averages were calculated for 0001 and 1200 GMT separately and for the two hours combined. The averages used in the construction of the charts are those for the two hours combined, and the standard deviations represent the variability of all the observations about this average value. No weighting factor was applied to a year with a small number of observations.

The many difficulties and uncertainties encountered in the analysis of stratospheric-level charts are well known and need not be repeated here in detail. However, it should be remembered that, at this level, there are very few areas of the hemisphere which provide a really adequate and homogeneous set of data for an eight-year period and there are some areas, for example China, where no data at all were available. The frequency with which radiosonde and radar wind ascents reach the 30-mb level is determined not only by the quality of the equipment and instruments used but also by the winds and temperatures prevailing at the time of the ascent. As a consequence more ascents reach this level in conditions of lighter winds and higher temperatures than is the case when winds are strong and the stratosphere is relatively cold.

In order to increase the number of individual observations of wind and temperature any observations in the range 25 to 35 mb which were included in the original data were extracted and used, but no attempt was made to interpolate or extrapolate to obtain the height of the 30-mb surface.

At tropical stations using the Meteorological Office radiosonde Mark 2B the temperature data for 1962–68 were used because, during the preparation of the 50-mb charts, it was found that the earlier data from these stations gave spuriously low average temperatures and large standard deviations which, it was established, were very largely due to instrumental errors. To make allowance for the different types of radiosonde instruments used some of the average values, particularly over Africa, were changed in accordance with values given by Hawson (1964).

In high latitudes in the North American and European sectors the winter and early spring monthly mean temperatures obtained from the pentad values gave very misleading values at some stations — particularly in any month when there were few observations during a significant warming and data for most of the remainder of the month were missing. Eight-year average temperatures derived from such monthly means were in error and additional errors occurred because, at some stations, no data at all were available for some of the years used. In order to ensure that the average temperatures were made more representative for the eight-year period the data and results for stations within this area were examined in detail. At each station special consideration was given to any month for which no data at all were available or for which any monthly mean temperature was suspect owing to data not being available for part of the month. An estimate of the monthly mean temperature for the particular station was made after examination of the data and results for surrounding stations. These estimated monthly mean temperatures were then used to obtain a revised eight-year average value and this value was used in the final analysis of the chart. The method is somewhat crude but it results in a more realistic analysis in an area which is of particular interest. In the winter months over high-latitude areas, the missing observations tend to increase the magnitude of the computed standard deviation and this was borne in mind when analysing the charts.

It will be appreciated that, throughout the analysis of the charts, a good deal of subjectivity was inevitable and, with projects of this nature, this will continue to be so until more homogenous and more plentiful data become available at the higher levels. In spite of the inadequacy of the data it is felt that the charts provide an acceptable and useful representation of the main features of the climatology of the middle stratosphere for use until such time as more homogeneous and more plentiful data do become available.

PART I — AVERAGE TEMPERATURES AT 30 MILLIBARS AND THEIR VARIABILITY

1 — GENERAL

The average temperatures at 30 mb for January, April, July and October for the whole of the northern hemisphere are presented on the charts in Plates 1, 3, 4 and 6. Those for February and March and for August and September are shown in Plates 2 and 5 respectively. These charts cover the area from the pole to 45°N and are included because the reorganization of the high-latitude stratospheric-temperature patterns in spring and autumn makes it difficult, or sometimes impossible, to interpolate between the January and April or the July and October charts. South of 45°N interpolation between the average charts for the mid-season months is considered adequate for most practical purposes.

Corresponding charts of standard deviation of temperature at 30 mb for the same months are contained in Plates 7–12 and, because of the bimodal character of the temperature distribution in high latitudes during winter and spring months, a selection of histograms showing observed and theoretical frequency distributions is included alongside the charts for January to April. Additional histograms for selected stations for all months considered are given in Figure 6.

The charts for the winter and spring months should be used with caution in those higher-latitude areas which are dominated by the two very different thermal regimes and it is hoped that the selection of histograms given will enable the reader to determine for himself the months and the areas in which temperatures do not conform to the normal distribution.

2 — DISCUSSION OF THE CHARTS

The January and February charts (Plates 1 and 2a) show isotherm patterns in middle and high latitudes which are typical of the winter regime. The principal climatological features are the cold area between north-east Greenland and north Norway, the warm region in the vicinity of Kamchatka and the warm belt around the hemisphere which varies from 50 to 60°N to the east and west of Kamchatka to about 30°N in other parts of the hemisphere. South of the temperature maximum in middle latitudes there is a decrease of temperature to −58 to −64 °C towards the equator By March (Plate 2b) the centre of the cold area has moved south-east to the Gulf of Bothnia and temperatures at the centre are appreciably warmer than in January and February. The centre of the 'Aleutian' warm area changes little from February to March. The changes which take place between January and March result in a marked decrease in the temperature gradient over much of the Arctic basin and this decrease is more marked on the April chart (Plate 3). By April the warm area has moved nearer the pole to be centred over the north of east Siberia while, on the other side of the hemisphere, in the region of the British Isles, there are still the remnants of a weak cold area with temperatures of about −54 °C and there are also small weak cold centres at a similar latitude over North America. The April chart bears a closer resemblance to the July chart (Plate 4) than it does to those of the earlier winter months. The main features of the mid-summer stratospheric-temperature regime are the warm area centred near the North Pole within which average temperatures are a little above −40 °C and the gradual decrease to values of −54 to −60 °C near the equator. It is noticeable that the warm area is not symmetrical about the North Pole but the warmer air is displaced towards the Canadian sector and also that, in high latitudes, the temperature gradient over Russia is appreciably stronger than the gradient over North America. The August isotherm pattern over middle and high latitudes (Plate 5a) resembles closely the July chart and the only significant difference between the two months is the seasonal cooling of 3 or 4 deg in higher latitudes. The average chart for September (Plate 5b) shows this to be the transitional month between the well-defined summer and winter patterns. Over the hemisphere north of 45°N temperature gradients are generally very weak. By October (Plate 6) the chart shows that the features associated with a mid-winter pattern are becoming established. There is a cold area centred near the pole where average temperatures are about -61 °C. The Aleutian warm area is evident although the highest temperatures, about -50.5 °C, appear to be centred over the Sea of Okhotsk and the warm belt, which is a characteristic feature of the winter stratosphere, is becoming established.

Figure 1 shows the 30-mb temperatures, for the months January to April and July to October, averaged around latitude circles. The averages were obtained from the charts using values at the

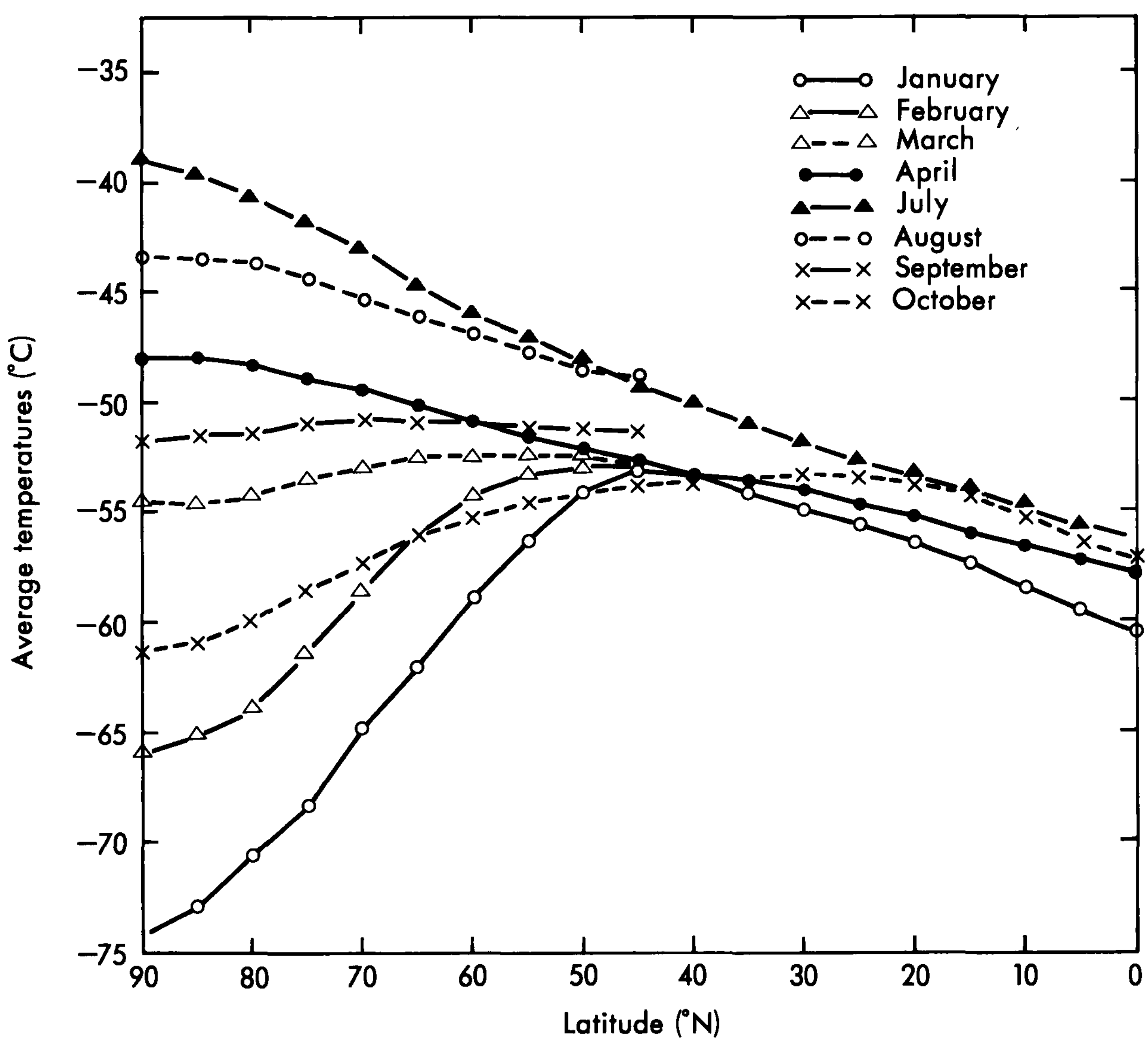

FIGURE 1. TEMPERATURES AT 30 MILLIBARS AVERAGED AROUND LATITUDE CIRCLES

intersections of every 10 degrees of longitude with every 5 degrees of latitude. This shows clearly the very large annual variation in high latitudes and the much smaller annual variation in other latitudes. The very large rise in temperature which takes place in the high-latitude stratosphere between January and April is a striking feature of this diagram. Most of this rise takes place from February to March although, in any individual year the time at which the final warming takes place varies considerably and the major rise may occur earlier or later. In both January and February there is a sharp rise in temperature from the polar region to the latitude of the warm belt (about 40 to 50°N) and then a relatively gradual decrease in temperature towards the equator. The July curve shows the gradual decrease in temperature from the warm area near the pole to the cold region near the equator. In higher latitudes the seasonal cooling from August to September is approximately double that from July to August and, although the winter features are present in October, as the winter advances the high-latitude stratosphere cools a further 15 deg or so to the January values of about −73 to −74 °C and the temperature gradients between high and middle latitudes increase considerably.

In low latitudes, in addition to the annual variation there is also a fluctuation in the monthly mean temperatures which is associated with the quasi-biennial oscillation (QBO) in the zonal wind component and analysis of the 30-mb temperature data at Canton Island (02° 46 ′S, 171° 43 ′W) shows that the QBO accounts for nearly half of the total variance whereas the annual oscillation accounts for only about a quarter.

The hemispheric pattern of these temperature variations from season to season is shown in more detail on the charts in Figures 2–5. In an area near the North Pole and north Greenland there is a rise of over 25 deg between January and April (Figure 2). Most of this warming takes place in the period January to March and is dealt with in more detail later in the text under the heading 'The final warming'. From April to July (Figure 3) there is a further warming in high latitudes with peak values of 10 deg off northern Norway. Figure 4 shows the marked seasonal cooling from summer to autumn in high latitudes. Over north Greenland and the pole there is a cooling of more than 20 deg most of which takes place between August and October. Figure 5 shows that the high-latitude stratosphere continues to cool between October and January. In the region of Spitsbergen this cooling exceeds 14 deg. However, in the Aleutian region the warm area intensifies with peak values exceeding 7 deg.

The charts of standard deviation of temperature at 30 mb are shown in Plates 7–12 and frequency distributions for a selection of stations between 45°N and the pole are included alongside the charts for January, February, March and April. Comments on the charts follow here, but, before using them, the reader is advised to refer to the section on 'The final warming' as the charts need to be used with caution and understanding of the events which take place during the late winter/spring period in high latitudes.

In January (Plate 7) the standard deviation exceeds 10 deg over a considerable area in high and some middle latitudes with the maximum occurring over the central districts of west Greenland. The trough in the pattern, indicating high standard deviations, over the North Sea and central Europe may be attributed to those stratospheric warmings which originate over or to the east of south-east Europe and move in a north-westerly direction. In the tropics from mid North Atlantic across central America and the Pacific to the Phillipines the standard deviation is between 2 and 3 deg but in low latitudes over Africa and the Indian Ocean there is evidence for suggesting that

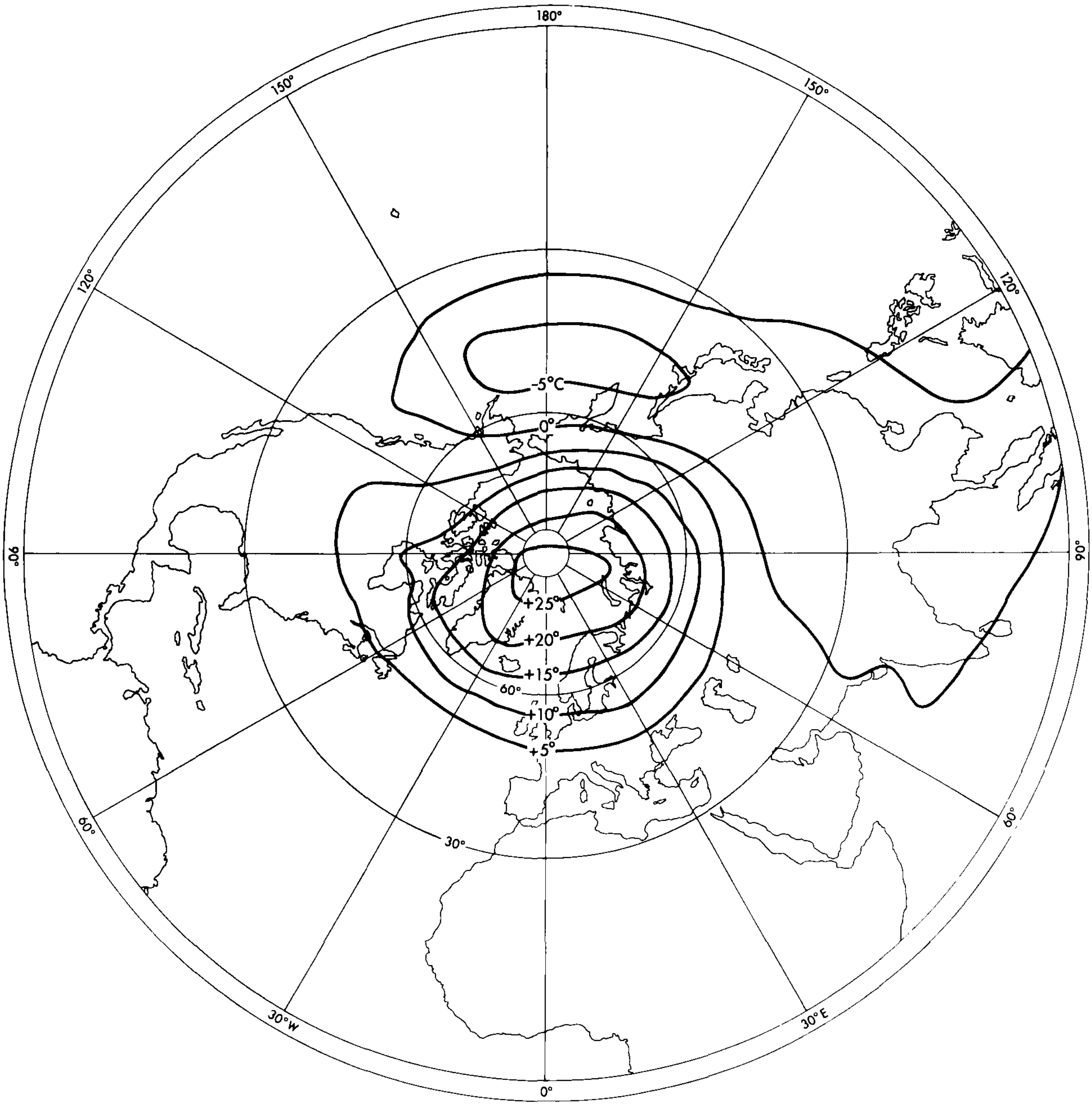

FIGURE 2. CHANGE OF AVERAGE TEMPERATURES AT 30 MILLIBARS FROM JANUARY TO APRIL, 1957–64

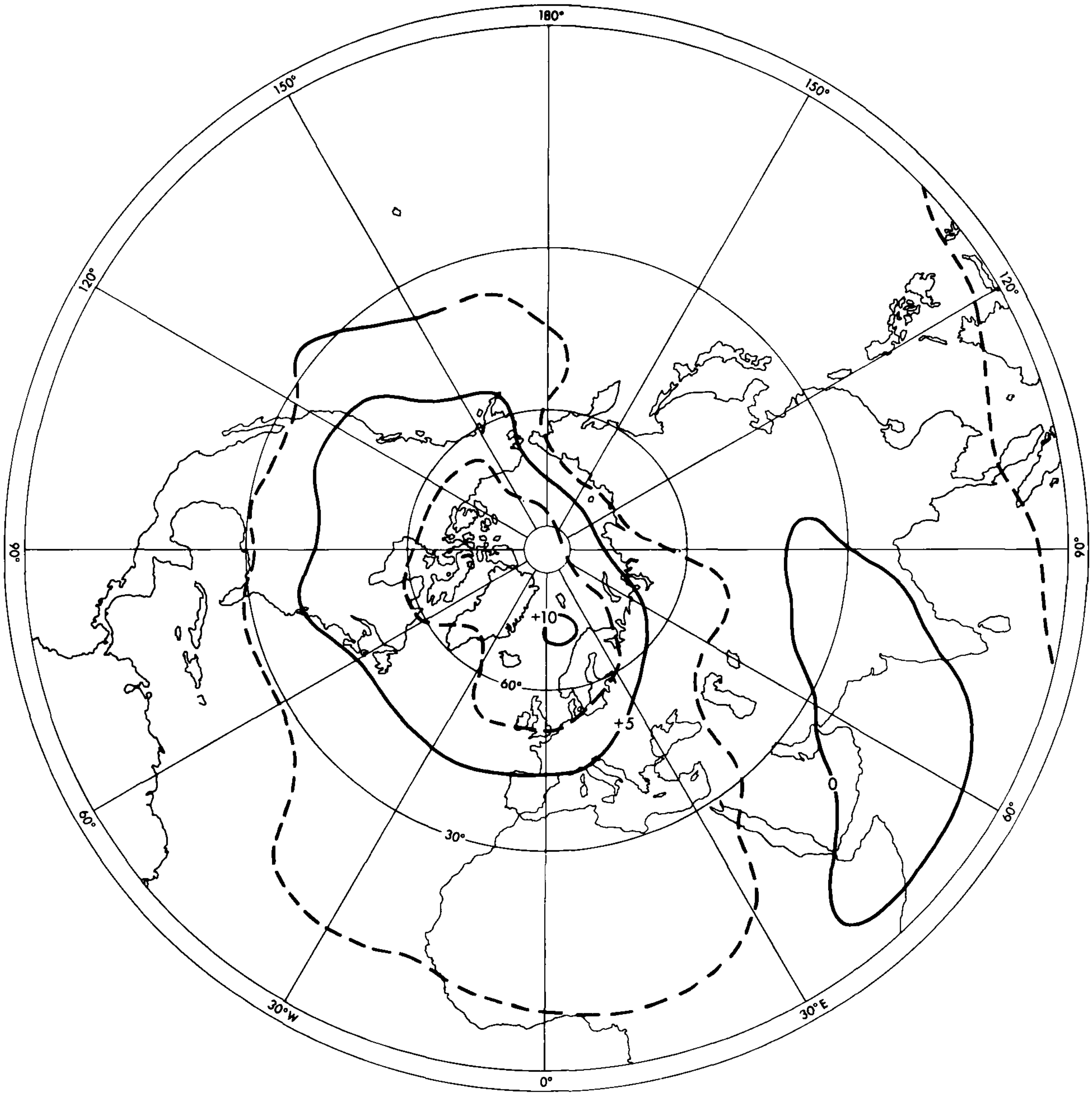

FIGURE 3. CHANGE OF AVERAGE TEMPERATURES AT 30 MILLIBARS FROM APRIL TO JULY, 1957–64

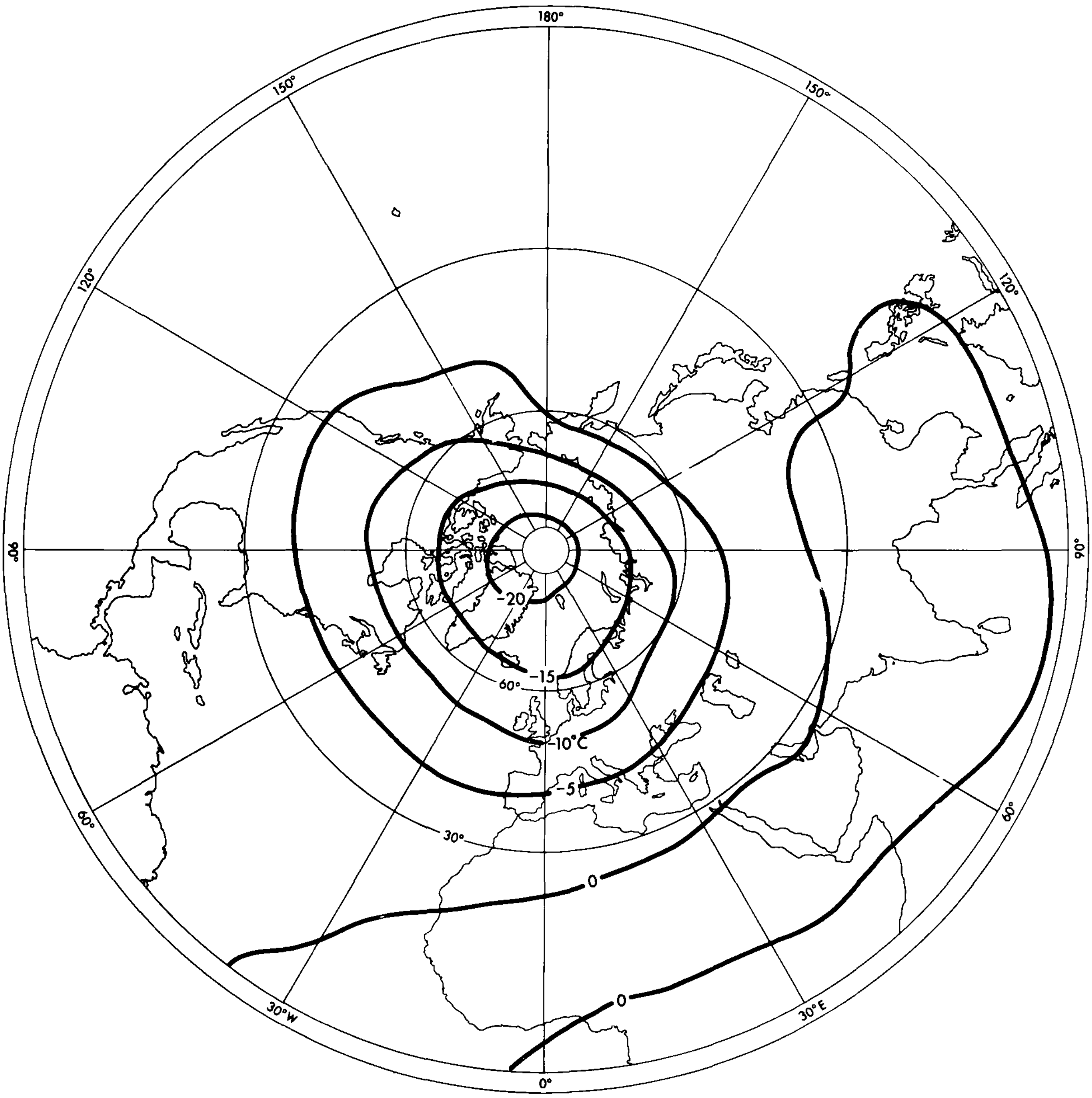

FIGURE 4. CHANGE OF AVERAGE TEMPERATURES AT 30 MILLIBARS FROM JULY TO OCTOBER, 1957–64

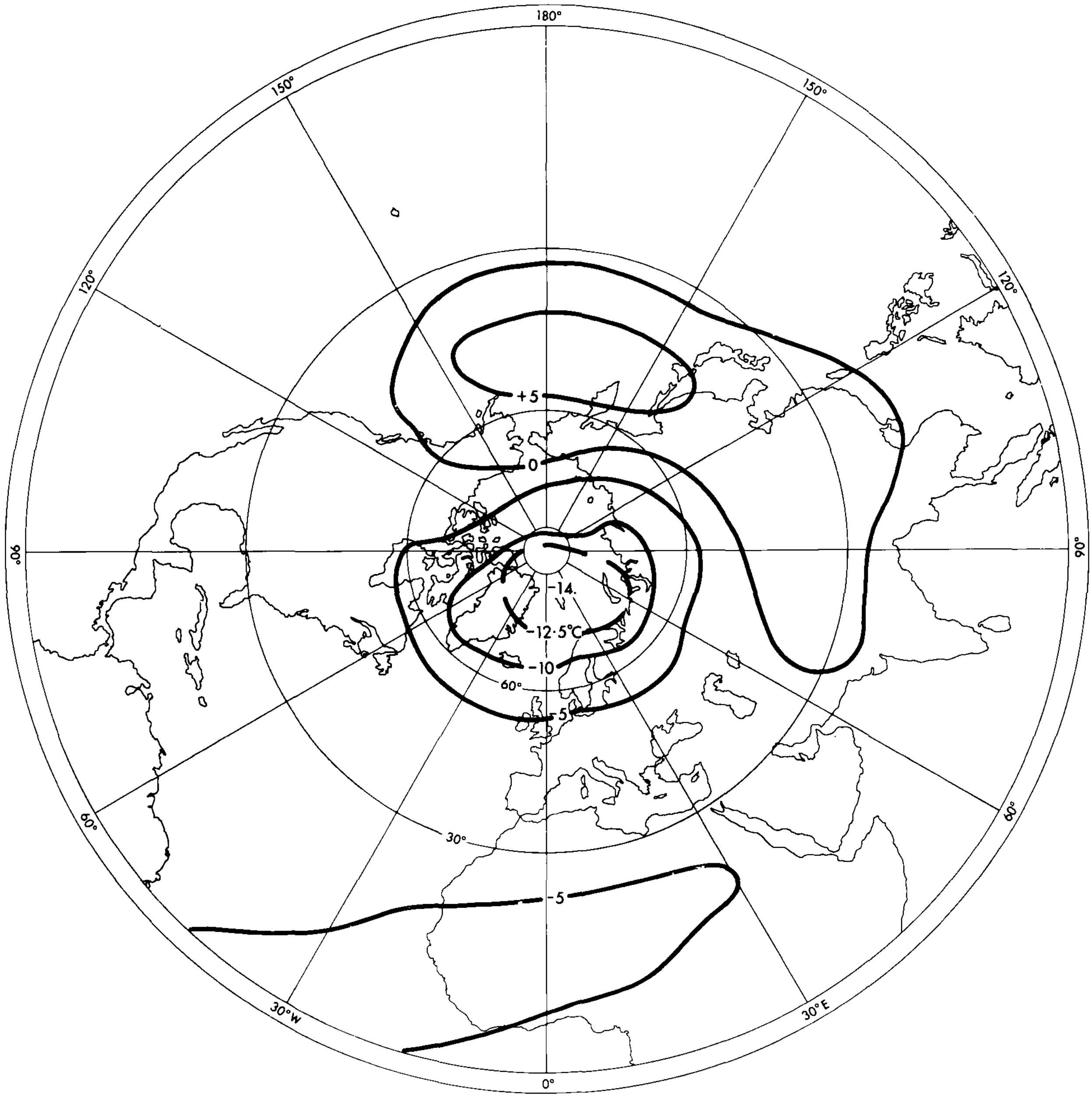

FIGURE 5. CHANGE OF AVERAGE TEMPERATURES AT 30 MILLIBARS FROM OCTOBER TO JANUARY, 1957–64

variability is a little higher with values exceeding 5 deg. The chart for February (Plate 8a) shows that, as in January, the standard deviations are large in high latitudes with values of more than 10 deg over much of the Arctic. In March (Plate 8b) the variability is still high with a maximum value of 12.3 deg at Alert (based on 383 observations in the eight-year period). Plate 9 shows that by April the high-latitude stratospheric-temperature regime is much less variable with maximum values of about 6 deg from northern Canada to northern Scandinavia. The charts for July, August and September (Plates 10, 11a and 11b) illustrate the very marked change in the variability between winter (Plate 7) and summer especially in high latitudes. Over a large part of the hemisphere north of 45°N the standard deviation is generally about 2 or 3 deg although, in July, there is some evidence for suggesting higher values over North Africa, India and into China. By October (Plate 12) over most high-latitude areas the standard deviation exceeds 3 deg with values higher than 4 deg from the North Atlantic across the Russian arctic to north-east Siberia. These relatively low values indicate that during summer and autumn, in high latitudes, there is nothing comparable with the sudden warmings which take place in winter and spring to disrupt the temperature regime. In October, as in the other mid-season months, the standard deviation exceeds 4 deg across Africa, the Indian Ocean and south-east Asia. However, these are areas with relatively few radiosonde stations and owing to the paucity of data it is not possible to be very confident about the analysis there.

The charts of average temperature and their standard deviations do provide useful and reliable information for the summer months and also, for a large part of the hemisphere, for the other months considered but those for the winter/spring months should be used with extreme caution in areas where the distribution is known to be bimodal. In those areas a considerable amount of additional useful information can be obtained from the relevant temperature-frequency diagrams.

The frequency distributions of 30-mb temperatures for a selection of stations in different latitudes are given in Figure 6 and the relevant statistics are presented in Table I. These histograms, and those for high-latitude stations which accompany the standard deviation charts (Plates 7–9) confirm that in winter and spring the frequency distributions of stratospheric temperatures in some high latitudes are distinctly bimodal. As at 50 mb, it is of interest to note that at Adak, situated within the Aleutian stratospheric warm area, the cold regime never became established during January to March in the years 1958–65 whereas at Crawley, at a comparable latitude on the other side of the hemisphere, much wider fluctuations of temperature occurred with a minimum of −85 °C in February. The lower-latitude stations all show a unimodal temperature distribution in January and the histograms for April, July, August, September and October all show that the 30-mb temperature distribution is nearly normal over the hemisphere generally.

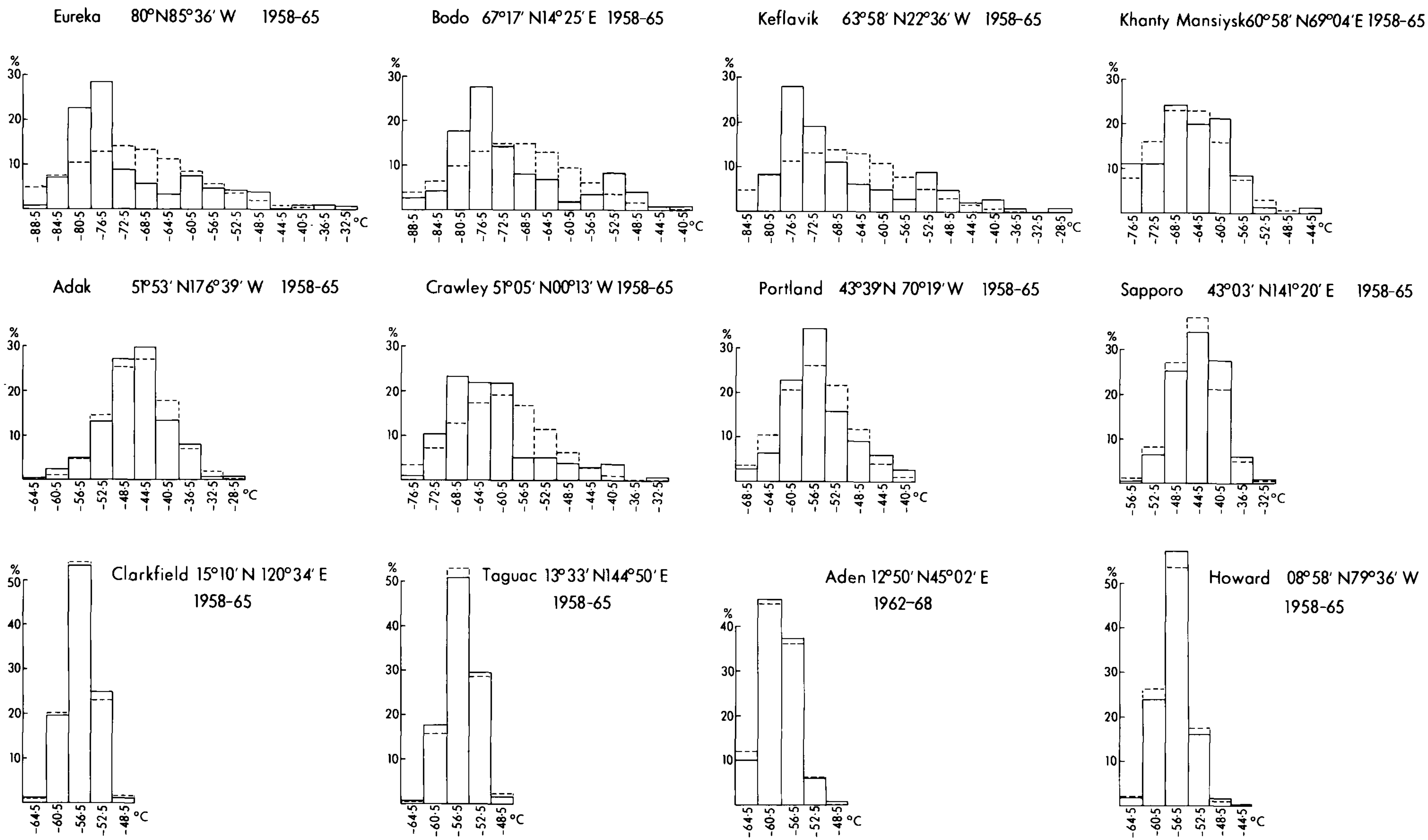

FIGURE 6. FREQUENCY DISTRIBUTIONS OF TEMPERATURE AT 30 MILLIBARS IN JANUARY

——— Observed distribution - - - - - Theoretical distribution

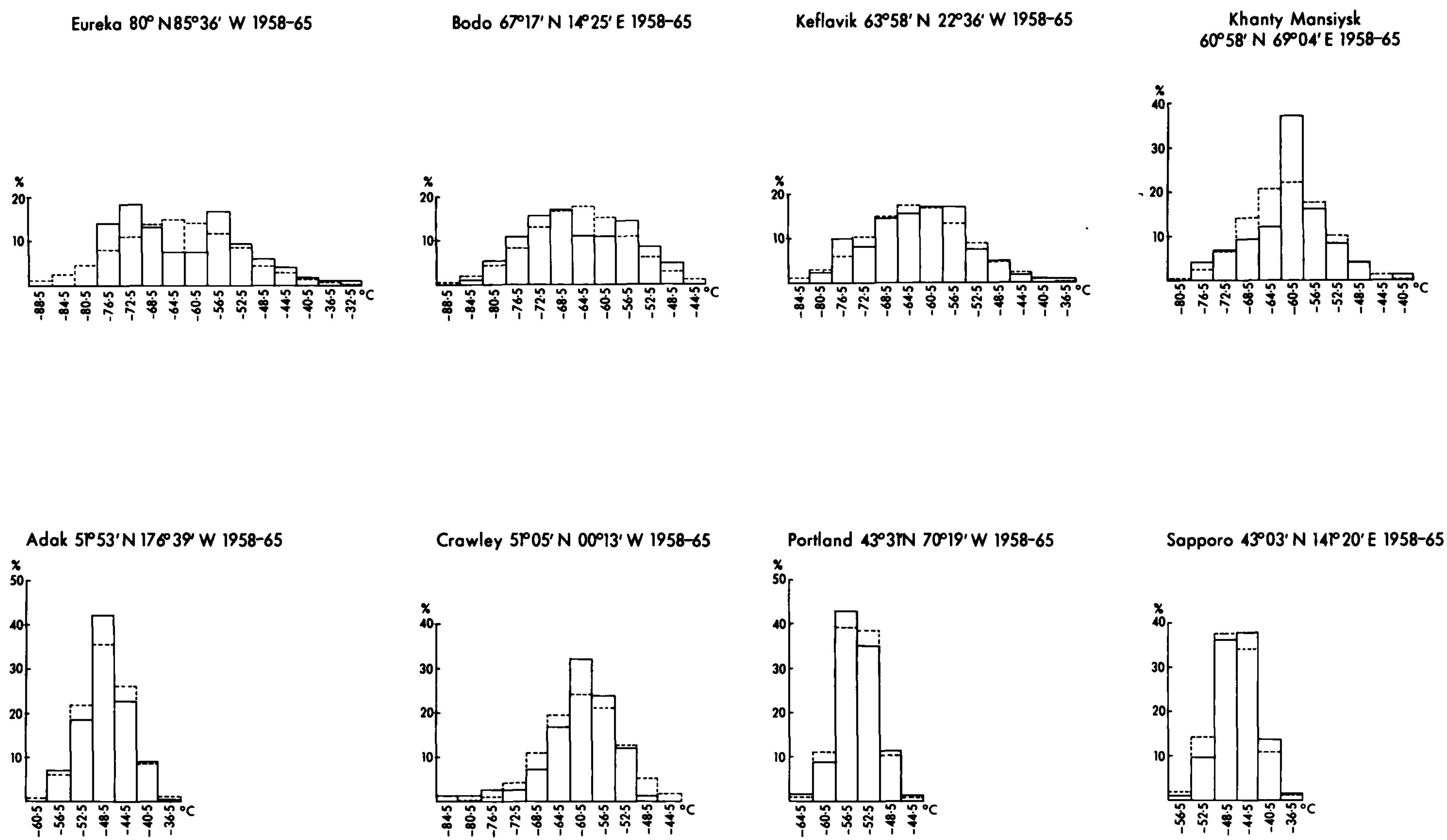

FIGURE 6. (*contd*) FREQUENCY DISTRIBUTIONS OF TEMPERATURE AT 30 MILLIBARS IN FEBRUARY

——— Observed distribution - - - - - Theoretical distribution

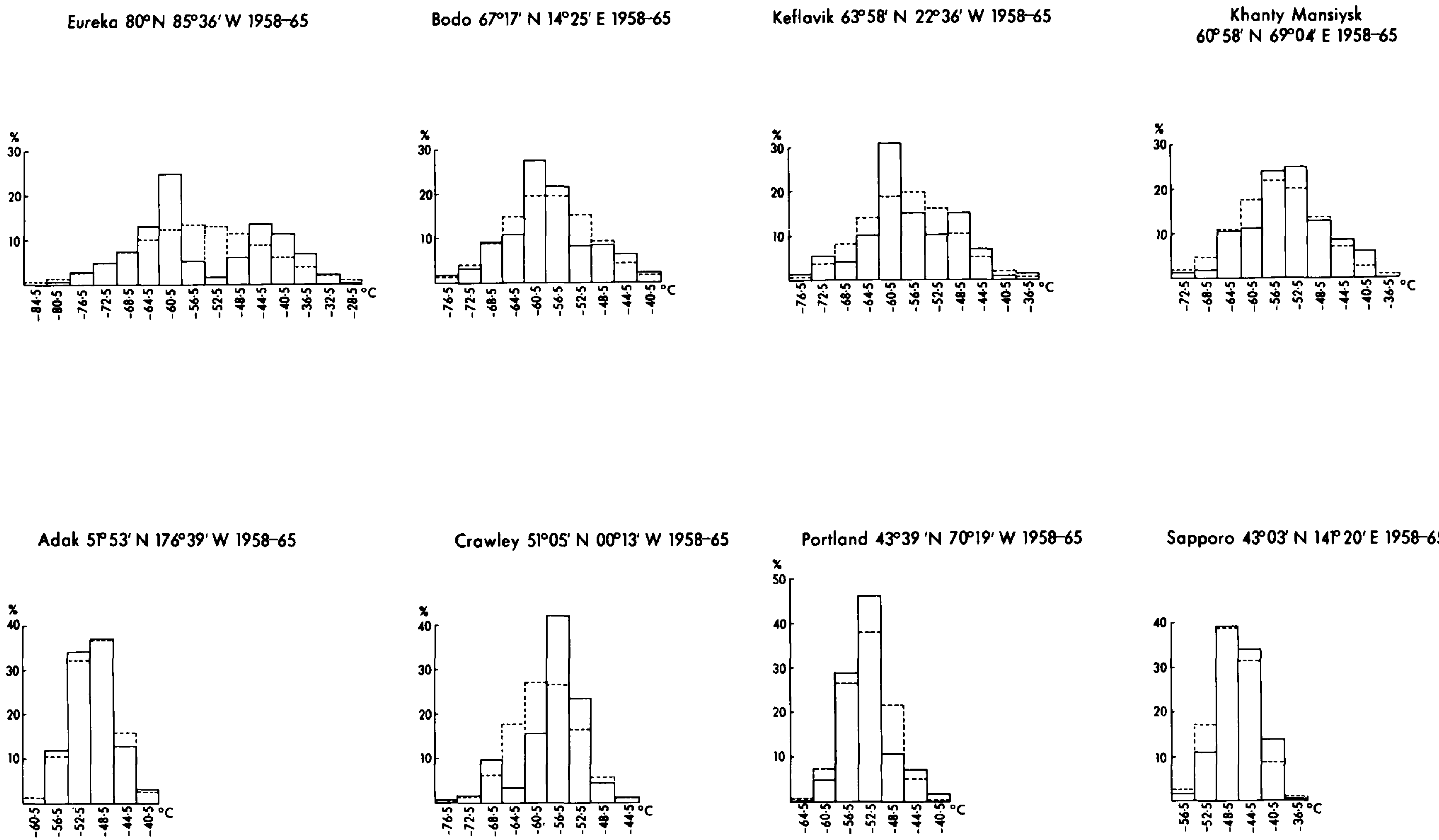

FIGURE 6. (*contd*) FREQUENCY DISTRIBUTIONS OF TEMPERATURE AT 30 MILLIBARS IN MARCH

——— Observed distribution ----- Theoretical distribution

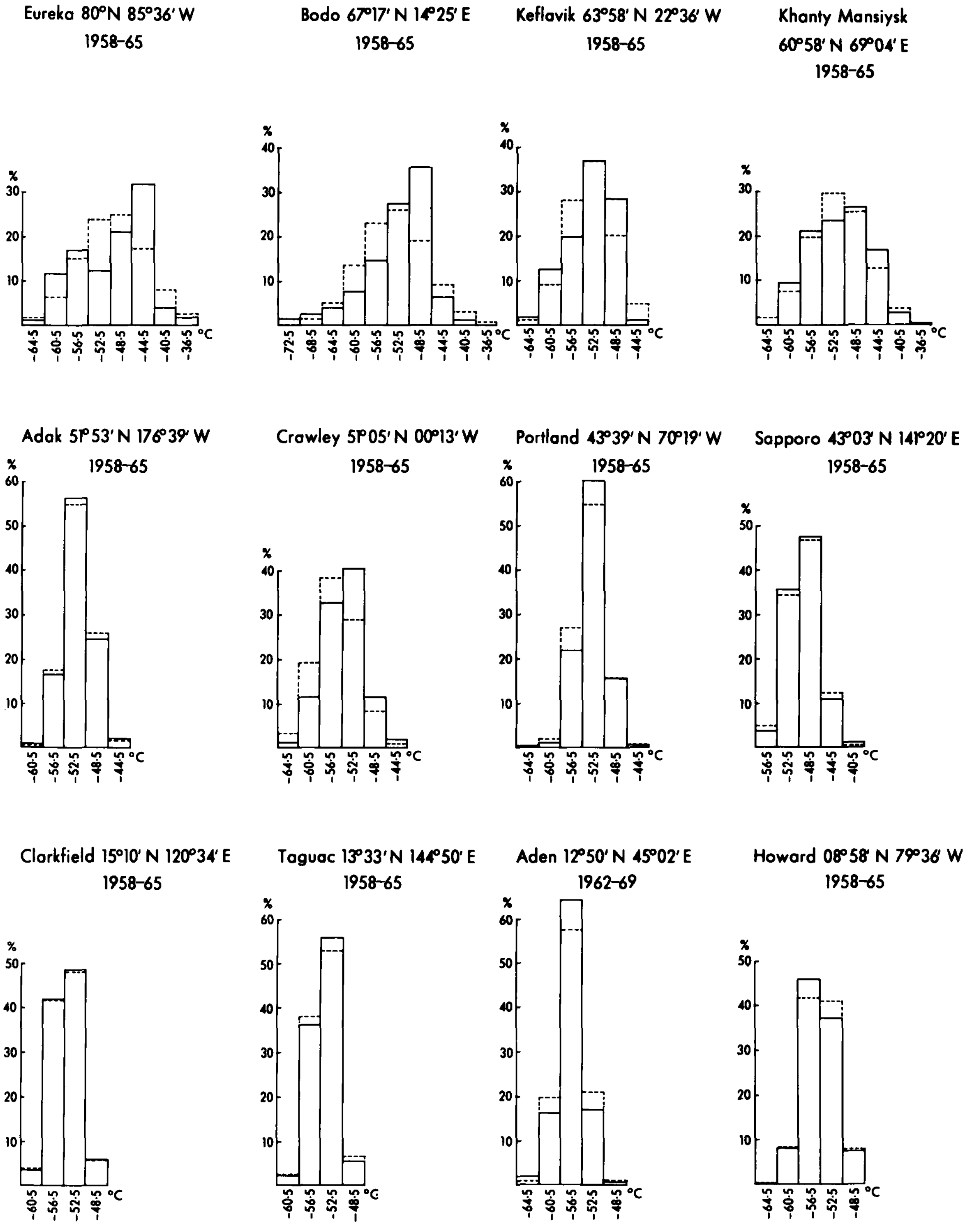

FIGURE 6. (*contd*) FREQUENCY DISTRIBUTIONS OF TEMPERATURE AT 30 MILLIBARS IN APRIL

——— Observed distribution - - - - - Theoretical distribution

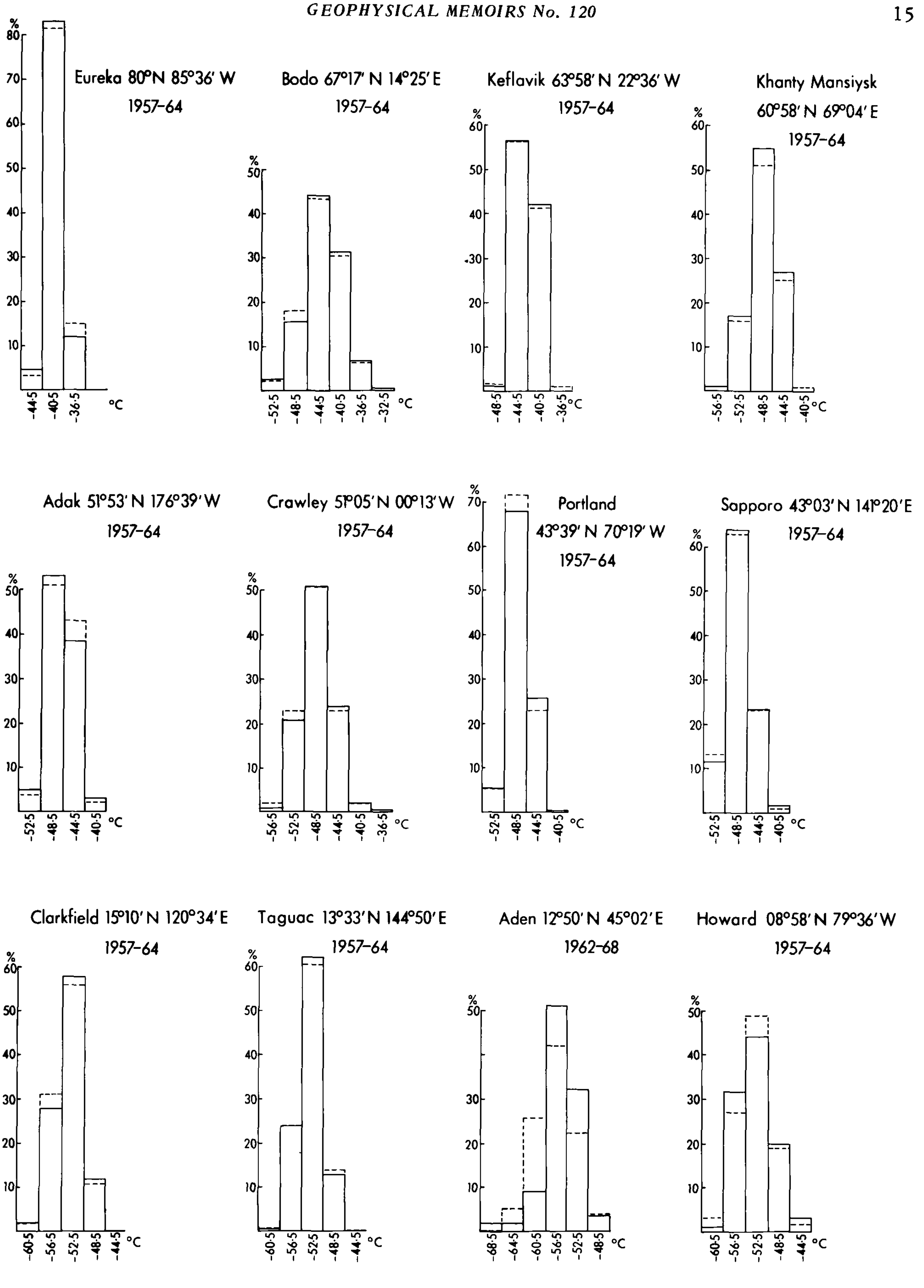

FIGURE 6. (*contd*) FREQUENCY DISTRIBUTIONS OF TEMPERATURE AT 30 MILLIBARS IN JULY

——— Observed distribution - - - - - Theoretical distribution

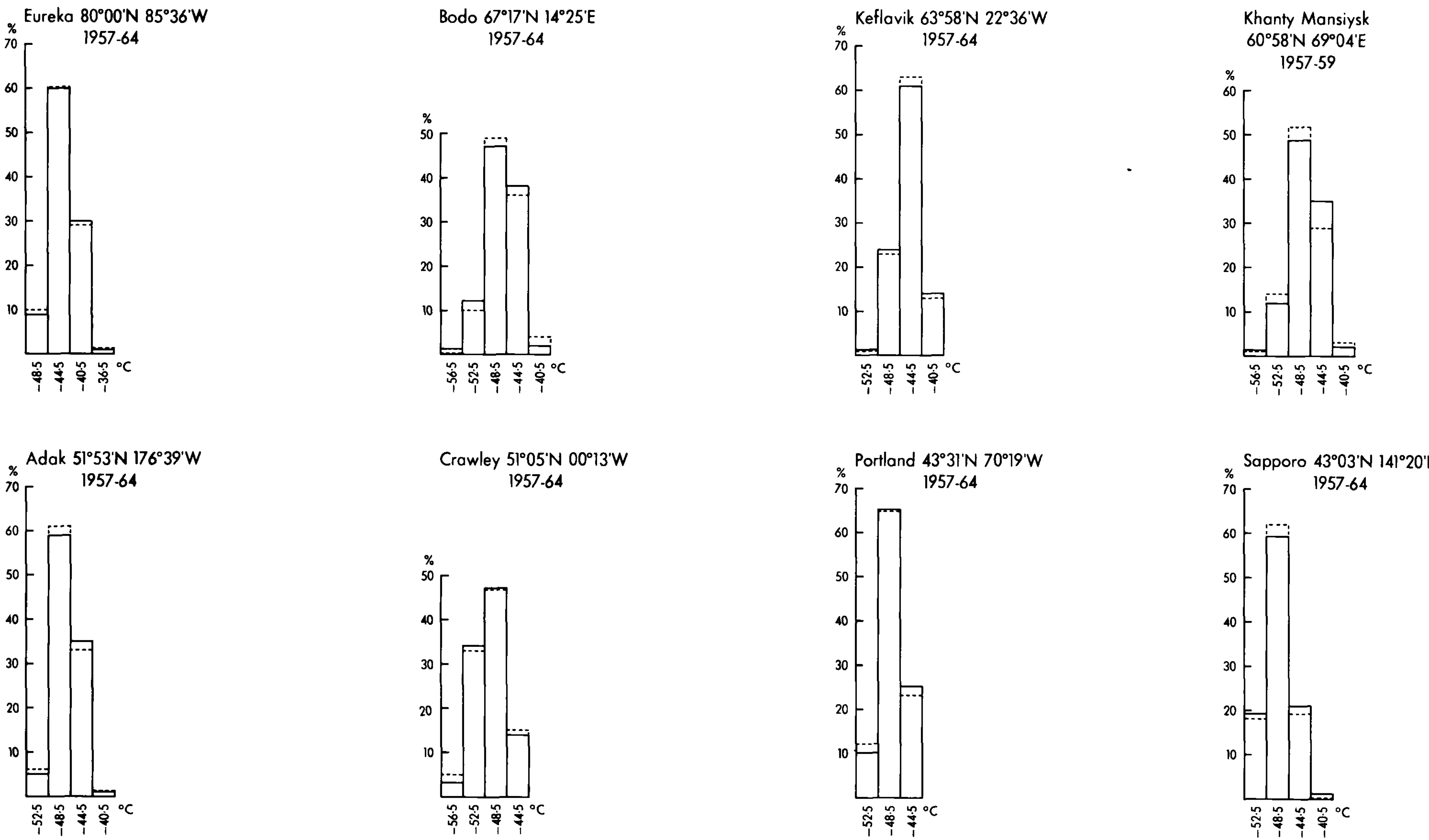

FIGURE 6. (*contd*) FREQUENCY DISTRIBUTIONS OF TEMPERATURE AT 30 MILLIBARS IN AUGUST

——— Observed distribution - - - - - Theoretical distribution

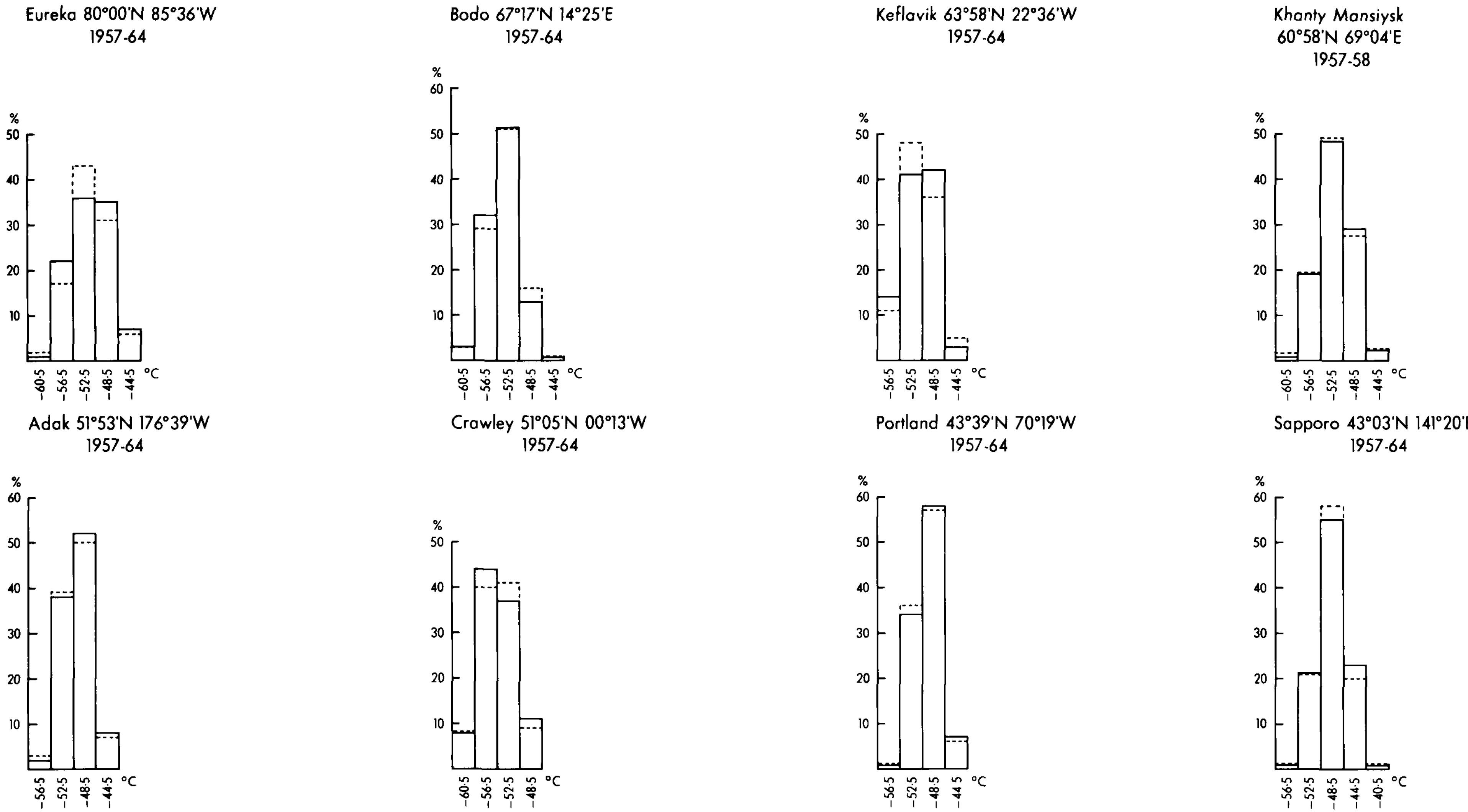

FIGURE 6. (*contd*) FREQUENCY DISTRIBUTIONS OF TEMPERATURE AT 30 MILLIBARS IN SEPTEMBER

——— Observed distribution - - - - - Theoretical distribution

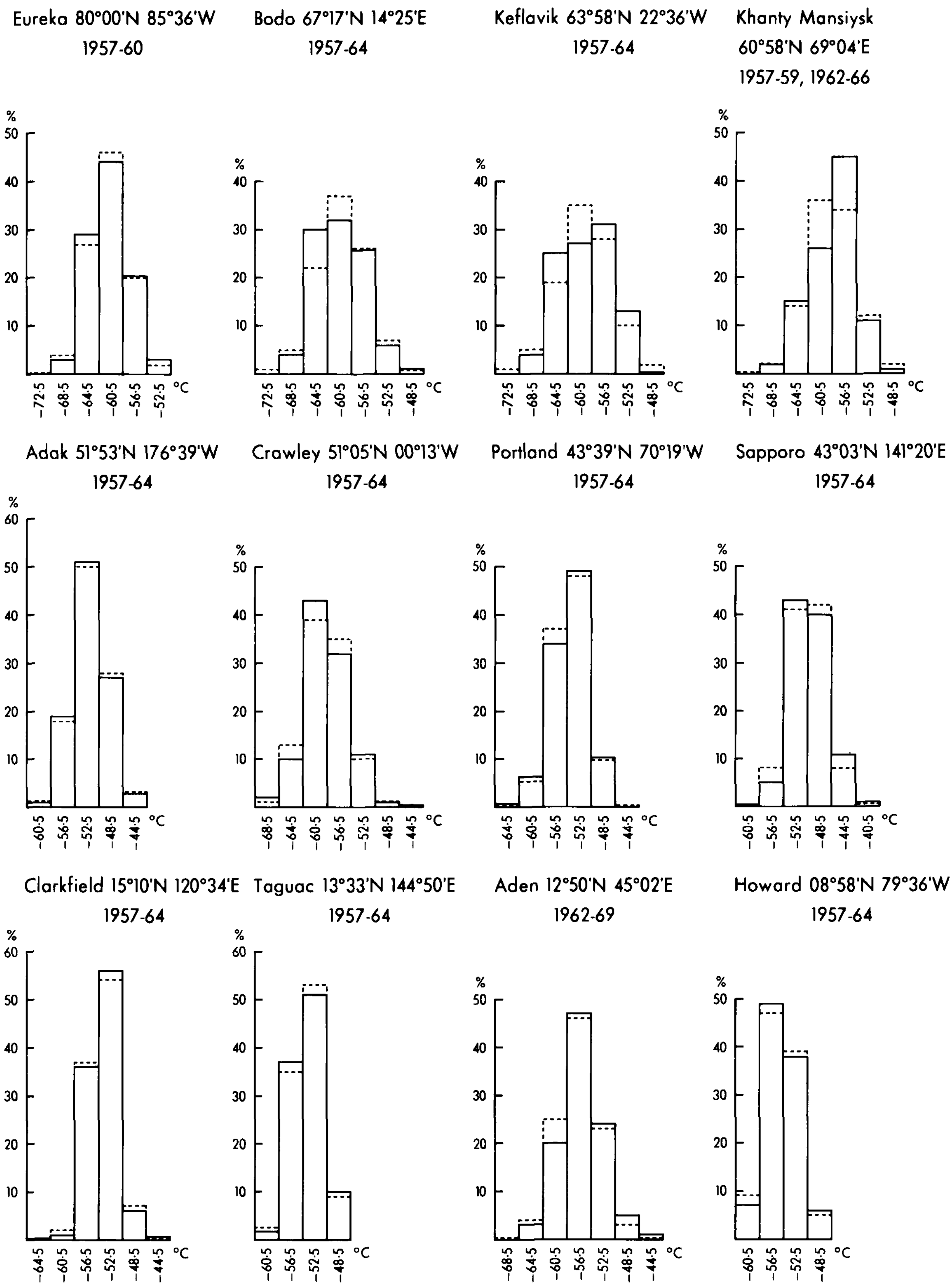

FIGURE 6. (*contd*) FREQUENCY DISTRIBUTIONS OF TEMPERATURE AT 30 MILLIBARS IN OCTOBER

——— Observed distribution - - - - - Theoretical distribution

TABLE I – AVERAGE 30-MILLIBAR TEMPERATURES AND STANDARD DEVIATIONS FOR THE STATIONS FOR WHICH HISTOGRAMS ARE GIVEN IN FIGURE 6.

	Eureka 80°00'N, 85°56'W						Bodø 67°16'N, 14°24'E						Keflavik 63°58'N, 22°36'W					
	$\overline{T}$	σ	N	n	T_{max}	T_{min}	$\overline{T}$	σ	N	n	T_{max}	T_{min}	$\overline{T}$	σ	N	n	T_{max}	T_{min}
Jan.	-71.8	11.5	296	8	-32.6	-87.4	-70.7	10.6	120	7	-42.4	-88.5	-68.8	11.6	288	8	-28.4	-83.3
Feb.	-64.0	10.7	332	8	-30.9	-77.7	-65.5	8.8	186	8	-46.8	-85.2	-63.2	9.0	276	8	-34.0	-82.0
Mar.	-55.5	11.8	428	8	-28.8	-80.0	-58.5	7.8	240	8	-38.3	-83.6	-57.8	7.9	319	7	-36.4	-75.6
Apr.	-50.1	6.1	425	8	-35.5	-63.4	-53.5	6.0	288	8	-40.0	-74.0	-53.3	4.1	420	8	-44.8	-66.0
July	-40.0	1.4	433	8	-34.5	-44.5	-43.7	3.4	319	8	-33.0	-52.0	-42.9	1.7	412	8	-38.6	-48.4
Aug.	-43.7	2.2	424	8	-36.7	-49.6	-47.2	2.7	191	8	-39.9	-56.0	-45.0	2.2	406	8	-39.0	-52.0
Sept.	-51.6	3.4	391	8	-43.0	-59.4	-53.2	2.8	144	8	-45.4	-62.1	-51.2	2.8	387	8	-44.4	-58.1
Oct.	-61.0	3.2	355	8	-49.1	-70.1	-60.2	4.1	224	8	-49.0	-70.1	-59.6	4.3	377	8	-50.3	-69.5

	Khanty-Mansiysk 60°58'N, 69°04'E						Adak 51°53'N, 176°39'W						Crawley 51°05'N, 00°13'W					
	$\overline{T}$	σ	N	n	T_{max}	T_{min}	$\overline{T}$	σ	N	n	T_{max}	T_{min}	$\overline{T}$	σ	N	n	T_{max}	T_{min}
Jan.	-66.6	6.5	70	5	-44.0	-78.0	-46.0	5.6	337	8	-28.8	-62.6	-60.9	8.3	137	7	-31.0	-76.0
Feb.	-61.6	7.0	75	3	-42.5	-78.0	-48.1	4.3	244	8	-33.7	-57.9	-60.1	6.5	84	7	-48.0	-85.0
Mar.	-55.7	7.2	117	5	-39.0	-72.0	-50.0	3.9	240	8	-37.5	-57.7	-58.7	5.5	183	8	-45.0	-76.0
Apr.	-51.6	5.2	162	5	-38.0	-62.1	-52.1	2.6	301	8	-42.5	-59.3	-55.7	3.9	162	8	-45.0	-66.0
July	-48.1	2.4	93	3	-43.0	-55.0	-46.8	2.1	221	8	-39.8	-52.9	-48.6	2.9	198	8	-37.0	-55.0
Aug.	-47.7	2.7	304	8	-40.8	-57.0	-47.4	2.0	273	8	-42.3	-52.6	-49.6	3.0	203	8	-40.0	-58.0
Sept.	-52.1	3.0	279	8	-44.2	-60.0	-50.1	2.4	285	8	-44.8	-56.4	-54.5	3.0	186	8	-47.0	-61.0
Oct.	-58.8	3.9	190	8	-49.0	-69.0	-52.0	2.9	335	8	-42.3	-60.3	-58.9	3.5	248	8	-45.0	-68.0

	Portland 43°39'N, 70°19'W						Sapporo 43°03'N, 141°20'E						Clark 15°10'N, 120°34'E					
	$\overline{T}$	σ	N	n	T_{max}	T_{min}	$\overline{T}$	σ	N	n	T_{max}	T_{min}	$\overline{T}$	σ	N	n	T_{max}	T_{min}
Jan.	-56.3	6.0	331	8	-37.8	-70.0	-45.1	4.1	251	8	-32.2	-55.9	-56.4	2.7	466	8	-47.4	-65.0
Feb.	-54.6	3.3	347	8	-44.2	-64.4	-46.9	3.7	196	8	-36.9	-55.7						
Mar.	-53.0	4.0	410	8	-39.3	-64.3	-47.4	3.7	247	8	-37.4	-59.2						
Apr.	-53.1	2.6	371	8	-45.3	-63.6	-49.8	2.9	234	8	-39.5	-56.5	-54.3	2.4	433	8	-47.6	-61.5
July	-47.8	1.7	386	8	-41.0	-52.5	-48.1	2.2	341	8	-41.5	-53.4	-53.5	2.4	394	8	-44.1	-61.0
Aug.	-48.1	2.1	395	8	-42.2	-60.5	-48.5	2.3	321	8	-41.1	-54.6						
Sept.	-49.9	2.1	361	8	-44.3	-57.0	-48.6	2.5	327	8	-42.3	-55.7						
Oct.	-54.0	2.7	374	8	-47.4	-62.7	-50.5	2.9	338	8	-41.9	-58.8	-53.9	2.3	460	8	-43.7	-65.0

	Taguac 13°33'N, 144°50'E						Aden 12°49'N, 45°02'E						Balboa 08°56'N, 79°34'W					
	$\overline{T}$	σ	N	n	T_{max}	T_{min}	$\overline{T}$	σ	N	n	T_{max}	T_{min}	$\overline{T}$	σ	N	n	T_{max}	T_{min}
Jan.	-55.9	2.7	421	8	-48.9	-63.9	-59.1	3.0	139	6	-47.0	-66.0	-57.0	2.7	387	8	-45.2	-65.2
Apr.	-54.0	2.3	402	8	-46.6	-61.6	-56.5	2.5	160	8	-49.0	-63.0	-54.6	2.9	404	8	-41.5	-63.9
July	-53.0	2.3	411	8	-46.2	-59.3	-56.8	3.6	111	7	-49.0	-70.0	-53.0	3.0	365	8	-44.3	-60.2
Oct.	-53.8	2.4	380	8	-46.8	-59.4	-56.7	3.3	169	8	-45.0	-65.0	-54.9	2.7	375	8	-46.5	-61.5

$\overline{T}$ is the average temperature (degrees Celsius).
σ is the standard deviation.
N is the number of observations.
n is the number of years used.
T_{max} is the warmest recorded temperature.
T_{min} is the coldest recorded temperature.

3 – THE FINAL WARMING

As stated earlier in the text the high-latitude stratospheric-temperature regime undergoes a radical change between January and April. In some years there are quite large temperature oscillations and, in most years, there is a final warming in late winter or early spring, after which 'summer' temperature patterns are established. The manner in which this change takes place varies quite considerably from year to year and presents difficulties in trying to describe the climatology by means of averages and standard deviations. Some of these difficulties can be readily seen in Figures 7 and 8 which show the 30-mb twice-daily temperatures from January to April at Alert and Keflavik for three different years.

At Alert in 1958 there was a warming in January. Temperatures were near –80 °C around the 25th and then rose sharply to –33 °C on 1 February to give a warming of about 45 deg. This was followed by a cooling, another warming and then a gradual cooling with temperatures near –60 °C throughout March. There was then a slow rise in April. In 1961 there was a warming from about –80 °C in early January to warmer than –55 °C towards mid month. This was followed by a cooling to below –70 °C until the end of February when a slow warming started and temperatures reached –28 °C by mid March, after which temperatures remained generally above –50 °C. In 1965 temperatures remained near –80 °C through January with only slight warming in February. There was no major warming until late March when two warmings of 10 to 20 deg occurred. There was a further warming in April after which temperatures remained above –50 °C.

At Keflavik (Figure 8) in 1958 there was a warming in January. Temperatures rose sharply from –82 °C on 22nd to –28 °C on 30th – a rise of 54 deg. This was followed by a cooling, another warming and then a gradual cooling with temperatures near –60 °C throughout March and early April. There was then a slow rise to –50 to –55 °C at the end of April. In 1964 there was a minor warming and cooling in January followed by several other minor warmings and coolings of about 15 to 20 deg during February, then, around mid March there was a warming of about 30 deg after which temperatures remained about –50 °C. In 1965 temperatures were around –80 °C through most of January and there were two warmings and coolings of 10 to 20 deg in February. During the second half of March a warming from –71 °C to –36 °C took place in two stages after which temperatures remained between –50 and –60 °C.

These data for Alert (Figure 7) and Keflavik (Figure 8) show that, apart from the 'final' warming, there can be a number of minor warmings in any one year. These minor warmings do not lead to a breakdown of the vortex and can be due to migration and intensification of the Aleutian high. Minor warmings also occur over the Atlantic and European sectors. The temperatures within these minor warmings may well reach values comparable with the major warmings but they move around the vortex and do not reach the pole to cause the vortex to break down.

Because of the sudden warmings or the 'final' warming it is apparent that there can be very large differences in the high-latitude temperature patterns within a particular month. This is illustrated in Figures 9–12. Between 1 and 5 January and from 26 to 31 January 1963 there was

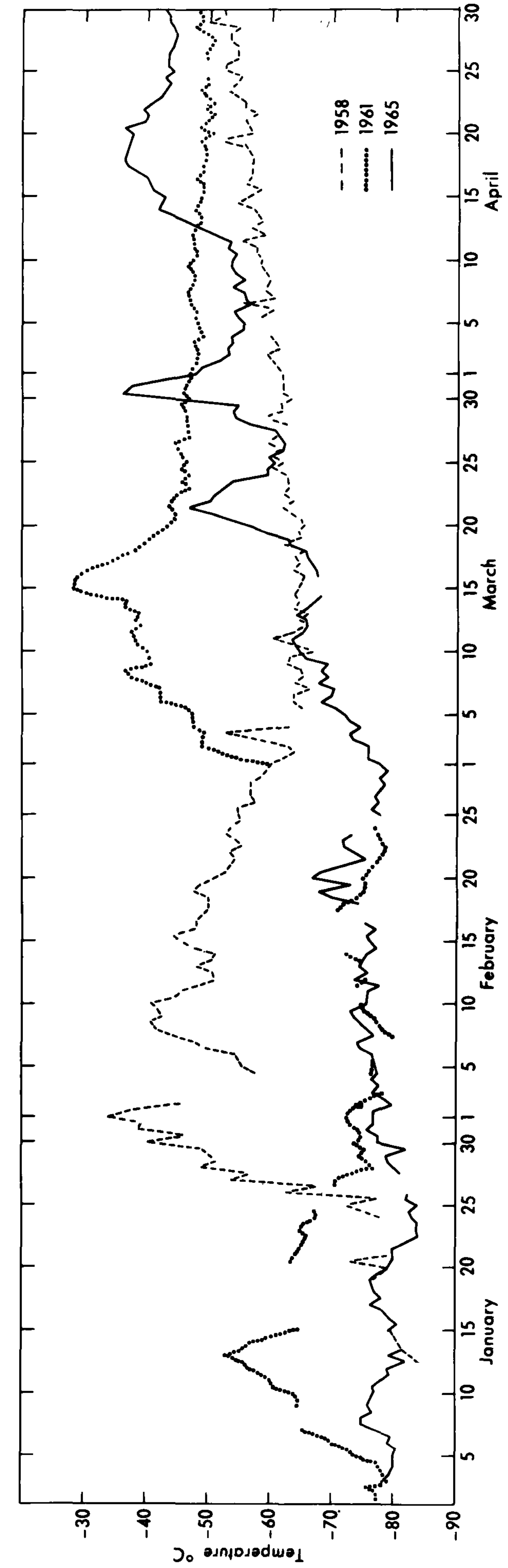

FIGURE 7. TWICE-DAILY 30-MILLIBAR TEMPERATURES AT ALERT 82°30′N, 62°20′W

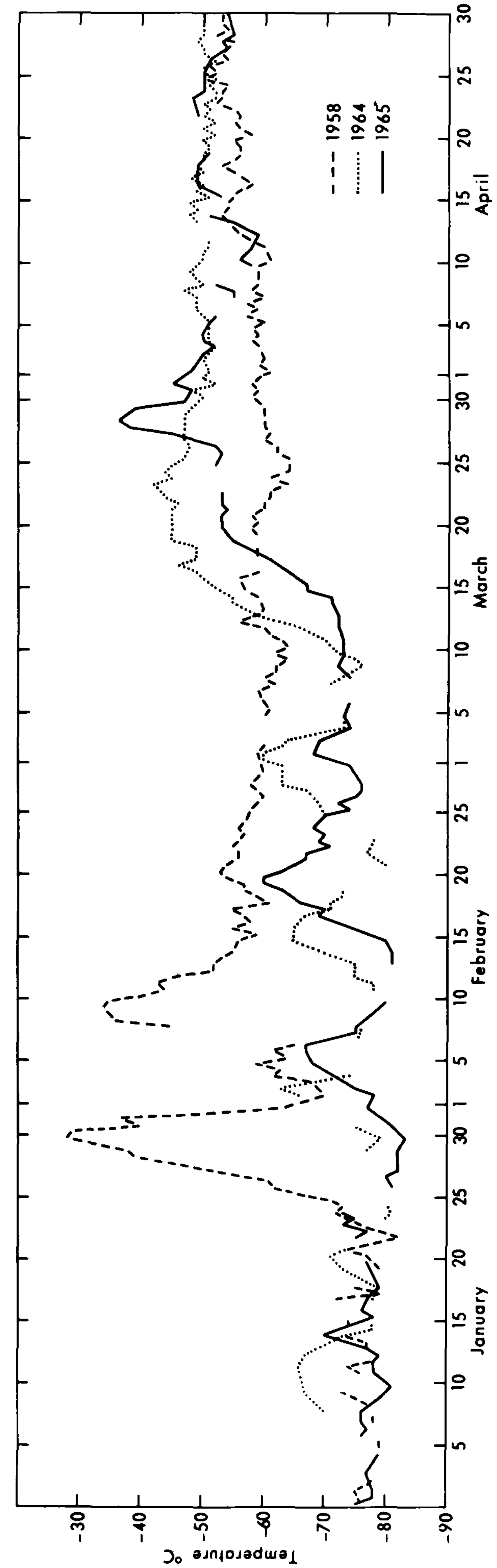

FIGURE 8. TWICE-DAILY 30-MILLIBAR TEMPERATURES AT KEFLAVIK 63°58′N, 22°36′W

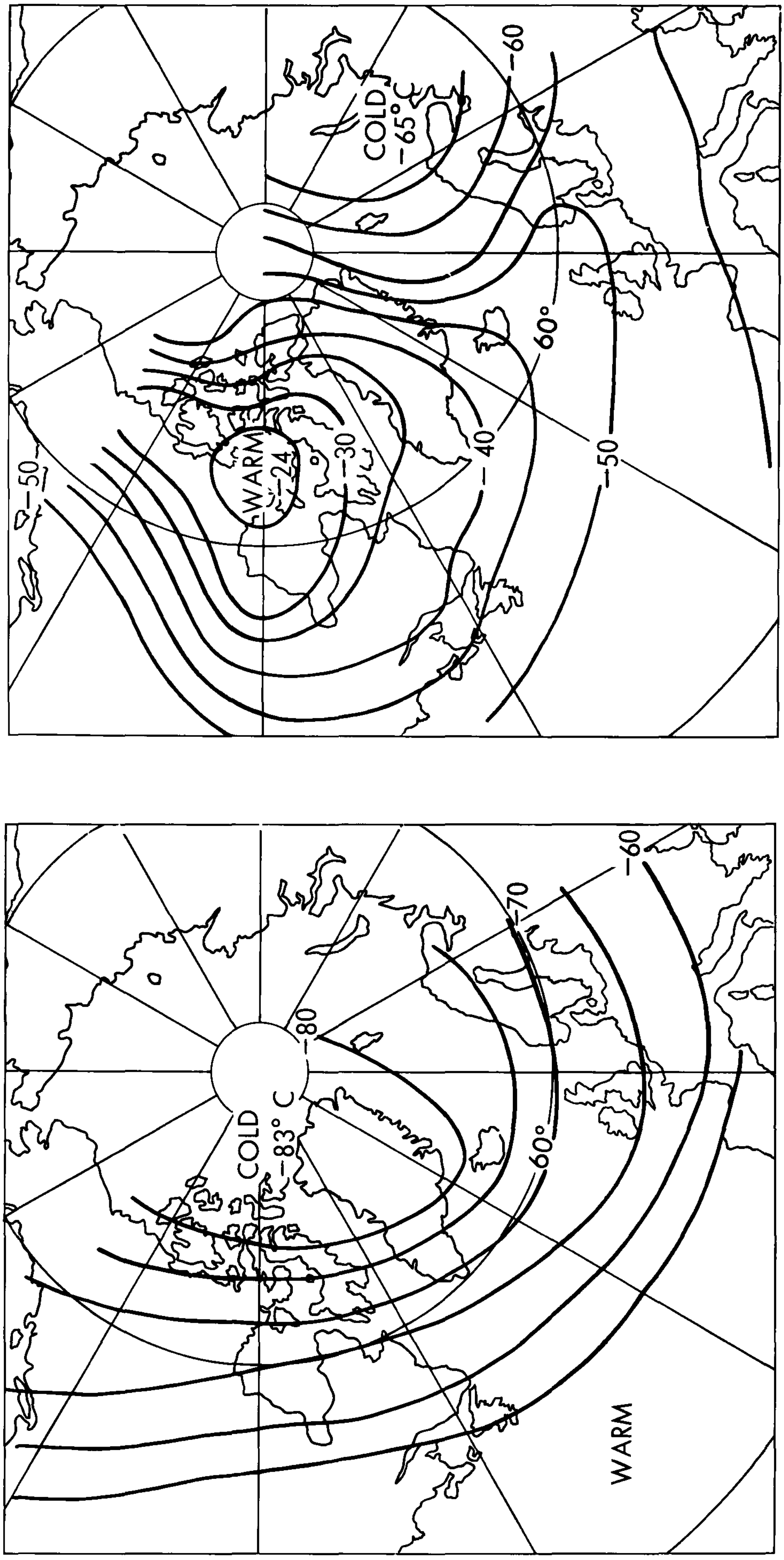

26-31 January 1963

1-5 January 1963

FIGURE 9. 30-MILLIBAR MEAN TEMPERATURES (DEGREES CELSIUS)
1–5 JANUARY 1963 26–31 JANUARY 1963

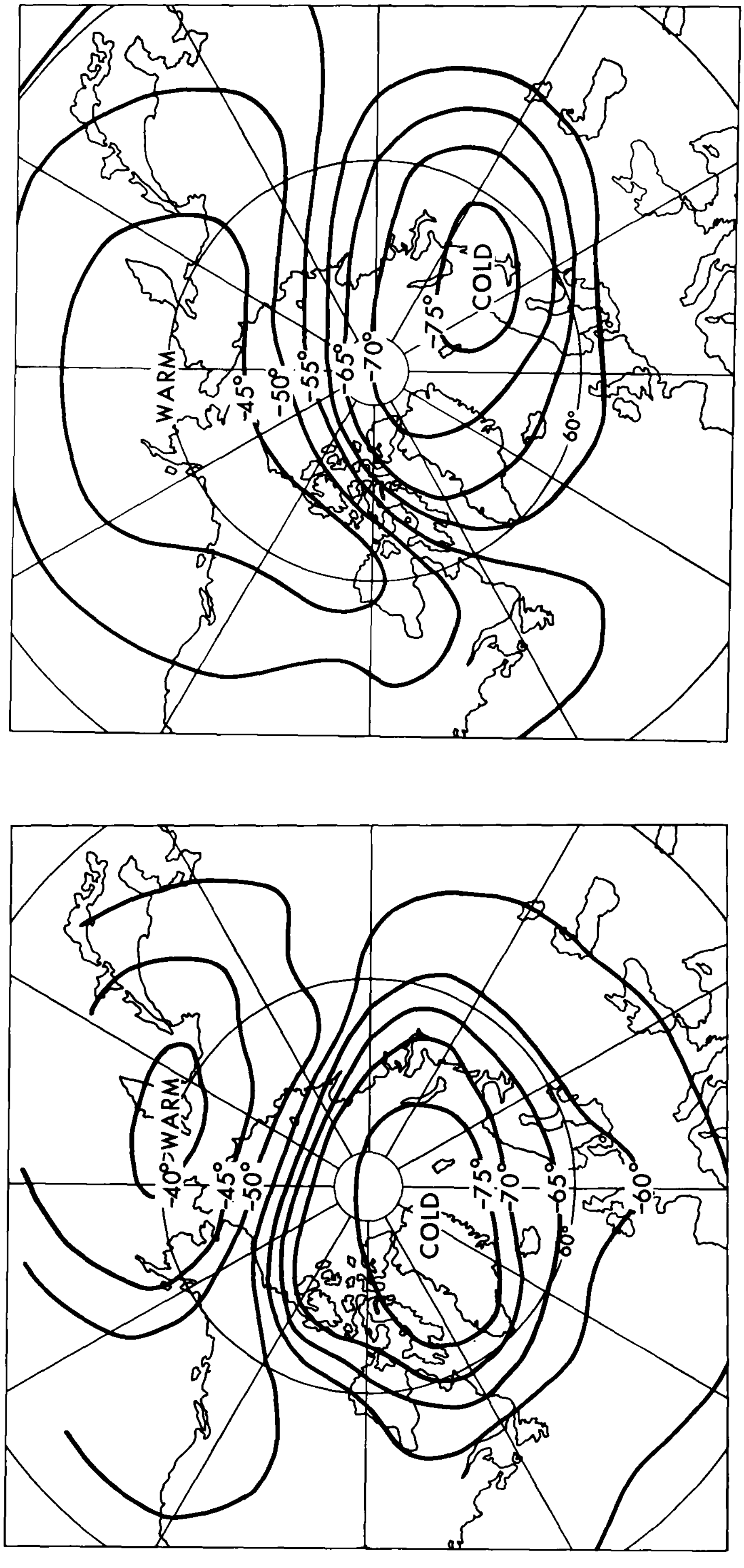

FIGURE 10. 30-MILLIBAR MEAN TEMPERATURES (DEGREES CELSIUS)
1–5 FEBRUARY 1964 26–29 FEBRUARY 1964

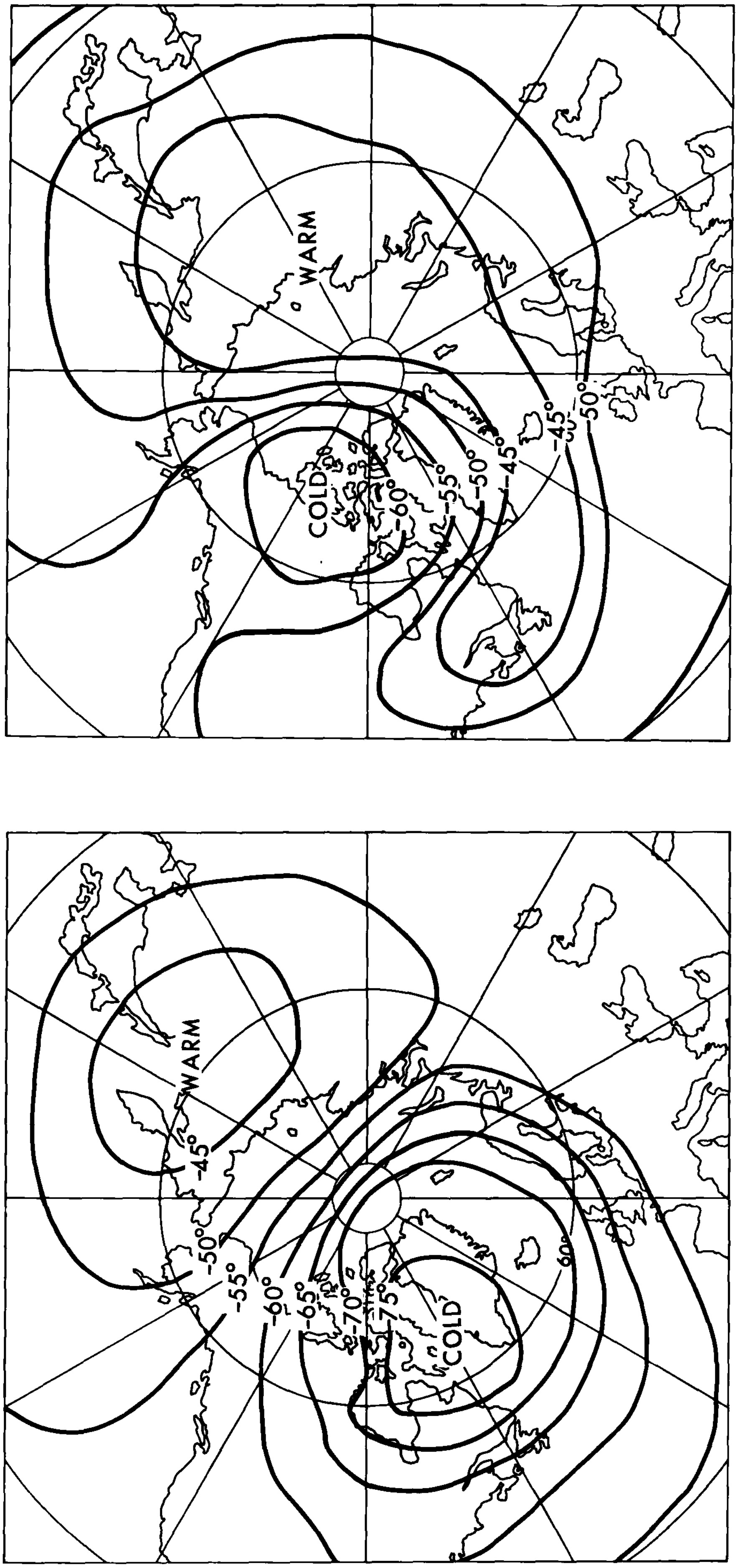

FIGURE 11. 30-MILLIBAR MEAN TEMPERATURES (DEGREES CELSIUS)
1–5 MARCH 1965 26–31 MARCH 1965

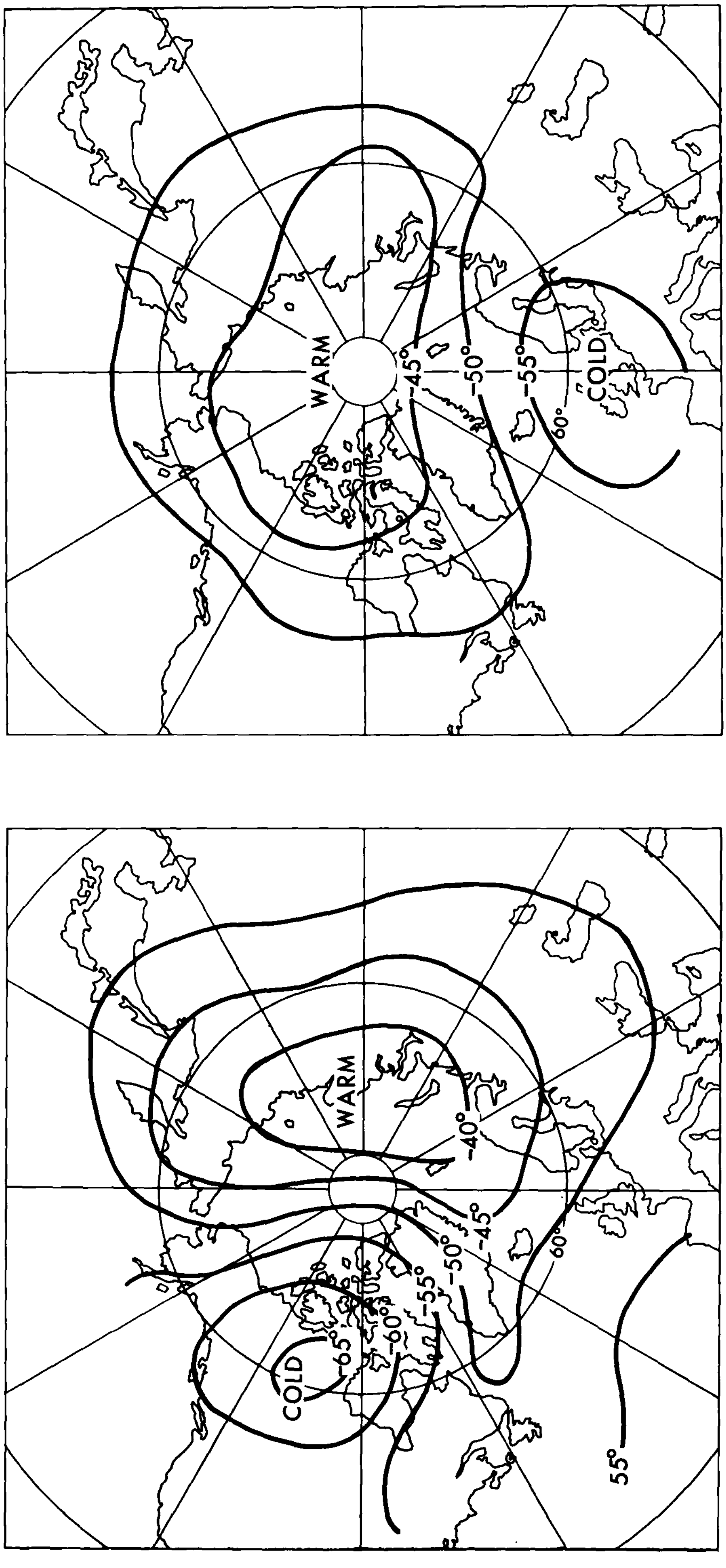

FIGURE 12. 30-MILLIBAR MEAN TEMPERATURES (DEGREES CELSIUS)
1–5 APRIL 1965 26–30 APRIL 1965

a warming of more than 50 deg over parts of northern Canada. The charts in Figure 10 show that in February 1964, over a large part of Canada, there was a warming of over 15 deg (more than 20 deg in some areas) whilst on the other side of the hemisphere, over Russia, there was a cooling of about 10 deg. In March 1965 (Figure 11) rises of 20 deg and above took place in high latitudes over a large area of the Canadian, Atlantic and European sectors with the maximum rise, of about 30 deg, centred near southern Greenland. Although sometimes in April variations of daily temperatures are small the mean charts for the first and last pentads in April 1965 (Figure 12) show that this is not always so. In that month the pentad means varied by as much as 15 deg in some places.

In considering the charts in Figures 9–12 it should be borne in mind that these are meaned over several days and so do not represent extreme values. The statistics for individual months for the three stations in Table II give an indication of the magnitude of the range of temperatures which occurs in high latitudes but over the area where stratospheric warmings are most pronounced (i.e. north Canada, Atlantic and European sectors) the absolute extremes of 30-mb temperature vary from several degrees colder than –80 °C to warmer than –30 °C in January, February and March.

Because of the very marked year-to-year differences in the date of the breakdown of the polar vortex and the manner in which the final warming occurs it must be emphasized that the monthly mean charts over high and some middle latitudes do vary quite considerably from one year to another during the winter/spring period and the chart for an individual month can be very different from the longer-period average. To illustrate this point charts for contrasting Januarys, Februarys, Marches and Aprils are shown in Figures 13, 14, 15 and 17.

In January 1963 (Figure 13a) no data were available for the area from 20 to 180°E in high latitudes but the data coverage over the remainder of the chart is sufficient to illustrate that a very marked warming took place over Canada. By the middle of the month there was an area over the Atlantic within which temperatures were as warm as those in the warm area which was centered over Kamchatka. This Atlantic warm area intensified and moved north-westwards to the north of Hudson Bay where 30-mb temperatures of about –20 °C were recorded for several days towards the end of the month. At the end of the month the coldest region was over the Gulf of Alaska. In January 1965 the coldest area was centred over the Greenland Sea and the warmest region was in the vicinity of Kamchatka. No major warming occurred and there were no very significant changes in the 30-mb isotherm pattern during the month. From these two charts it is clear that, in some areas, there can be differences of up to 20 deg between the monthly means for different Januarys. Comparing these two charts, this is so over Greenland and also in the Gulf of Alaska, whilst differences of up to 15 deg cover a wide area. The monthly mean chart for February 1965 (Figure 14a) shows a typical winter pattern with a cold area (colder than –75 °C) centred near Spitsbergen and a warm area (warmer than –45 °C) centred near Kamchatka with a strong thermal gradient between the pole and the Bering Strait region. On the chart for February 1958 (Figure 14b) the winter cold area has disappeared and in high latitudes temperature gradients are weak with the main warm area over north Siberia (–45 °C) and a secondary warm area (–50 °C) over north Canada. These two Februarys show differences of more than 20 deg in their monthly mean 30-mb temperatures over quite a large area.

In March 1960 (Figure 15a) the winter circulation continued to the end of the month and so the monthly mean chart shows a typical winter pattern. By contrast, the chart for March 1964 (Figure 15b) shows a warm area (warmer than −40 °C) extending from central Siberia across the Arctic Ocean towards northern Canada and so, over most high-latitude areas, this monthly mean pattern resembles the summer-temperature regime. These two March charts show differences of 20 to 30 deg in the monthly mean temperatures over quite a large area. The pentad mean maps for March 1964 are shown in Figures 16a–f as the sequence of events is particularly interesting in that it shows the marked warming of more than 30 deg which took place over the Russian arctic. The analysis over Russia is based on data supplied by the World Data Centre of the Institute of Aeroclimatology in Moscow.

The chart for April 1959, (Figure 17a) shows a typical summer pattern with a warm area (warmer than −45 °C) near the pole but in April 1963 (Figure 17b) temperatures over Canada were generally −55 to −60°C in association with a contour low cell which was centred north of Hudson Bay for much of the month. The year-to-year differences in April are not as large as in January to March but monthly mean temperatures on the two charts shown vary by more than 10 deg in some areas.

From the foregoing remarks it is apparent that in winter and spring much of the Arctic stratosphere is dominated by two very different thermal regimes. Consequently the temperature distributions in areas where this is so are not normal and there is a marked tendency for the distribution to be bimodal. The average monthly temperatures for the eight-year period being considered (or for any other period) cannot be regarded as representative of a single year and the standard deviations contain a large element of year-to-year variation. During the months of January to April, in those years when either the cold or the warm regime prevails, the variability about the monthly mean is relatively small (2 to 4 deg) but in months when a warming occurs the variability about the monthly mean increases to give a standard deviation of more than 15 deg in some Januarys and more than 7 deg in some Februarys.

After the final warming there is a rapid change from isotherm patterns typical of winter to those more representative of summer and in spite of the very large year-to-year differences in high latitudes during the months January to April these differences cease to be apparent during the summer months. The curves in Figures 18 and 19 showing the individual temperatures for Alert and Keflavik for three Julys illustrate the small variations from one July to another.

TABLE II – 30-MILLIBAR TEMPERATURES AT ALERT (82°30′N, 62°20′W), EUREKA (80°00′N, 85°56′W) AND FROBISHER (63°45′N, 68°33′W)
MONTHLY MEANS AND EXTREMES

YEAR		JANUARY					FEBRUARY					MARCH					APRIL				
		N	T_m	T_{max}	T_{min}	σ	N	T_m	T_{max}	T_{min}	σ	N	T_m	T_{max}	T_{min}	σ	N	T_m	T_{max}	T_{min}	σ
1958	Alert	25	-73.3	-38.6	-84.1	17.0	49	-50.3	-33.1	-59.1	5.8	55	-62.2	-49.3	-66.9	3.3	54	-56.5	-48.9	-61.9	2.9
	Eureka	39	-72.5	-39.9	-82.6	12.5	49	-51.7	-34.6	-58.1	5.0	54	-62.7	-57.1	-66.6	2.2	55	-56.3	-50.9	-60.3	2.7
	Frobisher	4	-70.2	-54.4	-76.3	8.7	8	-50.0	-38.9	-56.1	6.3	19	-60.0	-54.1	-63.0	2.1	16	-53.3	-48.9	-60.8	3.5
1959	Alert	12	-76.4	-67.5	-84.1	5.1	17	-74.9	-69.6	-79.8	2.3	51	-44.6	-33.0	-66.0	6.1	50	-43.3	-38.0	-46.2	2.0
	Eureka	11	-73.6	-61.6	-82.7	7.1	13	-69.3	-63.2	-75.1	3.7	56	-42.8	-34.1	-53.2	4.4	53	-44.2	-35.5	-46.9	2.6
	Frobisher	12	-75.3	-61.2	-82.2	5.6	19	-53.6	-39.3	-63.4	6.9	37	-46.1	-41.3	-53.8	2.4	28	-49.1	-46.4	-51.7	1.5
1960	Alert	50	-64.2	-50.1	-79.4	8.6	46	-68.8	-56.8	-77.1	7.0	42	-70.9	-46.7	-78.2	8.8	55	-41.8	-33.8	-49.4	4.1
	Eureka	21	-60.7	-48.3	-75.2	7.4	43	-65.5	-54.0	-77.4	7.3	43	-69.5	-43.9	-80.0	10.5	41	-48.0	-41.3	-55.7	3.8
	Frobisher	36	-65.6	-47.8	-74.6	8.2	36	-61.3	-54.3	-70.2	4.3	48	-59.8	-49.6	-73.9	6.8	43	-50.8	-41.7	-57.9	4.0
1961	Alert	41	-76.4	-52.8	-79.0	7.2	30	-73.7	-63.1	-79.6	3.7	49	-42.3	-28.0	-59.4	6.2	49	-48.4	-46.3	-50.9	1.1
	Eureka	48	-63.2	-50.5	-79.4	7.9	30	-68.6	-54.9	-77.2	7.1	59	-42.2	-28.8	-53.4	4.7	51	-48.5	-45.4	-50.8	1.2
	Frobisher	35	-58.5	-47.9	-72.8	7.1	37	-56.4	-45.7	-71.0	5.5	52	-46.7	-41.5	-52.6	2.5	47	-51.7	-48.0	-55.7	1.9
1962	Alert	7	-80.3	-75.2	-85.0	3.1	22	-66.1	-53.3	-75.8	6.2	44	-66.0	-57.8	-72.0	3.6	52	-55.8	-44.3	-64.8	6.1
	Eureka	53	-79.7	-75.3	-83.3	2.2	53	-61.2	-44.0	-72.4	7.6	59	-65.0	-55.1	-72.7	3.9	58	-55.2	-43.5	-63.4	6.0
	Frobisher	14	-72.2	-68.4	-78.7	2.9	43	-55.7	-31.4	-70.4	9.6	41	-60.2	-53.5	-66.6	3.6	53	-51.5	-44.8	-60.0	3.9
1963	Alert	4	-48.1	-38.8	-76.3	15.8	32	-50.5	-34.8	-57.9	7.0	40	-60.5	-56.9	-63.0	1.2 •	43	-54.5	-46.6	-62.1	4.7
	Eureka	48	-73 1	-32.6	-87.4	18.1	48	-50.8	-30.9	-59.8	7.9	52	-59.6	-55.5	-62.5	1.3	54	-55.4	-48.6	-61.1	5.7
	Frobisher	39	-59.8	-24.9	-80.6	20.5	44	-51.5	-41.3	-58.4	4.2	52	-57.6	-53.5	-62.3	2.0	52	-55.9	-47.9	-61.7	3.3
1964	Alert	1	-79.0				6	-75.9	-70.0	-78.8	3.1	47	-43.2	-28.4	-67.8	7.9	51	-45.5	-43.5	-47.5	0.8
	Eureka	26	-75.5	-67.9	-80.0	3.2	50	-72.6	-57.9	-77.7	5.0	50	-41.1	-30.9	-58.4	5.3	56	-45.9	-43.4	-48.1	1.0
	Frobisher	42	-72.2	-52.4	-80.0	7.2	46	-63.2	-47.6	-77.0	8.0	57	-43.4	-33.8	-53.8	4.0	54	-48.8	-43.8	-52.2	1.9
1965	Alert	52	-79.2	-74.7	-84.0	2.4	45	-75.0	-66.9	-79.7	3.0	55	-63.0	-36.0	-77.6	9.0	54	-46.6	-36.1	-61.3	6.8
	Eureka	50	-75.6	-67.0	-80.3	3.0	46	-72.4	-67.8	-77.4	2.2	55	-61.3	-38.9	-76.6	9.1	57	-47.2	-36.2	-60.6	7.0
	Frobisher	34	-70.1	-57.4	-78.0	5.6	20	-70.0	-55.6	-77.1	6.7	48	-57.9	-39.6	-78.9	9.2	52	-50.9	-44.0	-63.4	6.4

N is Number of observations.
T_m is monthly mean temperature (degrees Celsius).
T_{max} and T_{min} are highest and lowest recorded temperatures.
σ is standard deviation (degrees Celsius).

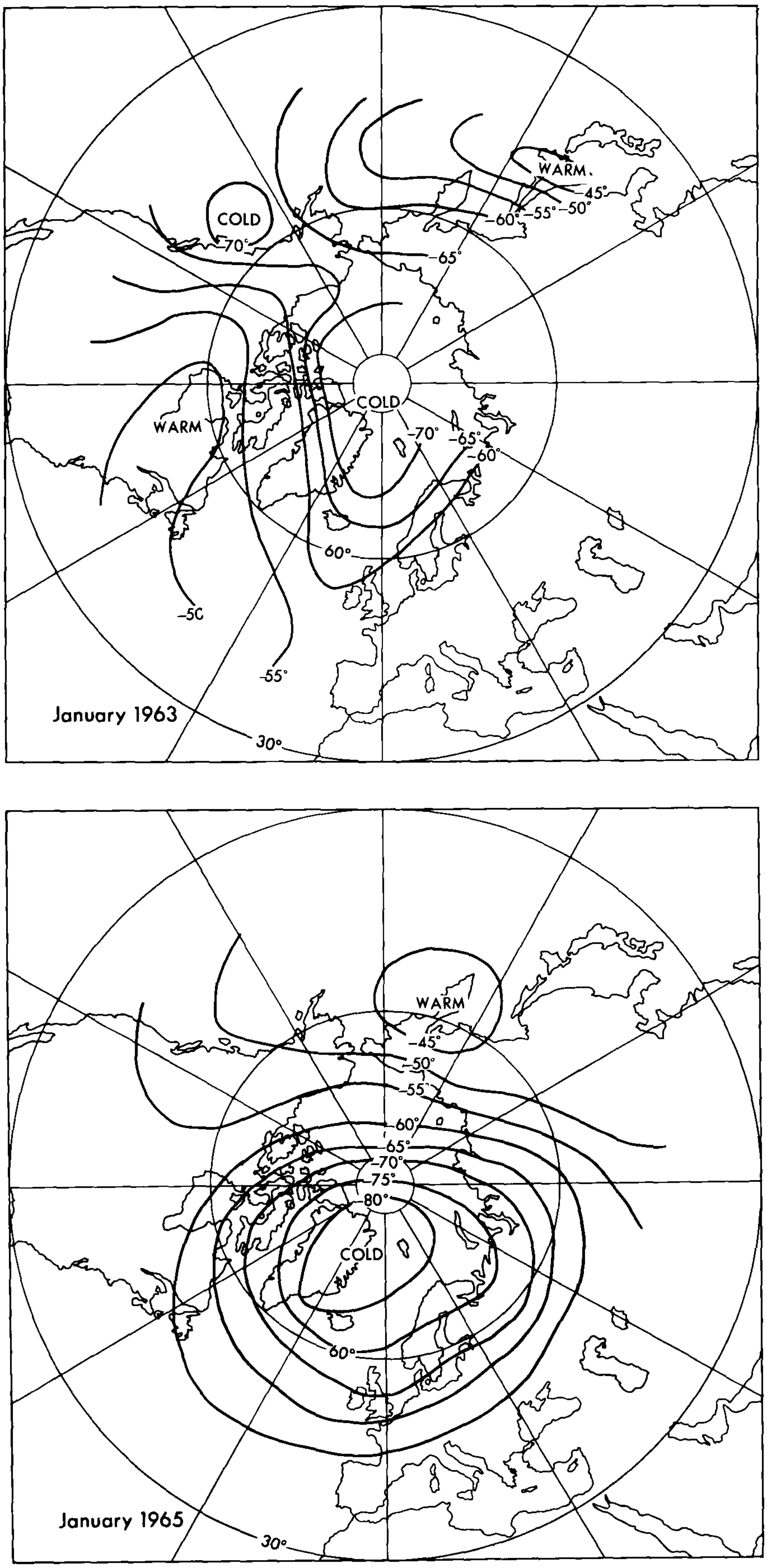

FIGURE 13. MONTHLY MEAN 30-MILLIBAR TEMPERATURES

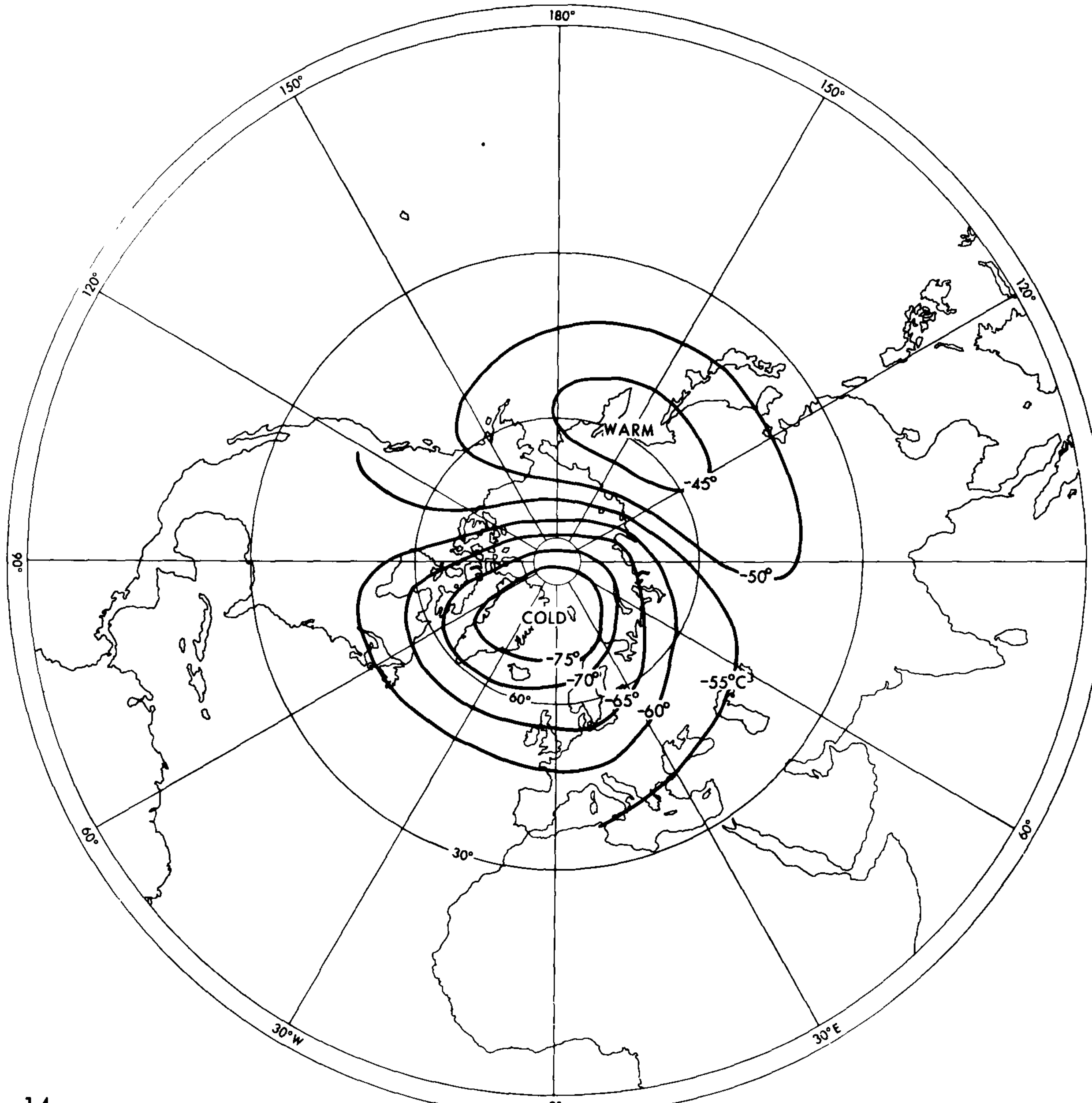

14a

FIGURES 14a AND 14b. MONTHLY MEAN 30-MILLIBAR TEMPERATURES FEBRUARY, 1965 (14a) AND 1958 (14b)

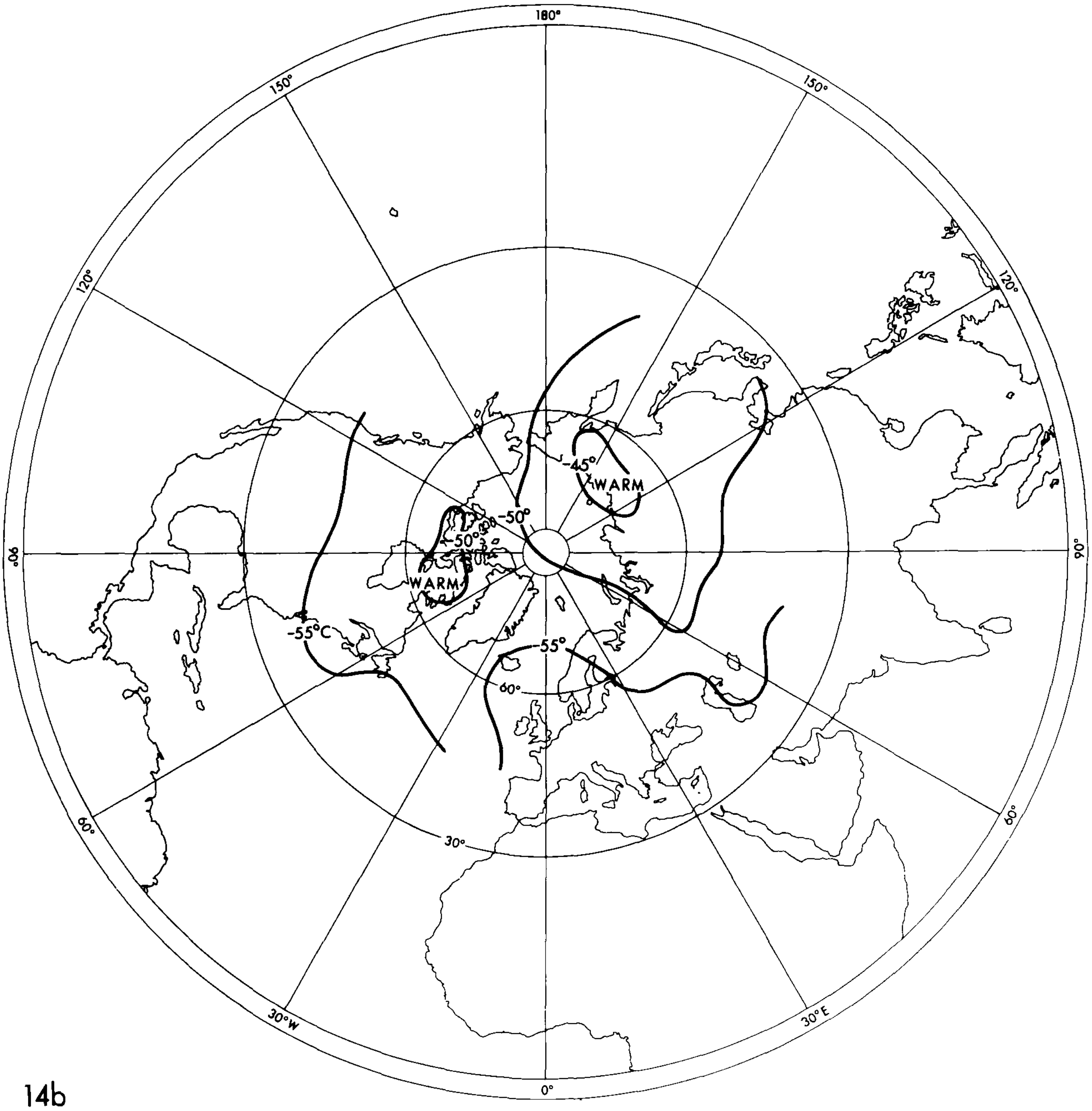
180°
150°
150°
120°
120°
90°
90°
60°
60°
30°W
30°E
0°
30°
60°
-45°
WARM
-50°
-50°
WARM
-55°C
-55°

14b

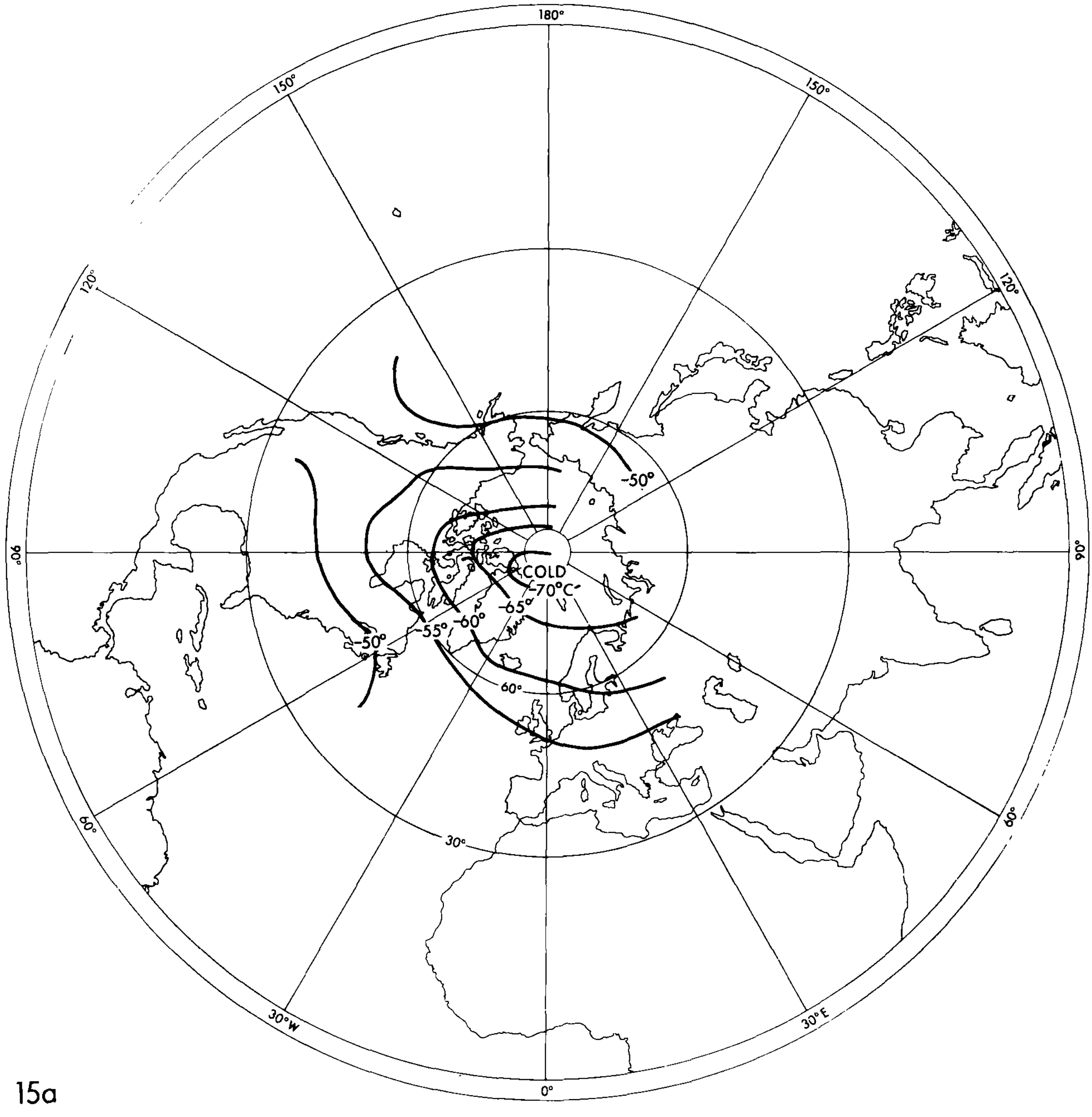

15a

FIGURES 15a AND 15b. MONTHLY MEAN 30-MILLIBAR TEMPERATURES MARCH 1960 (15a) AND 1964 (15b)

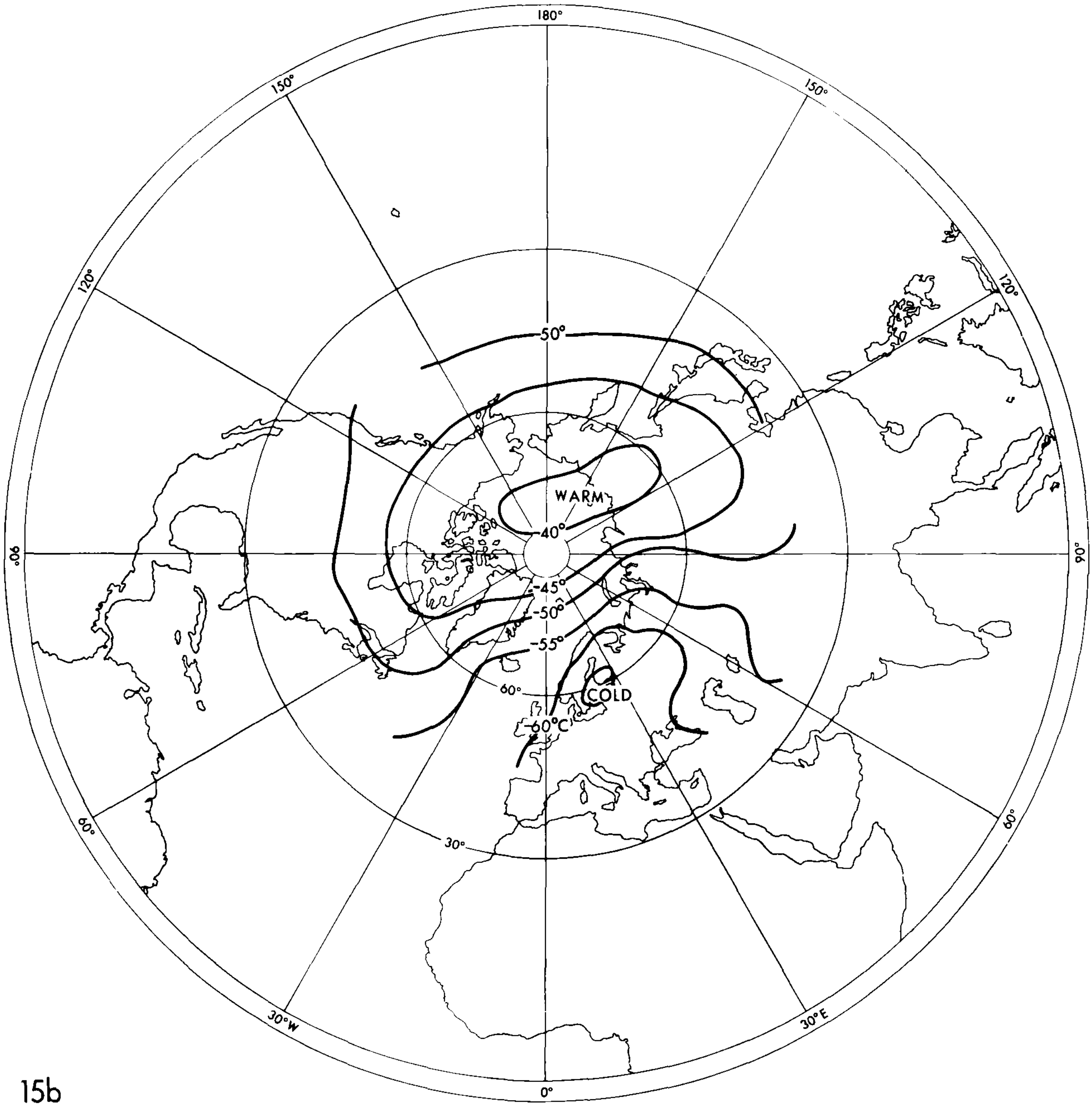
180°
150°
150°
120°
120°
90°
90°
60°
60°
30°W
30°E
0°
50°
WARM
40°
-45°
-50°
-55°
60°
COLD
-60°C
30°

15b

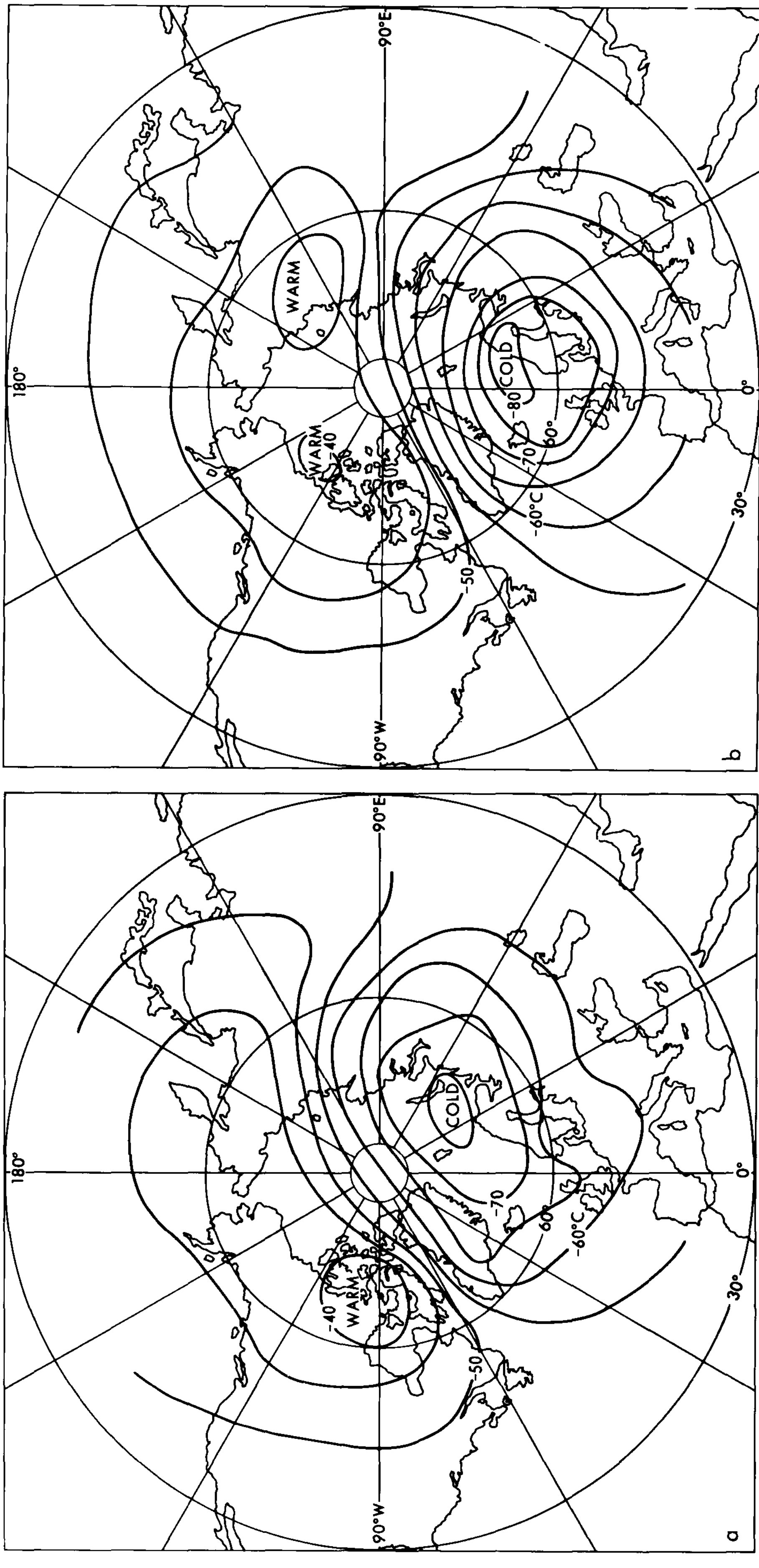

FIGURES 16a AND 16b. 30-MILLIBAR PENTAD MEAN TEMPERATURES

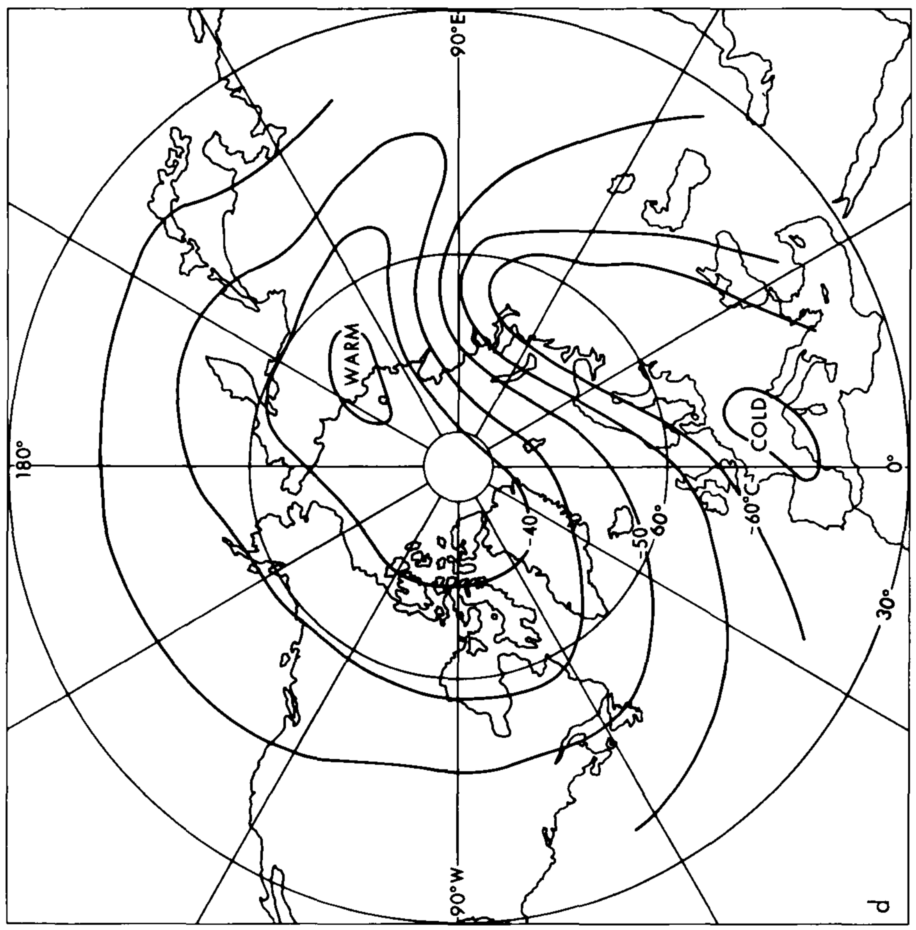

16—20 March 1964

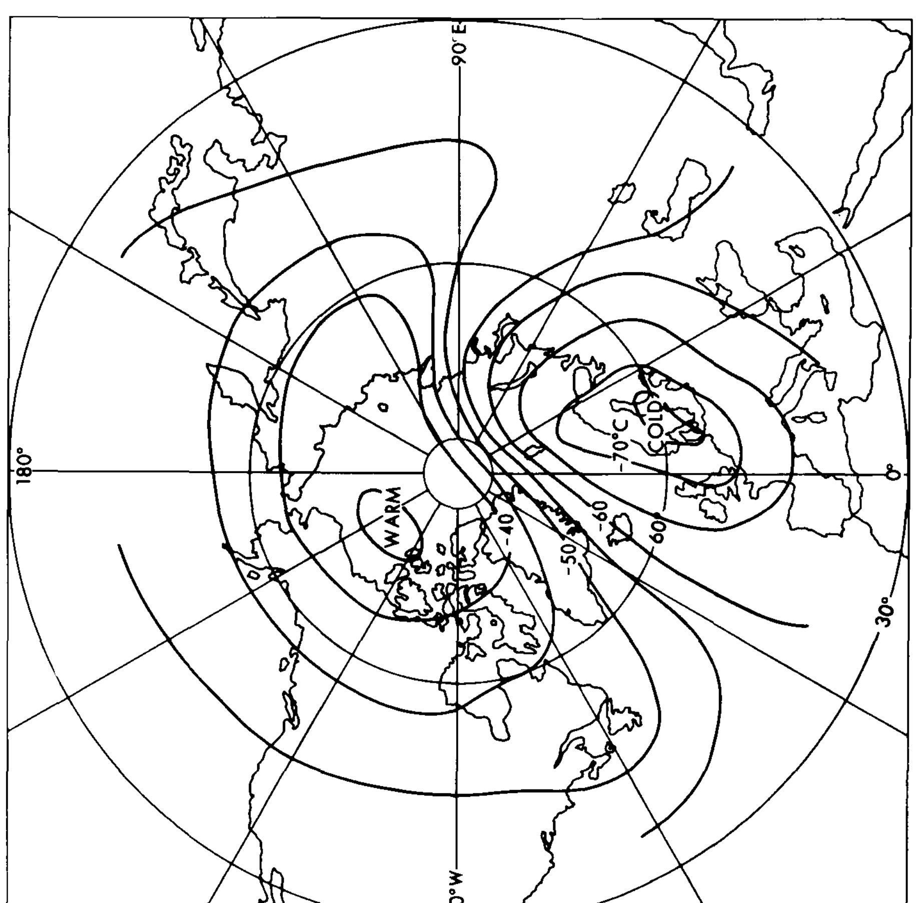

11—15 March 1964

FIGURES 16c AND 16d. 30-MILLIBAR PENTAD MEAN TEMPERATURES

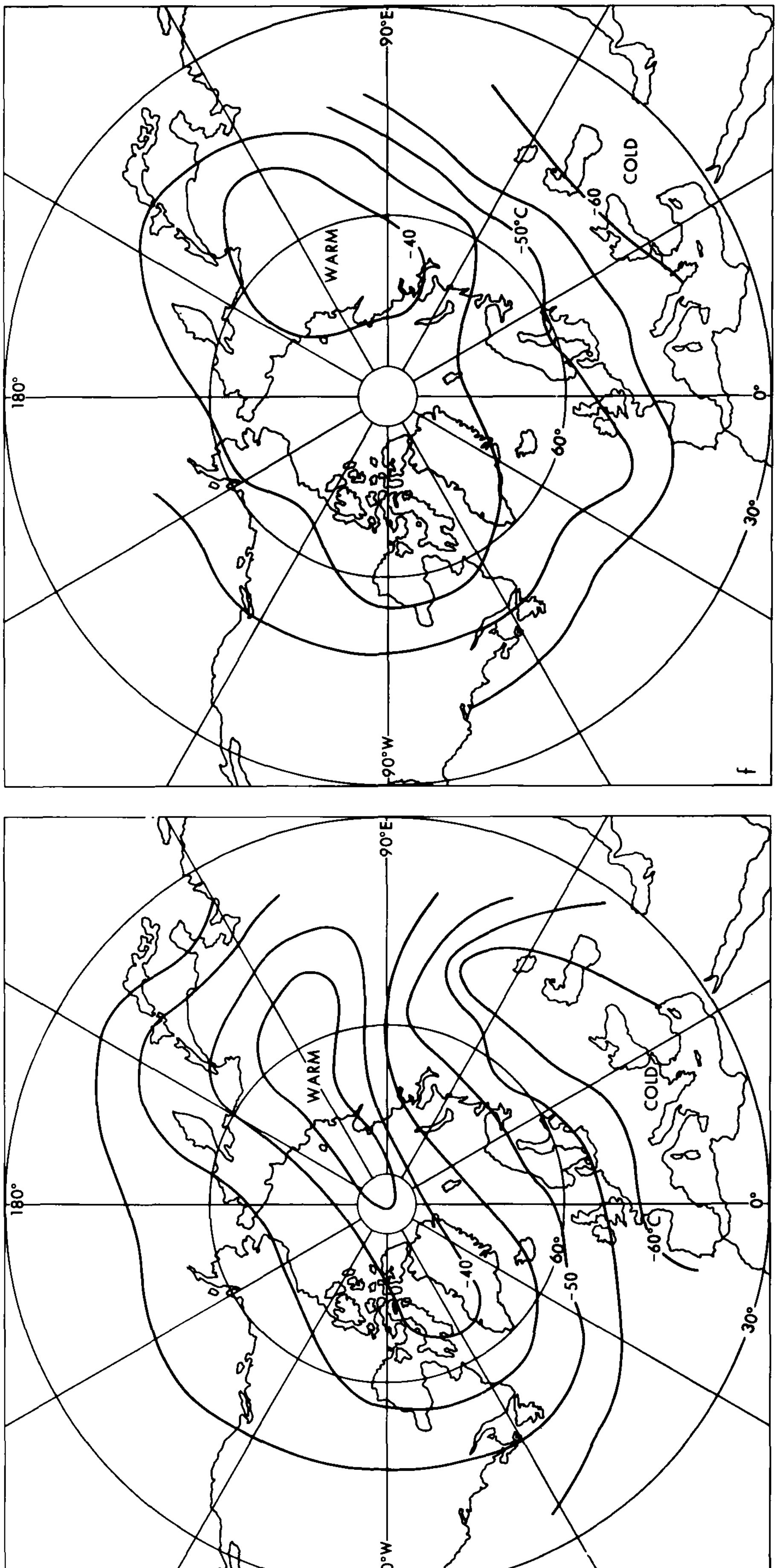

26—31 March 1964

21—25 March 1964

FIGURES 16e AND 16f. 30-MILLIBAR PENTAD MEAN TEMPERATURES

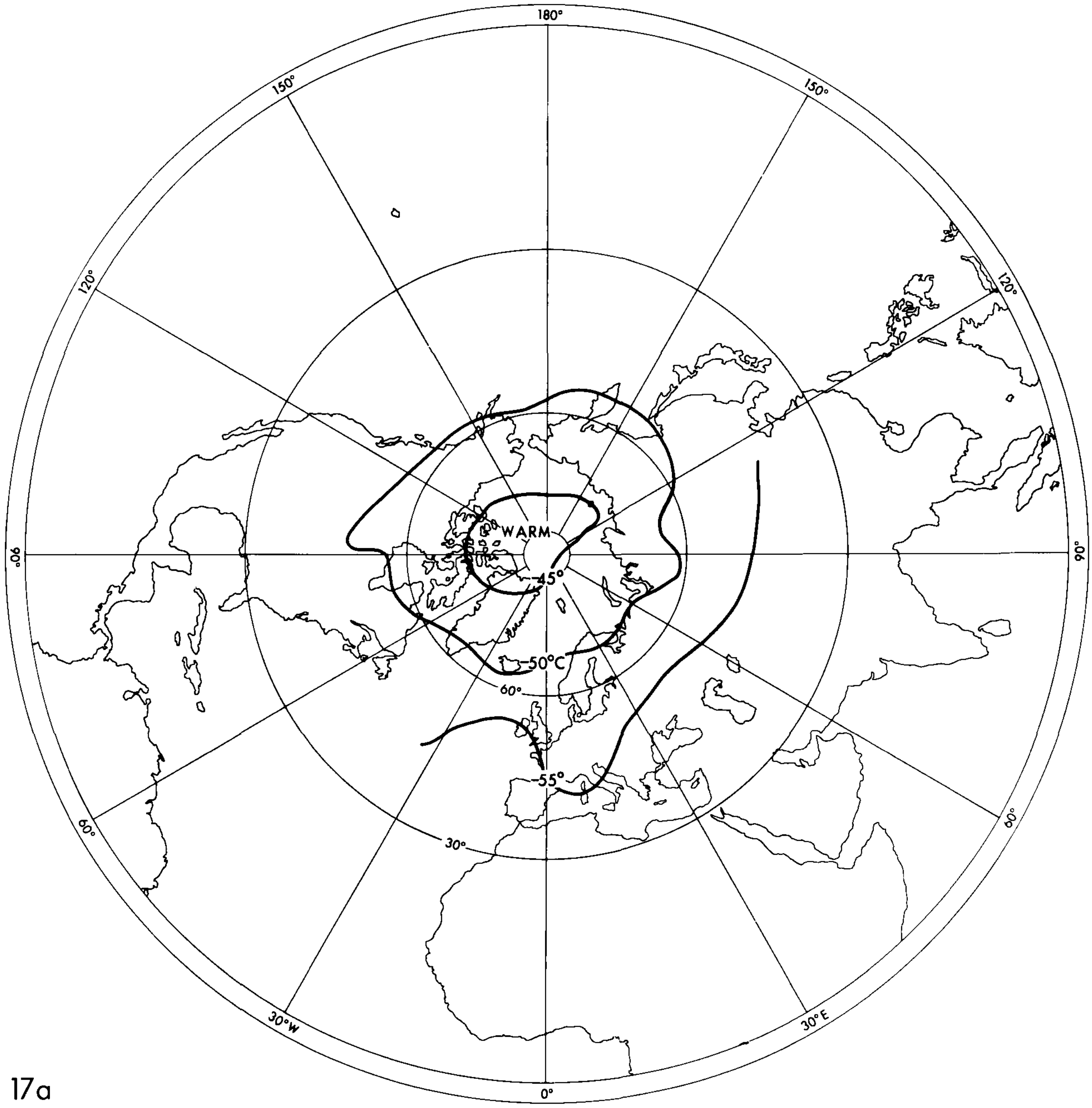

17a

FIGURES 17a AND 17b. MONTHLY MEAN 30-MILLIBAR TEMPERATURES APRIL, 1959 (17a) AND 1963 (17b)

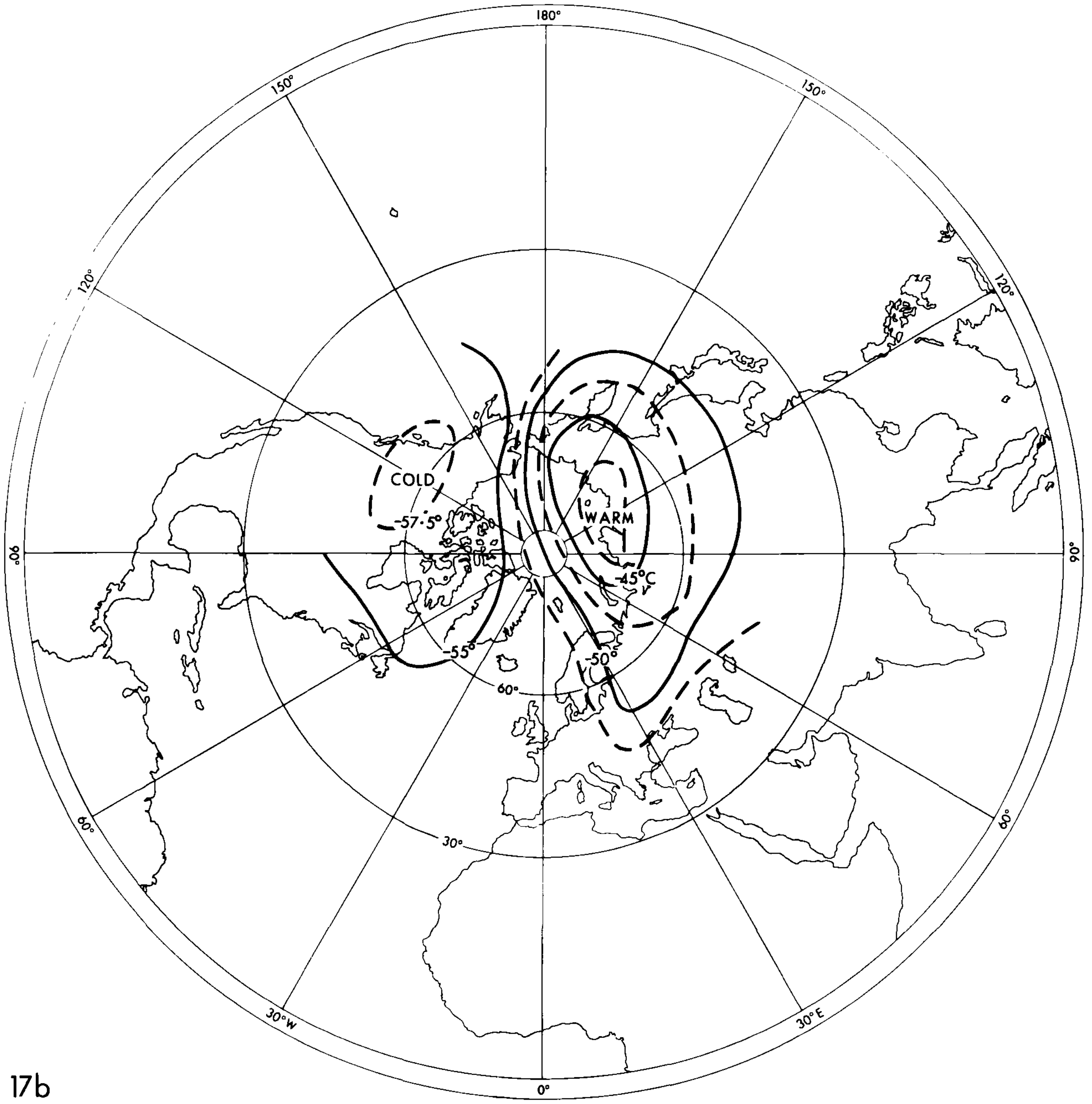
180°
150°
150°
120°
120°
90°
90°
60°
60°
30°W
30°E
0°
60°
30°
COLD
-57·5°
WARM
-45°C
-55°
-50°

17b

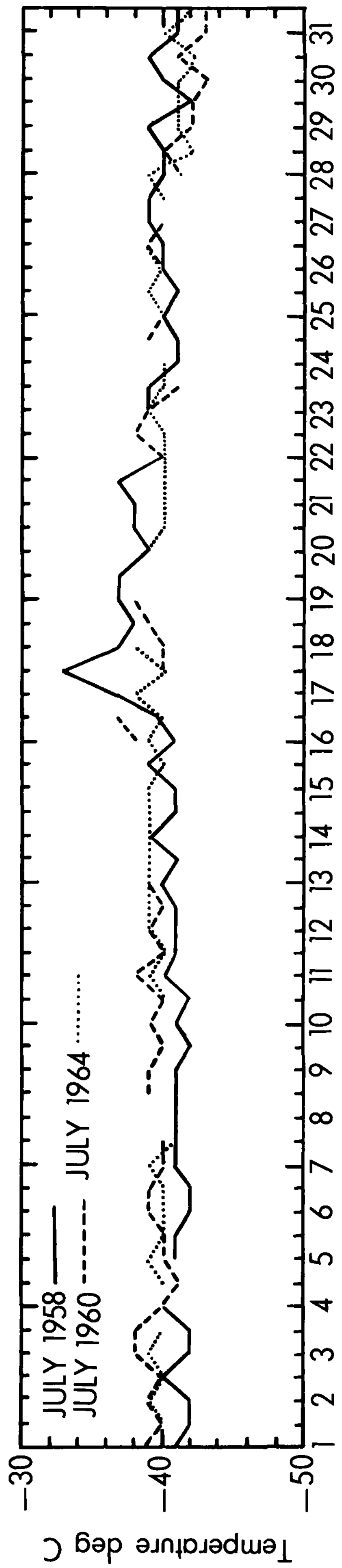

FIGURE 18. 30-MILLIBAR TEMPERATURES AT 0000 AND 1200 GMT, JULY, AT ALERT

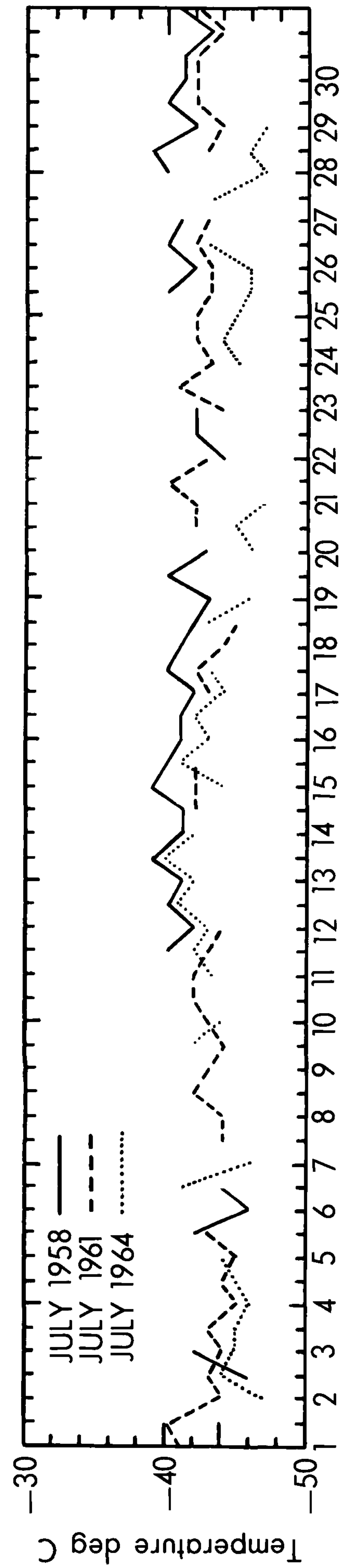

FIGURE 19. 30-MILLIBAR TEMPERATURES AT 0000 AND 1200 GMT, JULY, AT KEFLAVIK

PART II – AVERAGE CONTOUR HEIGHTS AT 30 MILLIBARS

The average contour charts for the 30-mb level are reproduced in Plates 13–18. As with the average temperatures the charts cover the northern hemisphere for the months of January, April, July and October but only from the pole to 45°N for February, March, August and September.

4 – DISCUSSION OF THE CHARTS

The average contour chart for January (Plate 13) shows the circumpolar vortex at this level to be well established and centred in the region of Spitsbergen. As at 50 mb there are two main troughs in the contour pattern – one over eastern Canada and the other over Siberia. Around the vortex there is a very strong westerly circulation which decreases towards the latitude of the higher contour heights. The highest values are recorded over the Pacific Ocean near 40°N and the high in that area is a well-marked feature of the January chart. The latitude of the belt of high contour heights varies somewhat with longitude being farthest north in the Pacific sector and farthest south (about 20°N) over central America. In lower latitudes gradients are small over large areas but there is a suggestion of lower average values across Africa and the Indian Ocean. The February chart (Plate 14a) shows the centre, with central values little changed, still situated in the Barents Sea and a strong westerly circulation around most of the hemisphere north of 45°N. The strongest gradients appear to be over the Arctic Ocean between the pole and the Bering Strait but farther south, over Alaska, gradients become weaker towards the North Pacific high. In March (Plate 14b) the vortex is still centred over the Barents Sea but it is less intense than on the February chart and the westerly circulation, although still quite strong, is considerably weaker than it is on the February chart. On the April chart (Plate 15) the contour pattern changes considerably. The main centre is probably situated over central Siberia with a trough to north east Canada and north Greenland but gradients in high latitudes are very much weaker than in January to March. In middle and low latitudes gradients are very weak with small high centres over Mexico and westwards into the Pacific and also to the south of Japan. In equatorial regions there is a decrease in the average heights.

From what has been said concerning the breakdown of the circumpolar vortex in the section on 'The final warming', it will be appreciated that in the period January to April there is appreciable year-to-year variation in the monthly mean position and intensity of the vortex and in the strength of the zonal circulation. In spite of these year-to-year differences the monthly mean charts for February and March usually show patterns fairly typical of winter but the individual April charts can vary between a well-defined winter type of circulation pattern and a pattern more closely resembling that of summer, with a high centred near the pole.

The July chart (Plate 16) shows the contour pattern typical of summer months. The polar high is well established with an easterly circulation around it and there is a gradual decrease of average heights towards the equator where the lowest heights are recorded. The average chart for August (Plate 17a) shows that, over high latitudes, the summer anticyclone is still the dominant feature although heights at the centre are about 200 metres lower than in July and the easterly gradient is somewhat weaker. By September, however, (Plate 17b) the pattern has changed considerably and there is a low vortex centred close to the pole with a high centred south of the Aleutians. The vortex increases in intensity and by October (Plate 18) the heights at the centre are below 23.2 km and the circulation has acquired the main features of the mid-winter circulation.

PART III – AVERAGE WINDS AT 30 MILLIBARS AND THEIR VARIABILITY

5 – GENERAL

The charts in this section consist of streamlines and isotachs (Plates 19–24), zonal wind components (Plates 25–30), meridional wind components (Plates 31–36) and standard deviations of the zonal and meridional components (Plates 37–42 and 43–48 respectively). Wind data were extracted and processed for nearly all available stations in the northern hemisphere and the streamline–isotach charts were constructed from the average winds.

The charts for the mid-season months have been analysed to the equator but, as is well known, the dominant feature in the equatorial lower stratosphere is the quasi-biennial oscillation (QBO) in the zonal wind component and some aspects of this phenomena are included in a separate section later in the text. It is apparent that, in areas where the QBO is the dominant feature, the wind distribution is not circular about the long-period average wind for a particular month. The problem of describing wind distributions in the stratosphere (at the 50-mb level) was dealt with in some detail in *Geophysical Memoirs* No. 112 and it was suggested that an acceptable solution was to regard the distribution as elliptical rather than circular. During the course of this work on the 30-mb level more has been done on the study of elliptical wind distributions and the results are included later in the text.

The charts for February and March and for August and September are included in order to describe the reorganization of the stratospheric flow patterns in spring and autumn. The way in which this particular aspect of the circulation affects the British Isles is described later in the two sections on the spring and the autumn reversals of 30-mb winds over Scotland.

6 – DISCUSSION OF THE CHARTS

On the streamline–isotach chart for January (Plate 19) the main feature is the westerly flow which covers most of the hemisphere north of about 20°N (over the North Pacific the latitude of the boundary of the westerly flow is north of this). These westerlies reach a maximum in the polar-night stratospheric jet with wind speeds exceeding 60 kn in a belt from southern Greenland to Scandinavia, thence across Russia and central Siberia to the Arctic Ocean and the North-west Territories of Canada. Within this belt of strong westerly winds the maxima appear to be situated near Iceland (greater than 70 kn), just east of the southern part of the Ural Mountains (greater than 70 kn) and over the East Siberian Sea where the average speed may exceed 100 kn. To the south of the polar-night jet there is a decrease to average speeds of less than 10 kn in low latitudes. In tropical and equatorial regions the winds at this level are dominated by the QBO in the zonal wind component and these areas will be referred to again later in the text.

The February chart (Plate 20a) shows a continuance of the strong westerly flow, over most middle- and high-latitude areas of the hemisphere, around the vortex which is centred in the Barents Sea. The zone of maximum wind speed is very close to that on the January chart but the strongest winds appear to be about 70 kn which represents a decrease from the maximum values of greater than 100 kn over the East Siberian Sea in January. The chart for March (Plate 20b) shows the average wind direction to be still westerly over middle and high latitudes and, although the maximum speeds still occur in similar areas to those on the charts for January and February, the average speeds are lower. The April chart (Plate 21) shows very marked changes from the preceding three months over middle and high latitudes with a considerable decrease in the average speeds. It has already been mentioned in the previous section that in some Aprils the circulation pattern can be typical of winter and in other Aprils there can be a high centred near the pole with a circulation pattern which more closely resembles that of a typical summer chart with a light easterly flow over higher latitudes. Clearly the time at which the hemispheric circulation changes to easterly is dependent upon the date, and the manner, of the final warming. In order to illustrate how the spring reversal varies from year to year over Scotland the 30-mb data for Leuchars/Shanwell have been analysed in some detail and they are discussed later.

Plate 21 shows that, in April, over a large part of the hemisphere the average wind speeds are less than 10 kn. There is an increase to 10 to 15 kn easterly, south of about latitude 20°N, but in equatorial regions the QBO is the dominant feature.

The average wind chart for July (Plate 22) shows a reversal of the predominantly westerly flow and the disappearance of the winter vortex. From the pole to low latitudes the wind directions are easterly. Over the Arctic the average speeds are very light but there is an increase to speeds of greater than 40 kn in a band which extends around most of the hemisphere between 15 and 25°N. South of this band of strong easterlies the average wind speeds decrease towards lower latitudes.

Over middle and high latitudes the average easterly circulation in August (Plate 23a) is weaker than that in July – being less than 10 kn over most areas north of about 45°N. The almost uniform easterly flow increases to 20 kn between 35 and 40°N. By September (Plate 23b) although average speeds in high latitudes are still less than 10 kn, the pattern shows a reversal of the predominantly easterly flow of July and August. Over an extensive area the average wind speeds increase to more than 10 kn and the mainly westerly flow exceeds 15 kn in a band from north of the Caspian Sea to north-east Siberia and into Alaska. South of this zone of stronger westerlies the average speeds decrease to a minimum (of less than 5 kn) with a reversal to light easterlies near 40°N around the whole hemisphere. The October chart (Plate 24) shows an increase in both the strength and geographical extent of the high-latitude westerly flow. In a band from north-east of the Caspian Sea to north-east Siberia and into northern Canada the average wind speeds exceed 30 kn and the westerly flow extends southwards to about 35°N before reversing to the lower-latitude easterly flow. This easterly flow increases to a maximum south of 20°N and the average chart then shows a decrease towards the equator. Although the chart has been analysed to the equator the presentation and interpretation of the relevant statistics is complicated by the QBO in equatorial stratospheric winds.

The hemispheric distribution of the average zonal wind components is shown in Plates 25–30. The main feature on the January chart (Plate 25) is the broad belt of westerly winds in middle and high latitudes with maxima of 70 kn near Iceland and over the Arctic Ocean near north-east Siberia. The westerly component decreases towards lower latitudes and in the tropics there is a definite easterly flow with average speeds in excess of 10 kn over the east Pacific and the Caribbean Sea. The February chart (Plate 26a) shows the pattern to be very similar to that of January and the main feature is still the belt of strong westerlies with maxima of greater than 60 kn centred north of Iceland, across Russia to 90°E (between 55 and 60°N) and also over the Laptev, East Siberian and Beaufort Seas. The westerly component decreases towards lower latitudes and over the North Pacific and eastern USA (in the region of the Aleutian high) the average zonal component is light easterly. A somewhat similar pattern continues on the March chart (Plate 26b) but the average zonal flow is much weaker with maxima of about 30 kn. The April chart (Plate 27) represents conditions at the time of year when the zonal flow over middle and high latitudes is changing from the westerlies of winter to the light easterlies of summer. Over much of the hemisphere the average zonal component is less than 10 kn and, in many areas, less than 5 kn In lower latitudes there is a definite easterly flow of greater than 10 kn. The July chart (Plate 28) shows that the average zonal component is easterly over the whole hemisphere. In high latitudes these easterlies are less than 10 kn but they increase in strength towards 20°N where the axis of the belt of the strongest easterlies is situated. The analysis suggests that within much of this belt around the hemisphere the average zonal wind component exceeds 40 kn. To the south of this easterly jet there is a decrease in strength but the available data indicate that, in spite of the QBO, the average zonal component near the equator is easterly. The August chart (Plate 29a) shows the average zonal component to be easterly over middle and high latitudes. Over most of the area north of about 55°N these easterlies are very light indeed and the average speeds of less than 5 kn are less than the July values. The average speed increases in lower latitudes but at about 45°N it is still only 10 kn. The September chart (Plate 29b) shows the reversal of the average zonal component over high latitudes from the very light easterlies of August to a well-established westerly regime. By October (Plate 30) the strongest westerly flow is still over Russia and the Canadian arctic where average speeds exceed 30 kn. The seasonal increase from September to October is such that average speeds reach 20 kn or more over most of Russia north of about 40°N. The westerly component decreases towards lower latitudes and south of about 30 to 35°N there is a definite easterly flow which reaches a maximum between 10 and 20°N. From east Africa to India to south-east Asia and the western Pacific the average zonal component exceeds 20 kn. It is interesting to note that the average October chart shows that, in high latitudes, the zonal circulation bears some similarity to the mid-winter pattern (Plate 25) whereas in low latitudes there is more similarity to the mid-summer pattern (Plate 28).

The average meridional components are shown in Plates 31–36. In January (Plate 31) with the strong flow around the vortex centred near Spitsbergen, the average meridional-component pattern is very pronounced over high latitudes. This is particularly so over central and east Siberia, Alaska, the north of Canada and much of the Arctic Ocean. In this area the values vary from +60 kn (a southerly component) over the Laptev and East Siberian seas to –40 kn (a northerly component) over the islands in the Canadian Arctic. The meridional components are much weaker than this over the Atlantic/European sector. In low-latitude areas the components are very much weaker, being often of the order of 1 kn. When observational and analytical errors are considered and also allowing for the fact that over large areas in low latitudes there are very few reporting stations, then it is apparent that in some places in the tropics it is not possible to determine the direction of the average meridional component with any degree of accuracy. In February (Plate 32a) the meridional flow pattern is still very pronounced with strong northerly components over north-east Canada and strong southerly components over Siberia, although these southerlies appear to be appreciably weaker than in January. The March chart (Plate 32b) shows a continuation of the basic winter meridional circulation pattern but with a general decrease in intensity. This decrease in average speeds continues and on the April chart (Plate 33) average meridional components of greater than 10 kn are restricted to small areas over north Canada (northerly) and Siberia (southerly). Over the remainder of the hemisphere the meridional components are comparatively light and in many areas, particularly in lower latitudes, they are less than 2 or 3 kn.

In July (Plate 34) the average meridional components are weak over the whole hemisphere being everywhere less than 5 kn. In August (Plate 35a) at many stations the average value is less than 1 kn and at only a few stations does it exceed 2 kn. In September (Plate 35b) the average value is generally less than 5 kn and only exceeds this in very limited areas. On the October chart (Plate 36) average meridional components of greater than 10 kn are restricted to north-east Siberia (southerly) and north-west Russia (northerly). Over the remainder of the hemisphere the meridional components are generally light and often less than 2 kn especially in lower latitudes. In all these months it is difficult to determine the zero isopleth with either confidence or precision over some parts of the hemisphere because of the very small average values involved.

The variability of the average wind is described by means of the charts of the standard deviation of the zonal and meridional components in Plates 37–48. It is envisaged that the main practical use of these charts will be the estimation of standard deviations for the construction of theoretical distribution ellipses for various positions on the charts and consequently the following remarks are confined to drawing attention to the principal features.

In January the standard deviation of the zonal wind component (Plate 37) exceeds 20 kn over most middle and high latitudes where the zonal component is strong (see Plate 25). The maximum variability (greater than 40 kn) appears to occur in an area across northern Canada and also near 60°N over parts of Sweden, Finland and west Russia. The lowest values (less than 10 kn) are found over the Pacific in the region of the light winds associated with the high area on the average contour chart (Plate 13). There is a zone around the hemisphere – the axis of which is practically coincident with the boundary between the higher-latitude westerlies and the lower-latitude easterlies – where the standard deviation is between 10 and 20 kn. South of this zone the variability increases but, near the equator, much of this increase is due to the easterly and westerly regimes of the QBO having been combined in obtaining the statistics for the eight-year period. The February chart (Plate 38a) shows that the variability of the zonal component is still high (standard deviation greater than 40 kn) in the region of the strongest winds and that the pattern is broadly similar to that of January. In March (Plate 38b) the standard deviation is still greater than 20 kn over most of the hemisphere north of 45°N but the region in which it is greater than 40 kn is confined to parts of Scandinavia. Although we know that in April the average zonal wind components in higher latitudes are not particularly strong (see Plate 21), we see from Plate 39 that the variability is quite high with a large area within which the standard deviation exceeds 20 kn. From the remarks made earlier this is to be expected as we know that April is a month when, over many middle- and high-latitude areas, the zonal component can vary between quite strong westerly and a light to moderate easterly. Around the hemisphere, near 30°N, the variability is at a minimum with values of less than 10 kn in some places but towards the equator values increase again. In July (Plate 40) the standard deviation of the zonal component is less than 10 kn over a large part of the hemisphere and is less than 5 kn near the pole. The increase to 10–20 kn occurs at about the latitude of the belt of strong easterlies on the average zonal component chart. The data suggest that variability is at a maximum near the equator but the spurious nature of the standard deviation there has already been mentioned. In August (Plate 41a) variability of the zonal component is at a minimum (less than 5 kn) over north Greenland whilst over North America, the Atlantic, Europe and the Arctic the standard deviation of the zonal component is within the range 5–10 kn. Variability is highest (greater than 15 kn) in the region to the north and west of the Caspian and Aral Seas and also over north-east China and south-east

Siberia. The pattern of standard deviation of the zonal component in September (Plate 41b) is broadly similar to the August pattern. In October, (Plate 42) the variability exceeds 15 kn over the Canadian Arctic and also over Asia north of about 50°N. The variability is at a minimum (less than 10 kn) in a zone around the hemisphere between approximately 20 and 40°N and this zone is more or less coincident with the contour-height high in Plate 18. Towards lower latitudes the variability increases.

The standard deviation of the meridional component in January (Plate 43), like that of the zonal component, is large over middle and high latitudes. The maximum variability appears to occur north of Hudson Bay where values are in excess of 50 kn, which is larger than the maximum values on the chart of standard deviation of the zonal component in January. Values in excess of 40 kn are recorded over parts of north-east Canada and also over a considerable area of the Arctic Ocean. The variability decreases towards lower latitudes and south of about 30°N the standard deviation is generally 5–10 kn. The standard deviations of the meridional components in February and March (Plates 44a and 44b) show that variability is highest over the Arctic (greater than 40 kn) and decreases towards lower latitudes. In general terms this is a continuation of the January pattern.

In April (Plate 45) the standard deviation is greater than 10 kn over many areas north of about 50°N and values reach a maximum of more than 20 kn over the Arctic. Over the remainder of the hemisphere, where average meridional components are very small, the standard deviation is in the range 5–10 kn. In July (Plate 46), over much of the hemisphere, the standard deviation is in the range 5–10 kn but it is less than 5 kn over much of North America, Greenland and western Europe and also over Japan. Over middle and high latitudes the standard deviation of the meridional component in August (Plate 47a) ranges between a little below 5 kn to a little over 10 kn and the overall pattern bears some resemblance to that for July. In September (Plate 47b) there is a slight increase in the variability, particularly over Canada, but the standard deviation is still in the range 5–10 kn over most areas. By October (Plate 48) over middle and high latitudes the standard deviation is generally greater than 10 kn and values reach a maximum of greater than 15 kn over the Arctic. In lower latitudes, where average meridional components are light, the standard deviation is in the range 5–10 kn. The chart for October is very similar to that for April.

7 – ELLIPTICAL DISTRIBUTION OF THE WINDS

In *Geophysical Memoirs* No. 112 it was shown that, at the 50-mb level over large parts of the hemisphere and in some seasons the observed wind distributions are not circular and that they are more adequately described by a series of ellipses. The wind distributions at the 30-mb level for over 50 stations were examined in some detail and were tested for circularity and ellipticity by means of the chi-square test. The average wind was subtracted from the individual winds and the test was applied to the distribution of these departures from average. The 30, 60 and 90 per cent probability circles were obtained by using radii appropriate to the normal circular distribution, i.e. 0.59, 0.96 and 1.52 times the standard vector deviation. The tests for ellipticity were made in two ways – in one case the axes were assumed to lie east–west and north–south and in the other case the angle of rotation of the true major axis was calculated for each set of data and these axes were then used for constructing the theoretical ellipses. The angle of rotation

(ψ), i.e. the angle between the assumed major axis and the true major axis was obtained from the expression

$$\tan 2\psi = \frac{2 r_{uv}\, \sigma_u\, \sigma_v}{\sigma_u^2 - \sigma_v^2}$$

where r_{uv} is the correlation coefficient between the zonal and meridional components, σ_u and σ_v the standard deviations of the zonal and meridional components.

The lengths of the semi-axes of the 30, 60 and 90 per cent probability ellipses were obtained by multiplying the standard deviations of the components by 0.84, 1.36 and 2.15.

The winds were assigned to four different ranges, each representing a quarter of the area of the circle or ellipse. For the circle the four boundaries were 045°, 135°, 225° and 315° and for the ellipse 270° and 090°

$$\pm \tan^{-1} \frac{\text{semi minor axis}}{\text{semi major axis}} .$$

In both the circularity and ellipticity tests the chi-square value for the one per cent significance level with three degrees of freedom has been used as the critical value and occasions in excess of this (i.e. greater than 11.3, indicating significant non-ellipticity or non-circularity) are summarized in Table III. In interpreting this summary of the results it should be borne in mind that the user is often interested in the distribution of large departures from average (the 60–90 per cent part of the distribution) rather than the distribution of winds which are near average (the 0–30 per cent part), also that in July, over much of the hemisphere except lower latitudes, wind speeds are very light and variability is at a minimum. Therefore, in July at many stations, and in the 0–30 per cent range for other months at some stations, winds are often so close to the average that very small variations in speed or direction result in large changes in the chi-square values. Line 10 of Table III shows that at the 60–90 per cent range there can be little doubt that the distribution is not circular. Of the 55 distributions tested, in January 47 could be said to be significantly non-circular, in April 54, in July 39 and in October 46.

The detailed statistics in Appendix 1 indicate that for those stations which had a chi-square value of less than 11.3 for the circularity test then, in almost all cases, the chi-square values for the ellipticity tests were also small.

If the chi-square values are considered in latitude bands (as arranged in Table III) it is clear that, in general, the theoretical elliptical distribution provides a much better estimate of the observed distribution than the theoretical circular distribution. Exceptions to this are confined mainly to the 0–30 per cent range of the distribution: between 20 and 35°N in January, north of 20°N in April, over the whole hemisphere in July and between 20 and 35°N in October. It should be noted that, for the larger departures from average (the 60–90 per cent range) a significant improvement is sometimes obtained by using the true major and minor axes (Column C of Table III) rather than assuming these axes to be east–west and north–south (Column B). This is particularly so when considering the larger departures from average for regions north of 20°N in

TABLE III – NUMBER OF OCCASIONS WITH CHI-SQUARE VALUE GREATER THAN 11.3

	Probability bands per cent	January A	January B	January C	April A	April B	April C	July A	July B	July C	October A	October B	October C
						South of 20°N 13 stations							
1	60–90	13	6	5	13	5	3	12	2	2	13	7	9
2	30–60	13	5	4	12	3	1	11	10	6	13	7	6
3	0–30	8	2	2	12	4	7	6	6	5	10	5	4
						20°N – 35°N 13 stations							
4	60–90	13	6	2	13	4	4	10	6	6	13	1	1
5	30–60	12	5	5	10	2	2	7	2	4	11	2	0
6	0–30	11	10	9	10	8	6	8	8	9	5	5	4
						North of 35°N 29 stations							
7	60–90	21	14	6	28	12	14	17	12	12	20	9	5
8	30–60	18	11	12	25	17	10	8	5	5	18	14	8
9	0–30	20	14	13	25	23	25	16	17	14	18	13	10
						All 55 stations							
10	60–90	47	26	13	54	21	21	39	20	20	46	17	15
11	30–60	43	21	21	47	22	13	26	17	15	42	23	14
12	0–30	39	26	24	47	35	38	30	31	28	33	23	18

Col. *A* – Circularity test.

Col. *B* – Ellipticity test assuming major axis of ellipse to be along east/west or north/south axes.

Col. *C* – Ellipticity test using true major and minor axes of ellipse and using standard deviations about these axes.

Note: Chi-square value greater than 11.3 indicates 1 per cent level with 3 degrees of freedom.

January and a chart of the angle of rotation of the true major axis of the ellipse for January is shown in Figure 20. For the other mid-season months, there is apparently little to be gained by making an allowance for the angle of rotation of the true major axis except perhaps in higher latitudes in October but, if required, the values are included in the statistics in Appendix I.

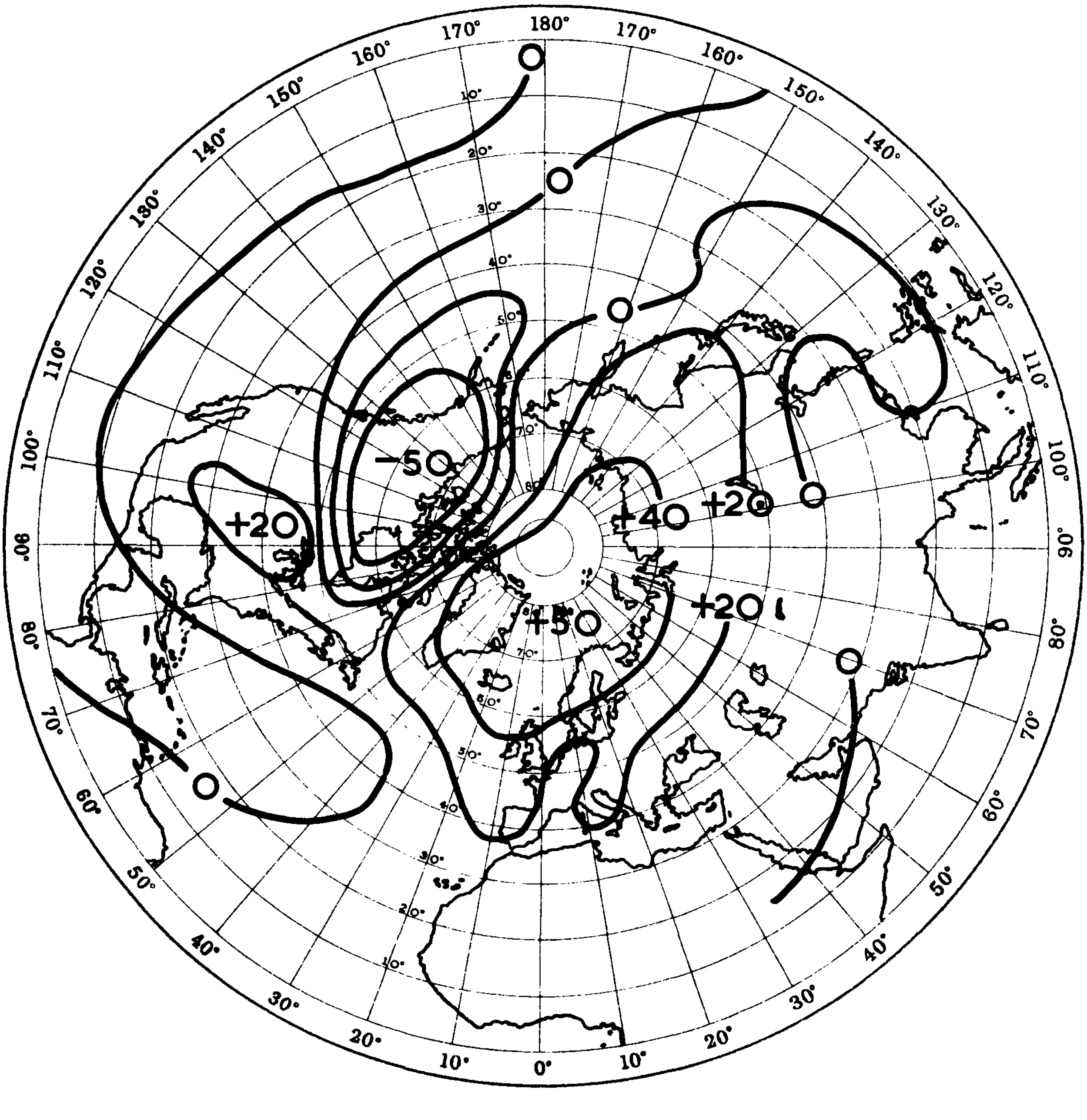

FIGURE 20. ANGLE OF ROTATION OF TRUE MAJOR AXIS OF ELLIPSE AT 30 MILLIBARS JANUARY, 1958–65

The 30, 60 and 90 per cent circles and ellipses of the theoretical distributions for the departures from the average 30-mb wind at three stations for the four mid-season months are shown in Figures 21–23 together with the numbers actually observed in each 'box'. The stations illustrated are Crawley (51° 05 'N, 00° 13 'W), Wakkanai (45° 25 'N, 141° 41 'E) and Ponape (6° 58 'N, 158° 13 'E). The Crawley diagrams (Figure 21) show that in April and October the theoretical elliptical distribution provides a much better estimate of the observed distribution. At Wakkanai (Figure 22) it is noticeable that, in all four months, the stronger departures from normal are much better described by the elliptical distribution. Ponape (Figure 23) is near 7 °N and, consequently, the winds are dominated by the QBO. Clearly the theoretical circular distribution is very misleading as only a very small number of observed winds actually occurred in the 30–90 per cent range in the sectors 315°–045° and 135°–225°. In general the observed distribution is much better described by either of the elliptical distributions.

From the foregoing results it is clear that, in the middle stratosphere, it can be very misleading to use the derived statistics in any way which assumes the wind distribution to be normal and circular. In many cases this will tend to overestimate the stronger meridional components and underestimate the stronger zonal components. In general, the observed distribution at 30 mb (as at 50 mb) is more adequately described by a series of ellipses with the length of the major and minor axes determined in terms of the standard deviation of the zonal and meridional components. The results for the stations considered in Appendix I indicate that it is usually acceptable to consider the east–west (or north–south) axis as the major axis of the ellipse. These ellipses do not provide a perfect representation of the observed distribution but they are, in general, more adequate than circles, especially when dealing with large departures from average.

The presentation of wind statistics has for long been recognized as a difficult problem and the reader requiring more information on this topic would do well to start by reading a paper entitled 'On the standard vector deviation wind rose' by Crutcher (1957). A paper by Rangarajan and Mokashi (1966) gives statistical parameters for all months for three Indian stations and describes their method of constructing the distribution ellipses. Maher and McRae (1964) present basic statistics for 23 Australian stations and also give three examples of the construction of probability ellipses.

8 – THE QUASI-BIENNIAL OSCILLATION AND ITS EFFECT ON WINDS AND TEMPERATURES AT 30 MILLIBARS IN LOW LATITUDES

This phenomenon was dealt with at some length in *Geophysical Memoirs* No. 112 and, for those who require a detailed description there is a very extensive literature on the subject. It is thought that the requirements of readers of this publication will be satisfied if the text and diagrams are limited to what is necessary for the better understanding of the climatology of the 30-mb level.

The 30-mb monthly mean zonal wind components for Canton Island (2° 46 'S, 171° 43 'W) for the period May 1954 – August 1967 and for Gan (00° 41 'S, 73° 09 'E) from September 1967 are shown in Figure 24. A noticeable difference between this Figure and the 50-mb monthly mean zonal wind components (Figure 17 of *Geophysical Memoirs* No. 112) is that at 30 mb the

Circular | Elliptical major axis east/west | Elliptical true major axis

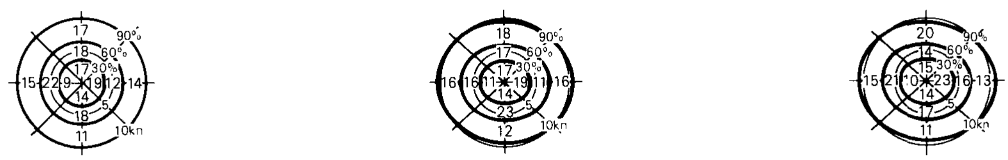

JULY 1957-64 (Expected frequency in each box 16)

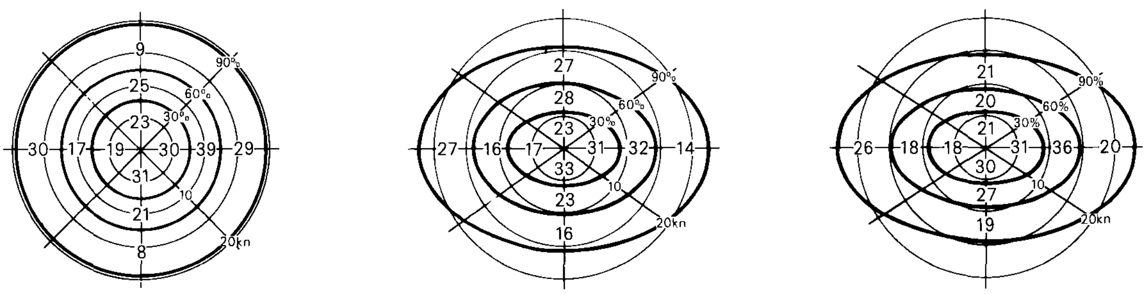

OCTOBER 1957-64 (Expected frequency in each box 23)

Circular | Elliptical major axis east/west | Elliptical true major axis

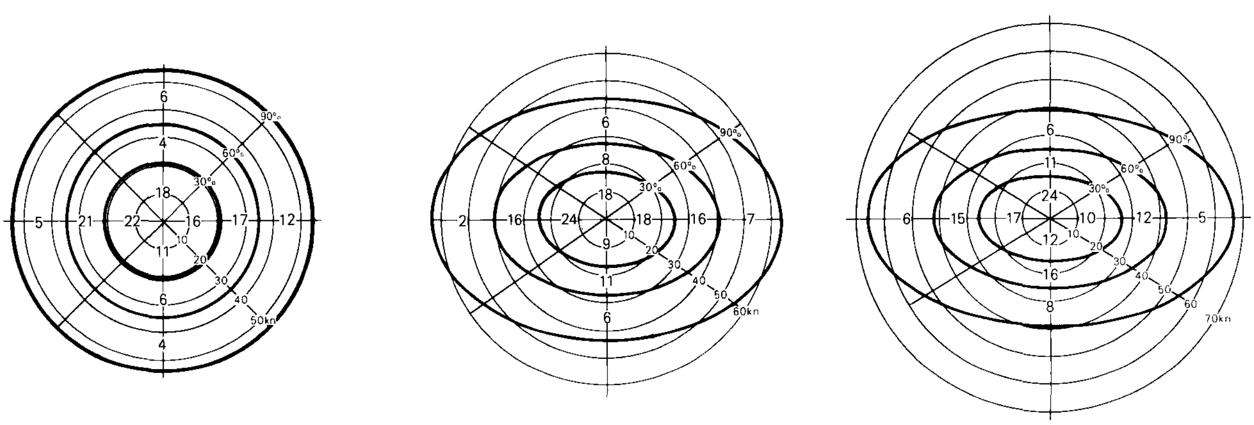

JANUARY 1958-65 (Expected frequency in each box 12)

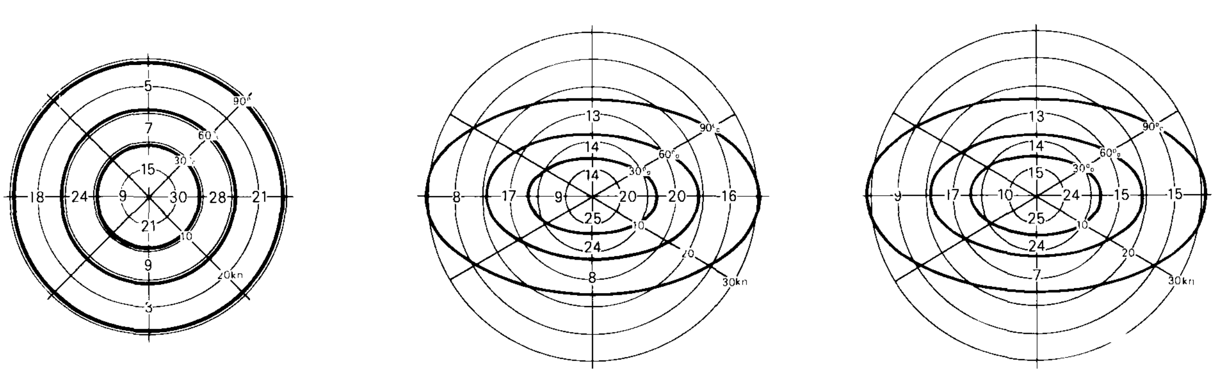

APRIL 1958-65 (Expected frequency in each box 16)

FIGURE 21. DISTRIBUTION OF DEPARTURES FROM THE AVERAGE 30-MILLIBAR WIND, FOR CRAWLEY 51°05′N, 00°13′W

See Appendix I for relevant statistics.

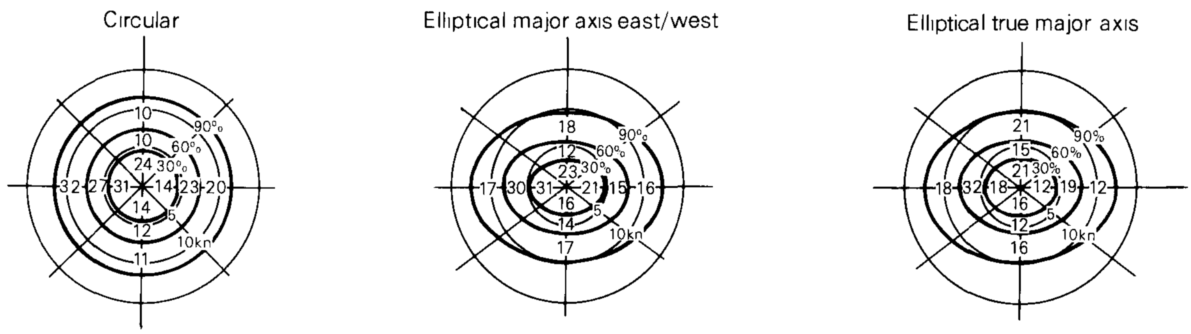

JULY 1957-64 (Expected frequency in each box 19)

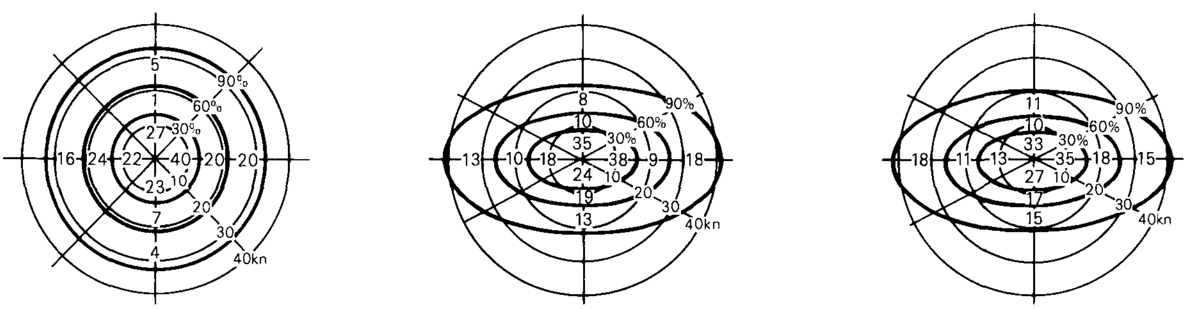

OCTOBER 1957-64 (Expected frequency in each box 18)

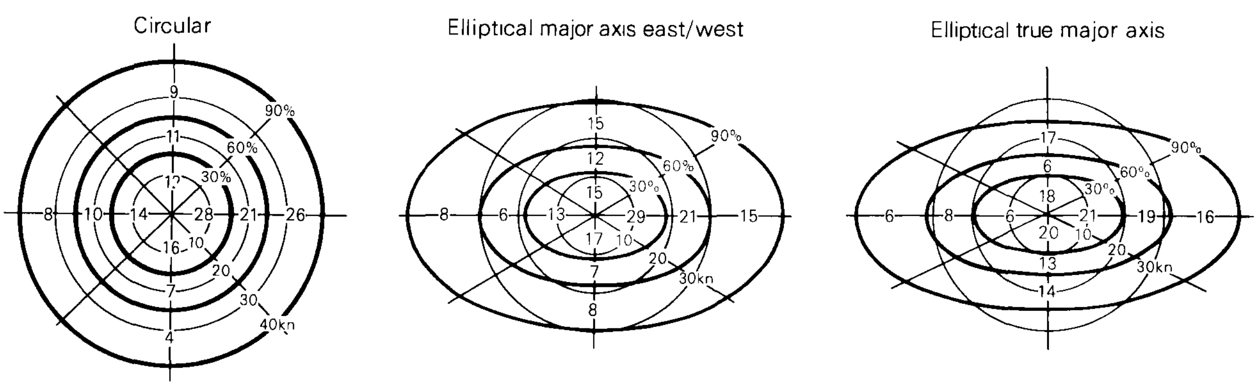

JANUARY 1958-65 (Expected frequency in each box 14)

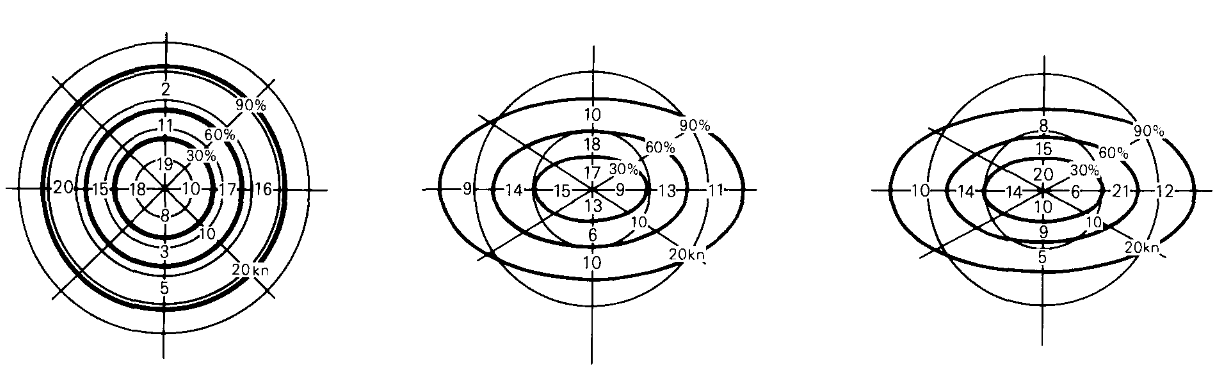

APRIL 1958-65 (Expected frequency in each box 12)

FIGURE 22. DISTRIBUTION OF DEPARTURES FROM THE AVERAGE 30-MILLIBAR WIND FOR WAKKANAI 45°25′N, 141°48′E

See Appendix I for relevant statistics.

Circular | Elliptical major axis east/west | Elliptical true major axis

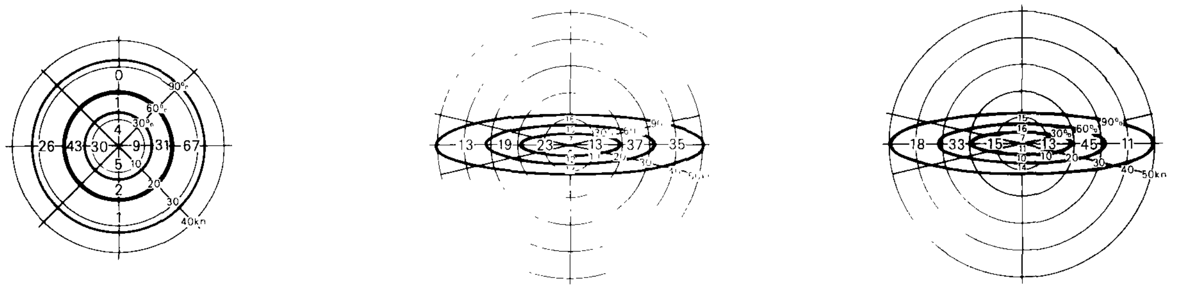

JULY 1957-64 (Expected frequency in each box 17)

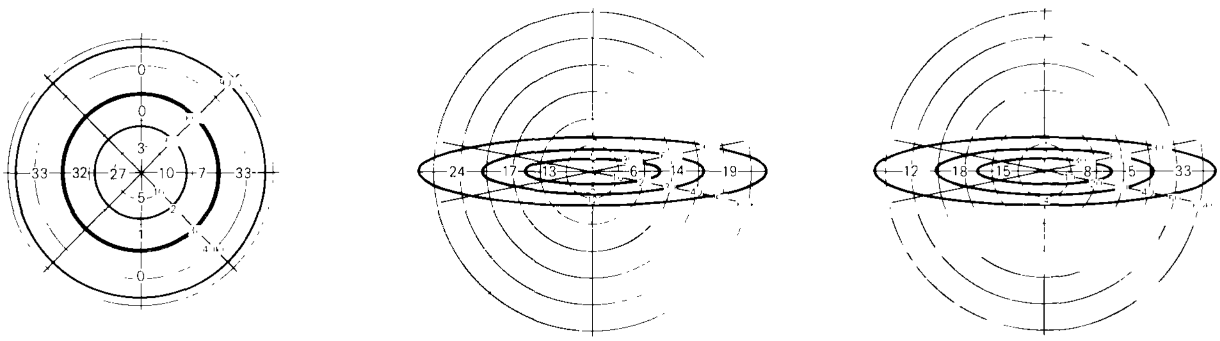

OCTOBER 1957-64 (Expected frequency in each box 12)

Circular | Elliptical major axis east/west | Elliptical true major axis

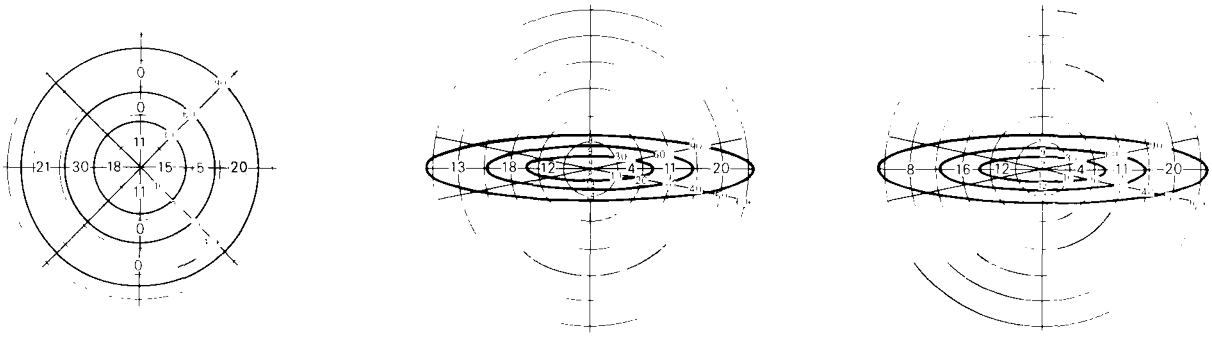

JANUARY 1958-65 (Expected frequency in each box 11)

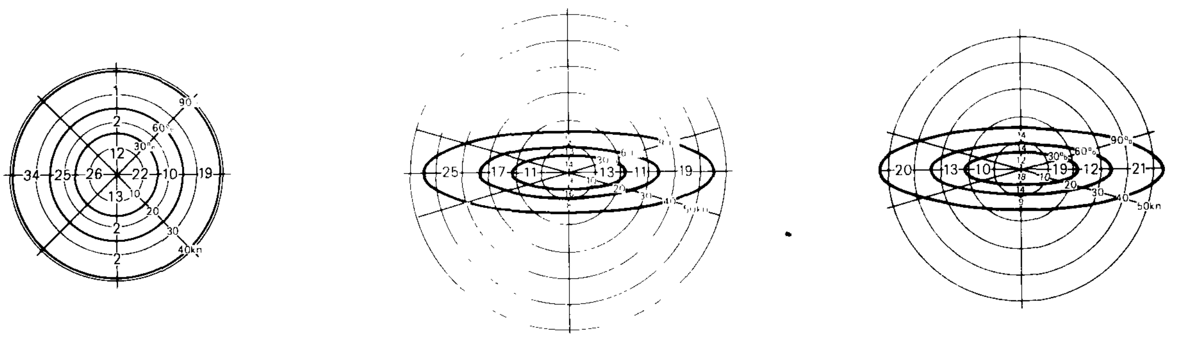

APRIL 1958-65 (Expected frequency in each box 14)

FIGURE 23. DISTRIBUTION OF DEPARTURES FROM THE AVERAGE 30-MILLIBAR WIND FOR PONAPE 6°58′N, 158°13′E

See Appendix I for relevant statistics.

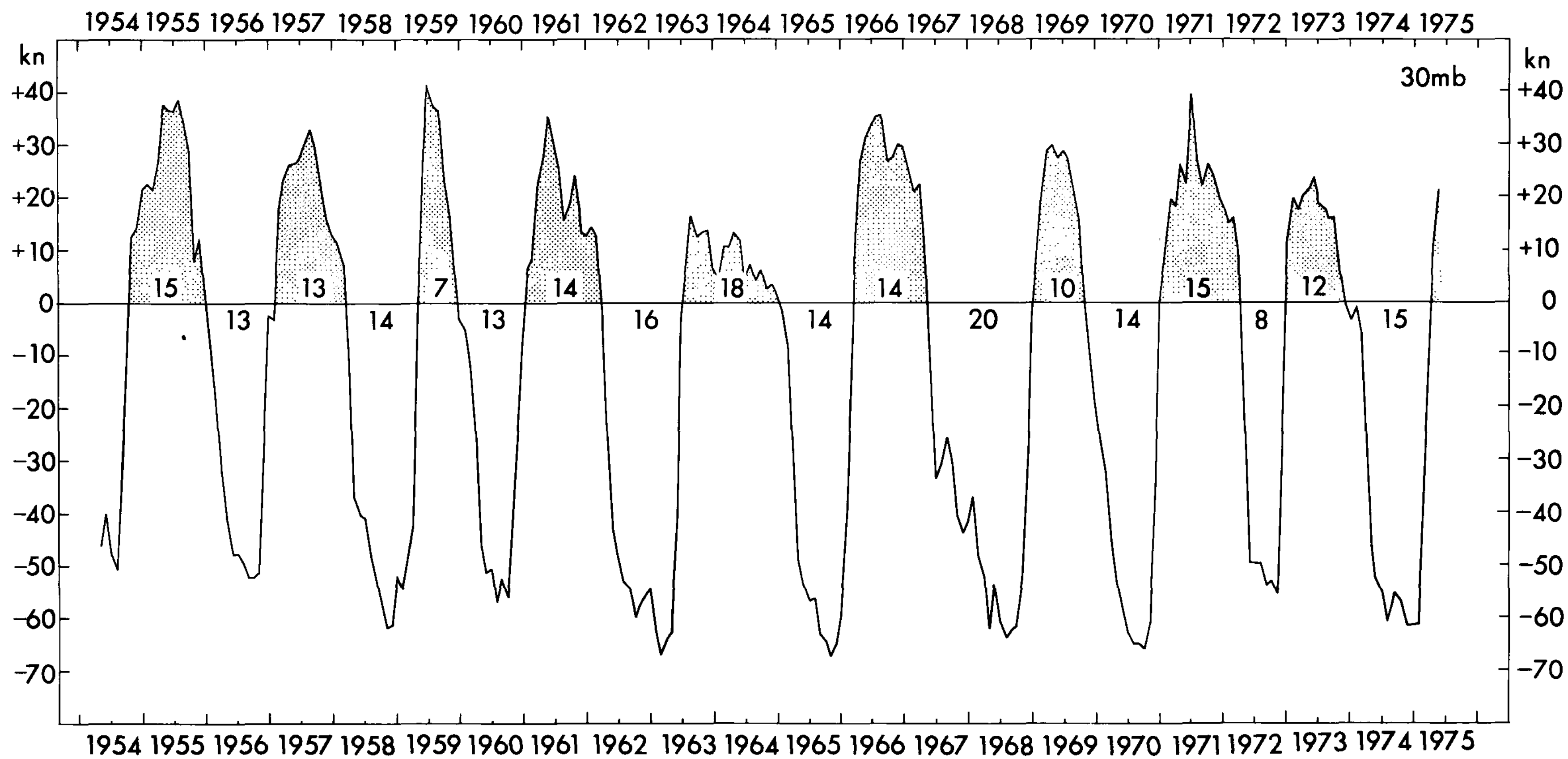

FIGURE 24. MONTHLY MEAN ZONAL WIND COMPONENTS AT 30 MILLIBARS FOR CANTON ISLAND FROM MAY 1954 TO AUGUST 1967 AND FOR GAN FROM SEPTEMBER 1967 ONWARDS

——— Canton Island - - - - - Gan

Components towards the east (shaded) are positive. The duration, in months, of each regime, is given near the zero line.

easterly regime persists longer than it does at 50 mb and, conversely, the westerlies are correspondingly shorter lived. At this higher level the easterlies not only persist longer but they are also appreciably stronger. Figure 24 shows nine westerly and nine easterly phases of the QBO and from these the average duration of the westerly regime is 13 months and of the easterly regime 14 months. In both cases the standard deviation is about three months. At 50 mb the average duration of the westerly regime is 16 months (with a standard deviation of 4 months) and of the easterly regime 11 months (with a standard deviation of 1 month).

Figures 24 and 25 (the pentad, i.e. 5-day, means of the 30-mb zonal wind component at Canton Island) illustrate that in low-latitude areas, where the QBO is the dominant feature, there is little to recommend taking an average for any individual month over a period of years. An average obtained in this way would be made up of both easterly and westerly regimes and would, therefore, suggest a relatively light average wind and a high standard deviation. This would be very misleading when we know that there are definite easterly and westerly regimes (albeit of variable length) within which the average wind is stronger and the variability is much less.

In order to present the climatological facts of the QBO in a more practical and meaningful way the Canton Island 30-mb data for the period from February 1956 to May 1967 were used to prepare the curves in Figure 26. These 136 months represent five full cycles of the oscillation and although this indicates an average period-length of about 27 months, it can be seen from Figure 24 that the period varies considerably. The data were processed to provide the average zonal components, meridional components and their standard deviations for five months which were all the first month of an easterly regime, the five which were the second month of an easterly regime and so on up to the 14th easterly month. The same procedure was followed for the westerly regime up to the 14th month. There was only one occasion when the monthly mean zonal wind component was easterly and only one when it was westerly after the 14th month and these months were not used. The statistics for the easterly regime are based on data for five individual months for months 1 to 13 and on three individual months for the 14th month. For the westerly regime the statistics for months 1 to 7 are based on five individual months, months 8 to 13 on four individual months and month 14 on three individual months. The averages were obtained by taking all the individual values together and the standard deviations describe the variability about this average.

Figure 26 shows that with the westerly regime the average zonal wind component quickly reaches a value near 20 kn and maintains that value until after the 10th month of the regime then falling to about 10 kn during the 12th, 13th and 14th months. The easterly regime behaves rather differently — there is a more gradual increase to a maximum (of nearly 60 kn) during the 8th and 9th months, then a gradual decrease to about 30 kn in the average for the 14th easterly month. The average meridional components are light in all months of both regimes with values in excess of one knot in only five of the months. It is of interest that the meridional component during these five full cycles of the QBO showed a very definite preponderance of northward flow. The curve of the standard deviation of the zonal wind component shows that in most months the standard deviation is within the range 10–15 kn except during the change-over from the easterly regime to the westerly when there is a marked increase. The standard deviation of the meridional wind component is within the range 5–10 kn throughout all months.

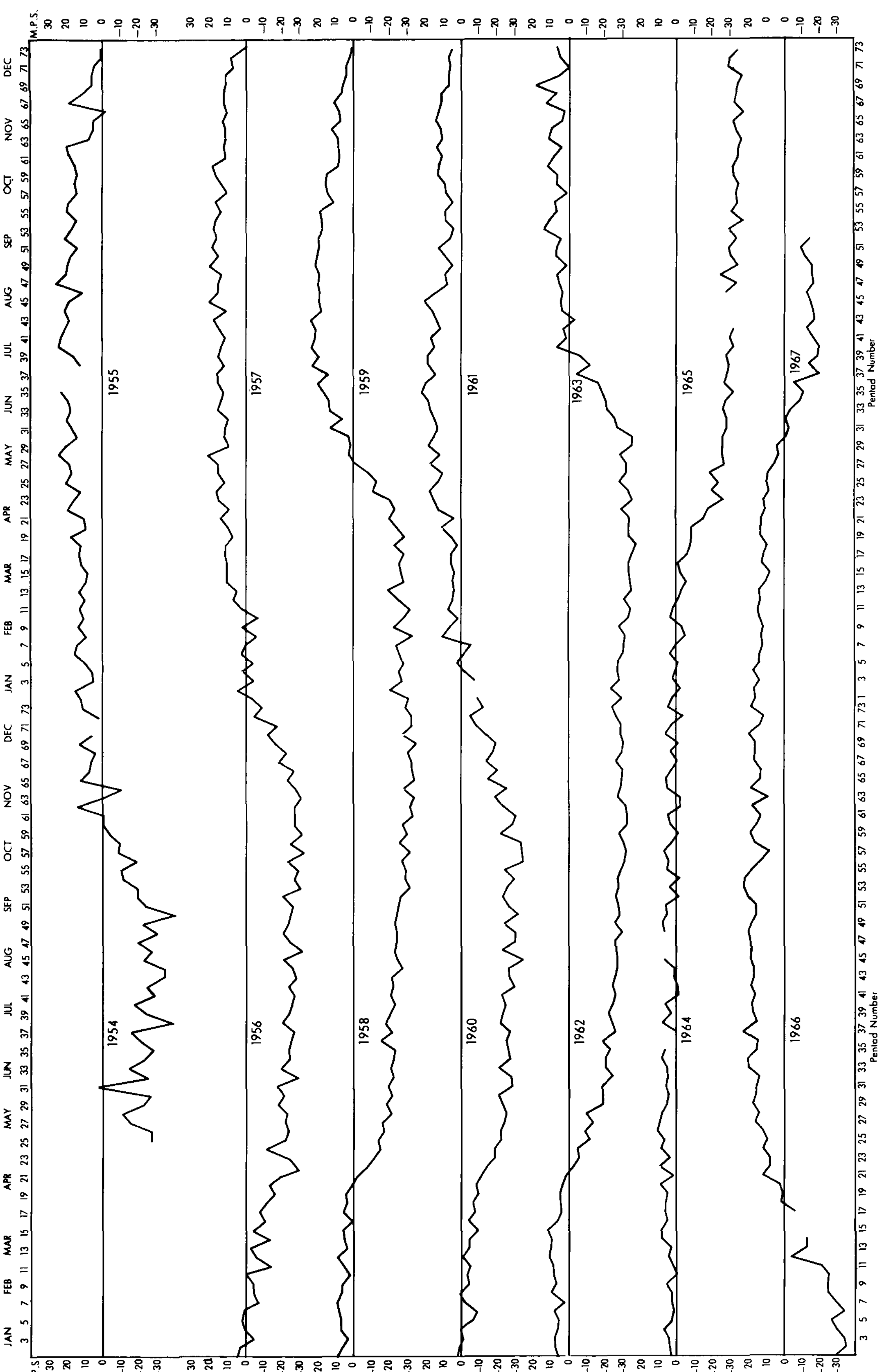

FIGURE 25. PENTAD MEAN ZONAL WIND COMPONENTS AT 30 MILLIBARS FOR CANTON ISLAND

Units are metres per second.

Components towards the east are positive.

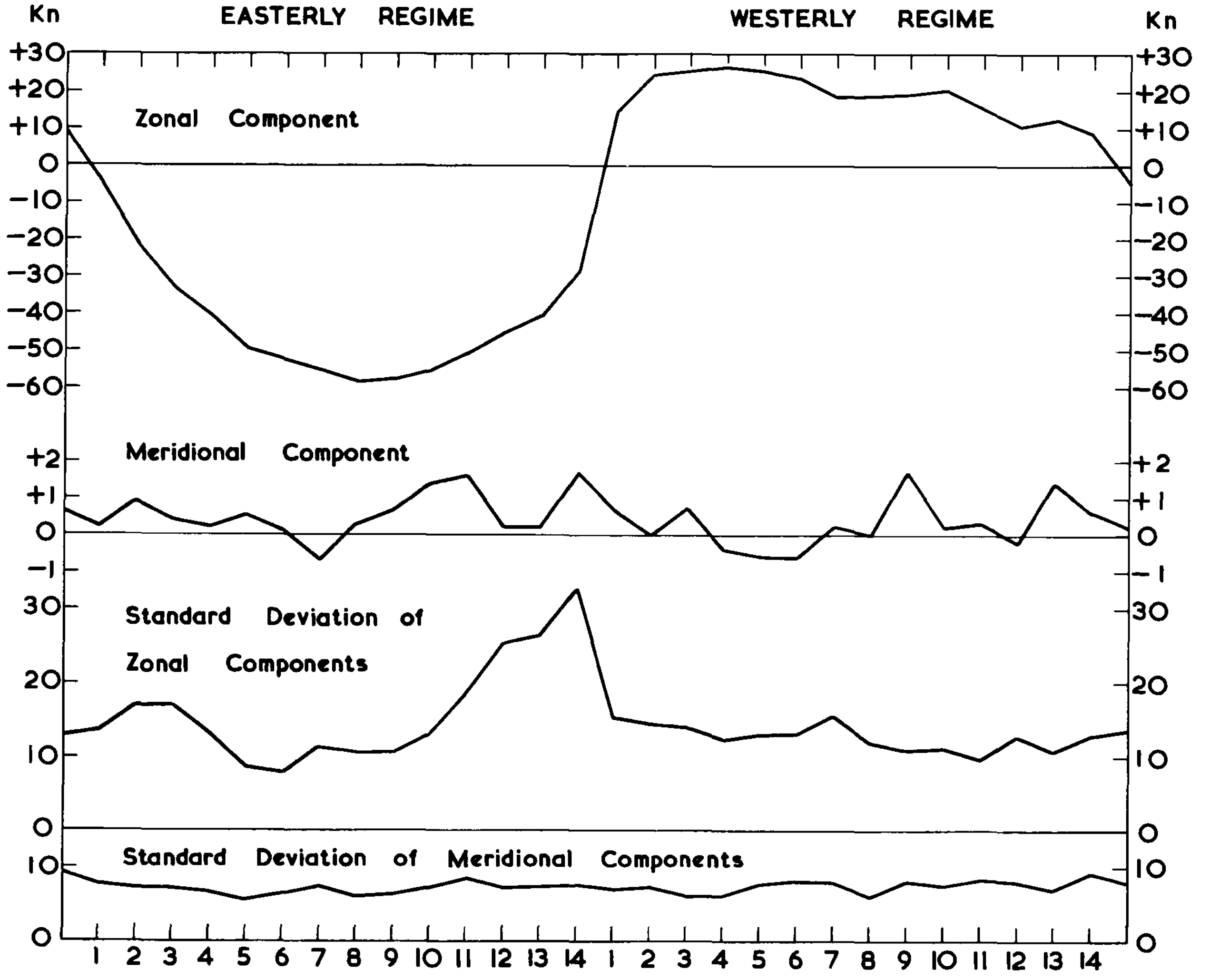

FIGURE 26. CANTON ISLAND (2°46′S, 171°43′W) 30-MILLIBAR AVERAGE ZONAL AND MERIDIONAL WIND COMPONENTS AND THEIR STANDARD DEVIATIONS BASED ON FIVE FULL CYCLES OF THE QUASI-BIENNIAL OSCILLATION FROM FEBRUARY 1956 TO MAY 1967

If one is required to provide 30-mb average winds for the area within say 5° or 7° north and south of the equator then the information contained in Figures 24–26 provides an adequate description, although it must be accepted that, because of the variable lengths of the easterly and westerly regimes, it is not possible to provide statistics which cover all eventualities.

The data for the easterly and westerly regimes were used to provide the statistics in Table IV. In calculating these statistics, if the monthly mean zonal wind component was less than 10 kn the data for that month were ignored. These statistics may be somewhat crude but, for many purposes, they provide an acceptable estimate of the parameters involved and there is the advantage that the user has only to decide whether the equatorial stratospheric-wind regime is an established easterly or westerly.

Stations close to the equator were included in the selection for which statistics were computed in investigating the nature of the observed wind distributions at 30-mb (see Table III and Appendix I) and the chi-square values showed that whilst the distribution is not circular neither can it be properly described as elliptical. In each case the statistics calculated were based on data for five individual months but, as indicated earlier, this is a most unsatisfactory and not very meaningful way of arriving at an average wind in the area where the QBO is most marked. The Canton Island 30-mb data during established easterly and westerly regimes separately, were therefore processed and tested for ellipticity and circularity. The results are shown in Figures 27a–d and the relevant statistics are included in Table IV. It is evident from these results that, when considering the separate regimes, as one would expect, the observed distribution is certainly not circular and the chi-square values suggest that, for both regimes, the distributions are significantly non-elliptical but more especially in the established easterly regime. In testing the distribution for ellipticity the assumption is made that the wind components are normally distributed and so histograms showing the observed and theoretical frequency distributions were prepared and these are shown in Figure 28. The histograms in Figure 28a and b were prepared using only those months when the mean zonal component was greater than 10 kn. In Figure 24 it can be seen that within the easterly regime the monthly average zonal component quickly reaches 20 kn and that the average remains above 20 kn until the last month of the easterly regime. Consequently the histogram in Figure 28c was prepared using data only for those months within the easterly regime when the mean zonal component exceeded 20 kn. These diagrams show that within the established easterly or westerly regimes the zonal components are not distributed normally. The zonal components during the established westerly regime (Figure 28a) suggest a bimodal distribution and during the established easterly regime both Figures 28b and c show the positive skewness of the distribution.

It can be concluded, therefore, that in the middle stratosphere, in those regions where the QBO is the dominant feature, the wind distributions cannot be adequately or satisfactorily represented either by the circular or by the elliptical normal distributions. However, in this work the data for five full cycles of the QBO have been used to provide the percentage frequencies of occurrence for various speed-ranges of the zonal components within either an established easterly or westerly regime and these are reproduced in Figures 29 and 30.

TABLE IV – STATISTICS OF 30-MILLIBAR WINDS (KNOTS) AT CANTON ISLAND DURING (a) ESTABLISHED EASTERLY AND (b) ESTABLISHED WESTERLY REGIMES

	Components		Standard deviation		Number of observations	Average wind		Standard vector deviation	Chi-square values for circularity test			Chi-square values for ellipticity test		
	zonal	meridional	zonal	meridional		*deg*	*kn*		*per cent* 0–30	30–60	60–90	*per cent* 0–30	30–60	60–90
(a)	–48.4	0.4	17.7	6.8	2216	091	48.4	18.8	348	364	321	179	116	60
(b)	22.7	0.2	13.0	7.4	2090	269	22.7	14.9	55	103	192	22	15	28

Note: The Chi-square value for the 5 per cent level with 7 degrees of freedom is 14.1 (i.e. values in excess of this indicate significant non-circularity or non-ellipticity).

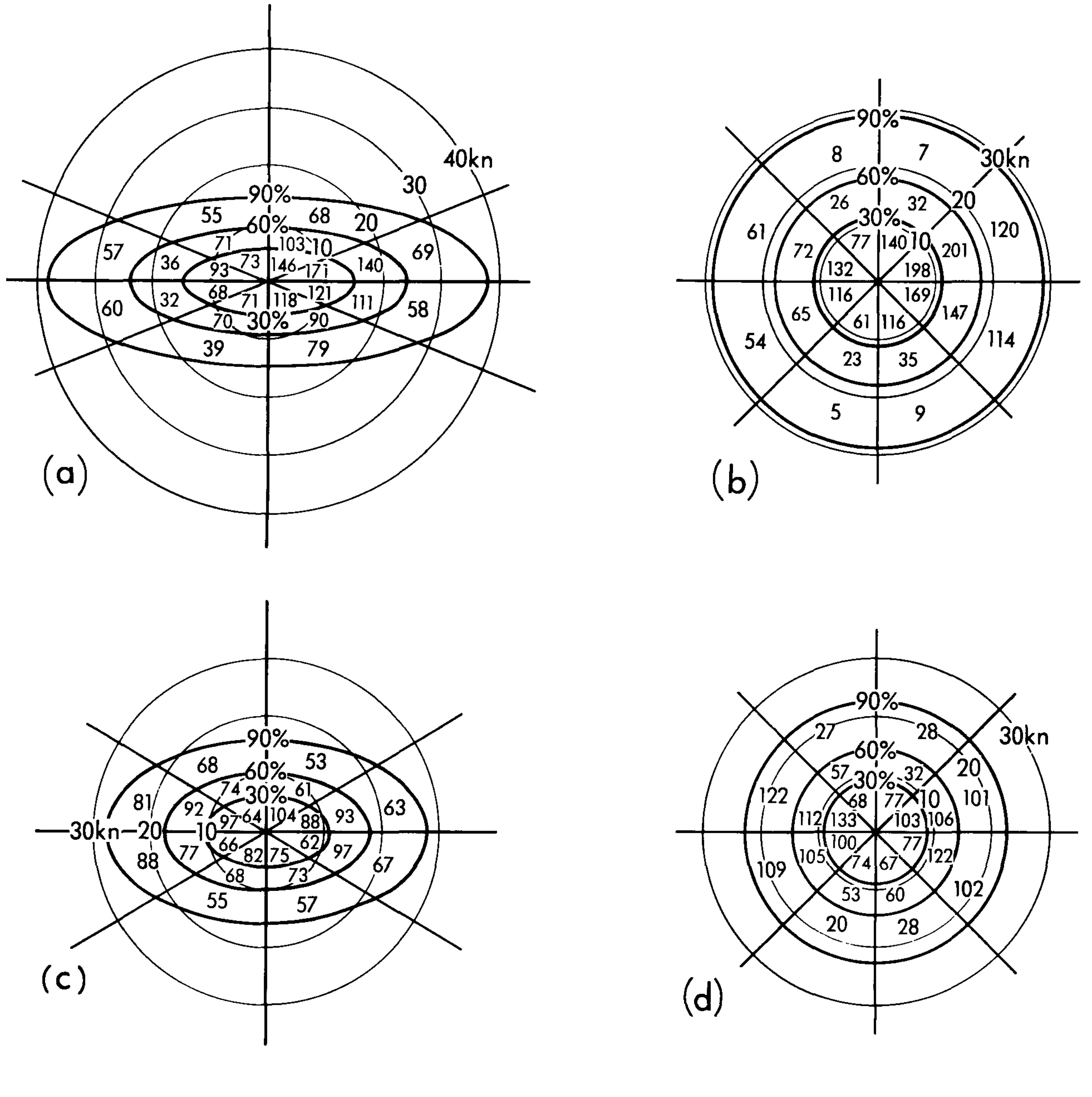

FIGURE 27. CANTON ISLAND (2°46′S, 171°43′W) 30-MILLIBAR WINDS – DISTRIBUTIONS OF DEPARTURES FROM THE AVERAGE DURING THE ESTABLISHED EASTERLY REGIME ((a) AND (b)) AND WESTERLY REGIME ((c) AND (d))

Expected frequency in each box is 83 in Figures (a) and (b), 78 in Figures (c) and (d). Months when mean zonal component was less than 10 knots were not included.

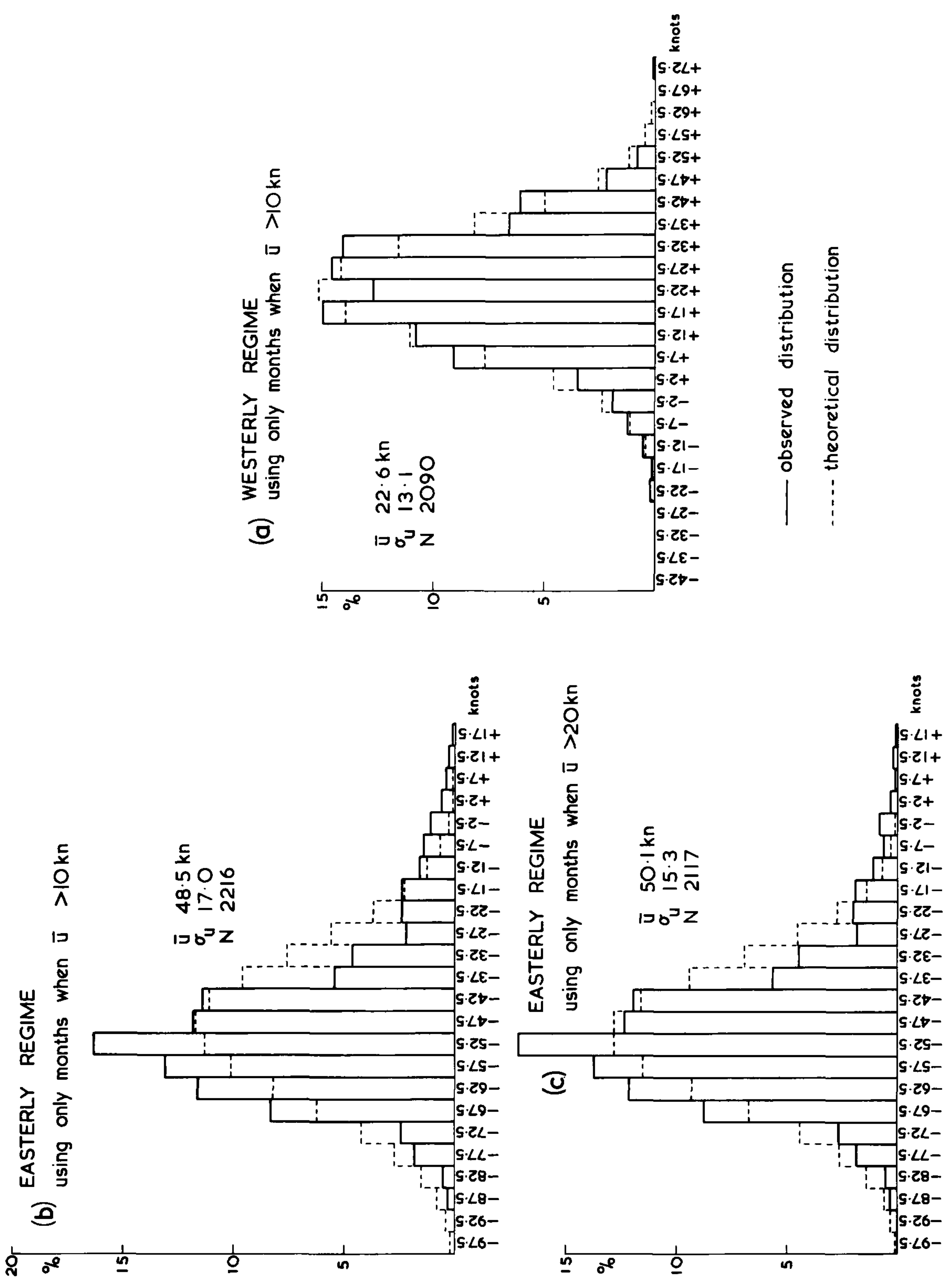

FIGURE 28. FREQUENCY DISTRIBUTIONS OF 30-MILLIBAR ZONAL WIND COMPONENTS AT CANTON ISLAND

$\bar{u}$ = average wind speed, σ_u = standard deviation, N = number of observations.

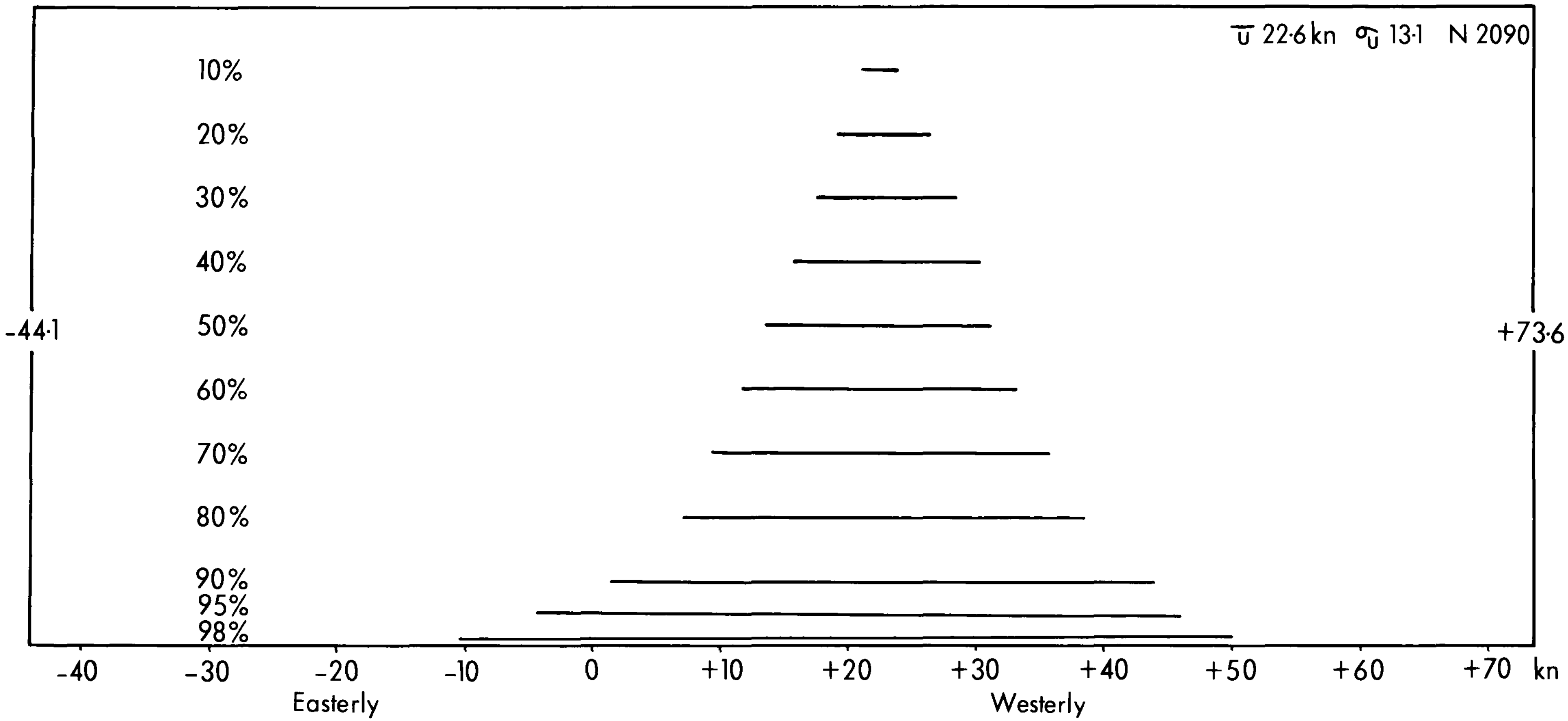

FIGURE 29. SPEED RANGES OF VARIOUS PERCENTAGES OF OCCURRENCE OF THE ZONAL WIND COMPONENT BASED ON OBSERVED WINDS DURING THE ESTABLISHED WESTERLY REGIME AT 30 MILLIBARS AT CANTON ISLAND

$\bar{u}$ = average wind speed, σ_u = standard deviation, N = number of observations. Months when mean zonal component was less than 10 knots were not included.

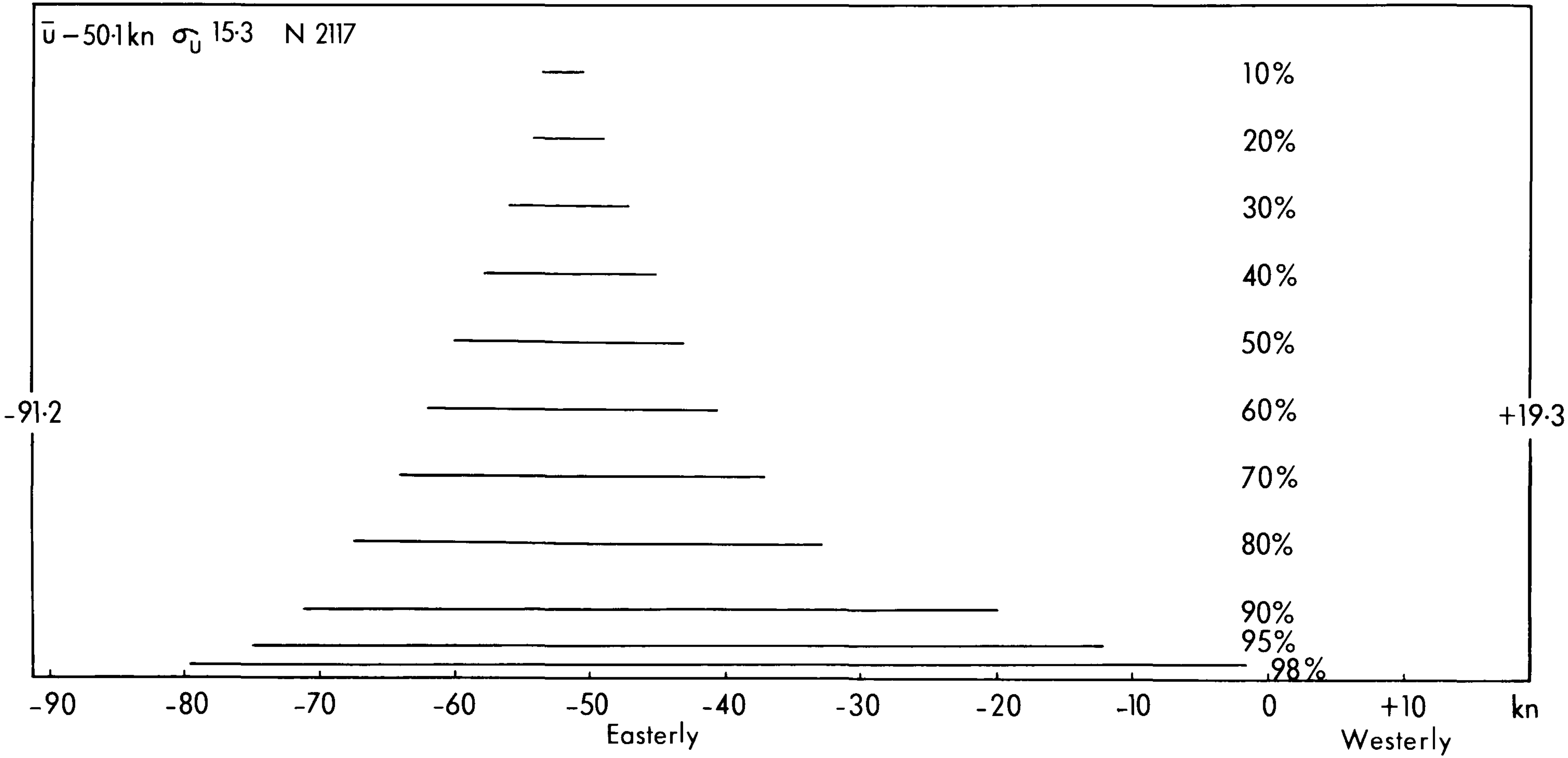

FIGURE 30. SPEED RANGES OF VARIOUS PERCENTAGES OF OCCURRENCE OF THE ZONAL WIND COMPONENT BASED ON OBSERVED WINDS DURING THE ESTABLISHED EASTERLY REGIME AT 30 MILLIBARS AT CANTON ISLAND

$\bar{u}$ = average wind speed, σ_u = standard deviation, N = number of observations. Months when mean zonal component was less than 10 knots were not included.

Any attempt to describe the climatology of the middle stratosphere in equatorial regions is complicated by the very variable behaviour of the length of the period of the QBO in the zonal component and also by the non-normal distribution of the zonal wind components. The former makes it difficult to arrive at a reliable average wind and the latter adds to the difficulty of describing the variability. In addition, the lack of stations with long and continuous records of stratospheric winds contributes to the problem. However, if one is required to provide statistics for areas in which the QBO is the dominant feature then the diagrams presented here, based on five full cycles of the oscillation, will enable an estimate to be made. The publication of more accurate and more reliable statistics seems unlikely until such time as adequate data from a representative network of stations become available.

In order to examine how hemispheric patterns might vary when equatorial winds are markedly easterly or westerly, monthly mean charts of 30-mb winds were prepared for selected Januarys, Aprils, Julys and Octobers and these are shown in Figures 31–42.

The charts for January 1959 (Figure 31) and July 1958 (Figure 32) are representative of months when the QBO is in a strong easterly phase and they show that there is a broad band of strong (greater than 50 kn) easterlies from the equator to about 20° into the summer hemisphere. The axis of this broad band of strong easterlies is not at the equator but is displaced into the summer hemisphere, where, beyond about latitude 20° the monthly mean winds are light easterly. In the winter hemisphere the easterlies extend to 25° or more from the equator before giving way to westerlies.

The charts for January 1958 (Figure 33) and July 1969 (Figure 34) are representative of months when the QBO is in a strong westerly phase and they show that, in both months, there is a narrow band of westerlies with speeds greater than 20 kn centred close to the equator. These westerlies extend to 5–10° into the summer hemisphere where a change-over to easterly takes place. The belt of stronger easterlies (greater than 20 kn) lies between approximately 12–37° in the summer hemisphere with lighter easterlies typical of the summer regime in higher latitudes. In the winter hemisphere the stronger westerlies in the zone near the equator decrease with increasing latitude and in both months easterly zonal wind components appear over quite considerable areas. In higher latitudes the zonal component increases again in the stronger westerly regime which is typical of the higher-latitude winter.

These charts indicate that the belts of strong easterlies or westerlies are continuous around the equator on a monthly time-scale. An examination of the 30-mb wind data on selected days during the established easterly or westerly regimes suggests that the easterly winds (with a speed of about 50 kn) and the westerly winds (with a speed of about 30 kn) do encircle the equatorial belt.

In studying mid-winter and mid-summer stratospheric wind patterns on a global scale there is a distinct advantage in knowing what the higher-latitude monthly mean regimes are in the two seasons. This advantage is lost when one considers the global patterns in some other months. We know that during the late winter and early spring period there can be very considerable year-to-year variations which are associated with the final warming and the breakdown of the winter stratospheric vortex. These differences can be quite noticeable in April when, in some years, the 30-mb monthly mean contour chart has a well-defined vortex, often centred in

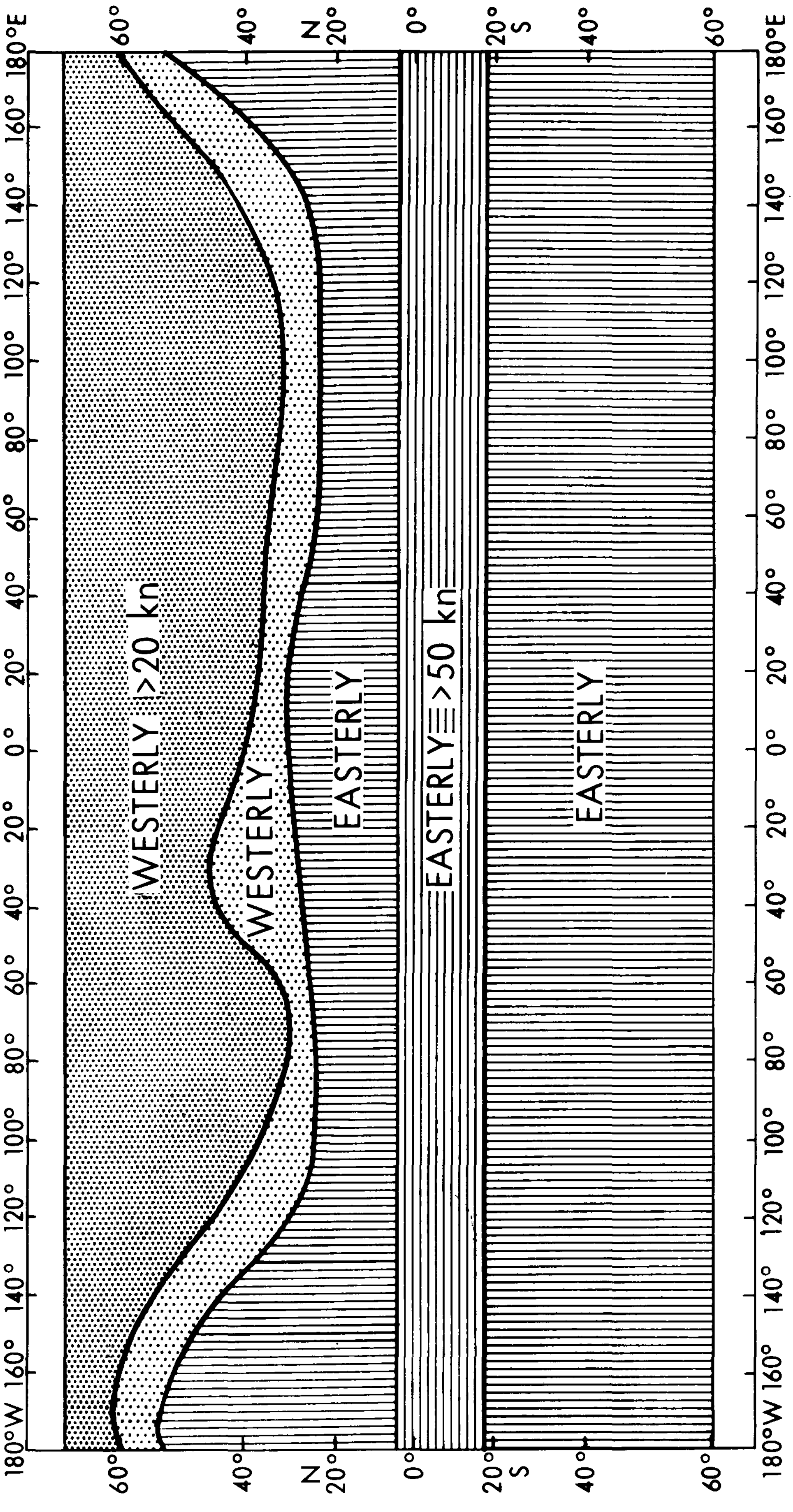

FIGURE 31. 30-MILLIBAR MONTHLY MEAN WINDS, JANUARY 1959

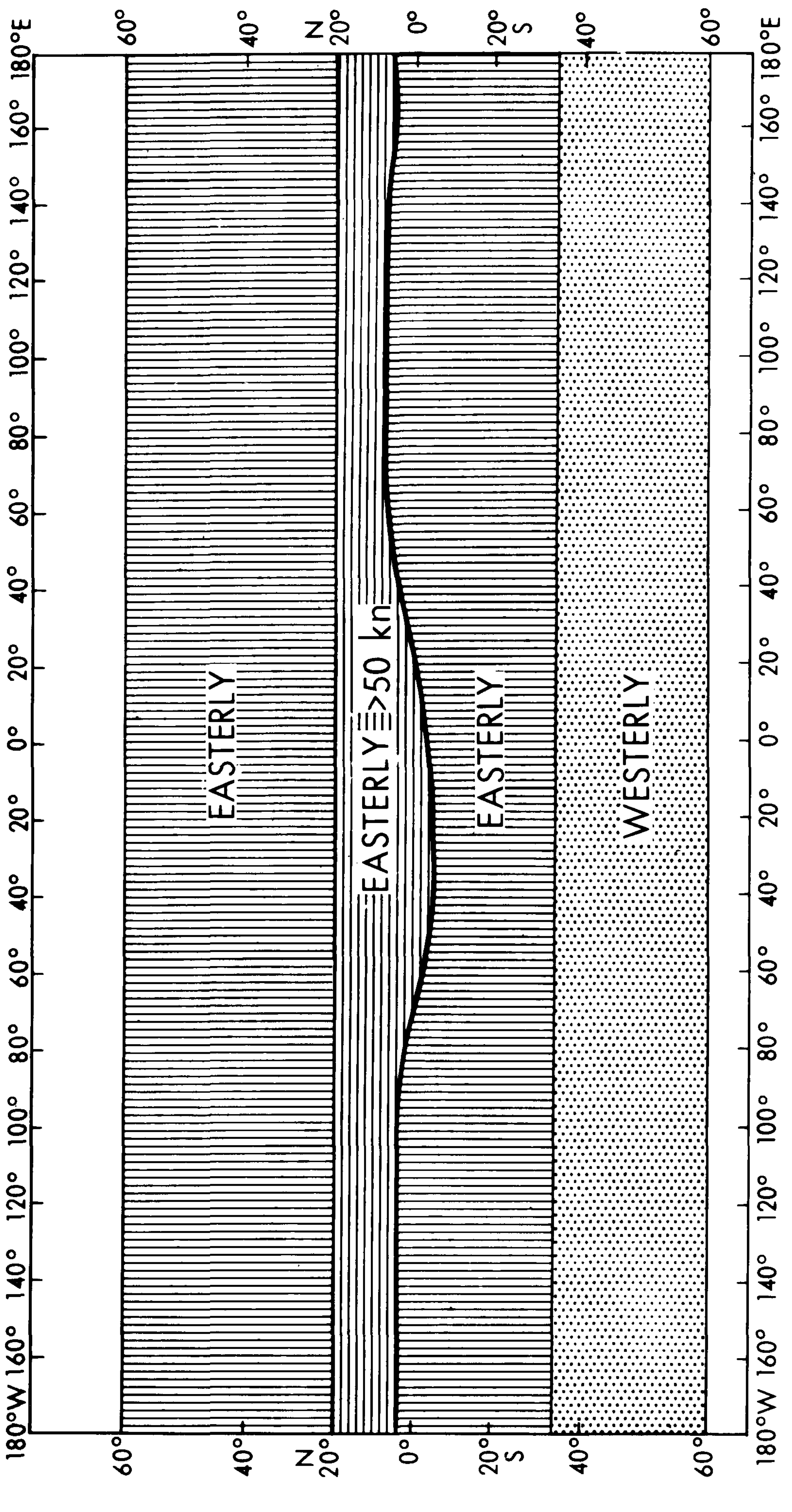

FIGURE 32. 30-MILLIBAR MONTHLY MEAN WINDS, JULY 1958

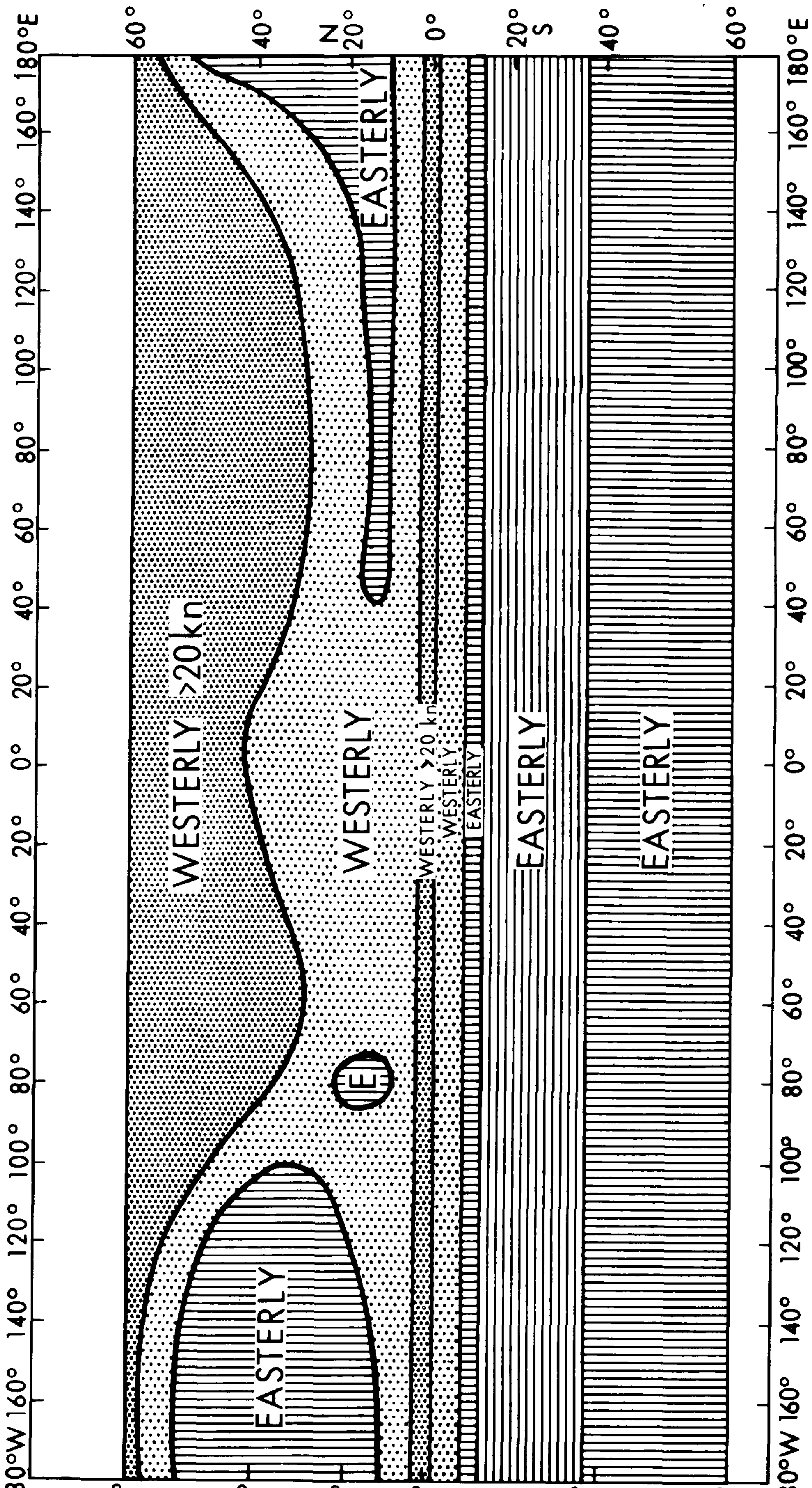

FIGURE 33. 30-MILLIBAR MONTHLY MEAN WINDS, JANUARY 1958

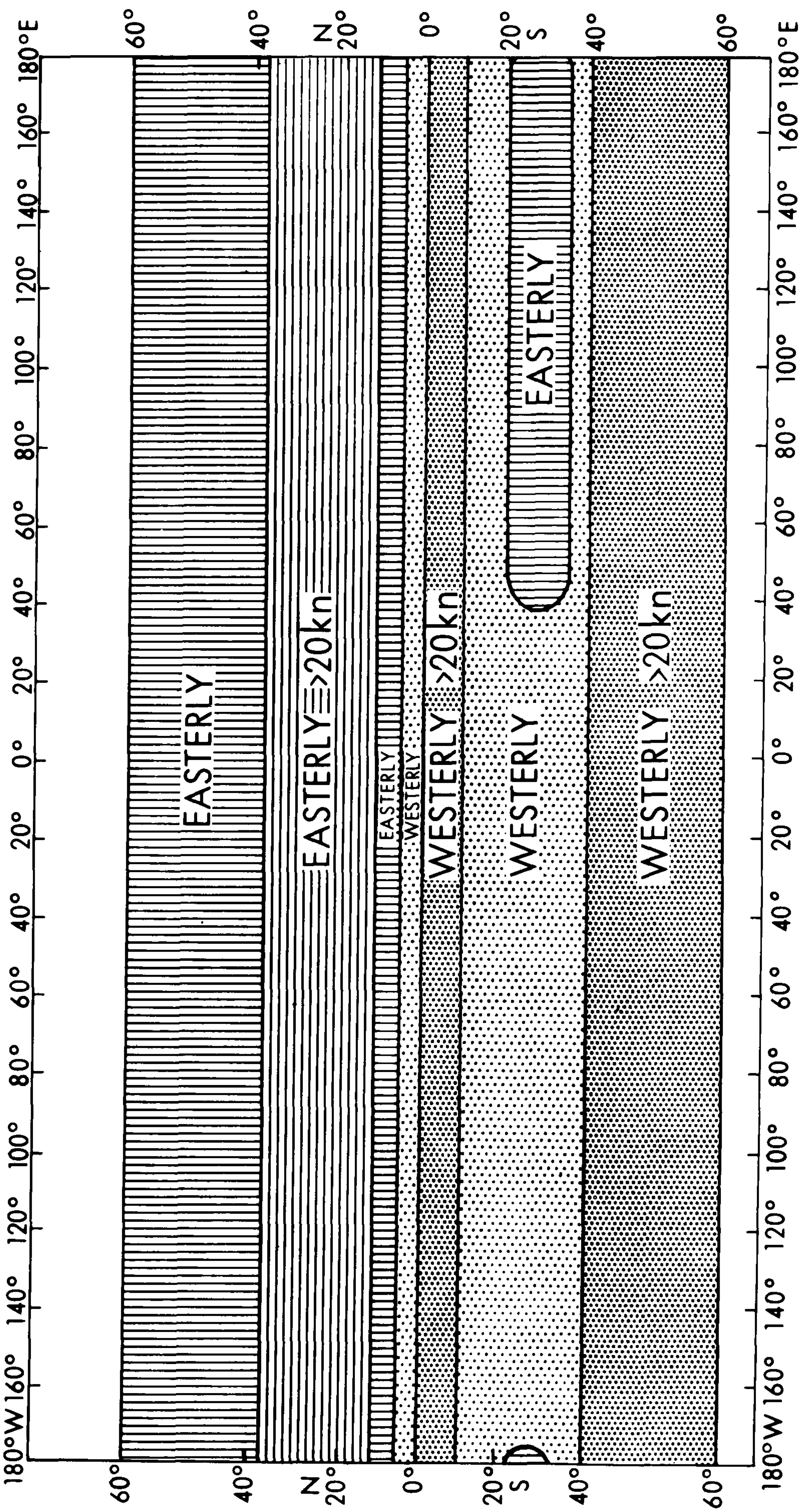

FIGURE 34. 30-MILLIBAR MONTHLY MEAN WINDS, JULY 1969

the region of Novaya Zemlya, with a strong westerly circulation associated with it. In some other years in April the 30-mb winds may be very light over a large part of the hemisphere in high latitudes. The charts in Figures 35–38 show how the monthly mean 30-mb wind patterns in April vary with different phases of the QBO. When the QBO is in a strong easterly phase as in April 1968 and April 1970 (Figures 35 and 36) then the easterly zonal component is 40–50 kn near the equator and the easterlies extend to 32–35° north and south.

When the QBO is in an established westerly phase (15–30 kn) near the equator, as in April 1969 and April 1971 (Figures 37 and 38) then the westerlies extend to about 8 or 9° north and south before reversing to easterlies in both hemispheres. These easterlies extend to about 30° in the northern hemisphere and to south of 30° in the southern hemisphere. The maximum easterlies occur in a band centred near 15–18°S with a secondary maximum occurring near 15–18°N. There may well be some small latitudinal differences in the boundaries between the easterlies and the westerlies which are related to the strength of the equatorial westerlies or to the phase of the QBO, but it is not possible to say this with any certainty until many more comparable charts have been analysed. The overall picture which emerges from these four charts for April is that of a broad band of easterlies (approximately 30–35° north and south) with the zone near the equator (say 9–10° north and south) dominated by either strong easterlies or westerlies depending on the phase of the QBO.

Over the middle and high latitudes of the northern hemisphere the 30-mb data for these four Aprils show considerable variability but suggest no obvious relationship between the phase of the QBO and the patterns observed north of, say, 40°N.

Monthly mean 30-mb wind charts were also prepared for a number of Octobers and four of these are shown in Figures 39–42. The diagrams for October 1965 and October 1972 (Figures 39 and 40) depict conditions when the QBO is in a strong easterly phase. The easterly zonal component is 50–60 kn near the equator and is generally strong in the band 10°N to 10°S. The easterlies extend to just north of 30°N and to south of about 35°S with westerlies in higher latitudes of both hemispheres.

When the QBO is in an established westerly phase (20–30 kn) as in October 1966 and 1971 (Figures 41 and 42) the strongest westerlies are confined to a narrow band close to the equator with westerlies extending to about 10°N and to 12–15°S. In the northern hemisphere the easterlies extend to 35–37°N with a well-defined maximum near 20°N. In the southern hemisphere the lack of data makes it difficult to define the boundary between the easterlies and the higher-latitude westerlies. However, there does appear to be a maximum in the easterly flow in the latitude of the Tropic of Capricorn and in October 1971 the monthly mean speed of the easterlies over much of Australia was stronger than 30 kn. These charts indicate that the belts of strong easterlies or westerlies are continuous around the equator on a monthly time-scale.

Both the April charts (Figure 35–38) and these four October charts suggest that, at the 30-mb level, there is a broad band of easterlies (approximately 30–40°N to 35–45°S) with the zone near the equator (say 9°N to 5°S) dominated by either strong easterlies or westerlies depending on the phase of the QBO.

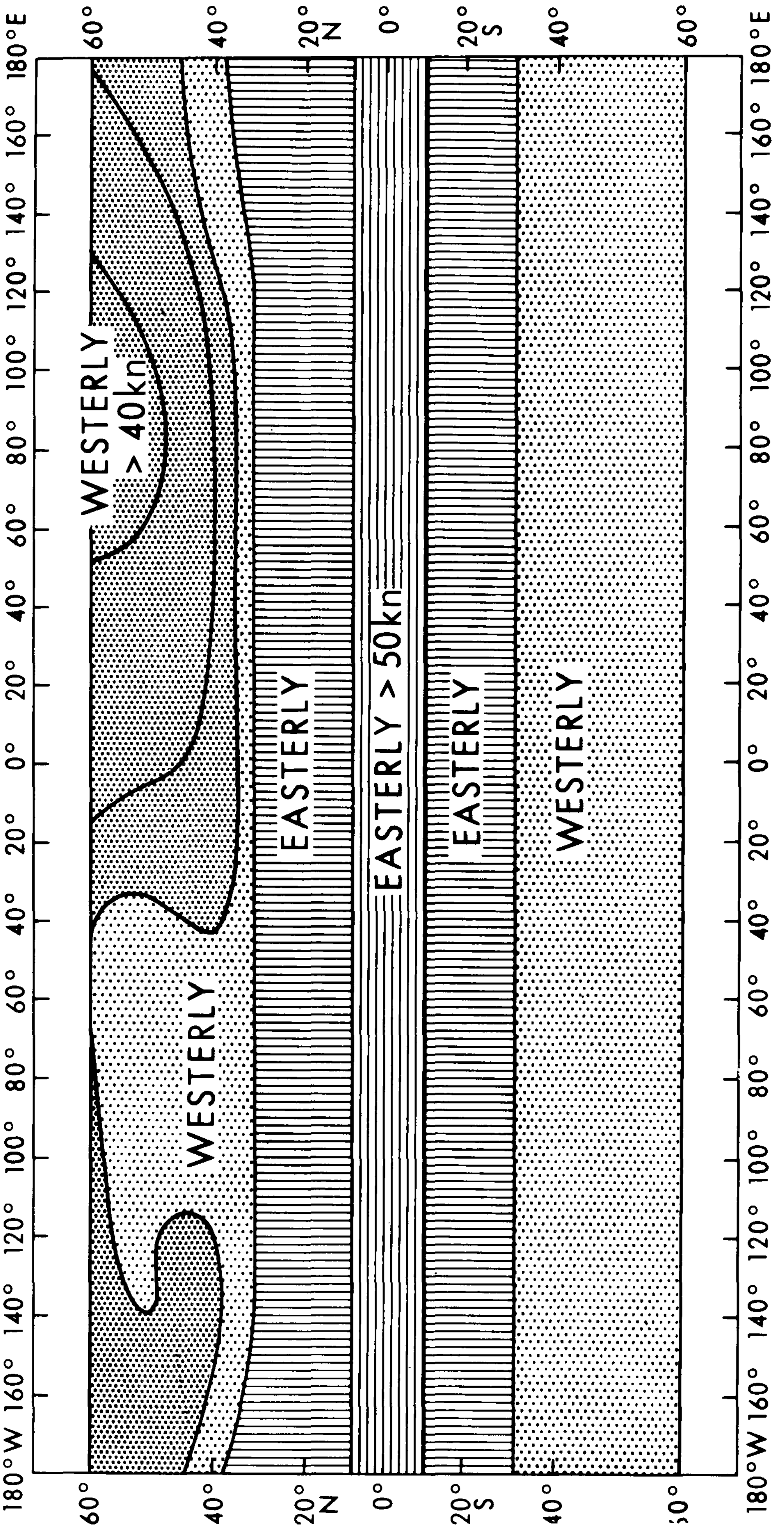

FIGURE 35. 30-MILLIBAR MONTHLY MEAN WINDS, APRIL 1968

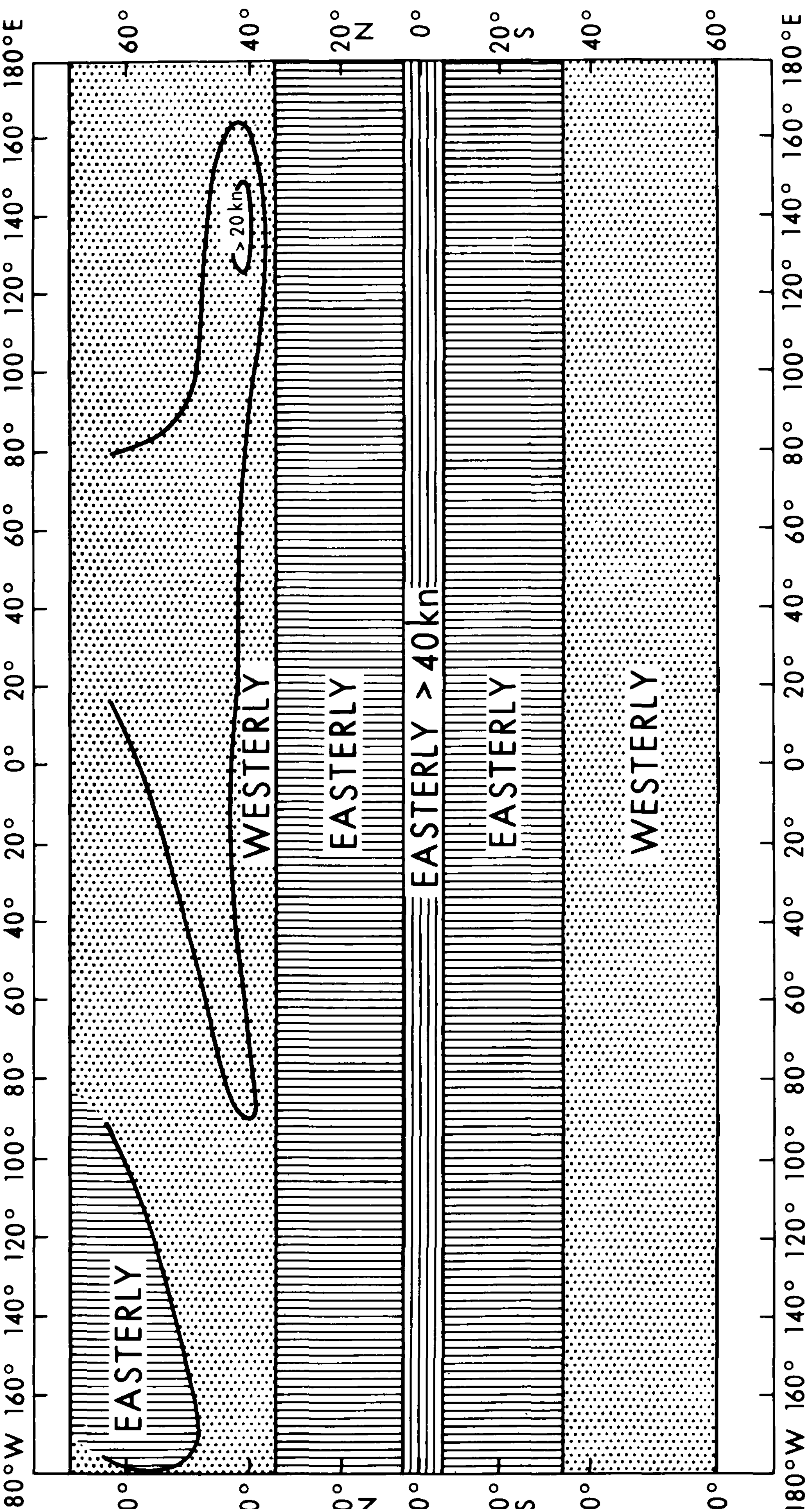

FIGURE 36. 30-MILLIBAR MONTHLY MEAN WINDS, APRIL 1970

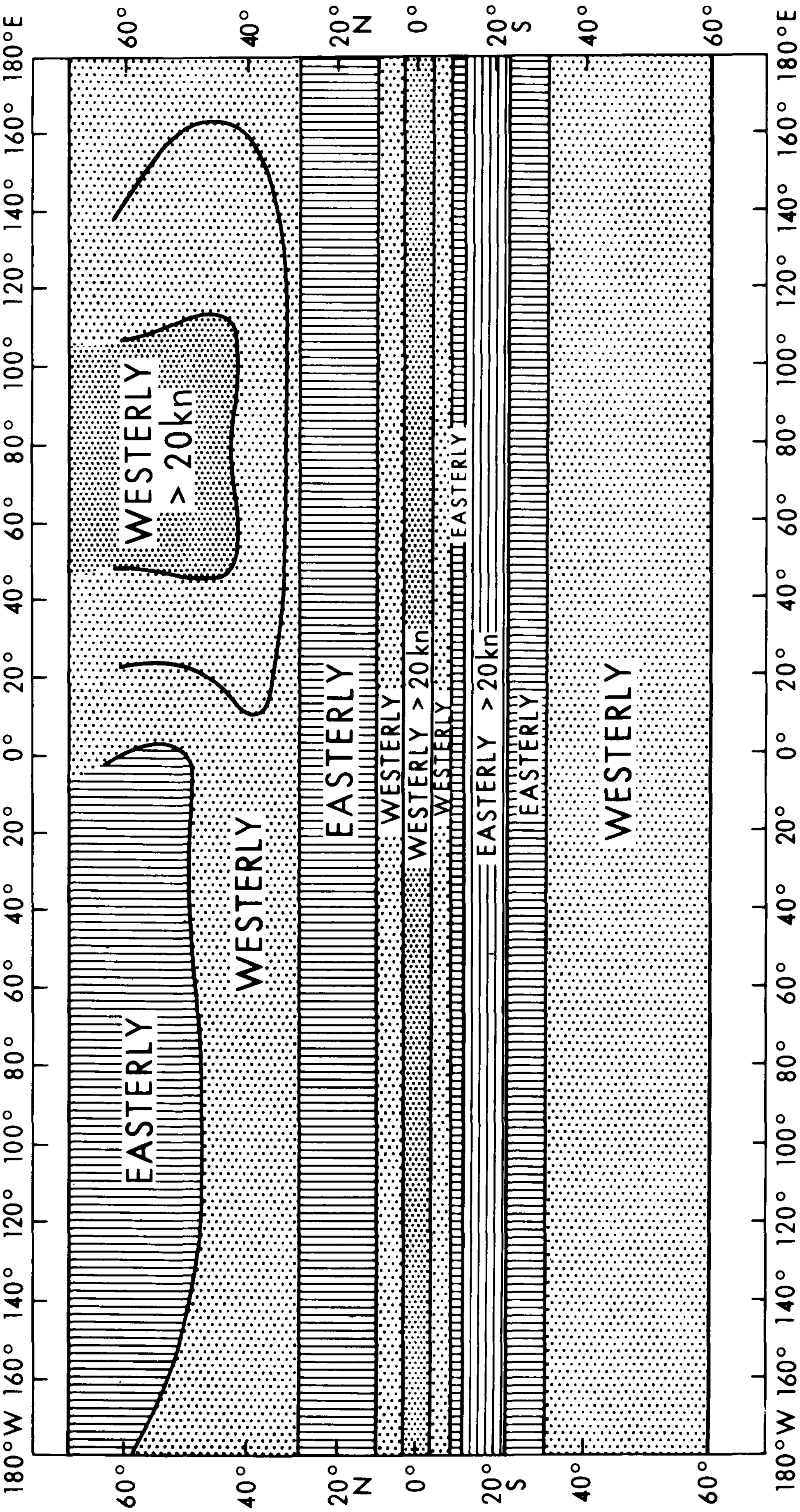

FIGURE 37. 30-MILLIBAR MONTHLY MEAN WINDS, APRIL 1969

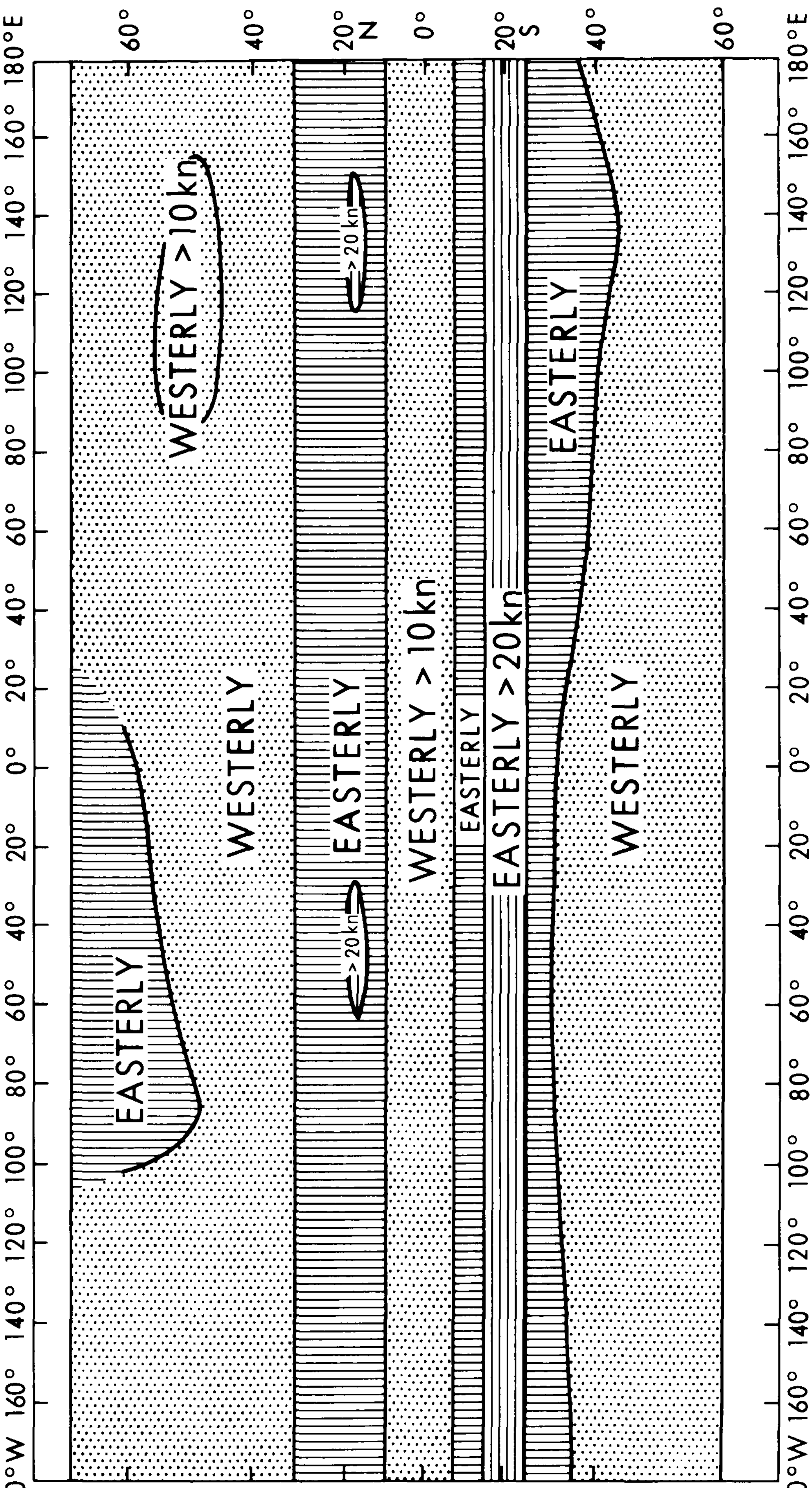

FIGURE 38. 30-MILLIBAR MONTHLY MEAN WINDS, APRIL 1971

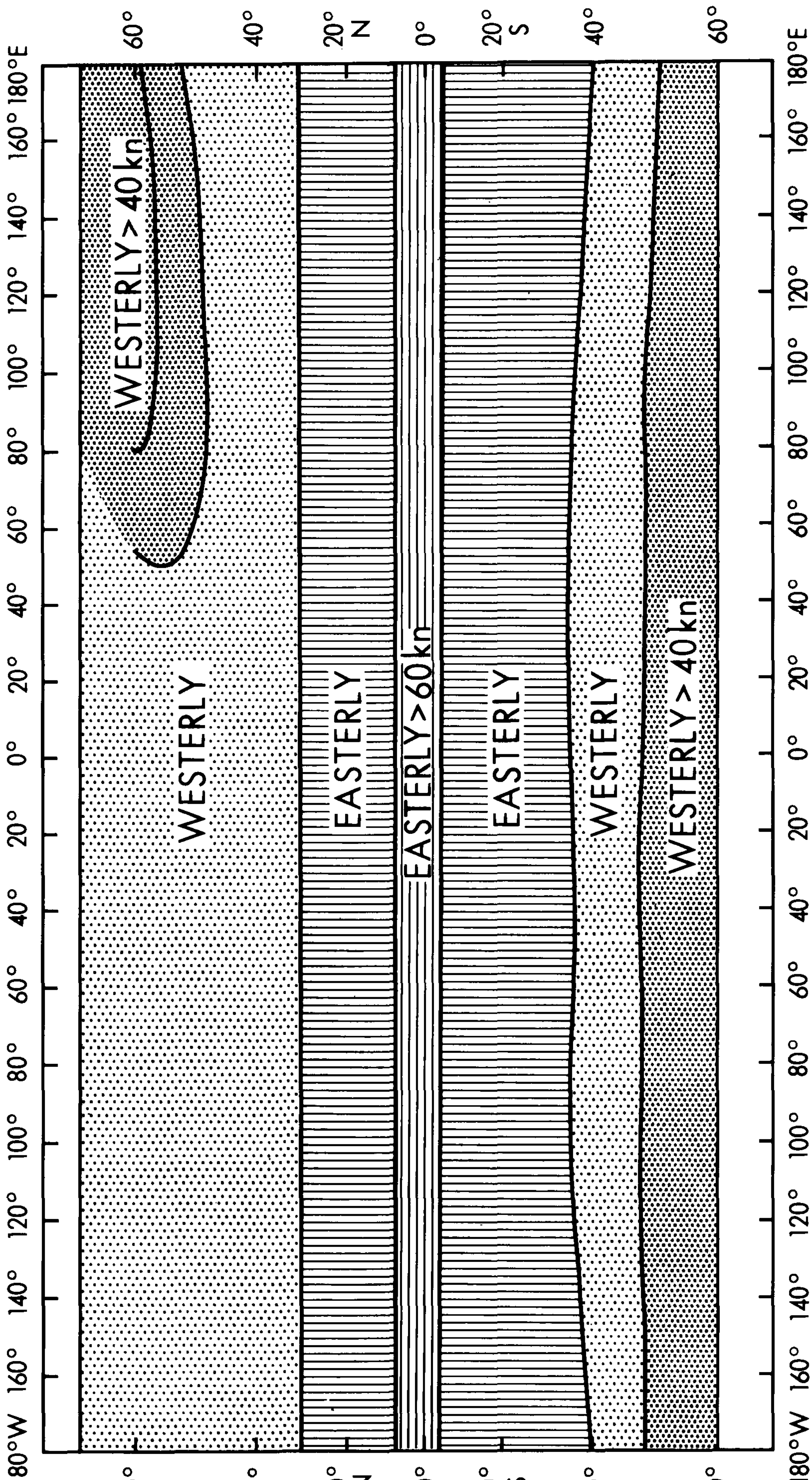

FIGURE 39. 30-MILLIBAR MONTHLY MEAN WINDS, OCTOBER 1965

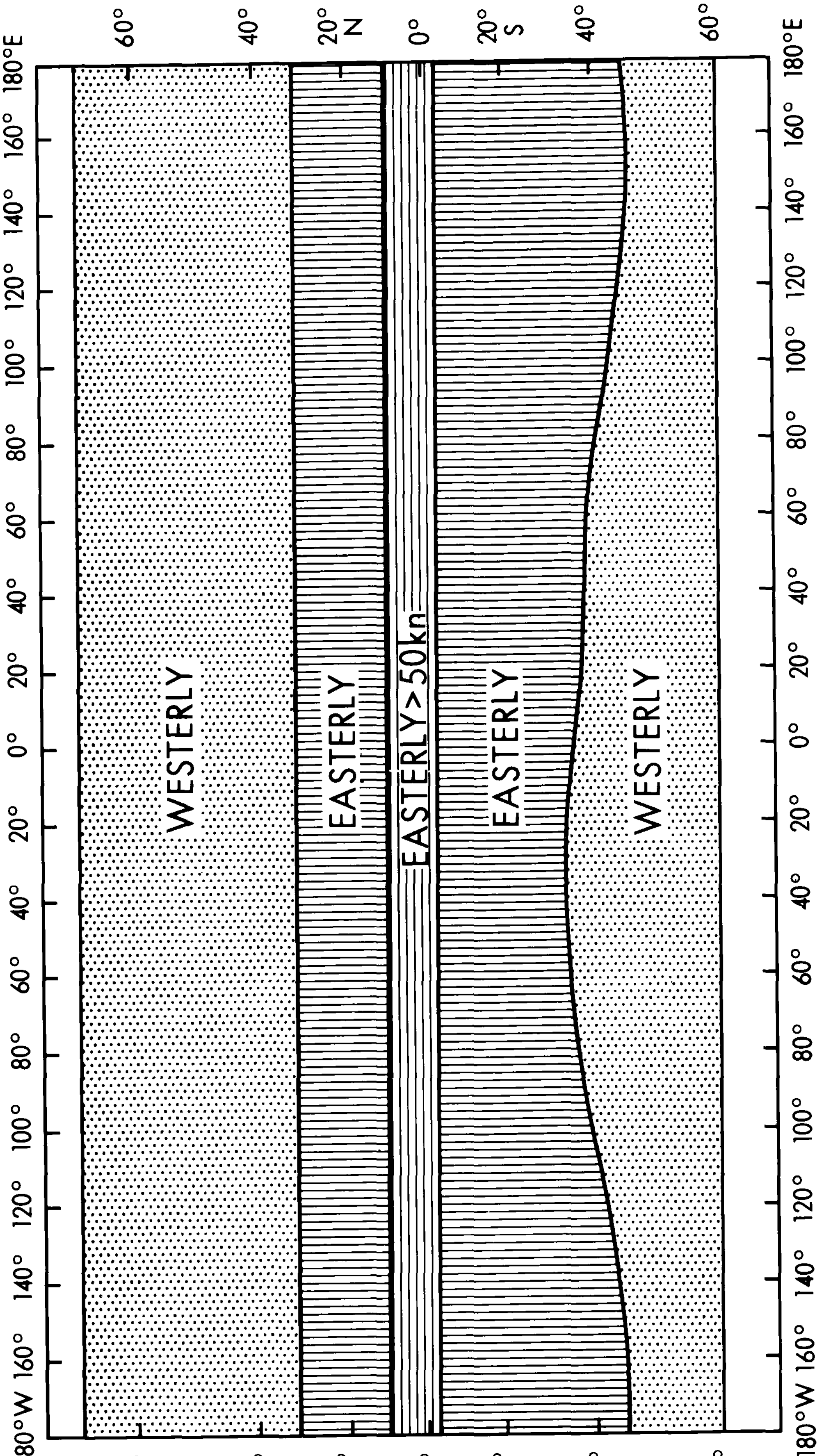

FIGURE 40. 30-MILLIBAR MONTHLY MEAN WINDS, OCTOBER 1972

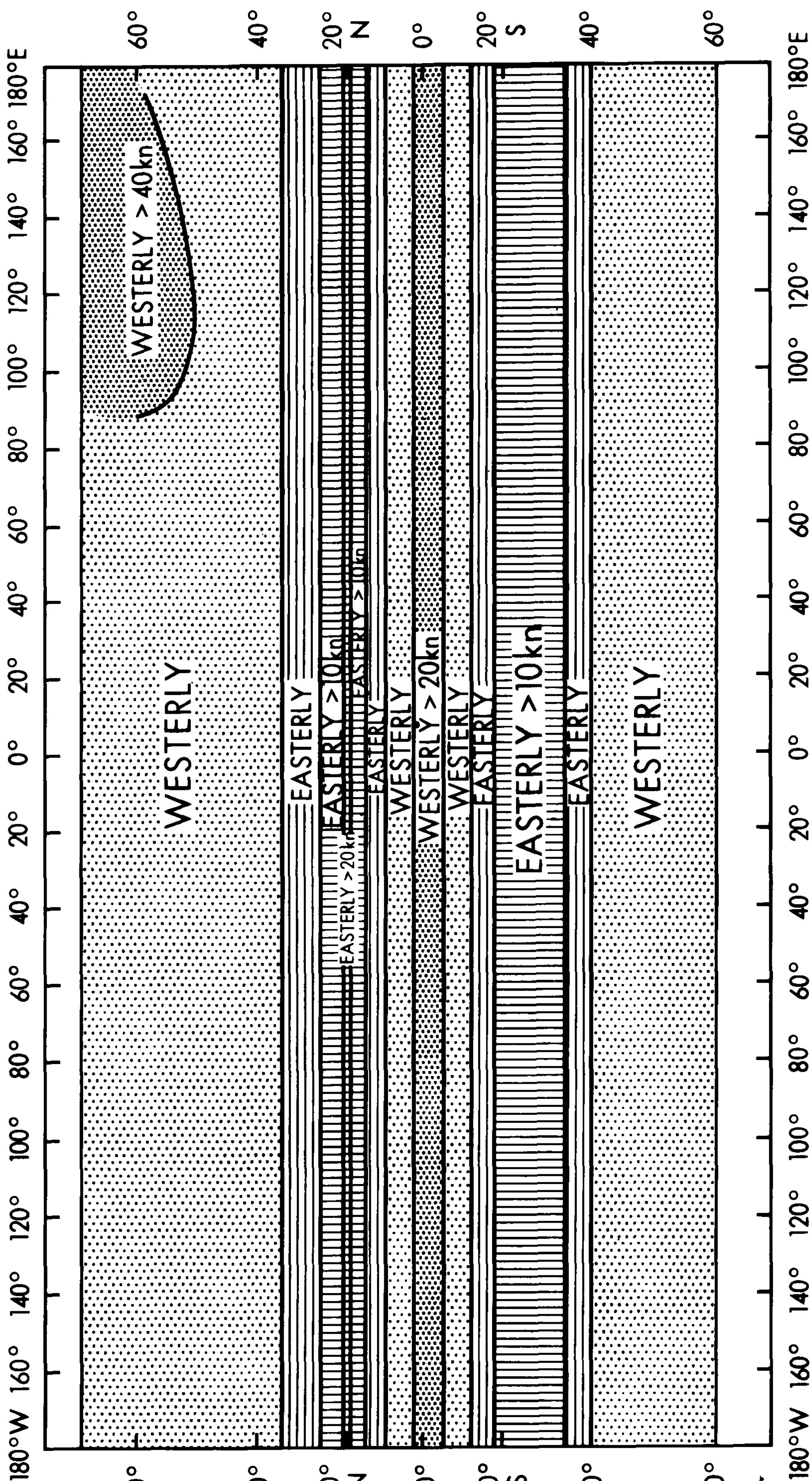

FIGURE 41. 30-MILLIBAR MONTHLY MEAN WINDS, OCTOBER 1966

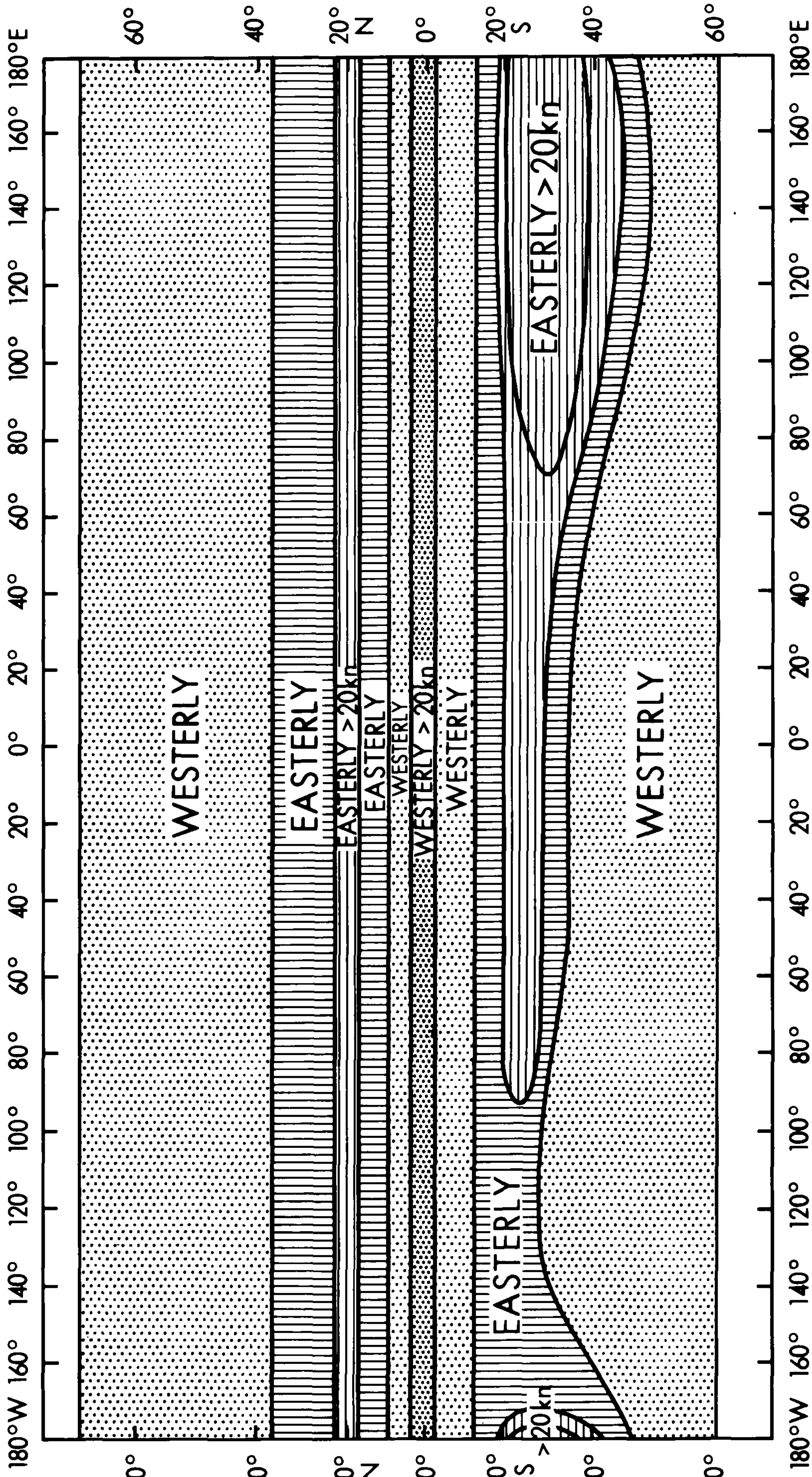

FIGURE 42. 30-MILLIBAR MONTHLY MEAN WINDS, OCTOBER 1971

Earlier in the text reference was made to the fact that the monthly mean temperatures in equatorial regions also show a fluctuation with a period of approximately 26 months. That this is so can be seen in Figure 43 which shows the 12-monthly running means of the 30-mb temperatures and the zonal wind components for Canton Island.

The range of the fluctuation in the monthly mean temperatures is about 4 deg and the two curves are out of phase by about 5 months. The annual variation in the monthly average 30-mb temperatures at Canton Island is shown in Figure 44. These values (based on data for 12 years from 1955 to 1966) show a maximum in July and a minimum in February with the range of this annual variation being about 4 deg. This annual temperature variation is a feature of the lower and middle stratosphere over the whole hemisphere but it is much more pronounced in high latitudes than near the equator. In the higher stratosphere (say 10 mb and above) there is a very marked semi-annual variation, the amplitude of which increases with height and latitude to show a maximum at the stratopause in polar regions. However, in low latitudes where the annual variation is smaller, the semi-annual variation (although not as large as in high latitudes) becomes a noticeable feature with maxima occurring in the spring and autumn and minima in winter and summer. The 30-mb average monthly temperatures for Canton Island (Figure 44) show that the semi-annual variation is not very evident at that level and accounts for only 5 per cent of the total variance whereas the annual variation accounts for 23 per cent. The QBO is the dominant feature and accounts for 46 per cent of the total variance.

9 – THE SPRING REVERSAL OF 30-MILLIBAR WINDS OVER SCOTLAND

From the charts included in this publication we know that in winter the high-latitude stratosphere is dominated by two features – a cold circumpolar vortex with a strong westerly circulation and a warm high centred over the Aleutian/Kamchatka area. In summer there is a complete reversal of the flow and the dominant feature in the stratosphere is a warm high centred near the North Pole with a very light easterly drift over high latitudes. The final warming (see section 3) is, of course, directly connected with this reversal of the flow and, as has been stated earlier in the text, the time at which this warming of the stratosphere and reversal of the circulation takes place and also the way in which it happens can and does vary quite considerably from year to year. In order to illustrate these variations in the region of the British Isles the 30-mb wind data from radiosonde stations in Scotland (namely Leuchars, Shanwell and Stornoway) were analysed for the period 1958–75. The 13-year average (1958–70) of the pentad (i.e. 5-day) mean values of the zonal wind component for January to October are shown in Figure 45. The winter westerlies, which are stronger than 40 kn for most of January and February, decrease in the spring and change to light easterly towards the end of April. The pentad average zonal component remains about 10 kn easterly throughout the summer and changes back to westerly again by late August or early September. The considerable year-to-year differences in the behaviour of the pentad mean zonal wind components in the spring can be seen in Figure 46. These diagrams show the mean zonal wind components for successive five-day periods during the months January to May in each of the years 1958–75. From these graphs it is evident that the years can be classified into three groups. There are the years 1958, 1965, 1966, 1968 and 1971 when the change-over can be said to be late. There are other years such as 1959, 1961, 1964, 1969, 1972, 1973, 1974 and 1975 when the easterlies were established early. There is another group of years when it is difficult to classify the onset of the easterlies with any degree of certainty although some of these might be considered as average, such as 1963, 1967 and 1970. The two years 1960 and 1962 are

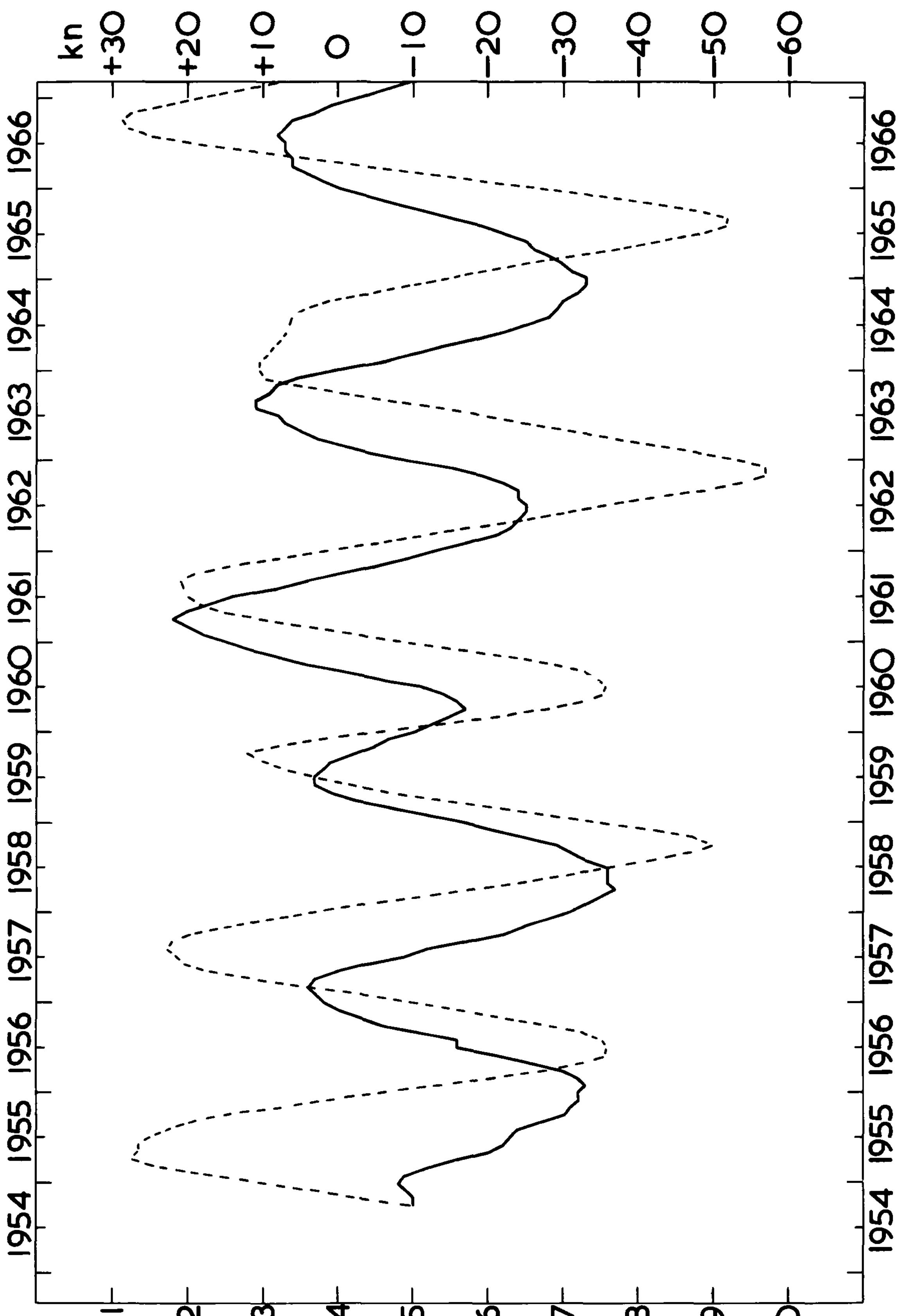

FIGURE 43. CANTON ISLAND 12-MONTHLY RUNNING MEANS OF TEMPERATURE (DEGREES CELSIUS) AND ZONAL WIND COMPONENTS (KNOTS) AT 30 MILLIBARS

——— Temperature   - - - - - - Wind

complicated by the reappearance of short-lived periods of westerly zonal component after the onset of the easterlies and, in view of the initial well-defined change-over it is considered that they are best described as 'average'.

FIGURE 44. 30-MILLIBAR MONTHLY AVERAGE TEMPERATURES AT CANTON ISLAND (1955–66)

In a year when the change-over occurs early the easterlies can be established as early as mid March but in years which can be classified as late, the first pentad mean easterly component may not occur until the end of April or early May and the final disappearance of the westerlies may not occur until towards the end of May. In presenting statistics of 30-mb winds during the early months of the year the spring reversal is obviously an important feature to bear in mind.

The curves in Figure 46 show that important year-to-year variations can also occur in the weeks before the summer easterlies are established. In many of the winters since 1958 the pentad mean zonal wind components have exceeded 70 kn – for short periods in some years, for longer periods in other years. On the other hand, there are years, such as 1961 when the pentad mean remained below 40 kn throughout most of the winter and years like 1963, 1971 or 1973 when it was near or below 20 kn for a considerable time. The diagrams presented in Figure 46 suggest that there is no simple connection between the strength of the zonal circulation early in the year and the date of the spring reversal. In years when the zonal component exceeded 80 kn

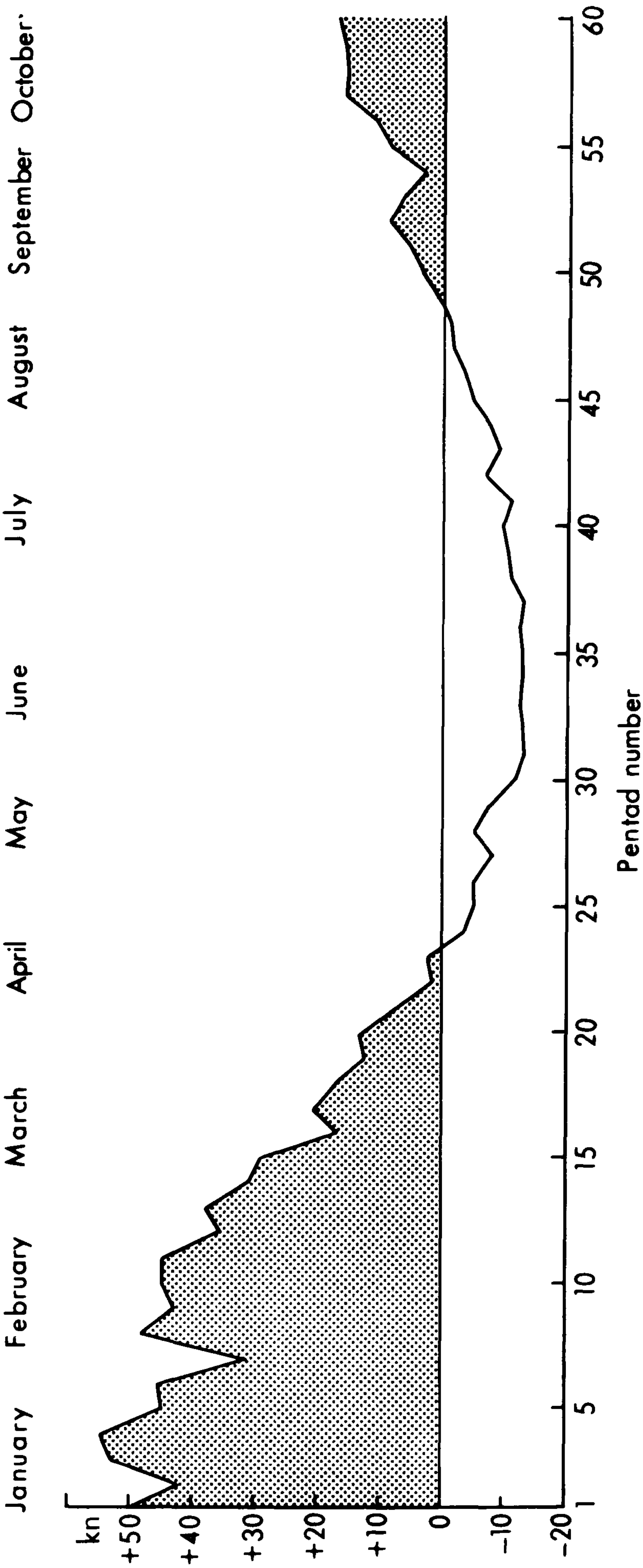

FIGURE 45. PENTAD AVERAGE ZONAL WIND COMPONENTS AT 30 MILLIBARS OVER SCOTLAND FOR JANUARY–OCTOBER (1958–70)

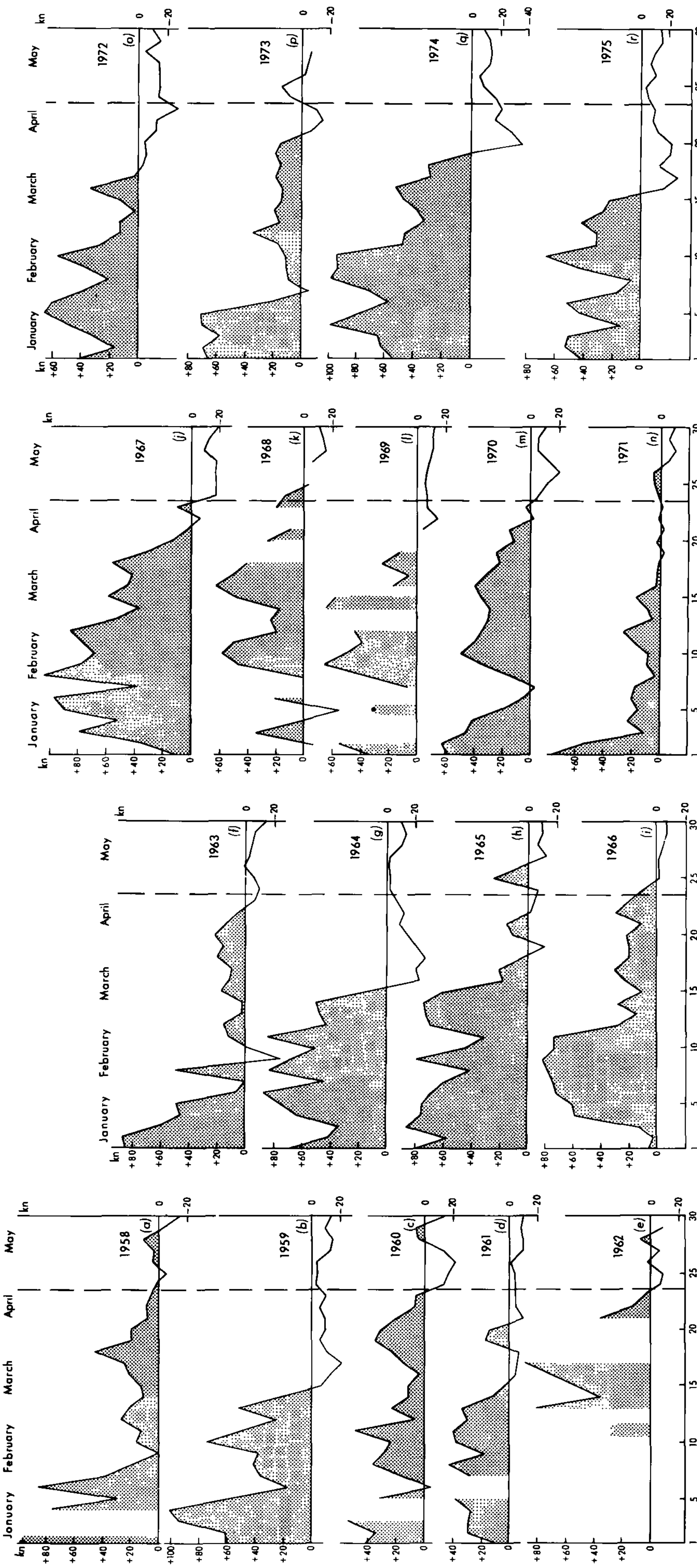

FIGURE 46. PENTAD MEAN ZONAL WIND COMPONENTS AT 30 MILLIBARS OVER SCOTLAND FOR JANUARY TO MAY OF EACH OF THE YEARS 1958–75

in some pentads the following spring reversals were late (as in 1958 and 1962) or early (as in 1959, 1964 and 1974). In years when the zonal circulation was generally much lighter, as in 1960 and 1961, the reversal to easterlies occurred at quite different times.

It has been suggested that the phase of the QBO in equatorial stratospheric winds may have a bearing on the spring reversal of stratospheric winds and the final warming in high latitudes. If the phase of the equatorial QBO in the 30-mb zonal wind component is such that, in the spring there is an increasing westerly (or decreasing easterly) component then there is a tendency for the change-over to stratospheric summer easterlies over Scotland to occur early. The converse is also true and a decreasing westerly (or increasing easterly) in the spring at 30 mb over the equator tends to be associated with a non-early (i.e. average or late) reversal to easterly at 30 mb over Scotland. However, the record shows that there are exceptions and so these 'suggestions' cannot be regarded as 'rules'. It may very well be that, in time, convincing theoretical arguments which are consistent with the observations, will be advanced to demonstrate that the equatorial and polar stratospheres are linked in such a way as that outlined above. A further possibility is that a connection might be found between the characteristics of the mid-winter circulation in the high-latitude stratosphere and the date of the spring reversal. At present there is no way of reliably forecasting the exact time of the change over to summer easterlies and it is unlikely that this will be possible until we have a better understanding of how known changes in the stratospheric circulation fit into the general circulation.

10 – THE AUTUMN REVERSAL OF 30-MILLIBAR WINDS OVER SCOTLAND

From the average contour charts for July and August (Plates 16 and 17a) we know that in summer the high-latitude stratosphere is dominated by a warm high centred near the North Pole with a very light easterly drift over high latitudes. By September (Plate 17b) the average chart shows a low vortex centred near the pole with a light westerly flow established over high latitudes. The pentad average zonal components at 30 mb, based on data for Leuchars, Shanwell and Stornoway (Figure 47) indicate that, over Scotland, this reversal takes place around late August or early September, i.e. pentads 48 to 49. The curves of the extreme values in Figure 47 show that the pentad mean zonal wind component can be easterly until towards the end of October and the pentad means for the individual years from 1958 to 1975 (Figure 48) indicate the variability which occurs, at the 30-mb level, from one autumn to another. In most years the initial reversal to westerly takes place within a short period near the average time of late August. However, in most of the years, following the initial onset of the pentad mean westerly zonal wind components, the easterlies reappear at some stage during the autumn. This reappearance of the easterlies leads to a wide range (more than 30 kn) of mean zonal wind components during each pentad of October. Figure 47 shows that from late September to mid October (pentads 54–57) the pentad average zonal wind component increases from less than 5 kn to more than 15 kn. During pentad 57 (8–12 October), although all the years have a mean westerly component, the variability is considerable with values ranging between 36 kn and 1 kn. In six of the years (1960, 1966, 1968, 1969, 1971 and 1973) the pentad mean was greater than 20 kn whereas in 1958, 1959 1961, 1972 and 1974 it was less than 10 kn.

Although the autumn reversal from summer easterlies to winter westerlies takes place within a short period around the average date it is apparent from Figures 47 and 48 that the subsequent behaviour of the 30-mb winds over Scotland can be very different from one year to another, especially during October.

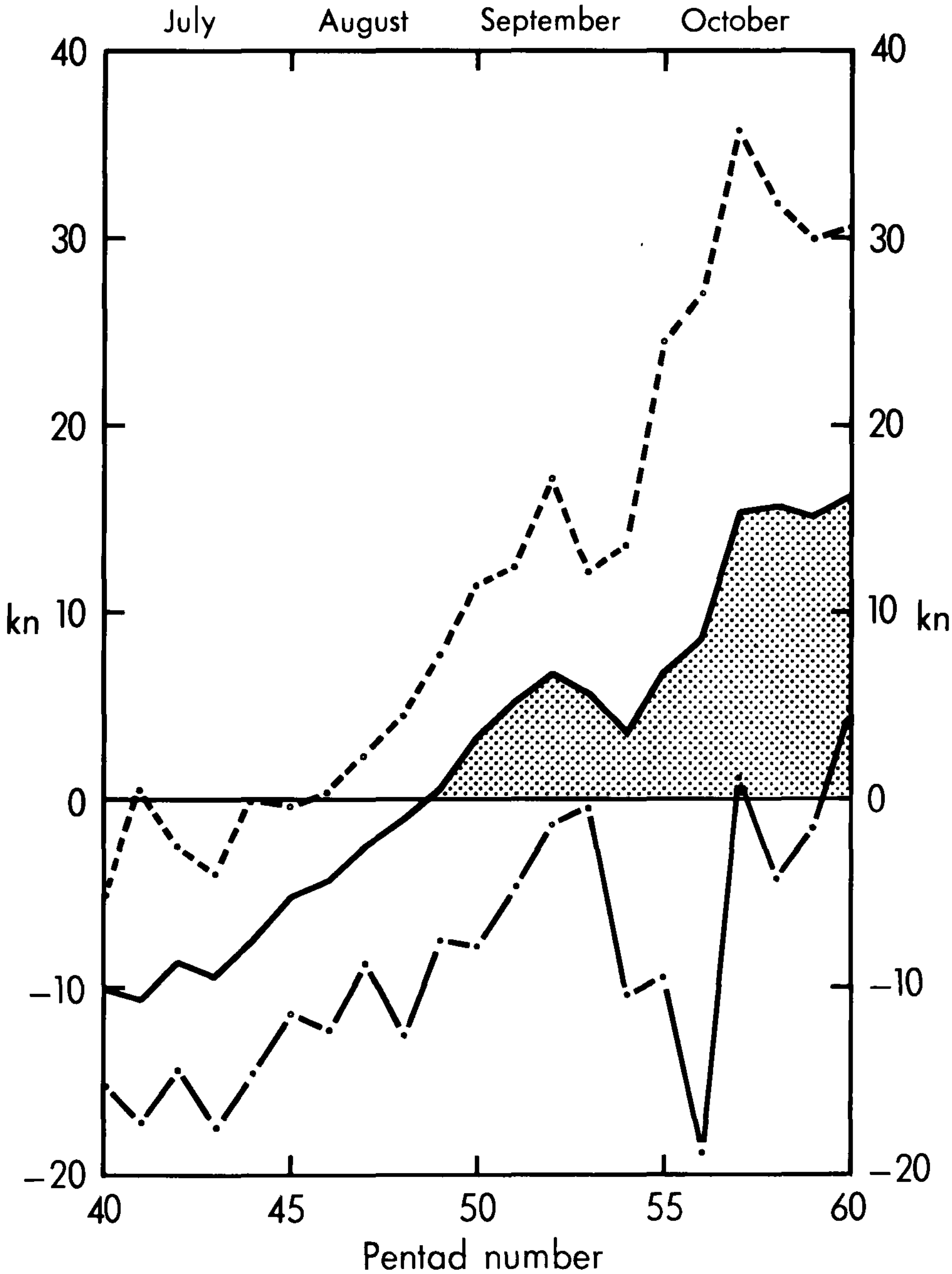

FIGURE 47. PENTAD AVERAGE ZONAL WIND COMPONENTS AT 30 MILLIBARS OVER SCOTLAND FOR JULY–OCTOBER (1958–74)

———— Maximum – – – – – Minimum Extreme values for each pentad

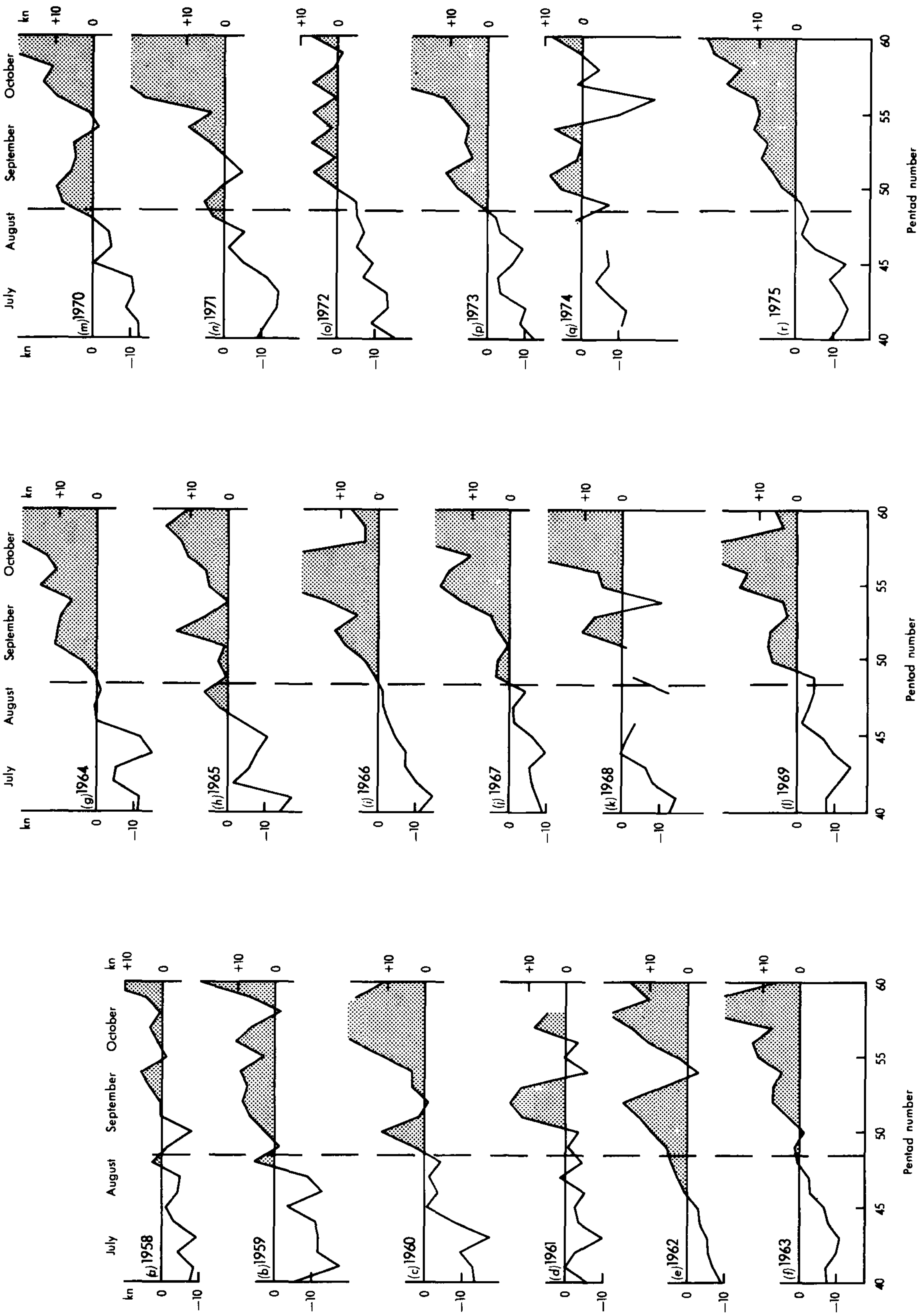

FIGURE 48. PENTAD MEAN ZONAL WIND COMPONENTS AT 30 MILLIBARS OVER SCOTLAND FOR JULY TO OCTOBER OF EACH OF THE YEARS 1958–75

ACKNOWLEDGEMENTS

Thanks are due to all those meteorological services whose data have been used and in particular to those who very kindly supplied data which supplemented their published material. Grateful acknowledgement is made to those who have given helpful advice and guidance during the preparation of this *Memoir* and also to the members of the staff of the Synoptic Climatology Branch of the Meteorological Office who were responsible for assembling the data.

REFERENCES

CRUTCHER, H.L.	1957	On the standard vector-deviation wind rose. *J Met, Lancaster, Pa,* 14, p. 28.
EBDON, R.A.	1970	Average temperatures, contour heights and winds at 50 millibars over the northern hemisphere. *Geophys Mem, London,* 15, No. 112.
HAWSON, C.L.	1964	Notes for the Central Forecast Office on analysis at 100-mb, 50-mb and 30-mb levels. (Unpublished, available in the Meteorological Office Library.)
MAHER, J.V. AND McRAE, J.N.	1964	Upper wind statistics, Australia, June 1975 to May 1961. Bureau of Meteorology, Melbourne.
RANGARAJAN, S. AND MOKASHI, R.Y.	1966	Some aspects of the statistical distribution of upper winds over India. *Indian J Met Geophys, New Delhi,* 17, p. 25.
Washington, United States Weather Bureau	1955–64	Northern hemisphere. Part II. Data tabulations. Washington, D.C. 1955–64.

APPENDIX I – STATISTICS FOR THE STATIONS USED IN THE CHI-SQUARE TESTS

Station	Position	Month	Vector mean wind deg kn	Standard deviation of wind components zonal kn	Standard deviation of wind components meridional kn	Number of observations	Circularity test per cent *0–30	Circularity test per cent 30–60	Circularity test per cent 60–90	Chi-square values for ellipticity test with axes E/W or N/S per cent *0–30	Chi-square values for ellipticity test with axes E/W or N/S per cent 30–60	Chi-square values for ellipticity test with axes E/W or N/S per cent 60–90	Ellipticity test using true major axis per cent *0–30	Ellipticity test using true major axis per cent 30–60	Ellipticity test using true major axis per cent 60–90	Angle of rotation ** deg	Correlation coefficient
Canton Island	2°46′S, 171°43′W	Jan.	094 10	30.1	7.3	311	52.6	191.5	101.7	22.1	32.8	84.4	25.5	83.1	44.5	−2.0	−0.1
		Apr.	090 19	31.1	7.4	352	17.1	74.7	119.5	6.9	16.0	17.9	7.7	17.9	16.0	0.6	0.0
		July	084 05	36.3	7.7	396	20.7	97.4	421.7	42.6	138.6	9.9	39.4	109.9	16.1	0.2	0.0
		Oct.	093 10	36.9	7.7	331	56.8	297.0	219.4	61.7	76.6	45.1	70.6	34.4	109.3	−0.2	−0.0
Ponape	6°58′N, 158°13′E	Jan.	081 07	29.0	5.7	151	5.1	57.0	37.6	6.2	4.7	8.5	5.5	2.5	8.4	0.9	0.1
		Apr.	088 16	25.5	7.3	191	14.1	30.5	51.5	2.4	1.6	12.7	4.2	0.5	7.3	0.9	0.0
		July	089 28	23.5	5.3	228	32.2	79.0	182.5	13.8	25.9	20.8	9.4	63.3	3.0	1.5	0.1
		Oct.	089 17	30.7	5.8	159	30.1	57.8	98.3	11.4	6.8	18.6	8.8	9.5	39.0	−0.3	−0.0
Balboa	8°56′N, 79°34′W	Jan.	082 06	28.1	6.9	383	35.6	71.4	124.2	0.6	3.8	52.1	2.8	6.4	43.3	−1.2	−0.1
		Apr.	089 15	24.7	6.5	403	31.9	65.9	128.8	15.3	11.9	16.9	11.4	9.4	12.3	−1.1	−0.1
		July	090 29	23.5	7.1	357	34.4	129.8	197.6	39.9	48.1	1.5	37.3	31.2	3.9	−0.2	−0.0
		Oct.	088 14	29.2	5.5	367	22.4	115.2	236.1	12.7	33.6	7.9	13.5	33.8	6.0	−2.2	−0.2
Yap	9°29′N, 138°05′E	Jan.	098 07	28.9	6.9	136	33.4	29.8	38.9	8.3	11.7	0.9	7.9	3.7	4.1	−3.2	−0.2
		Apr.	089 15	26.0	9.0	130	32.9	19.6	53.6	6.3	10.3	25.7	18.8	8.2	8.3	−4.3	−0.2
		July	093 34	16.0	7.3	101	5.2	75.2	14.8	2.8	35.8	4.6	9.8	5.1	6.2	−2.2	−0.1
		Oct.	095 20	25.7	6.4	144	19.7	25.9	62.0	0.8	12.3	8.8	1.8	7.2	12.9	−3.9	−0.3
Chaguaramas Bay	10°41′N, 61°37′W	Jan.	080 08	29.4	7.2	241	26.1	34.3	132.2	7.2	13.0	11.6	10.5	10.6	8.9	2.1	0.1
		Apr.	083 16	22.5	7.1	280	39.2	37.9	47.4	10.7	2.4	8.1	10.7	3.2	6.3	1.7	0.1
		July	088 34	20.1	5.2	268	54.6	100.6	78.3	36.7	23.6	4.7	20.0	18.9	13.4	2.9	0.2
		Oct.	092 18	27.9	8.8	249	16.8	38.6	206.5	4.6	69.8	15.0	0.9	63.6	16.8	1.1	0.1
Eniwetok Atoll	11°21′N, 162°21′E	Jan.	093 10	24.1	6.6	395	29.8	64.8	103.0	4.4	17.3	29.0	3.1	19.3	30.8	−0.6	−0.0
		Apr.	094 18	20.2	6.3	384	85.6	55.2	99.2	13.0	8.9	14.9	13.1	9.1	16.8	−0.7	−0.0
		July	091 38	14.8	5.9	405	17.3	62.1	175.7	18.6	48.1	0.8	19.0	52.2	3.6	−1.8	−0.1
		Oct.	092 21	23.7	7.5	382	37.1	55.4	191.0	13.5	30.7	39.5	16.0	36.8	31.2	−3.2	−0.2
San Andrés	12°35′N, 81°42′W	Jan.	095 10	21.7	11.2	218	34.2	16.0	34.3	9.1	5.1	20.1	15.9	2.1	15.7	−7.3	−0.2
		Apr.	087 15	19.3	9.2	248	20.2	29.4	29.1	8.7	14.0	6.5	12.4	5.9	8.8	3.9	0.1
		July	098 32	19.6	11.6	195	16.1	15.8	14.4	12.3	21.6	8.3	14.2	11.3	9.7	3.3	0.1
		Oct	095 15	20.5	8.7	207	24.2	25.0	50.4	3.9	10.4	12.1	4.0	5.6	22.5	−6.5	−0.2
Aden	12°50′N, 45°02′E	Jan.	106 03	24.0	6.6	113	7.9	28.9	39.1	10.2	1.1	3.2	8.6	1.1	3.9	−0.1	−0.0
		Apr	094 16	18.0	6.1	110	1.4	22.3	42.2	4.0	3.0	1.7	2.4	3.4	3.9	−2.7	−0.1
		July	089 40	14.3	5.4	55	4.7	9.0	9.1	3.2	5.1	1.1	2.3	9.9	3.1	−3.9	−0.2
		Oct.	090 21	23.0	5.2	81	8.0	12.9	19.5	0.7	5.0	12.7	3.3	0.3	3.2	−0.3	−0.0
Guam	13°33′N, 144°50′E	Jan.	091 10	19.0	5.3	415	17.6	60.0	114.1	12.2	3.1	13.1	7.3	1.2	13.5	−0.1	0.0
		Apr.	092 17	15.9	5.1	390	42.1	43.5	77.5	3.7	10.0	1.6	2.9	8.6	3.1	−0.7	−0.0
		July	089 40	12.9	5.4	403	11.1	66.6	78.4	8.5	12.8	8.8	4.6	4.8	8.7	−0.9	−0.0
		Oct.	090 24	19.7	5.3	366	25.9	87.3	134.7	14.4	16.2	7.9	12.3	14.0	12.2	−0.2	−0.0

* Probability bands

** The angle between the true major axis of the ellipse and the east–west (or occasionally north–south) axis. A negative sign represents rotation in the clockwise direction.

APPENDIX I – STATISTICS FOR THE STATIONS USED IN THE CHI-SQUARE TESTS *(CONTD)*

Station	Position	Month	Vector mean wind *deg kn*	Standard deviation of wind components zonal *kn*	meridional *kn*	Number of observations	Circularity test *per cent* *0–30	30–60	60–90	Chi-square values for Ellipticity test with axes E/W or N/S *per cent* *0–30	30–60	60–90	Ellipticity test using true major axis *per cent* *0–30	30–60	60–90	Angle of rotation ** *deg*	Correlation coefficient
Clark	15°10′N, 120°34′E	Jan.	086 09	17.0	6.3	458	9.7	61.0	84.0	3.1	23.4	6.0	1.6	14.7	6.7	5.2	0.2
		Apr.	083 15	14.0	6.3	423	33.3	25.8	47.2	11.8	10.2	2.0	11.7	10.3	0.9	3.7	0.1
		July	086 42	12.5	7.1	390	9.9	28.9	39.1	7.4	21.5	12.7	5.0	19.6	11.3	3.3	0.1
		Oct.	085 23	17.8	6.3	451	28.4	88.6	122.7	3.6	26.8	9.8	4.6	30.2	12.8	1.3	0.1
Johnston Island	16°44′N, 169°31′W	Jan.	079 04	15.3	7.3	239	9.1	17.4	41.8	2.8	7.9	8.9	2.4	13.5	6.3	−3.9	−0.1
		Apr.	095 14	12.2	5.8	233	28.7	10.3	24.3	16.4	5.7	5.1	14.8	8.9	3.8	2.5	0.1
		July	091 39	9.8	4.8	196	6.4	7.1	18.8	0.8	1.6	7.2	2.8	2.0	1.1	2.4	0.1
		Oct.	091 18	16.5	7.4	252	14.6	30.6	41.8	6.3	4.9	13.0	6.8	4.8	12.8	−0.3	−0.0
Kingston	17°56′N, 76°47′W	Jan.	085 09	14.9	6.6	241	34.1	16.8	26.3	8.0	7.3	8.3	9.4	4.3	4.4	−2.2	−0.1
		Apr.	091 13	11.4	6.8	232	13.2	15.0	18.9	7.3	3.8	6.9	14.7	3.1	5.8	−2.9	−0.1
		July	091 42	11.3	7.3	311	4.0	23.0	30.3	5.6	12.1	5.4	6.1	11.2	5.3	1.3	0.0
		Oct.	090 19	14.5	5.3	263	7.8	44.9	39.2	7.5	1.5	4.5	7.3	2.3	5.3	−1.2	−0.1
Wake Island	19°17′N, 166°39′W	Jan.	094 06	10.7	5.8	414	8.7	22.7	34.6	8.9	2.9	8.0	11.3	5.6	10.0	−5.2	−0.1
		Apr.	094 12	11.4	5.0	430	25.7	51.9	48.5	8.3	7.3	3.9	7.2	6.1	4.8	1.8	0.1
		July	091 43	9.0	5.4	408	2.7	18.6	25.4	7.5	7.5	1.7	6.5	3.8	0.7	−5.5	−0.1
		Oct.	090 22	11.2	6.0	361	3.1	20.0	50.4	3.4	1.8	4.1	4.3	2.5	3.4	1.5	0.0
Merida	20°56′N, 89°41′W	Jan.	082 02	15.5	6.1	293	44.3	32.9	39.3	16.1	4.9	11.3	7.8	8.8	9.1	2.5	0.1
		Apr.	083 12	11.4	6.0	304	4.4	10.3	29.5	5.6	1.3	8.2	3.2	1.8	6.6	5.5	0.1
		July	089 40	9.0	5.9	346	2.8	4.5	17.0	4.1	1.5	2.7	3.8	2.4	0.3	−0.7	−0.0
		Oct.	085 19	11.2	5.2	338	10.8	20.4	40.5	3.7	2.6	3.9	4.2	3.1	1.5	1.5	0.0
Lihue	21°59′N, 159°21′W	Jan.	097 04	11.3	6.5	338	6.6	12.9	38.0	4.9	1.3	2.0	4.0	0.4	2.7	3.1	0.1
		Apr.	093 10	9.4	4.8	366	18.2	12.9	41.0	3.7	7.9	2.1	4.0	4.6	2.1	6.0	0.2
		July	092 43	8.6	6.0	378	20.2	5.2	18.6	13.0	10.3	7.1	6.3	12.3	6.0	−21.7	−0.3
		Oct	092 17	9.5	5.3	393	4.9	23.9	41.7	3.4	4.7	0.3	4.1	8.3	0.1	−3.7	−0.1
Central Airfield Iwo Jima	24° 47′N, 141°20′E	Jan.	096 04	22.6	7.5	315	68.7	38.0	41.0	16.7	4.8	9.0	19.4	3.3	8.4	6.6	0.3
		Apr.	095 07	11.4	5.9	349	18.0	27.8	42.5	3.7	5.5	1.9	3.8	5.8	4.0	2.8	0.1
		July	093 41	7.3	7.6	360	13.8	9.7	10.7	12.3	10.7	11.8	15.7	13.9	11.5	79.5	0.0
		Oct.	095 17	9.3	5.9	338	5.2	10.5	22.1	13.7	4.7	3.0	13.0	4.4	3.4	−1.9	−0.0
Miami	25°48′N, 80°16′W	Jan.	262 02	14.7	5.2	312	61.3	22.7	47.4	28.6	8.2	11.3	26.2	5.3	10.6	5.6	0.2
		Apr.	079 07	10.0	4.8	345	23.4	12.6	38.0	10.2	8.3	2.5	9.3	8.0	2.4	3.2	0.1
		July	090 39	7.6	5.3	357	1.1	3.1	17.1	1.0	1.5	2.5	2.7	1.2	2.2	3.7	0.0
		Oct.	081 11	9.6	5.6	337	12.0	4.3	28.0	13.4	8.4	2.5	9.5	7.3	3.9	2.9	0.1
Kadena	26°21′N, 127°45′E	Jan.	220 02	15.8	7.4	366	10.5	10.1	51.2	8.7	1.3	2.7	13.5	0.9	1.1	4.3	0.1
		Apr.	090 03	11.2	6.5	431	7.4	34.0	26.6	12.4	9.2	2.7	8.9	5.9	3.1	6.3	0.1
		July	091 41	7.8	6.8	462	23.3	9.0	2.6	23.9	11.2	4.5	34.5	8.2	2.8	−15.0	−0.1
		Oct.	091 13	8.7	5.2	452	5.6	19.4	36.4	7.1	3.7	2.1	4.0	2.1	1.6	4.3	0.1

* Probability bands

** The angle between the true major axis of the ellipse and the east–west (or occasionally north–south) axis.
A negative sign represents rotation in the clockwise direction.

APPENDIX I – STATISTICS FOR THE STATIONS USED IN THE CHI-SQUARE TESTS *(CONTD)*

Station	Position	Month	Vector mean wind *deg kn*	Standard deviation of wind components zonal *kn*	Standard deviation of wind components meridional *kn*	Number of observations	Circularity test *per cent* *0–30	Circularity test 30–60	Circularity test 60–90	Chi-square values for Ellipticity test with axes E/W or N/S *per cent* *0–30	30–60	60–90	Ellipticity test using true major axis *per cent* *0–30	30–60	60–90	Angle of rotation ** *deg*	Correlation coefficient
Midway Island	28°13′N, 177°22′W	Jan.	094 08	16.5	6.9	116	17.6	15.5	24.0	2.9	26.0	4.0	14.1	12.3	4.5	0.5	0.0
		Apr.	081 04	9.8	6.4	271	39.3	4.5	20.7	24.4	5.5	5.3	26.4	5.2	3.2	15.7	0.3
		July	089 31	11.7	7.1	314	51.8	47.3	28.2	44.1	9.9	24.1	61.5	7.6	27.9	1.2	0.0
		Oct.	090 08	9.0	5.6	276	3.9	14.2	23.8	0.9	12.2	2.8	8.6	3.5	2.2	−0.3	−0.0
El Paso	31°48′N, 106°24′W	Jan.	279 08	18.5	8.9	285	72.6	31.5	37.1	33.8	20.3	16.6	24.5	15.7	4.1	18.4	0.6
		Apr.	075 03	11.1	6.8	310	14.5	15.9	20.7	12.7	5.1	6.6	10.9	2.8	12.2	10.7	0.2
		July	089 31	8.1	4.6	427	18.4	38.1	27.9	31.1	2.2	15.5	28.7	5.4	12.5	−5.1	−0.1
		Oct.	276 01	11.8	5.6	330	12.6	56.7	49.3	9.7	3.4	5.4	3.5	4.3	4.3	9.9	0.3
Kindley Field	32°22′N, 64°41′W	Jan.	260 15	23.2	11.1	352	85.9	16.7	54.4	53.6	10.3	25.5	51.5	8.3	14.4	−7.0	−0.2
		Apr.	114 02	11.7	6.2	424	38.8	40.8	41.8	18.5	4.6	17.0	17.2	19.1	20.1	11.3	0.3
		July	090 29	8.1	6.3	444	75.6	13.7	49.0	51.5	17.8	47.4	44.3	16.2	42.7	10.4	0.1
		Oct.	073 03	9.4	5.7	428	3.1	19.3	45.1	1.2	3.8	6.4	2.0	1.6	8.0	4.7	0.1
San Diego	32°44′N, 117°10′W	Jan.	323 05	19.5	7.1	401	45.1	92.1	61.8	49.6	16.3	8.5	30.5	14.2	5.1	7.3	0.3
		Apr.	068 01	8.8	4.8	391	23.2	21.0	30.4	17.5	2.1	12.5	18.7	3.7	10.7	8.0	0.2
		July	089 29	5.6	3.7	392	10.5	16.0	10.1	8.9	2.7	7.3	13.8	3.8	7.1	−0.4	−0.0
		Oct.	298 01	9.3	4.5	432	5.9	36.1	70.8	4.2	6.0	1.0	5.8	4.5	1.5	2.2	0.1
Fort Worth	32°54′N, 97°02′W	Jan.	270 13	15.1	8.9	336	11.8	60.0	33.2	18.7	27.4	16.9	10.0	4.5	9.7	23.0	0.6
		Apr.	047 01	8.8	5.4	391	50.8	9.2	22.2	19.3	11.6	14.2	13.7	9.7	16.7	9.6	0.2
		July	089 29	6.0	3.8	411	4.2	53.7	28.2	9.1	2.5	3.1	5.3	6.9	3.3	2.5	0.0
		Oct.	283 02	11.4	4.9	391	16.9	40.5	61.0	15.6	6.9	8.9	17.9	7.8	1.0	8.1	0.3
Wheelus Field	32°54′N, 13°17′E	Jan.	279 10	24.7	12.6	412	32.0	29.8	52.1	14.8	7.2	16.8	7.1	12.4	9.2	14.6	0.4
		Apr.	215 01	14.1	9.1	406	94.8	24.1	43.9	80.1	5.6	36.4	73.6	4.8	38.2	14.0	0.2
		July	090 29	7.9	6.4	440	40.1	20.8	28.0	36.6	5.1	27.1	35.9	4.7	21.8	11.6	0.1
		Oct.	252 07	12.6	7.2	441	8.1	30.5	39.4	4.2	2.6	1.5	5.4	0.1	8.6	17.5	0.4
Mosulpo	33°12′N, 126°13′E	Jan.	267 10	28.2	13.5	268	32.2	45.4	32.0	25.7	8.7	16.1	25.3	5.4	16.4	−7.4	−0.2
		Apr.	272 06	15.9	7.1	367	8.8	48.9	52.8	6.0	11.9	4.3	6.2	12.4	3.9	0.0	0.0
		July	095 28	7.6	6.1	393	6.0	6.8	16.1	9.5	4.1	8.3	11.9	4.9	8.5	−11.6	−0.1
		Oct.	233 01	12.2	5.9	417	42.3	40.2	40.4	13.0	13.4	12.8	12.9	8.7	12.0	1.5	0.0
Kenitra	34°18′N, 6°36′W	Jan.	332 05	22.0	12.1	397	39.2	46.3	39.6	28.1	12.4	23.3	17.6	14.1	10.9	14.1	0.3
		Apr.	231 03	10.7	7.3	397	14.1	33.6	25.9	14.2	5.3	6.2	15.6	2.7	4.2	12.6	0.2
		July	090 27	9.2	5.2	410	60.2	14.1	31.5	23.6	12.8	18.2	20.6	13.8	17.6	1.4	0.0
		Oct.	258 08	12.1	6.7	433	23.6	23.4	49.4	13.1	3.7	7.7	11.8	5.3	6.7	3.3	0.1
OWS 'E'	35°00′N, 48°00′W	Jan.	242 02	11.8	6.5	136	12.7	17.7	17.6	9 3	4.3	8.1	15.0	3.7	1.4	−13.9	0.3
		Apr.	018 04	13.5	8.3	142	16.1	27.7	9.0	12.1	10.9	7.1	14.0	5.4	6.7	14.7	0.3
		July	089 23	12.1	9.3	171	10.8	13.3	15.0	14.3	15.6	12.0	12.4	9.9	12.5	− 4.1	−0.0
		Oct.	076 02	11.8	8.1	153	16.5	11.9	10.3	13.7	10.9	14.6	16.4	6.7	13.2	3.2	0.0

* Probability bands

** The angle between the true major axis of the ellipse and the east–west (or occasionally north–south) axis. A negative sign represents rotation in the clockwise direction.

APPENDIX I – STATISTICS FOR THE STATIONS USED IN THE CHI-SQUARE TESTS *(CONTD)*

Station	Position	Month	Vector mean wind *deg kn*	Standard deviation of wind components zonal *kn*	Standard deviation of wind components meridional *kn*	Number of observations	Circularity test *per cent* *0–30	Circularity test *per cent* 30–60	Circularity test *per cent* 60–90	Chi-square values for Ellipticity test with axes E/W or N/S *per cent* *0–30	Chi-square values for Ellipticity test with axes E/W or N/S *per cent* 30–60	Chi-square values for Ellipticity test with axes E/W or N/S *per cent* 60–90	Ellipticity test using true major axis *per cent* *0–30	Ellipticity test using true major axis *per cent* 30–60	Ellipticity test using true major axis *per cent* 60–90	Angle of rotation ** *deg*	Correlation coefficient
Qrendi	35°50′N, 14°26′E	Jan.	283 12	17.9	11.0	124	17.7	6.1	4.3	3.8	2.4	5.5	5.2	1.2	2.6	13.3	0.3
		Apr.	265 04	10.5	6.7	146	7.0	17.8	19.4	9.4	12.1	12.0	6.0	4.2	7.8	21.3	0.4
		July	091 24	7.0	5.0	216	9.2	1.1	8.4	8.7	3.8	3.6	6.0	6.0	4.4	8.3	0.1
		Oct.	259 12	11.6	8.2	185	3.2	7.2	11.5	3.9	2.0	6.8	2.0	0.9	3.1	23.1	0.4
Osan	37°06′N, 127°02′E	Jan.	257 14	23.9	7.7	349	40.0	100.0	106.1	4.9	39.0	16.0	9.1	24.5	7.4	2.3	0.1
		Apr.	255 09	17.9	7.4	415	38.7	122.9	79.6	16.5	41.8	7.7	16.5	51.0	10.2	5.7	0.2
		July	088 22	13.8	6.3	426	188.9	96.7	68.7	156.4	33.6	55.1	131.6	26.4	58.8	−7.0	−0.2
		Oct.	255 09	13.2	6.6	431	20.4	35.0	70.1	11.1	10.6	9.5	8.4	7.5	8.4	8.6	0.2
Wajima	37°23′N, 136°54′E	Jan.	241 12	28.2	9.1	180	21.9	45.9	38.7	7.2	10.3	8.5	2.6	15.2	9.6	2.0	0.1
		Apr.	265 05	16.7	7.0	215	3.7	85.5	37.8	4.6	14.1	6.1	12.6	2.1	5.4	4.8	0.2
		July	088 25	9.9	5.7	259	82.6	5.0	45.4	51.1	8.1	31.6	58.1	7.6	31.6	1.9	0.0
		Oct.	244 05	10.3	5.6	260	19.3	8.7	34.3	6.6	17.3	12.8	10.6	17.3	10.2	10.1	0.2
Sendai	38°16′N, 140°54′E	Jan.	220 07	24.6	8.4	227	48.6	40.3	35.0	16.8	3.4	7.0	23.8	3.1	8.0	0.2	0.0
		Apr.	243 04	13.0	6.4	210	19.1	25.6	28.9	13.6	19.3	1.6	13.3	11.2	3.3	10.7	0.3
		July	090 25	6.1	4.1	220	19.8	6.1	9.9	15.8	1.4	2.1	11.1	0.5	1.2	−12.0	−0.2
		Oct.	196 01	10.8	5.9	263	14.7	17.0	28.8	21.2	1.0	9.1	11.8	1.2	8.8	10.8	0.3
Lajes	38°45′N, 27°05′W	Jan.	264 11	26.7	11.7	373	37.7	38.7	40.0	38.4	2.5	17.9	25.4	13.1	12.4	8.6	0.3
		Apr.	010 03	11.0	7.3	418	29.9	9.6	28.7	29.5	4.2	11.2	23.9	5.1	15.8	16.4	0.3
		July	090 23	5.1	4.3	470	20.1	19.3	17.8	16.6	38.3	15.8	17.4	28.6	13.0	−5.0	−0.0
		Oct.	294 05	11.3	7.1	429	4.9	9.1	23.3	8.8	0.9	4.1	5.0	1.9	2.3	13.7	0.2
Denver	39°45′N, 104°52′W	Jan.	298 18	24.7	11.0	384	29.6	90.8	79.1	33.9	66.7	20.5	24.4	38.1	11.4	9.3	0.3
		Apr.	293 04	12.2	6.2	439	43.9	27.0	46.0	23.7	5.3	7.7	18.3	1.7	8.8	11.4	0.3
		July	089 20	5.4	3.7	406	7.1	4.1	27.2	1.5	5.8	1.5	3.0	2.9	1.6	1.1	0.0
		Oct.	285 07	9.1	5.2	419	8.2	15.5	28.6	2.0	2.7	2.2	2.4	1.5	0.2	4.5	0.1
Zaragoza	41°39′N, 1°00′W	Jan.	291 18	23.8	15.4	397	20.3	29.4	41.5	11.5	14.1	19.2	5.2	12.9	6.1	20.3	0.4
		Apr.	264 03	11.4	6.9	420	12.4	26.2	40.6	6.9	7.3	6.6	3.3	5.6	7.8	10.3	0.2
		July	096 20	5.6	4.3	397	4.2	4.7	9.5	9.0	1.6	1.6	9.3	13.5	3.1	12.5	0.1
		Oct.	266 11	12.6	8.3	384	21.4	10.0	36.2	14.5	19.3	11.5	13.1	11.0	6.1	25.1	0.5
Portland	43°39′N, 70°19′W	Jan.	260 39	25.7	17.9	286	11.5	29.0	21.3	5.6	16.1	10.0	8.8	32.3	9.6	12.4	0.2
		Apr.	274 07	13.7	7.5	345	76.9	62.1	27.2	80.4	30.6	16.4	69.9	21.2	20.2	7.8	0.2
		July	084 16	6.0	4.0	369	6.3	7.1	17.3	5.0	3.8	6.6	4.0	5.5	8.4	9.6	0.1
		Oct.	268 13	10.6	7.7	357	2.6	44.2	33.0	1.6	19.5	5.0	3.6	12.6	5.3	28.2	0.5
O.W.S. 'D'	44°00′N, 41°00′W	Jan.	257 11	13.6	7.6	179	23.0	10.8	13.1	7.4	7.8	6.9	4.8	0.8	8.2	−2.2	−0.0
		Apr.	050 01	13.5	9.5	95	25.4	8.6	15.7	19.5	7.3	11.2	14.1	5.0	6.5	23.7	0.4
		July	085 11	9.3	7.6	164	10.7	5.0	7.2	7.5	5.8	9.7	7.2	4.8	5.6	−14.0	−0.1
		Oct.	277 08	12.0	8.1	102	15.7	8.5	17.4	5.7	7.7	15.1	4.5	9.1	4.5	12.2	0.2

* Probability bands

** The angle between the true major axis of the ellipse and the east–west (or occasionally north–south) axis. A negative sign represents rotation in the clockwise direction.

APPENDIX I – STATISTICS FOR THE STATIONS USED IN THE CHI-SQUARE TESTS *(CONTD)*

Station	Position	Month	Vector mean wind *deg kn*	Standard deviation of wind components: zonal *kn*	Standard deviation of wind components: meridional *kn*	Number of observations	Circularity test *per cent* *0–30	Circularity test 30–60	Circularity test 60–90	Chi-square values for Ellipticity test with axes E/W or N/S *per cent* *0–30	Ellipticity test E/W or N/S 30–60	Ellipticity test E/W or N/S 60–90	Ellipticity test using true major axis *per cent* *0–30	Ellipticity test true major axis 30–60	Ellipticity test true major axis 60–90	Angle of rotation ** *deg*	Correlation coefficient
Beograd	44°47′N, 20°32′E	Jan.	279 35	27.7	20.6	147	3.3	7.8	8.5	1.3	6.8	11.8	3.0	8.5	6.7	3.9	0.0
		Apr.	251 08	16.6	9.0	168	8.7	49.3	12.3	7.1	26.5	10.2	6.0	10.0	9.0	19.9	0.5
		July	097 19	7.2	5.9	155	29.1	2.1	8.4	20.7	1.3	9.3	25.6	1.1	6.1	10.6	0.1
		Oct.	271 18	13.7	9.0	202	12.3	5.1	17.5	5.5	6.3	8.1	2.8	11.7	1.3	20.1	0.4
Salem	44°55′N, 123°01′W	Jan.	332 17	26.0	13.3	361	37.0	77.0	46.1	25.1	80.0	19.4	27.2	80.6	19.8	–4.5	–0.1
		Apr.	277 02	14.1	6.0	398	97.8	78.6	60.0	44.1	35.8	10.9	45.0	9.4	15.1	11.1	0.4
		July	089 15	4.7	3.4	416	8.8	13.7	18.4	5.3	3.3	16.1	4.4	3.0	15.2	8.5	0.1
		Oct.	285 08	10.0	6.5	386	4.1	47.5	24.1	2.3	43.0	2.0	8.6	21.4	2.8	17.0	0.3
Wakkanai	45°25′N, 141°41′E	Jan.	220 19	22.0	13.5	181	16.0	8.7	22.0	18.6	11.7	4.9	12.8	8.7	5.5	21.6	0.5
		Apr.	229 06	11.7	7.4	161	8.6	9.6	19.0	3.6	6.3	1.6	8.9	8.4	5.9	18.4	0.4
		July	087 19	5.9	4.5	254	11.5	11.0	16.6	9.0	11.1	1.0	6.4	12.3	3.4	–9.0	–0.1
		Oct.	250 17	18.8	10.1	239	34.1	24.9	20.6	40.8	11.5	8.2	34.9	6.2	9.1	–9.3	–0.2
Milano/Linate	45°26′N, 09°17′E	Jan.	282 31	27.9	22.2	255	12.0	19.4	9.1	14.4	4.7	13.1	9.1	4.1	3.8	29.5	0.4
		Apr.	271 04	13.8	6.9	266	88.3	37.1	23.2	52.3	3.6	22.3	46.0	4.4	18.2	6.6	0.2
		July	092 16	9.8	6.3	256	26.8	3.4	24.0	29.3	4.5	8.3	28.9	4.4	5.5	–5.1	–0.1
		Oct.	274 11	12.8	7.6	254	12.2	55.7	16.4	13.5	15.0	14.9	14.3	13.3	7.4	16.6	0.4
Chateauroux	46°51′N, 1°43′E	Jan.	288 33	31.7	19.5	286	17.2	16.8	57.4	10.7	7.0	15.0	16.5	5.8	3.5	11.2	0.2
		Apr.	314 03	13.9	6.7	359	70.4	25.3	32.1	24.8	7.9	14.9	26.4	5.8	16.0	0.2	0.0
		July	103 17	5.8	5.1	393	20.4	4.9	21.5	22.2	3.0	22.1	30.2	1.0	23.4	11.3	0.1
		Oct.	281 12	13.3	7.9	364	63.8	65.3	41.7	45.2	44.3	18.9	30.7	22.6	16.9	20.4	0.5
Wien	48°15′N, 16°22′E	Jan.	277 50	35.2	28.1	372	11.4	16.2	18.6	9.4	8.5	20.3	14.2	18.6	10.3	21.8	0.2
		Apr.	210 02	15.8	7.0	147	60.4	17.0	28.2	23.5	14.8	9.1	41.8	6.0	8.5	13.0	0.4
		July	099 16	5.1	3.5	372	35.8	14.9	17.7	25.4	30.2	2.5	15.6	17.7	11.7	15.4	0.2
		Oct.	286 15	8.7	8.7	194	12.1	13.2	5.8	12.6	14.1	5.8	2.9	5.2	2.7	45.0	0.5
International Falls	48°34′N, 93°23′W	Jan.	290 43	28.1	21.5	292	10.0	38.6	33.8	12.0	33.7	15.3	45.2	8.8	1.6	23.3	0.3
		Apr.	298 06	17.5	8.0	394	70.7	120.9	53.4	60.2	16.5	19.0	29.6	14.6	20.7	6.4	0.2
		July	085 13	6.7	4.4	387	19.9	20.0	20.7	22.9	7.3	14.3	19.3	7.8	17.5	4.2	0.1
		Oct.	289 12	10.6	7.7	345	14.0	41.2	14.5	17.3	15.5	13.2	10.2	5.7	6.8	17.6	0.2
Crawley	51°05′N, 00°13′W	Jan.	289 44	29.6	20.3	163	11.8	16.9	13.0	17.7	3.9	17.1	13.6	1.9	12.1	20.7	0.3
		Apr.	329 02	14.1	8.2	211	17.4	21.5	19.8	9.6	5.6	8.2	11.7	4.6	8.4	–0.1	–0.0
		July	097 15	4.9	4.4	207	3.8	4.3	1.6	2.4	5.1	1.2	5.7	2.2	3.0	18.1	0.1
		Oct.	288 13	10.4	7.4	309	5.4	12.8	22.1	8.5	6.6	7.1	6.0	9.3	1.7	19.2	0.3
Adak	51°53′N, 176°39′W	Jan.	154 06	19.2	14.4	258	9.0	6.8	14.7	10.3	12.1	6.1	12.8	6.5	9.4	–20.1	–0.2
		Apr.	141 05	15.3	9.9	246	45.1	13.6	17.2	42.3	6.3	8.8	28.3	5.0	12.0	–0.3	–0.0
		July	095 15	9.4	6.7	198	36.4	7.6	22.4	29.5	5.0	18.7	20.7	7.5	14.8	3.2	0.0
		Oct.	271 10	17.2	11.9	252	48.1	12.0	25.8	35.5	8.0	10.9	21.6	6.3	7.7	–14.0	–0.2

* Probability bands

** The angle between the true major axis of the ellipse and the east–west (or occasionally north–south) axis. A negative sign represents rotation in the clockwise direction.

APPENDIX 1 – STATISTICS FOR THE STATIONS USED IN THE CHI-SQUARE TESTS *(CONTD)*

Station	Position	Month	Vector mean wind *deg kn*	Standard deviation of wind components zonal *kn*	meridional *kn*	Number of observations	Circularity test *per cent* *0–30	30–60	60–90	Chi-square values for Ellipticity test with axes E/W or N/S *per cent* *0–30	30–60	60–90	Ellipticity test using true major axis *per cent* *0–30	30–60	60–90	Angle of rotation ** *deg*	Correlation coefficient
Hannover	52°28′N, 9°42′E	Jan.	288 47	25.3	18.3	78	1.9	10.1	4.2	2.8	6.9	5.0	1.4	3.3	6.3	14.0	0.2
		Apr.	327 03	13.9	7.2	176	18.9	28.6	27.8	12.5	15.8	6.6	14.3	6.6	8.2	2.0	0.0
		July	097 14	5.0	3.4	156	18.7	11.2	3.4	3.0	8.2	6.3	3.3	7.7	4.6	3.3	0.0
		Oct.	291 15	9.3	8.5	106	14.0	19.4	3.9	19.0	15.5	4.7	2.4	4.3	1.6	37.3	0.3
Goose	53°19′N, 60°25′W	Jan.	263 55	34.4	30.5	175	19.4	7.0	12.0	20.2	5.0	14.9	17.9	10.5	11.5	19.6	0.1
		Apr.	235 05	16.9	8.3	337	22.6	110.8	65.3	25.7	74.9	4.3	35.8	49.2	10.5	11.0	0.3
		July	094 12	5.9	4.7	334	3.9	13.9	17.7	19.3	3.6	9.3	11.3	2.4	8.7	2.8	0.0
		Oct.	266 20	13.5	10.6	334	2.5	16.2	9.1	0.5	13.1	4.6	1.7	9.4	5.5	29.4	0.4
Annette Island	55°02 N, 131°34′W	Jan.	324 30	21.8	24.5	210	16.6	11.4	2.7	25.9	8.7	6.5	15.4	27.4	16.2	−52.4	−0.4
		Apr.	003 04	13.1	7.7	275	42.0	18.1	26.0	19.4	7.0	10.8	22.3	3.7	7.6	−16.6	−0.4
		July	091 11	5.4	4.3	324	8.1	10.9	11.0	16.2	9.9	7.4	8.2	6.6	10.4	−18.5	−0.2
		Oct.	284 09	10.5	7.1	175	12.9	28.7	11.0	7.3	18.1	15.4	5.0	20.9	13.8	20.2	0.3
Churchill	58°45′N, 94°04′W	Jan.	305 41	32.6	34.9	103	17.1	7.5	15.9	17.5	11.7	14.7	1.7	12.5	7.7	−50.6	−0.3
		Apr.	323 08	20.0	10.0	249	35.7	39.9	27.3	18.4	16.3	19.6	24.4	6.1	15.0	0.3	0.0
		July	077 12	5.6	4.3	206	10.4	4.8	4.9	8.6	4.0	8.1	8.7	4.5	5.6	−3.1	−0.0
		Oct.	293 19	13.6	11.8	253	6.3	6.7	8.6	8.7	4.5	4.5	2.0	1.6	3.9	29.5	0.2
Orland	63°42′N, 09°36′E	Jan.	291 54	32.7	33.5	153	3.6	7.3	10.5	5.0	4.8	10.5	5.0	7.3	8.5	−2.4	0.1
		Apr.	300 13	24.5	18.0	284	36.7	19.2	23.3	47.5	5.2	24.7	30.2	11.4	24.4	4.0	0.0
		July	109 11	8.8	7.2	261	33.9	6.2	18.0	30.1	4.5	17.9	26.4	7.0	15.2	12.9	0.1
		Oct.	290 22	13.3	13.0	266	16.1	31.9	7.9	13.3	26.8	7.3	13.9	27.8	8.5	−11.2	−0.0
Keflavik	63°58′N, 22°36′W	Jan.	265 71	33.5	33.4	261	4.8	3.4	0.8	5.5	3.7	0.7	9.7	1.2	3.3	43.5	0.1
		Apr.	263 11	21.5	13.0	401	48.7	122.8	18.0	62.3	141.3	24.2	73.9	99.2	29.8	7.5	0.1
		July	085 11	5.4	4.3	399	25.8	1.9	10.7	23.1	3.5	11.6	23.1	5.7	7.0	12.0	0.1
		Oct.	257 21	14.2	13.6	347	6.0	10.4	3.2	5.7	12.7	4.2	2.5	2.6	6.1	40.1	0.3
Kotzebue	66°52′N, 162°38′W	Jan.	277 54	36.5	30.7	286	1.0	25.0	4.2	1.2	10.3	6.1	2.8	11.4	9.3	5.2	0.0
		Apr.	267 05	19.5	13.3	337	102.7	7.9	28.7	75.6	14.7	24.9	129.0	16.2	22.1	−0.4	−0.0
		July	084 10	5.0	4.5	347	12.0	16.1	25.1	16.3	13.5	23.8	30.9	0.6	18.8	6.6	0.0
		Oct.	259 31	13.1	14.0	339	9.5	3.4	4.1	11.0	4.5	5.1	11.1	6.9	5.0	54.4	0.2
Barter Island	70°08′N, 143°38′W	Jan.	304 73	30.8	32.8	260	8.5	20.9	34.9	9.3	18.4	37.2	2.0	1.5	7.8	−51.7	−0.3
		Apr.	302 12	28.0	13.4	356	273.4	79.8	70.4	191.5	39.3	49.0	204.3	25.9	46.6	−7.4	0.2
		July	088 09	4.8	4.8	315	16.0	5.5	15.7	16.0	5.7	16.4	21.0	2.2	13.7	45.0	0.2
		Oct.	269 31	15.4	13.6	321	79.2	15.2	28.0	20.4	6.1	7.0	19.1	6.1	13.7	32.0	0.3
Mould Bay	76°14′N, 119°20′W	Jan.	310 72	38.1	29.9	198	7.4	25.9	12.5	11.4	18.4	6.0	3.7	12.3	2.5	−21.9	−0.2
		Apr.	322 13	24.4	14.0	336	36.2	66.9	33.6	27.0	62.0	17.8	46.1	28.1	25.0	−16.8	−0.4
		July	087 07	4.4	4.0	361	3.6	8.2	4.4	3.5	6.4	1.3	7.0	6.1	5.2	−20.7	−0.1
		Oct.	275 27	18.7	15.3	273	52.3	8.3	21.9	55.3	5.1	20.4	34.0	8.0	11.9	−16.3	−0.1

* Probability bands
** The angle between the true major axis of the ellipse and the east–west (or occasionally north–south) axis.
A negative sign represents rotation in the clockwise direction.

APPENDIX I – STATISTICS FOR THE STATIONS USED IN THE CHI-SQUARE TESTS *(CONTD)*

Station	Position	Month	Vector mean wind		Standard deviation of wind components		Number of observations	circularity test			Chi-square values for Ellipticity test with axes E/W or N/S			Ellipticity test using true major axis			Angle of rotation **	Correlation coefficient
			deg	kn	zonal kn	meridional kn		per cent			per cent			per cent			deg	
								*0–30	30–60	60–90	*0–30	30–60	60–90	*0–30	30–60	60–90		
Thule	76°31′N, 68°50′W	Jan.	316	36	37.3	39.7	120	13.4	7.0	12.4	13.0	8.4	10.6	5.9	5.4	8.3	51.0	0.3
		Apr.	314	04	16.3	19.7	405	90.9	16.7	36.6	108.0	14.5	34.7	145.0	22.2	31.6	–71.3	–0.1
		July	093	08	3.8	3.7	427	3.4	9.4	3.2	3.4	7.4	3.2	10.0	5.8	6.6	35.0	0.1
		Oct.	268	17	13.6	18.0	370	8.2	9.4	18.9	10.5	3.7	6.9	7.4	2.4	7.7	–66.6	–0.3

* Probability bands

** The angle between the true major axis of the ellipse and the east–west (or occasionally north–south) axis. A negative sign represents rotation in the clockwise direction.

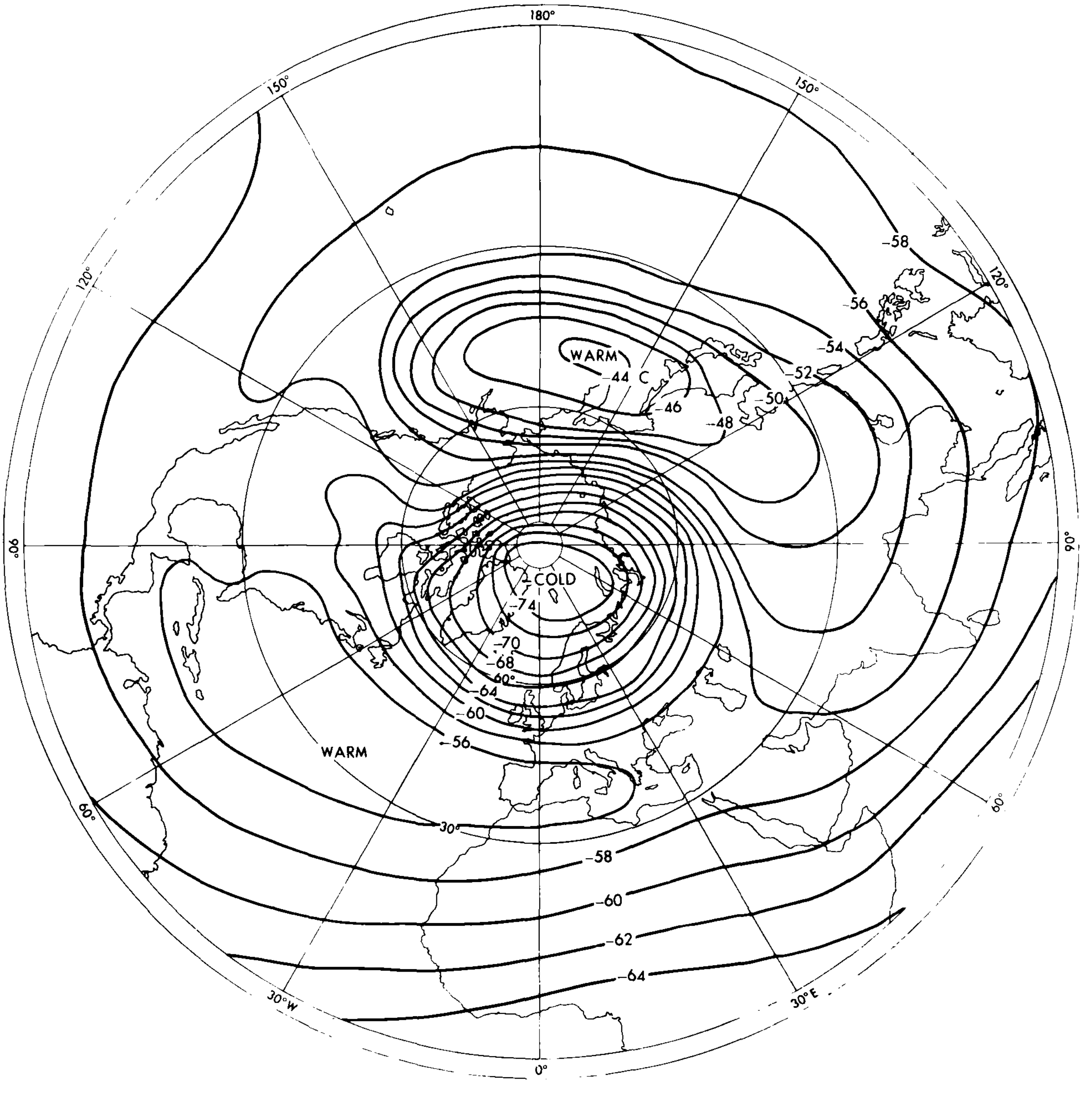

PLATE 1. AVERAGE TEMPERATURES AT 30 MILLIBARS OVER THE NORTHERN HEMISPHERE IN JANUARY, 1958–65

Temperatures are in degrees Celsius.

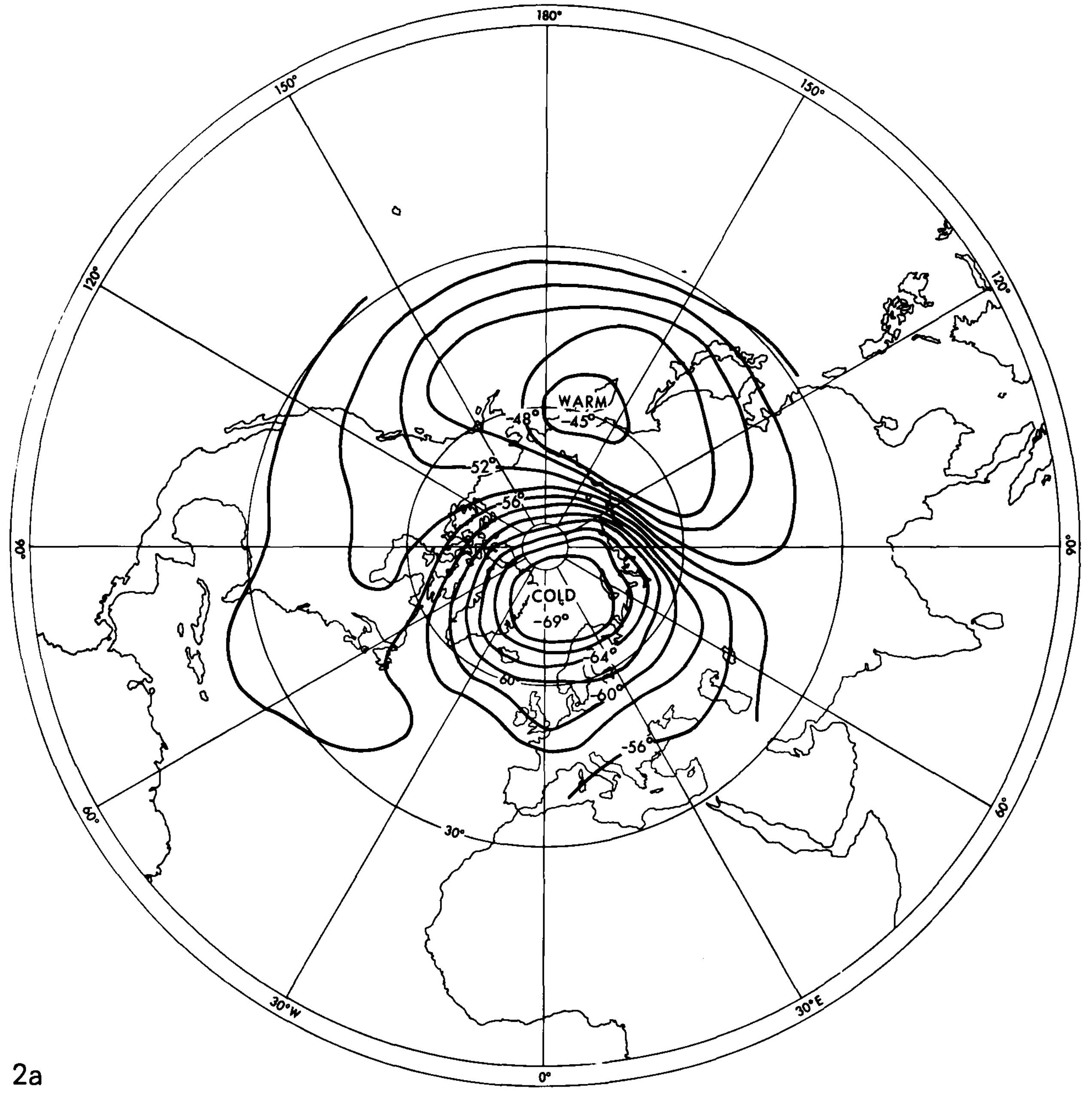

2a

PLATES 2a AND 2b. AVERAGE TEMPERATURES AT 30 MILLIBARS OVER THE NORTHERN HEMISPHERE (NORTH OF LATITUDE 45°N) IN FEBRUARY (2a) AND MARCH (2b), 1958–65

Temperatures are in degrees Celsius.

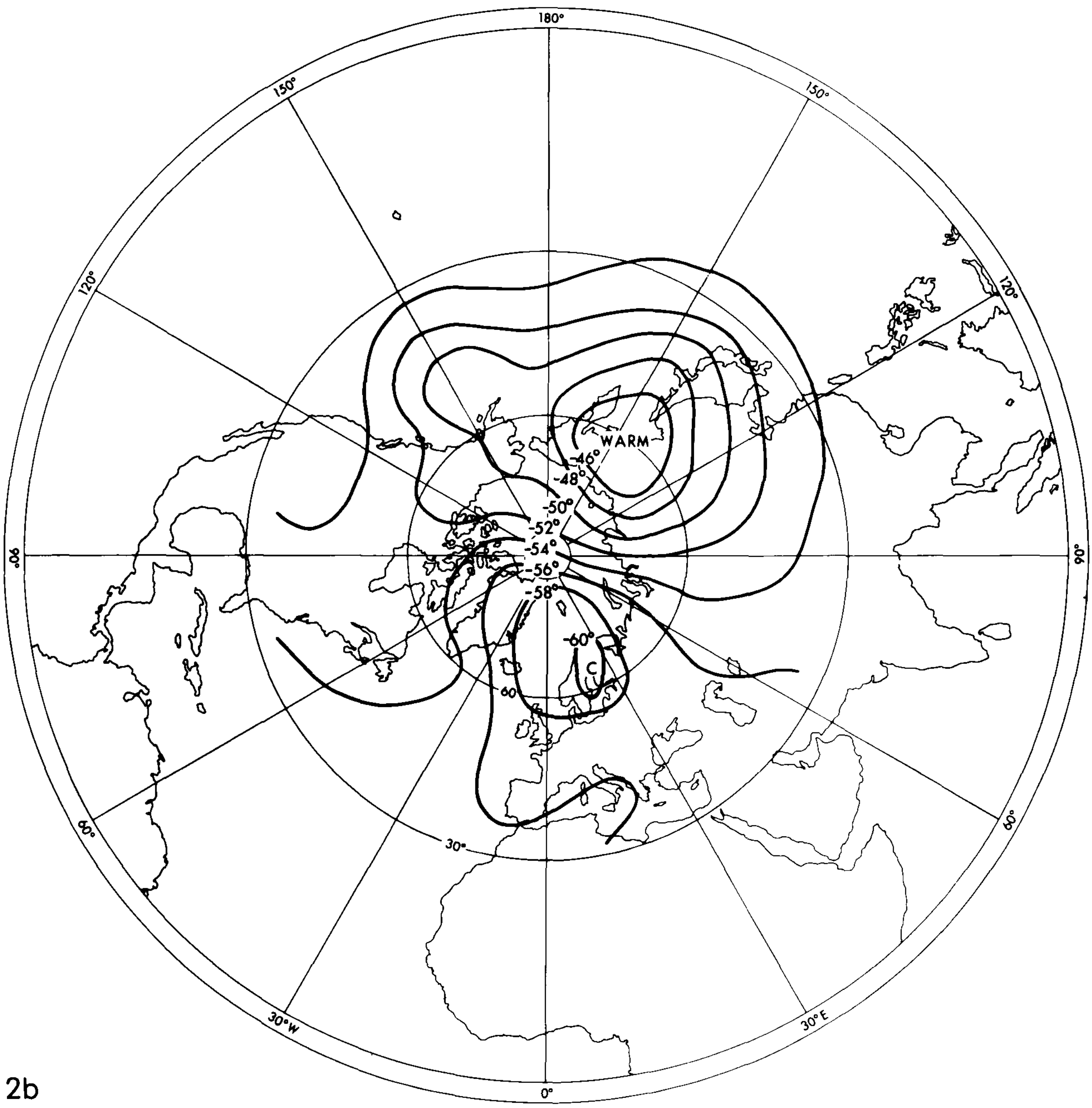
180°
150°
150°
120°
120°
90°
90°
60°
60°
30°W
30°E
0°
30°
WARM
-46°
-48°
-50°
-52°
-54°
-56°
-58°
-60°
C
60

2b

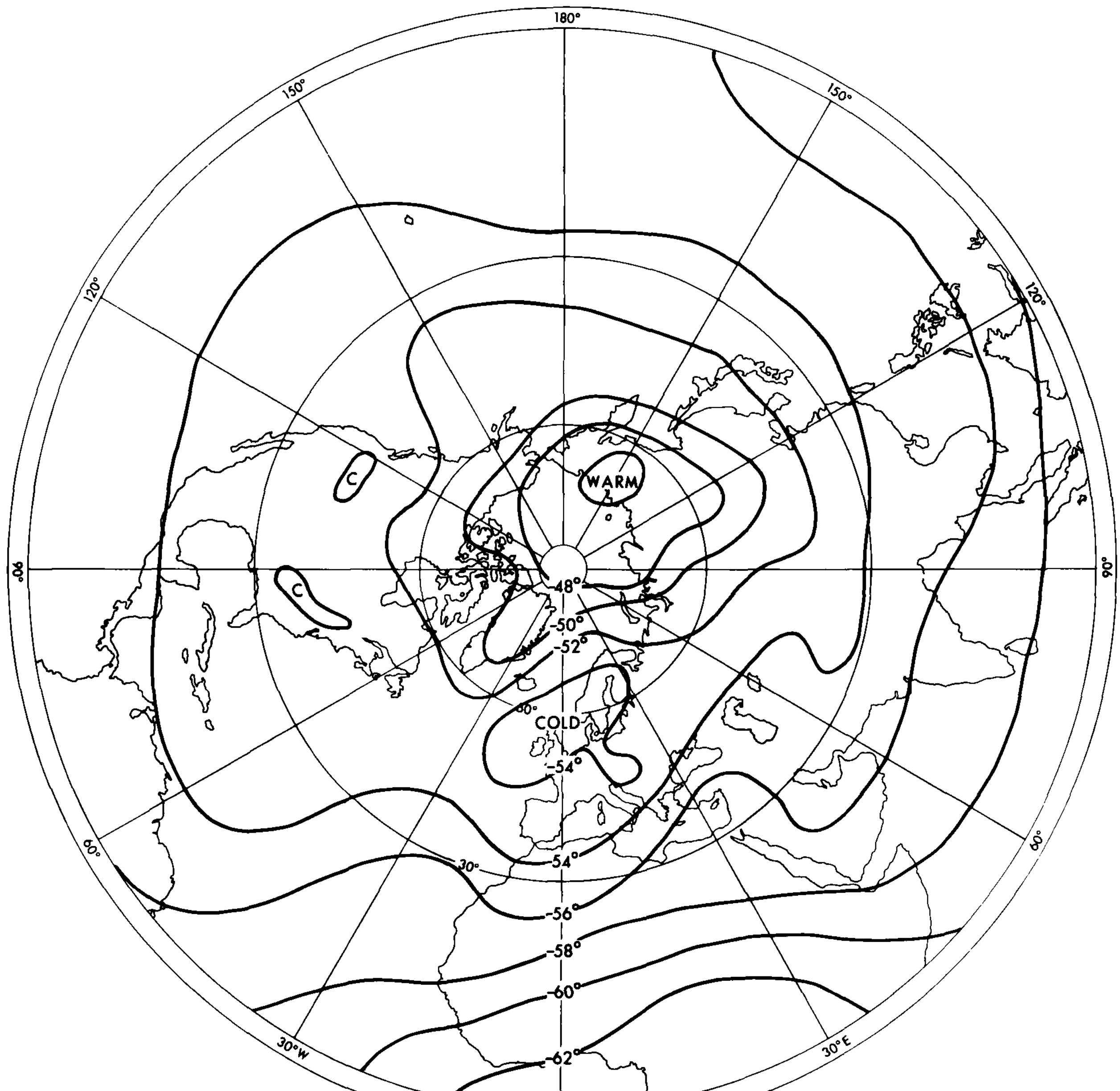

PLATE 3. AVERAGE TEMPERATURES AT 30 MILLIBARS OVER THE NORTHERN HEMISPHERE IN APRIL, 1958–65

Temperatures are in degrees Celsius.

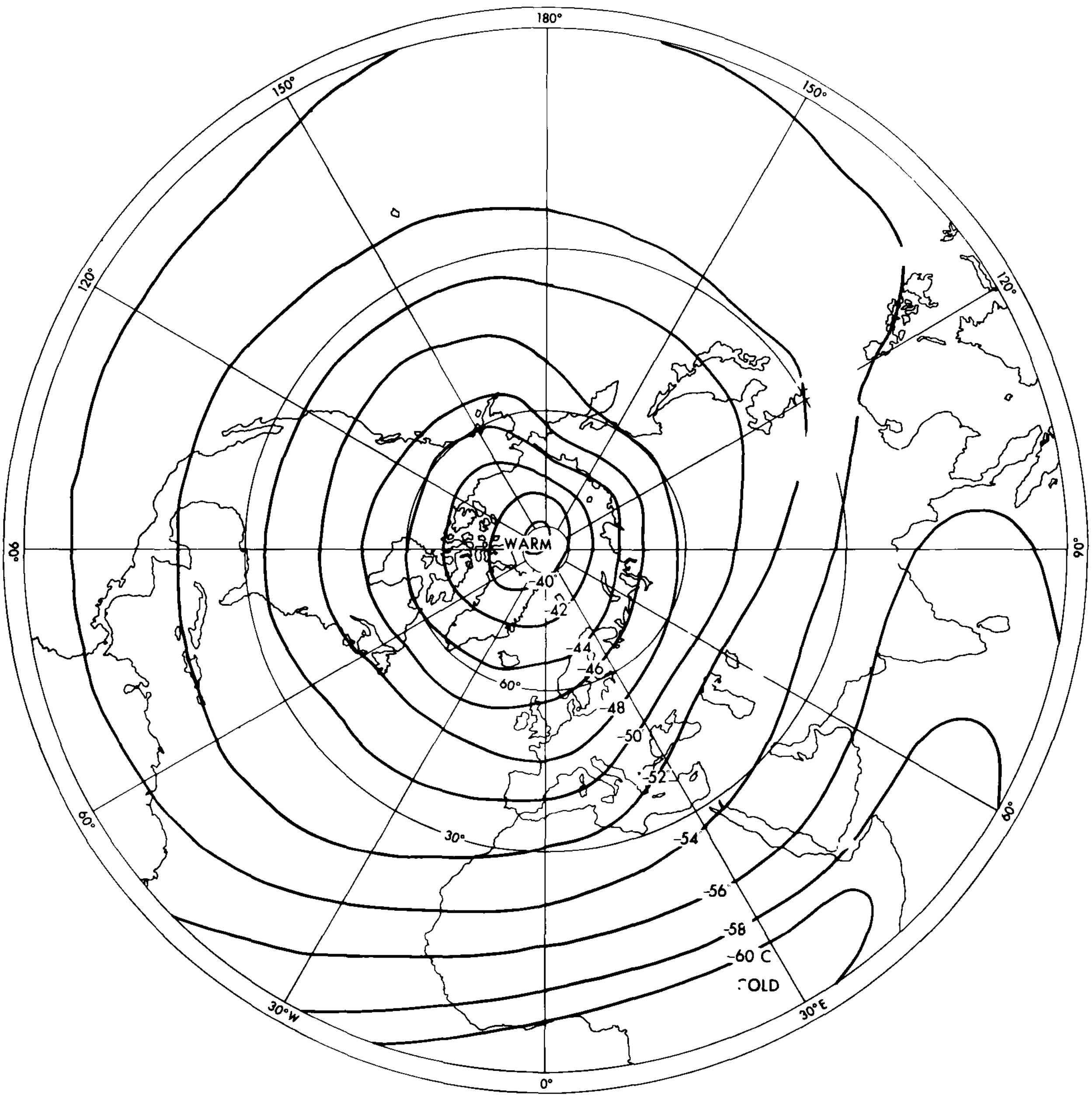

PLATE 4. AVERAGE TEMPERATURES AT 30 MILLIBARS OVER THE NORTHERN HEMISPHERE IN JULY, 1957–64

Temperatures are in degrees Celsius.

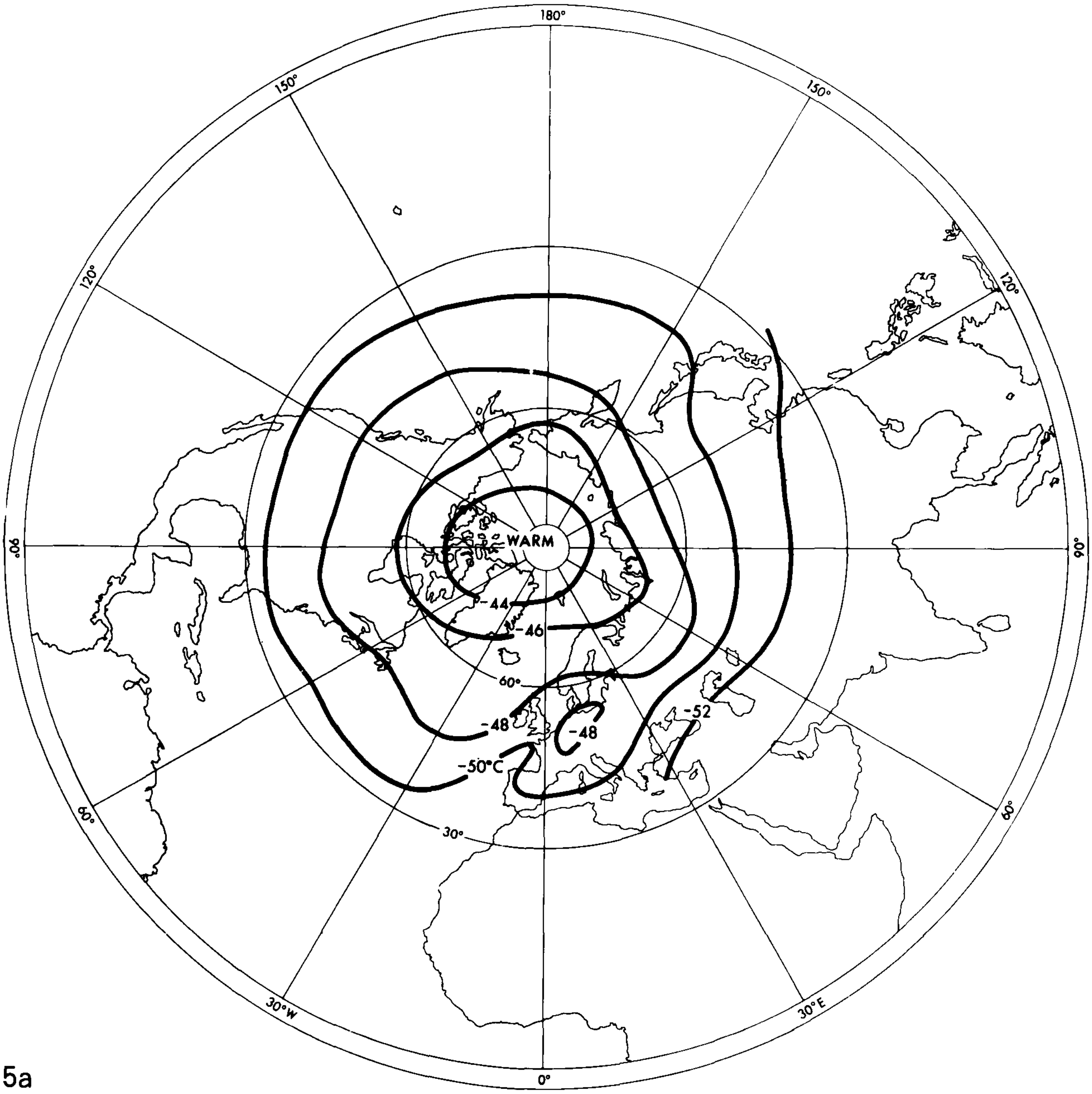

5a

PLATES 5a AND 5b. AVERAGE TEMPERATURES AT 30 MILLIBARS OVER THE NORTHERN HEMISPHERE (NORTH OF LATITUDE 45°N) IN AUGUST (5a) AND SEPTEMBER (5b), 1957–64
Temperatures are in degrees Celsius.

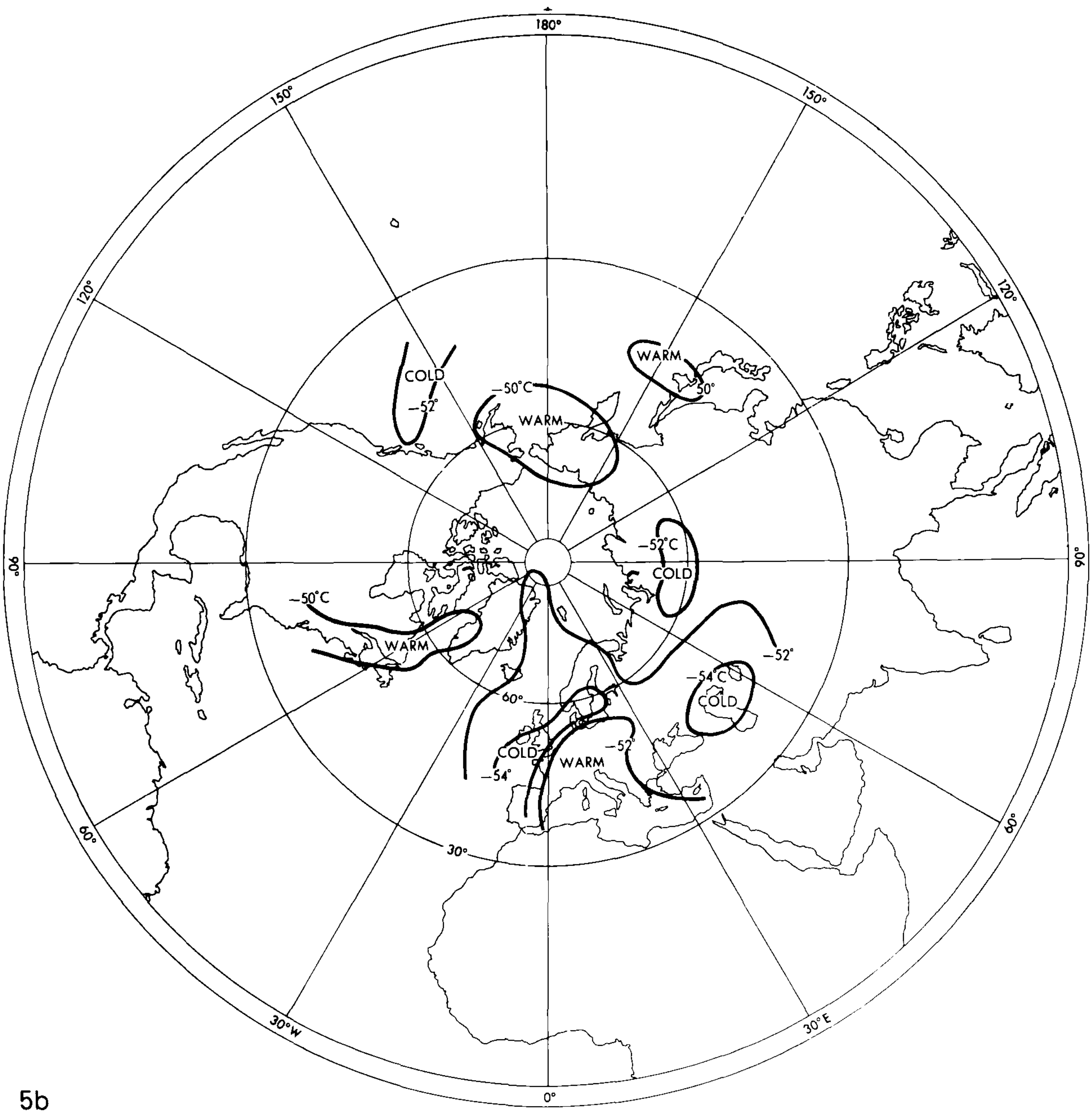
180°
150°
150°
120°
120°
90°
90°
60°
60°
30°W
30°E
0°
30°
60°
COLD
−52°
−50°C
WARM
WARM
50°
−52°C
COLD
−50°C
WARM
−52°
−54°C
COLD
60°
COLD
−54°
WARM
−52°

5b

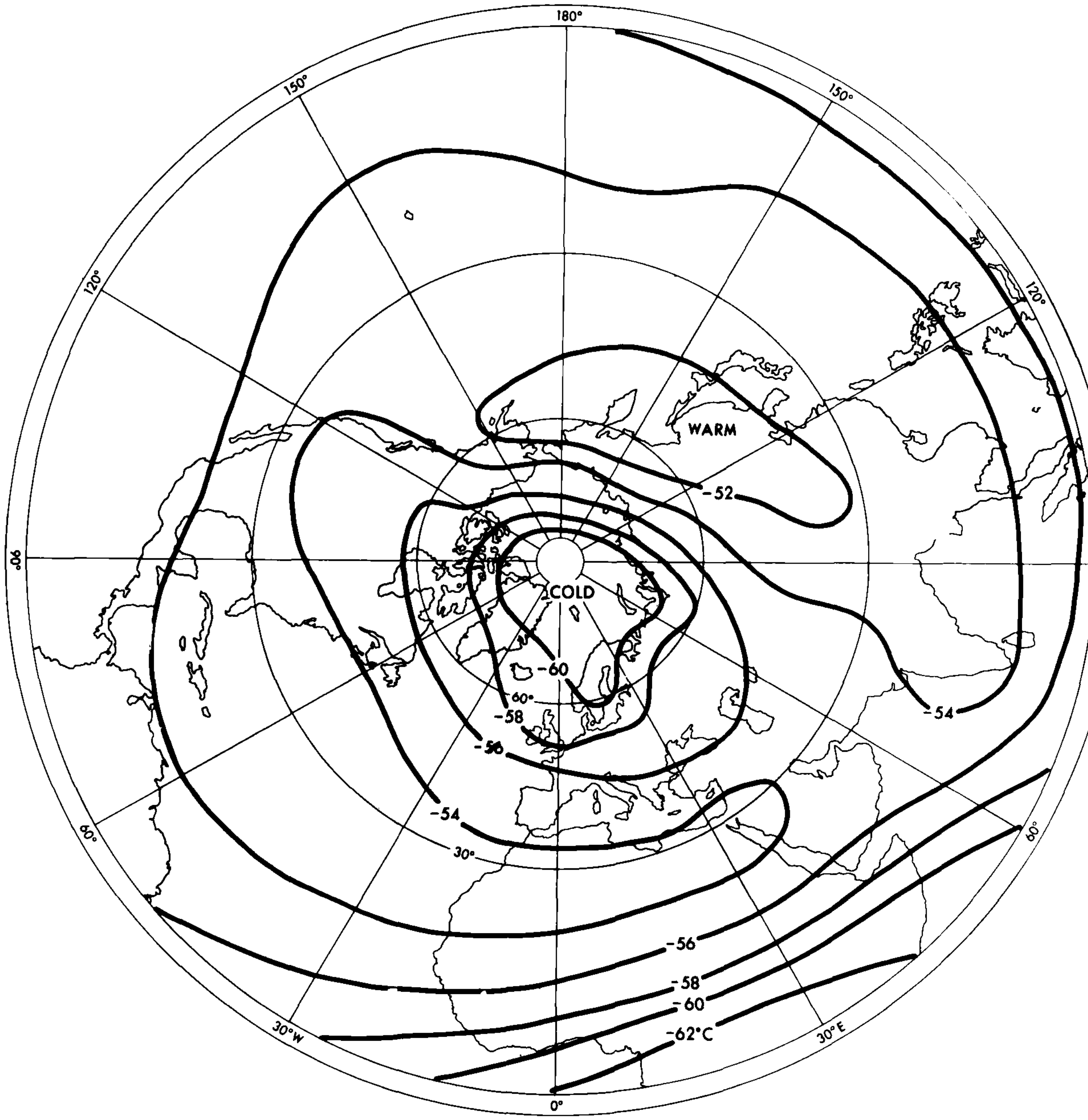

PLATE 6. AVERAGE TEMPERATURES AT 30 MILLIBARS OVER THE NORTHERN HEMISPHERE IN OCTOBER, 1957–64

Temperatures are in degrees Celsius.

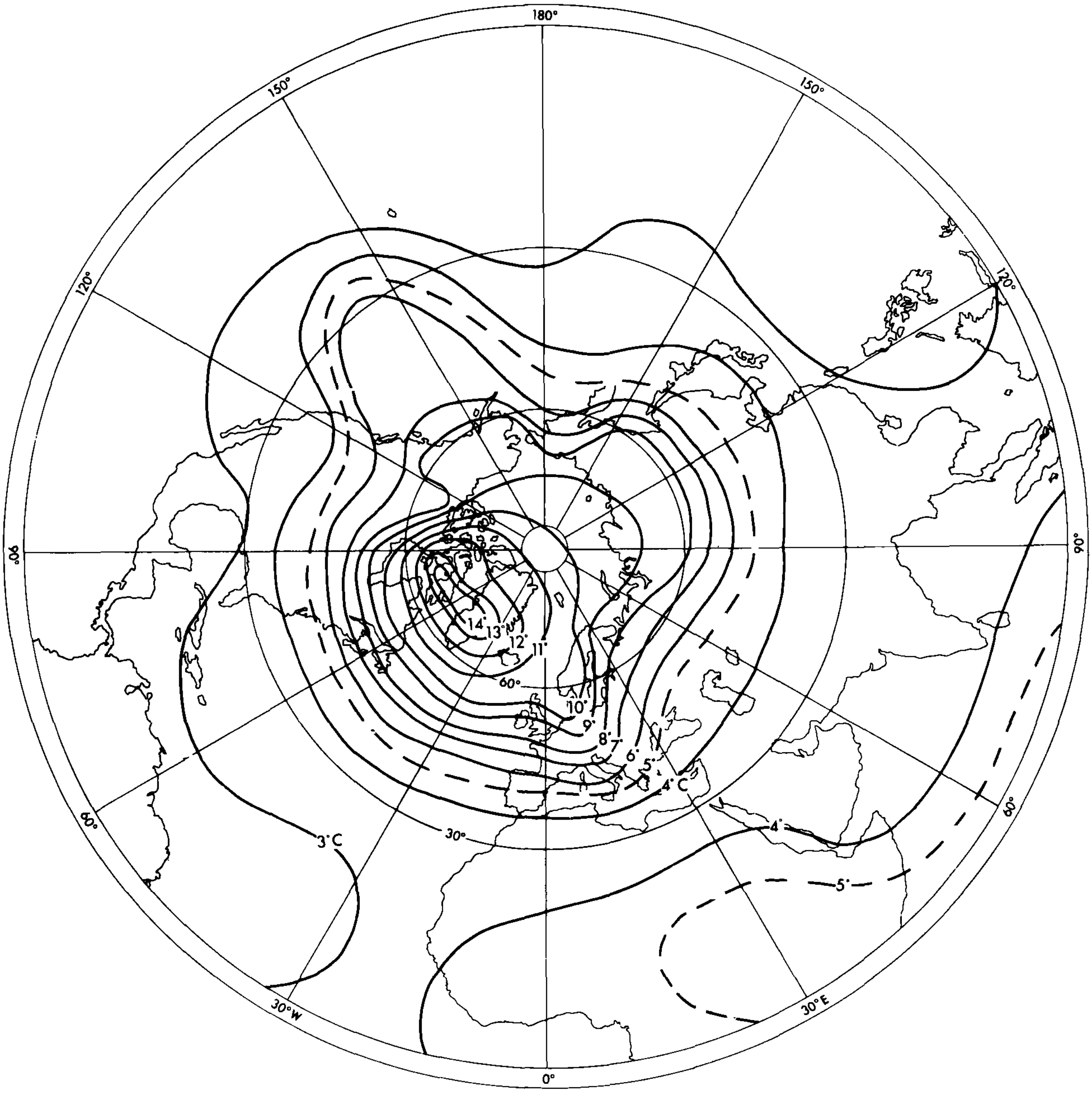

PLATE 7(i). STANDARD DEVIATION OF TEMPERATURES AT 30 MILLIBARS OVER THE NORTHERN HEMISPHERE IN JANUARY, 1958–65

Temperatures are in degrees Celsius.

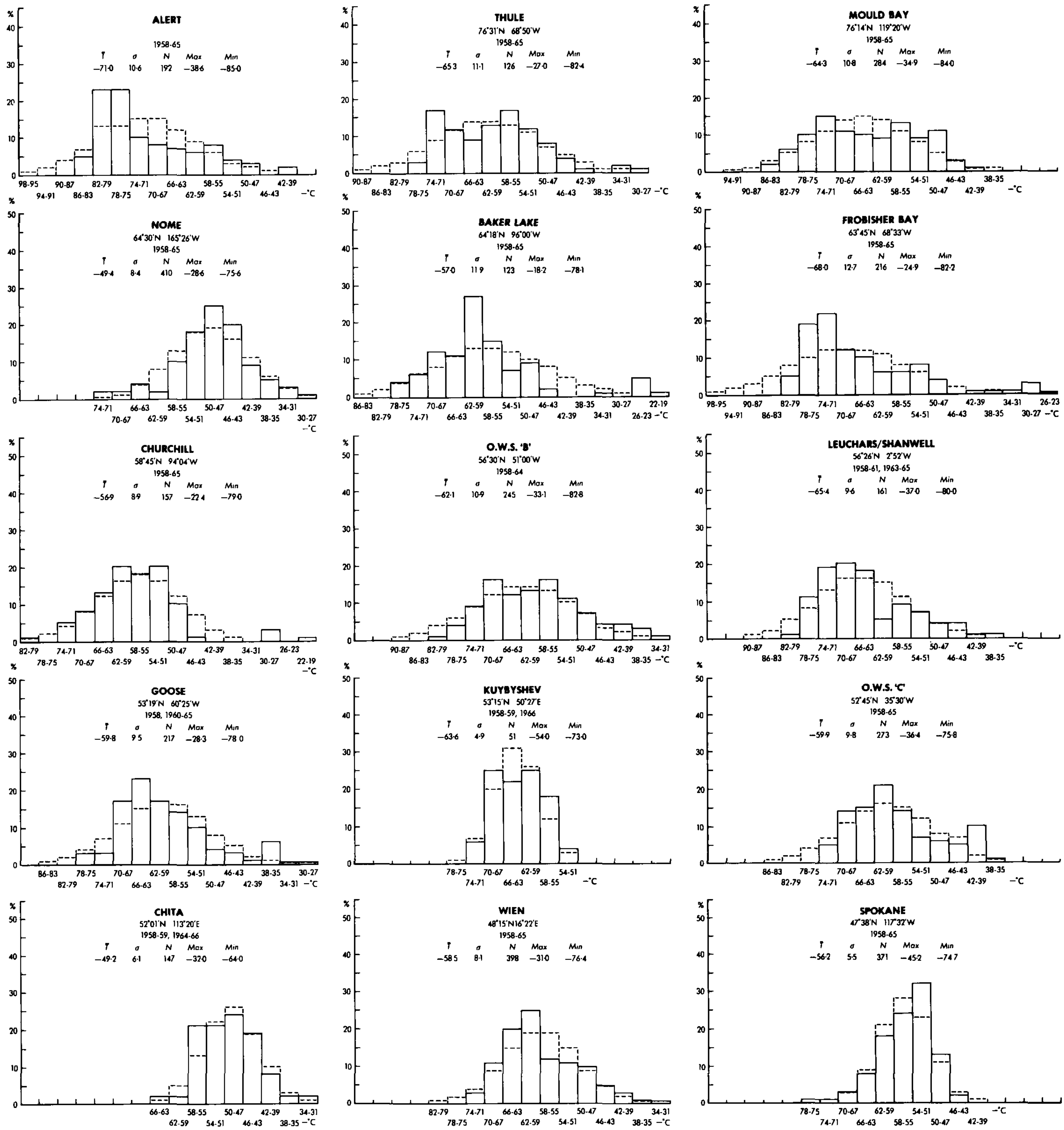

PLATE 7(ii). FREQUENCY DISTRIBUTIONS OF TEMPERATURES AT 30 MILLIBARS FOR SELECTED STATIONS IN JANUARY, 1958–65

——— Observed distribution - - - - - Theoretical distribution

N = number of occasions, $\overline{T}$ = average temperature, σ = standard deviation,

Max. = highest recorded temperature, *Min.* = lowest recorded temperature,

in degrees Celsius.

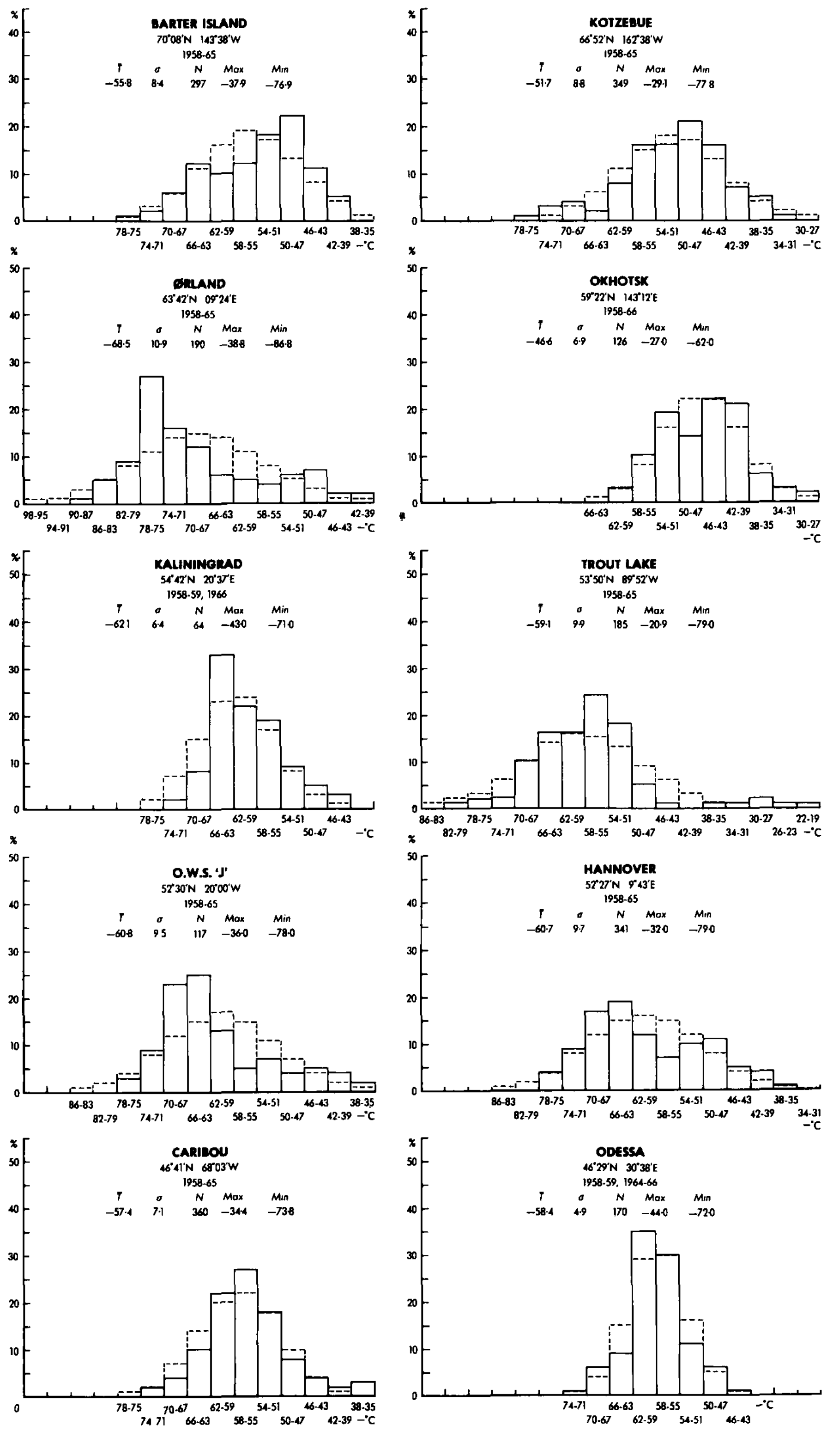

PLATE 7 (ii) (*contd*)

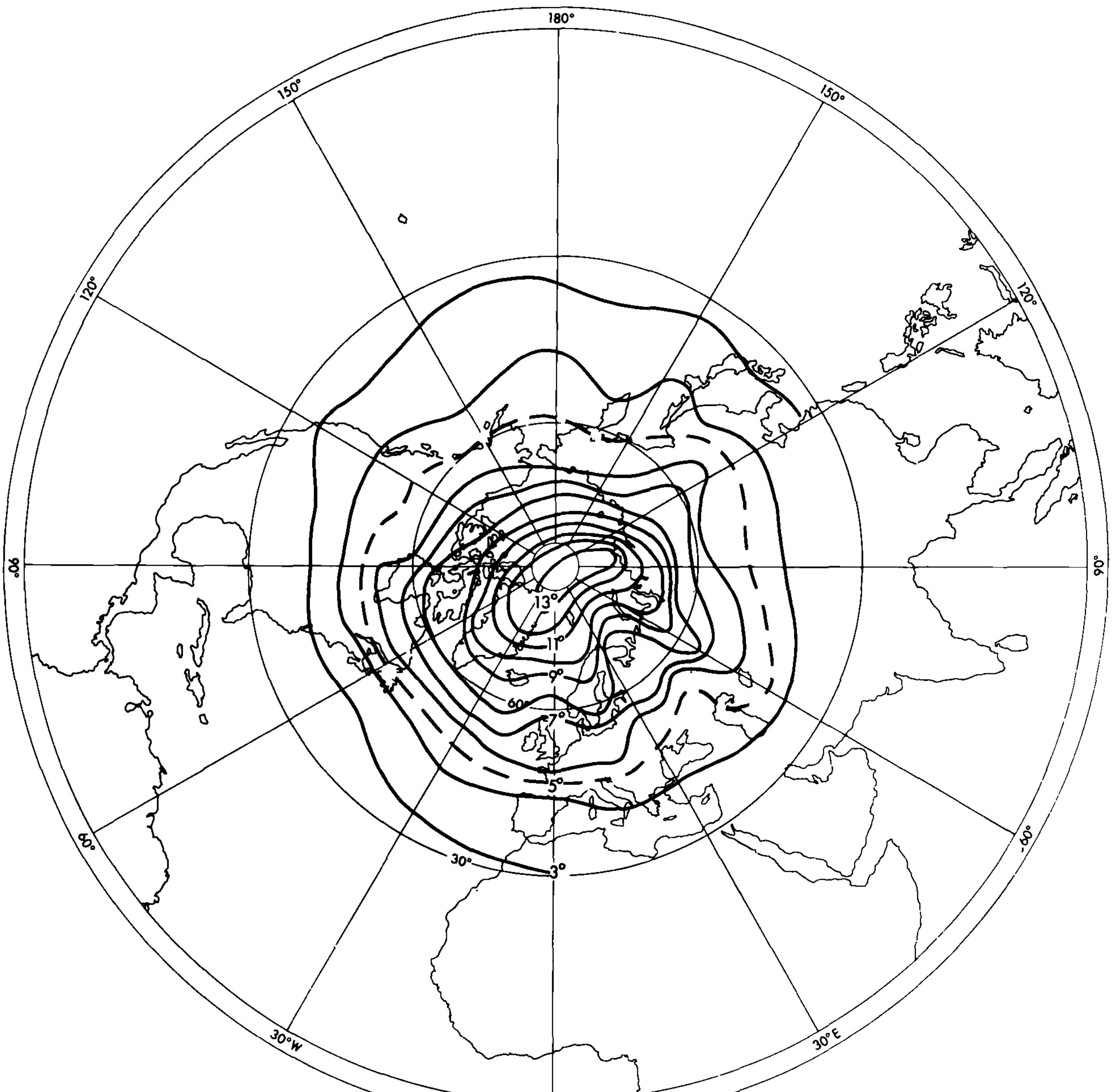

PLATE 8a(i). STANDARD DEVIATION OF TEMPERATURES AT 30 MILLIBARS OVER THE NORTHERN HEMISPHERE (NORTH OF LATITUDE 45°N) IN FEBRUARY, 1958–65

Temperatures are in degrees Celsius.

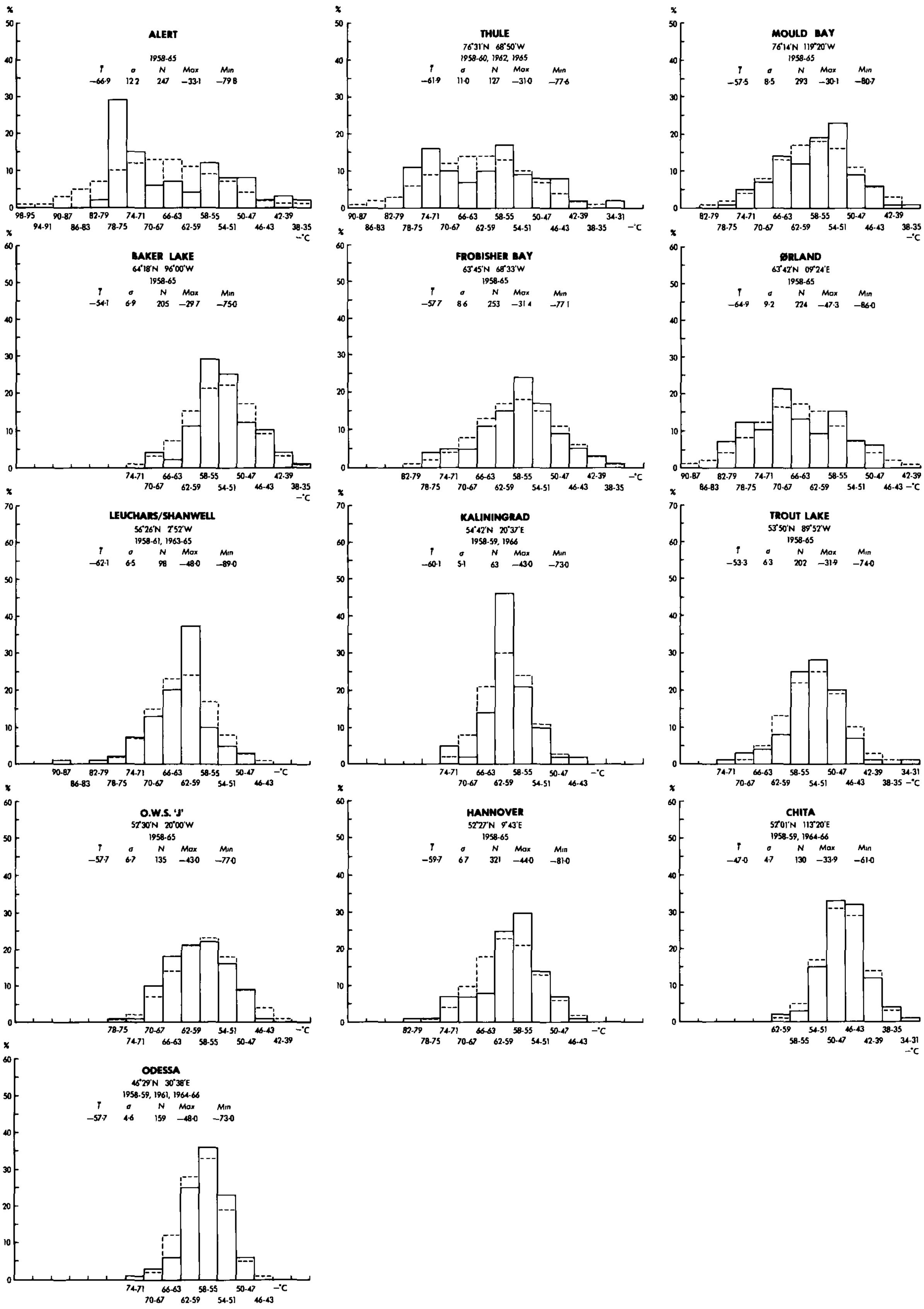

PLATE 8a(ii). FREQUENCY DISTRIBUTIONS OF TEMPERATURES AT 30 MILLIBARS FOR SELECTED STATIONS IN FEBRUARY, 1958–65

———— Observed distribution   – – – – – Theoretical distribution

N = number of occasions. $\overline{T}$ = average temperature, σ = standard deviation,
Max. = highest recorded temperature,   *Min.* = lowest recorded temperature,
in degrees Celsius.

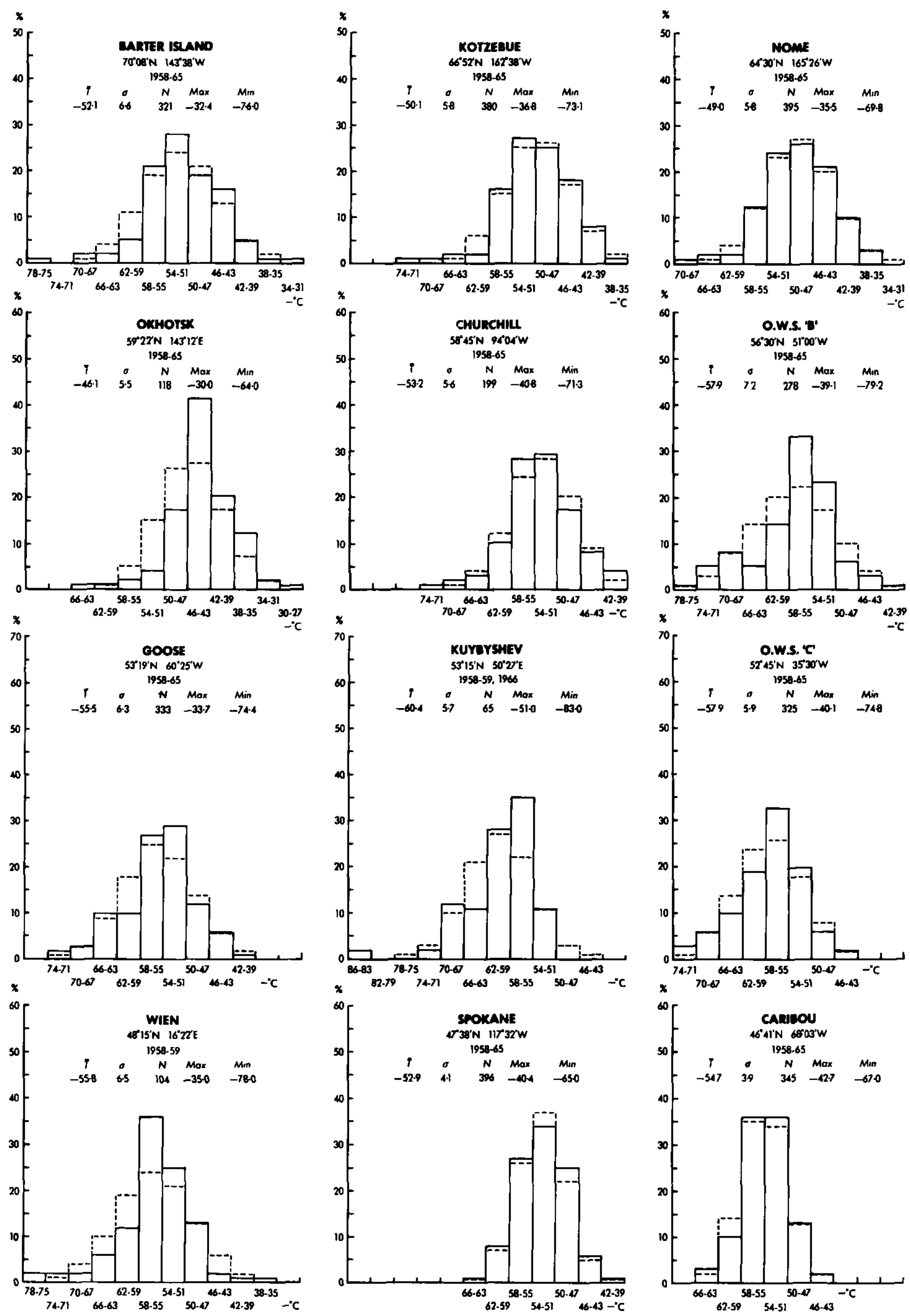

PLATE 8a (ii) (*contd*)

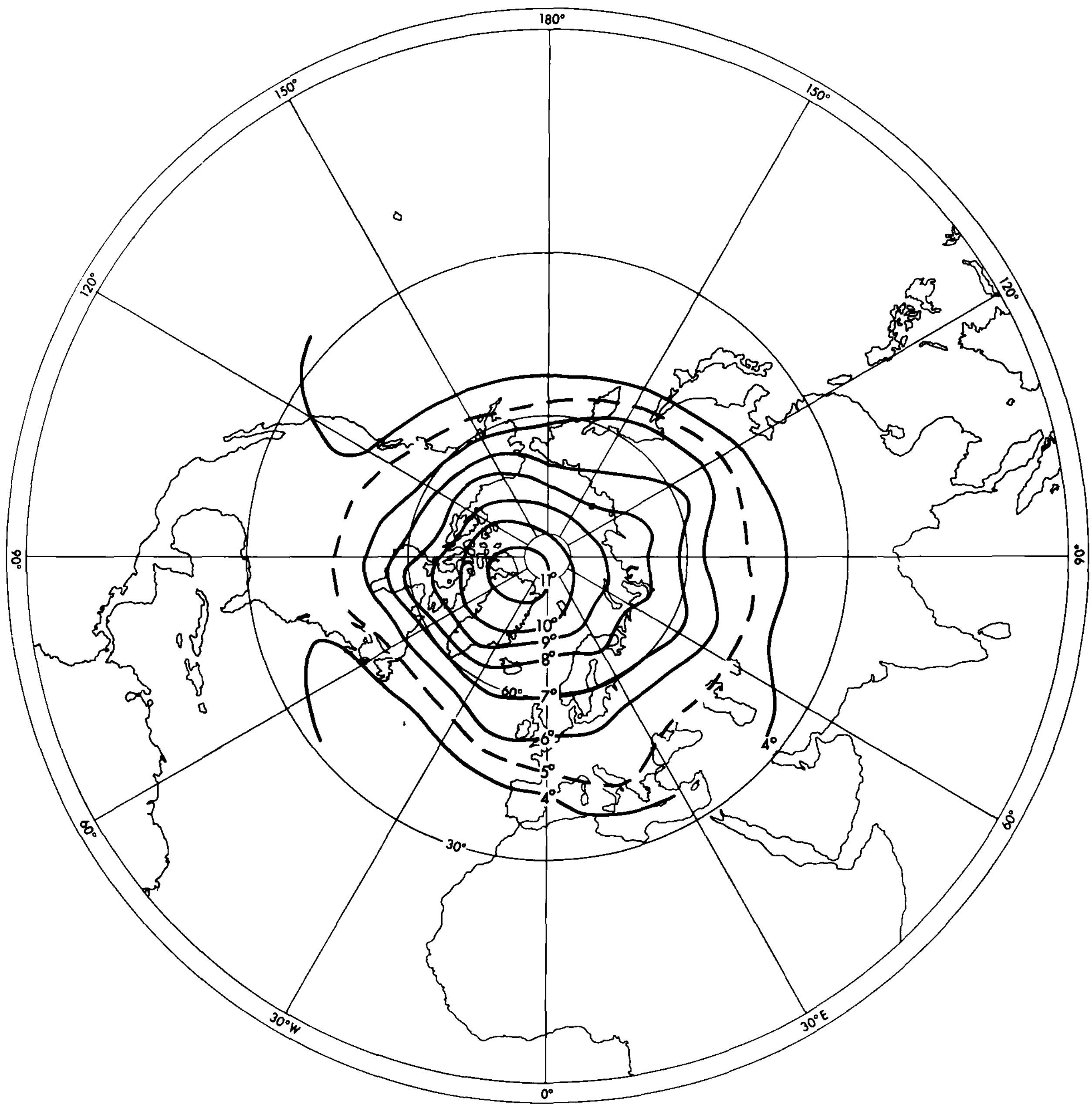

PLATE 8b(i). STANDARD DEVIATION OF TEMPERATURES AT 30 MILLIBARS OVER THE NORTHERN HEMISPHERE (NORTH OF LATITUDE 45°N) IN MARCH, 1958–65

Temperatures are in degrees Celsius.

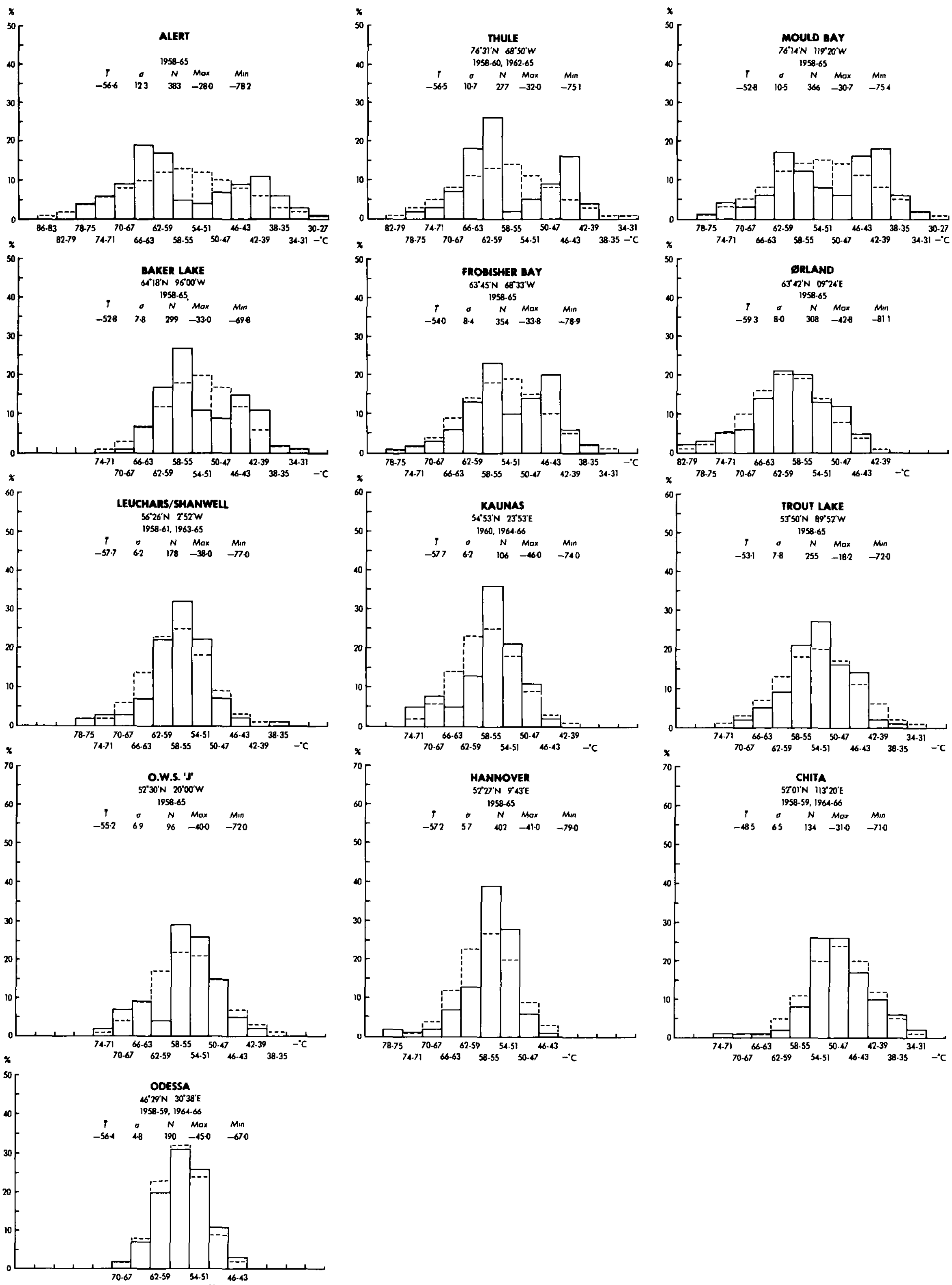

PLATE 8b(ii). FREQUENCY DISTRIBUTIONS OF TEMPERATURES AT 30 MILLIBARS FOR SELECTED STATIONS IN MARCH, 1958–65

——— Observed distribution – – – – – Theoretical distribution

N = number of occasions. $\overline{T}$ = average temperature, σ = standard deviation,

Max. = highest recorded temperature, *Min.* = lowest recorded temperature, in degrees Celsius.

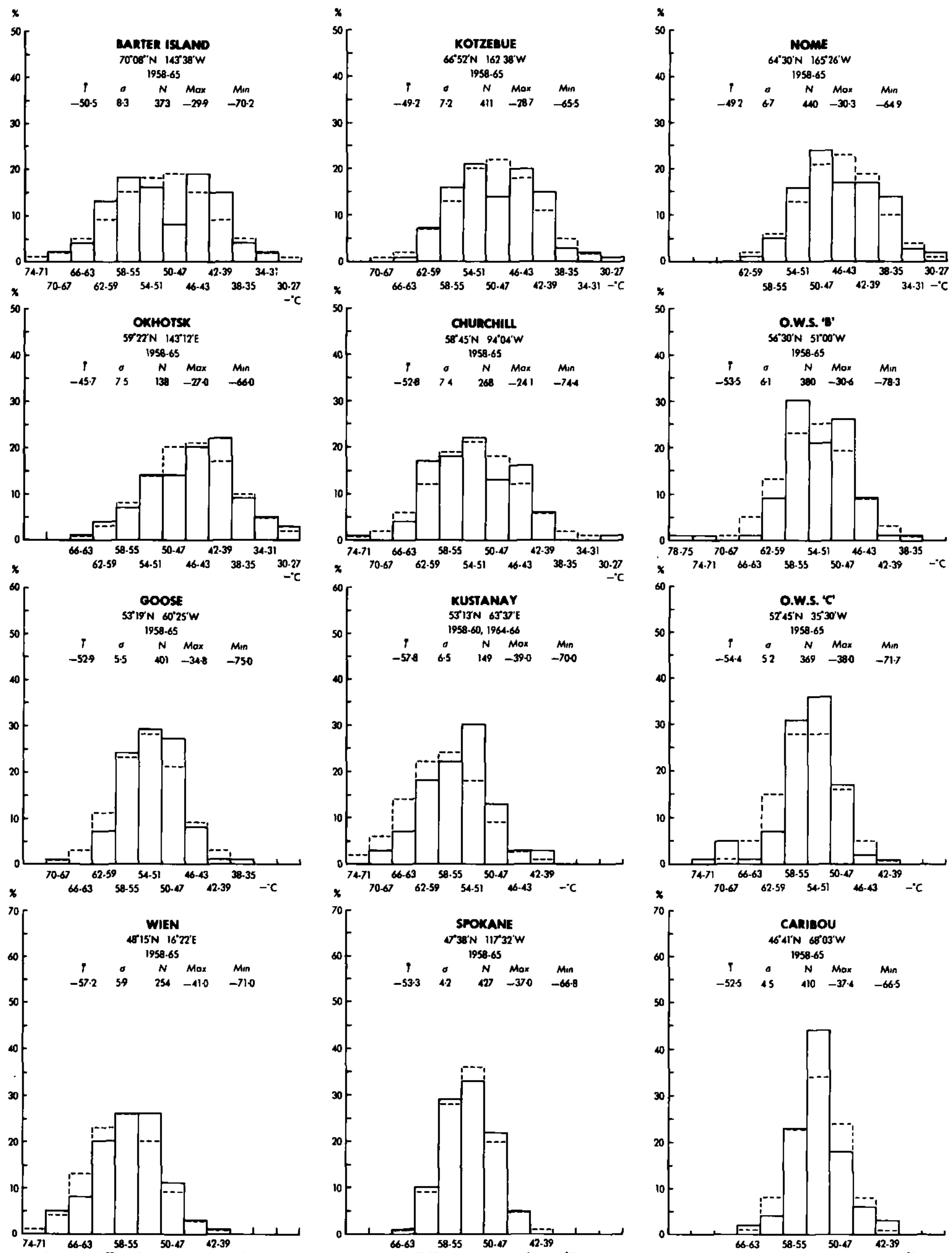

PLATE 8b (ii) (*contd*)

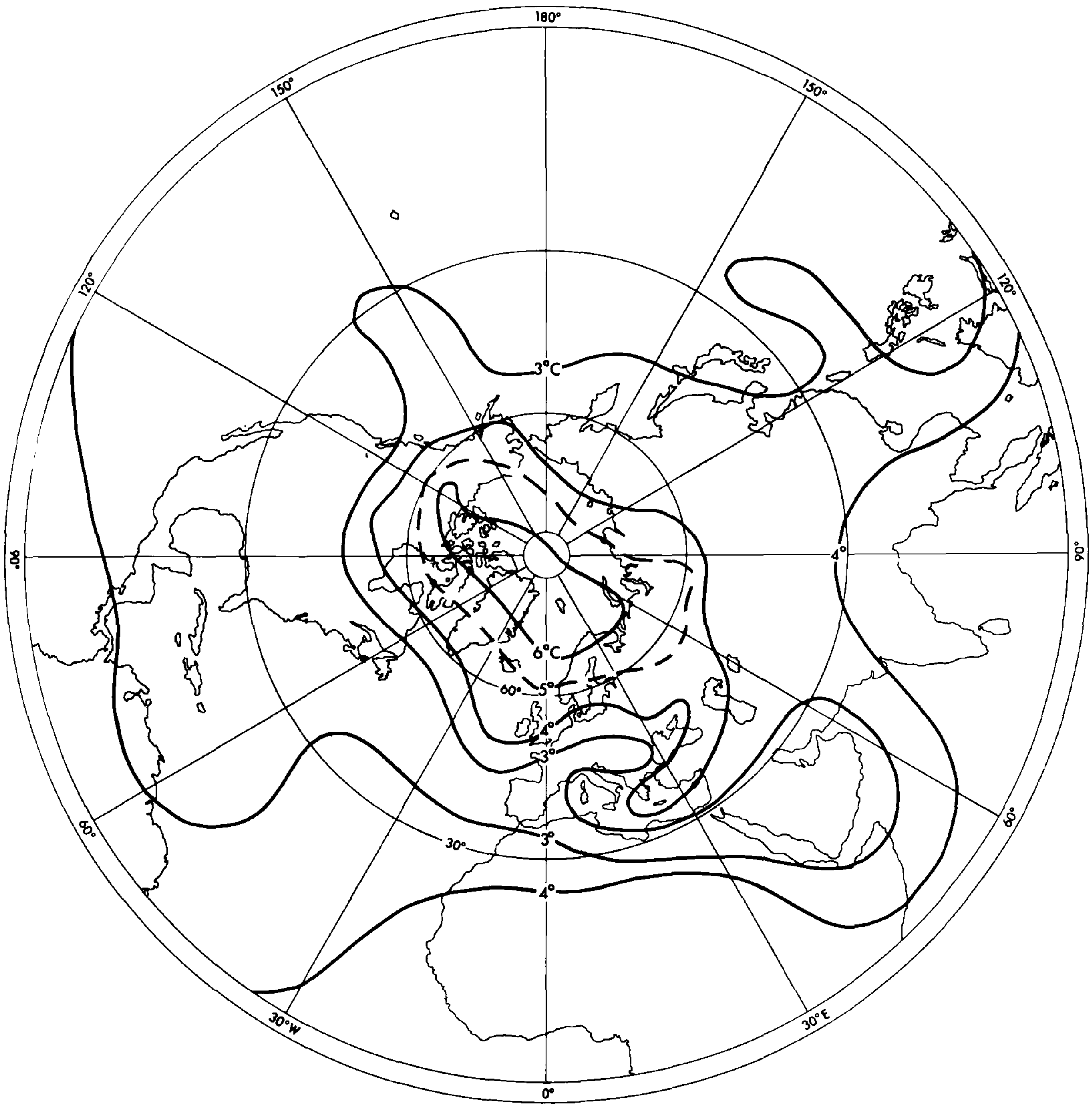

PLATE 9(i). STANDARD DEVIATION OF TEMPERATURES AT 30 MILLIBARS OVER THE NORTHERN HEMISPHERE IN APRIL, 1958–65

Temperatures are in degrees Celsius.

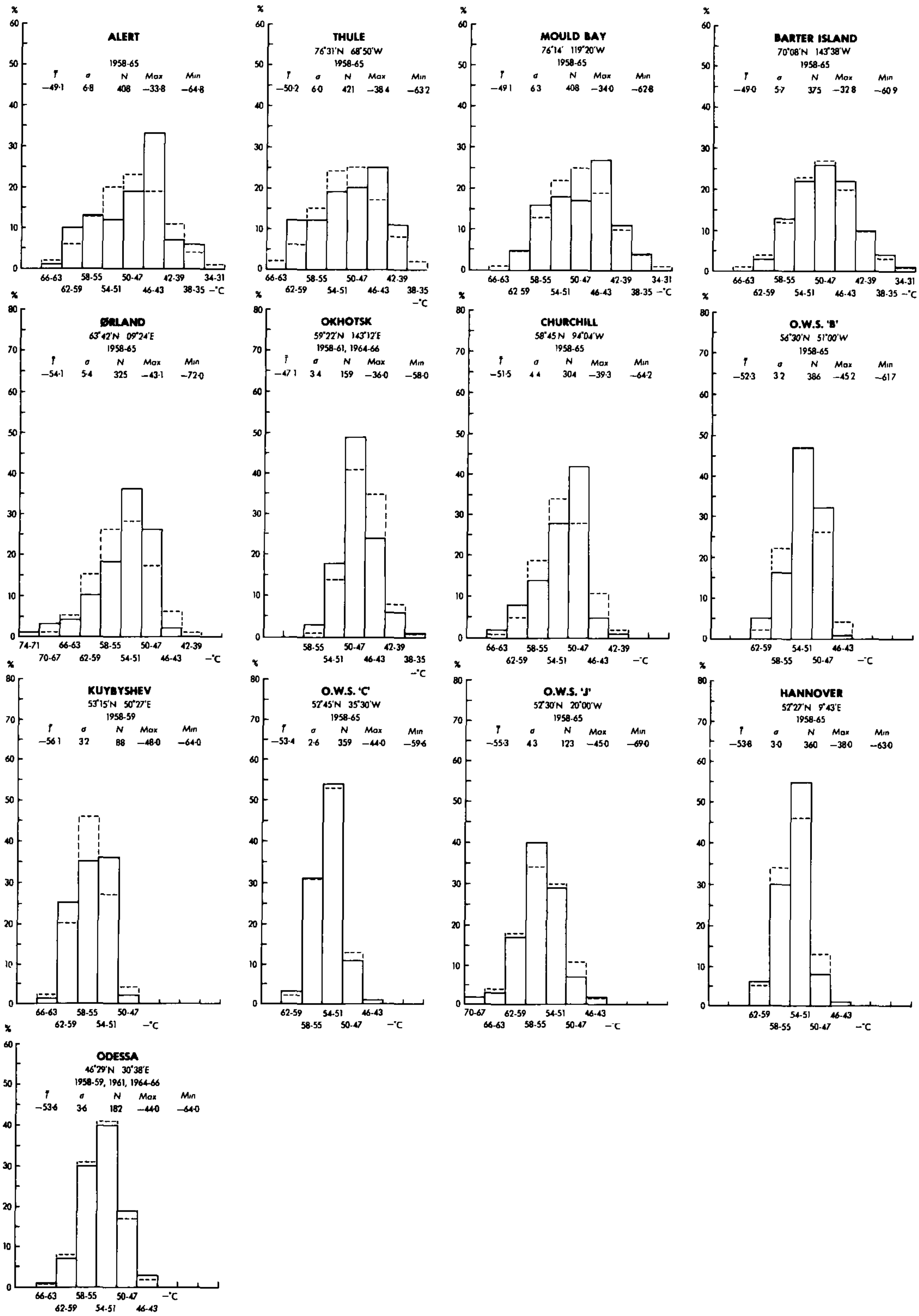

PLATE 9(ii). FREQUENCY DISTRIBUTIONS OF TEMPERATURES AT 30 MILLIBARS FOR SELECTED STATIONS IN APRIL, 1958–65

——— Observed distribution - - - - - Theoretical distribution

N = number of occasions. $\overline{T}$ = average temperature, σ = standard deviation,

Max. = highest recorded temperature, *Min.* = lowest recorded temperature,

in degrees Celsius.

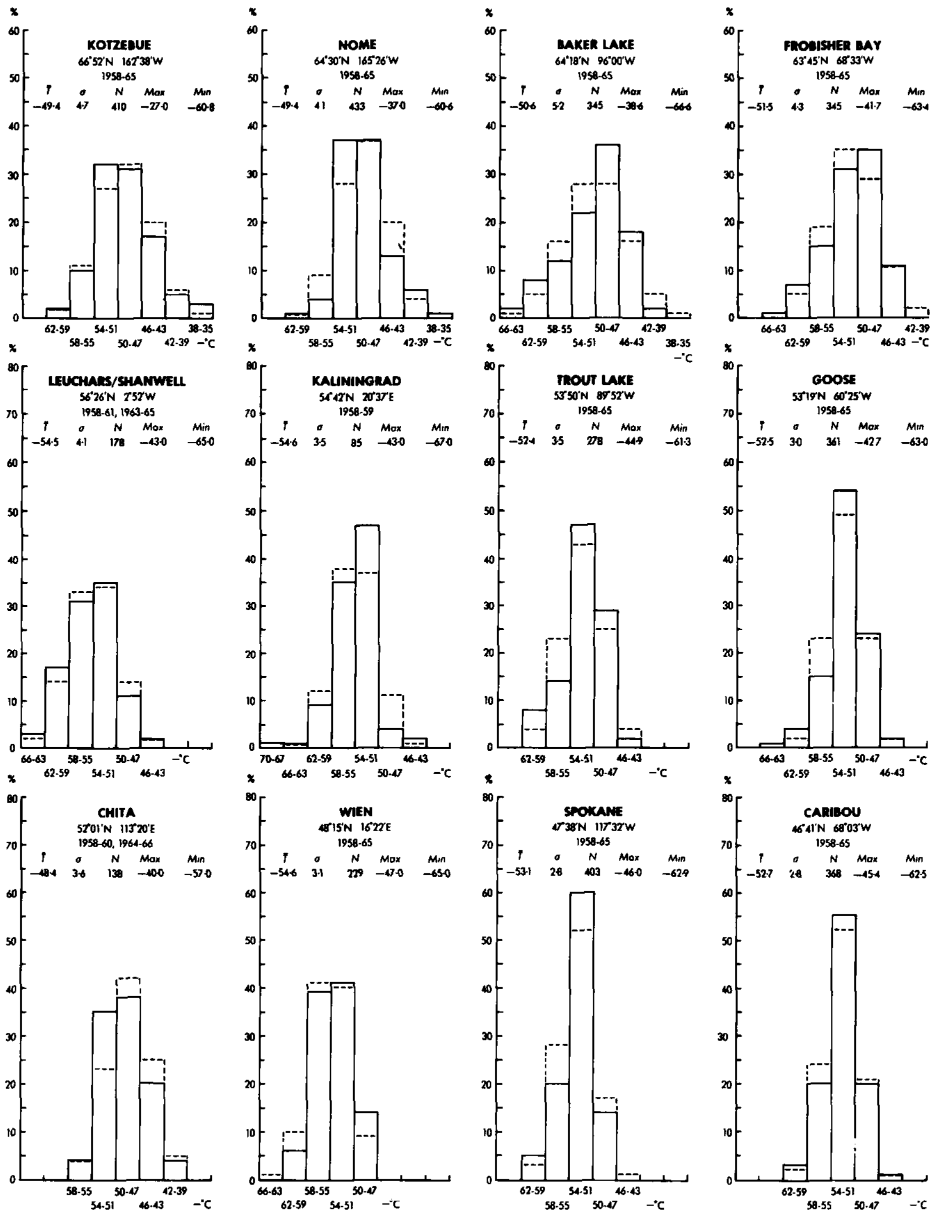

PLATE 9 (ii) (*contd*)

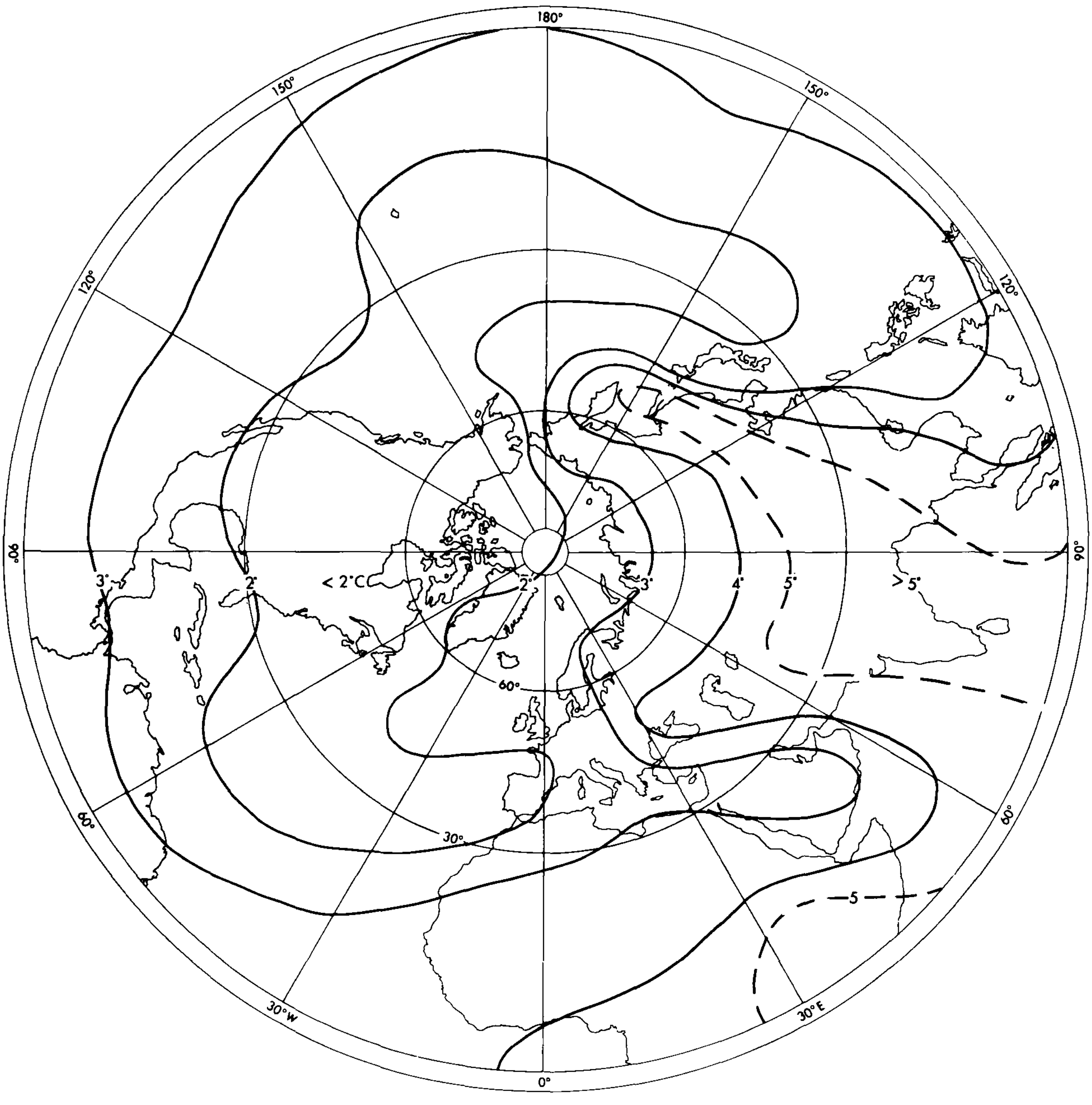

PLATE 10. STANDARD DEVIATION OF TEMPERATURES AT 30 MILLIBARS OVER THE NORTHERN HEMISPHERE IN JULY, 1957–64

Temperatures are in degrees Celsius.

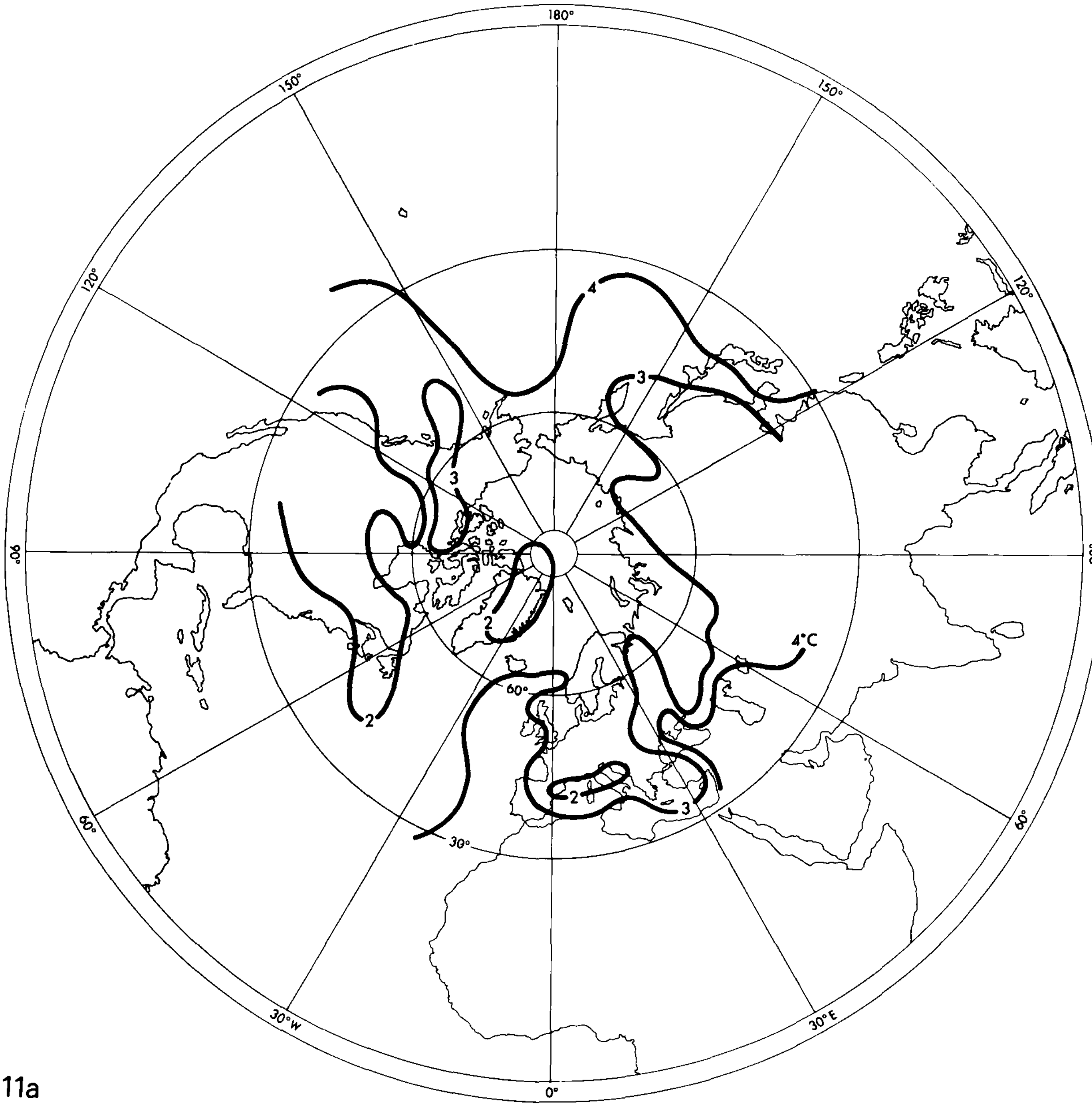

11a

PLATES 11a AND 11b. STANDARD DEVIATION OF TEMPERATURES AT 30 MILLIBARS OVER THE NORTHERN HEMISPHERE (NORTH OF LATITUDE 45°N) IN AUGUST (11a) AND SEPTEMBER (11b), 1957–64

Temperatures are in degrees Celsius.

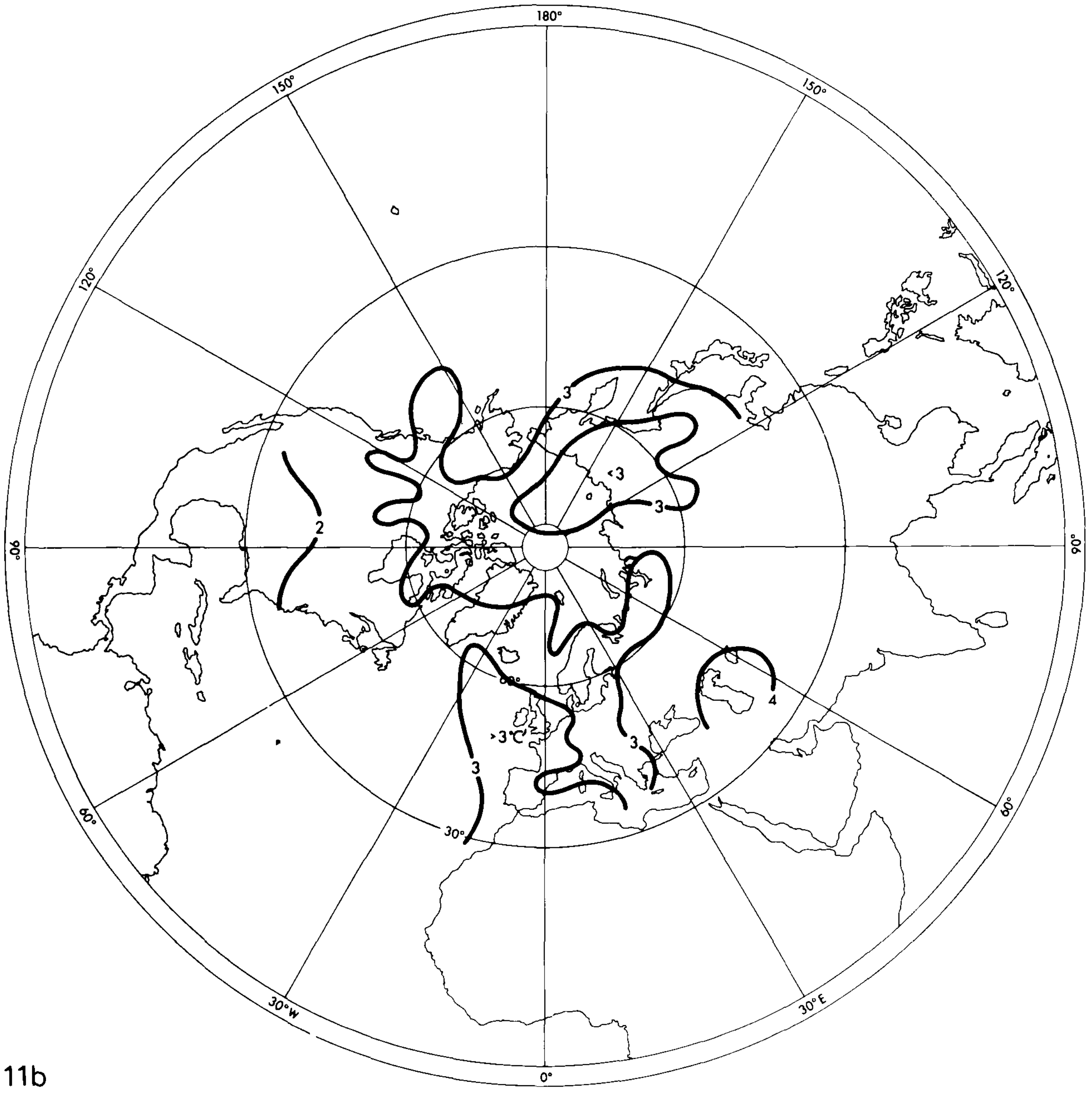

11b

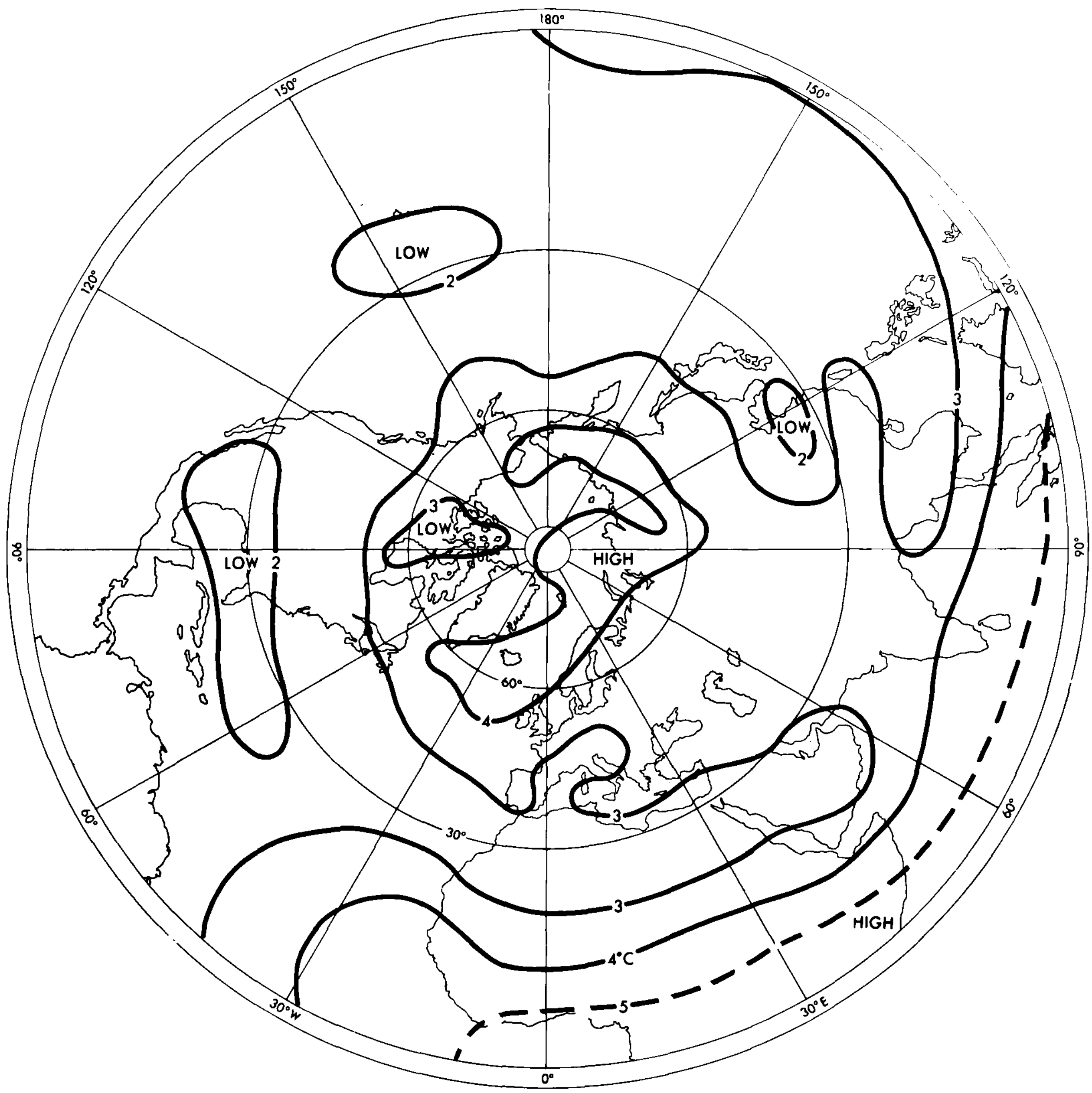

PLATE 12. STANDARD DEVIATION OF TEMPERATURES AT 30 MILLIBARS OVER THE NORTHERN HEMISPHERE IN OCTOBER, 1957–64

Temperatures are in degrees Celsius.

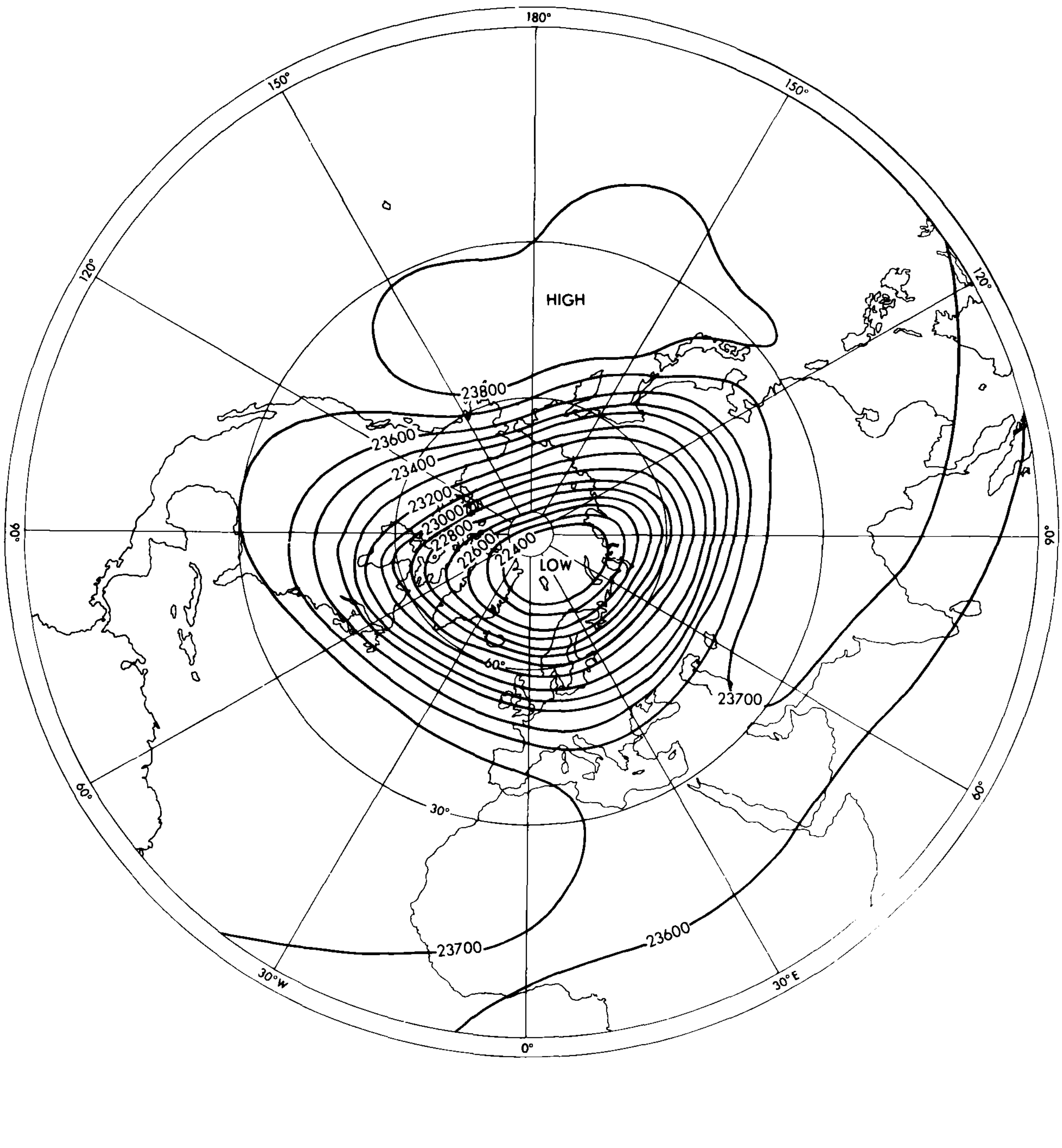

PLATE 13. AVERAGE CONTOUR HEIGHTS AT 30 MILLIBARS OVER THE NORTHERN HEMISPHERE IN JANUARY, 1958–65

Heights are in geopotential metres.

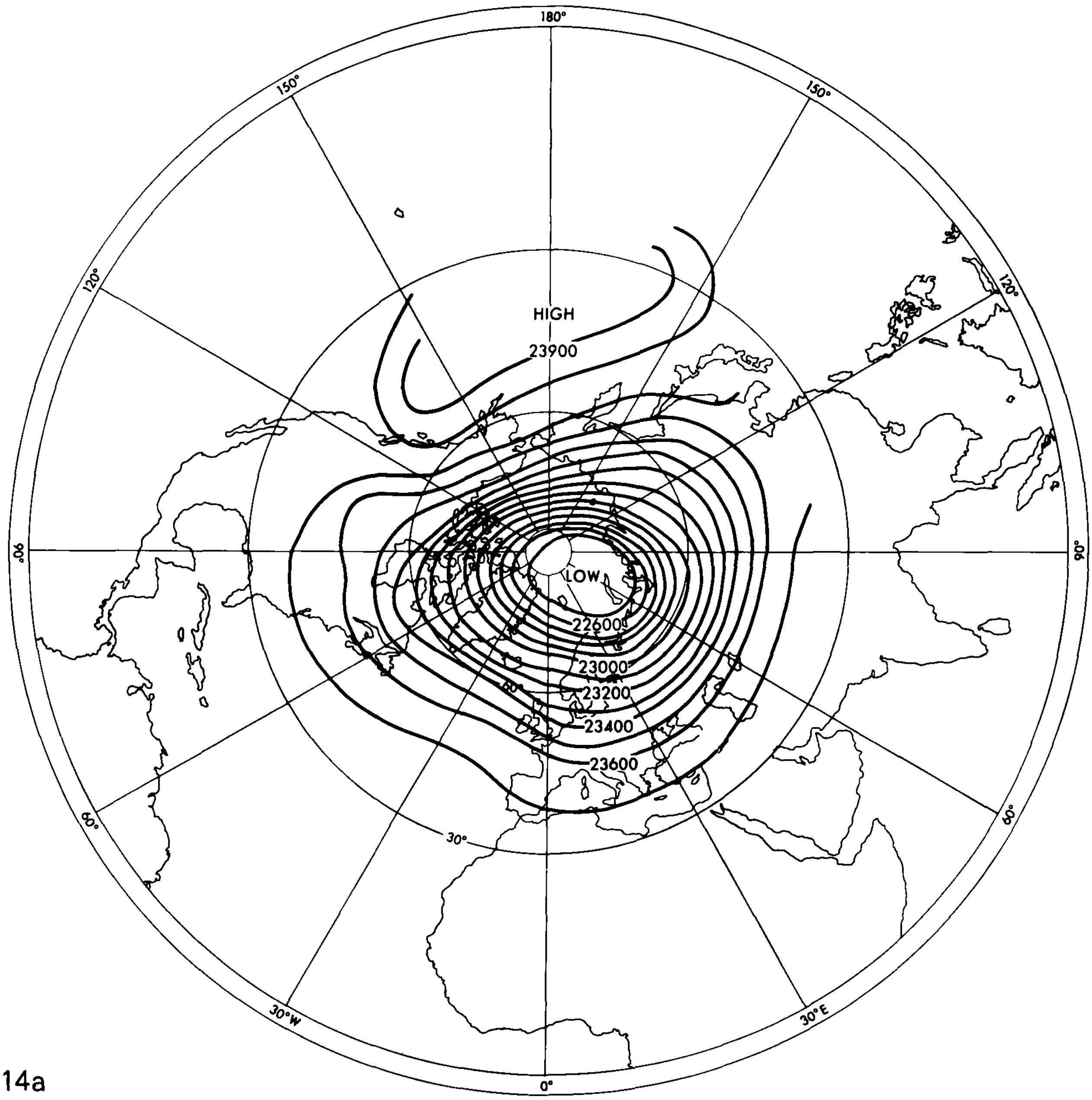

14a

PLATES 14a AND 14b. AVERAGE CONTOUR HEIGHTS AT 30 MILLIBARS OVER THE NORTHERN HEMISPHERE (NORTH OF LATITUDE 45°N) IN FEBRUARY (14a) AND MARCH (14b), 1958–65

Heights are in geopotential metres.

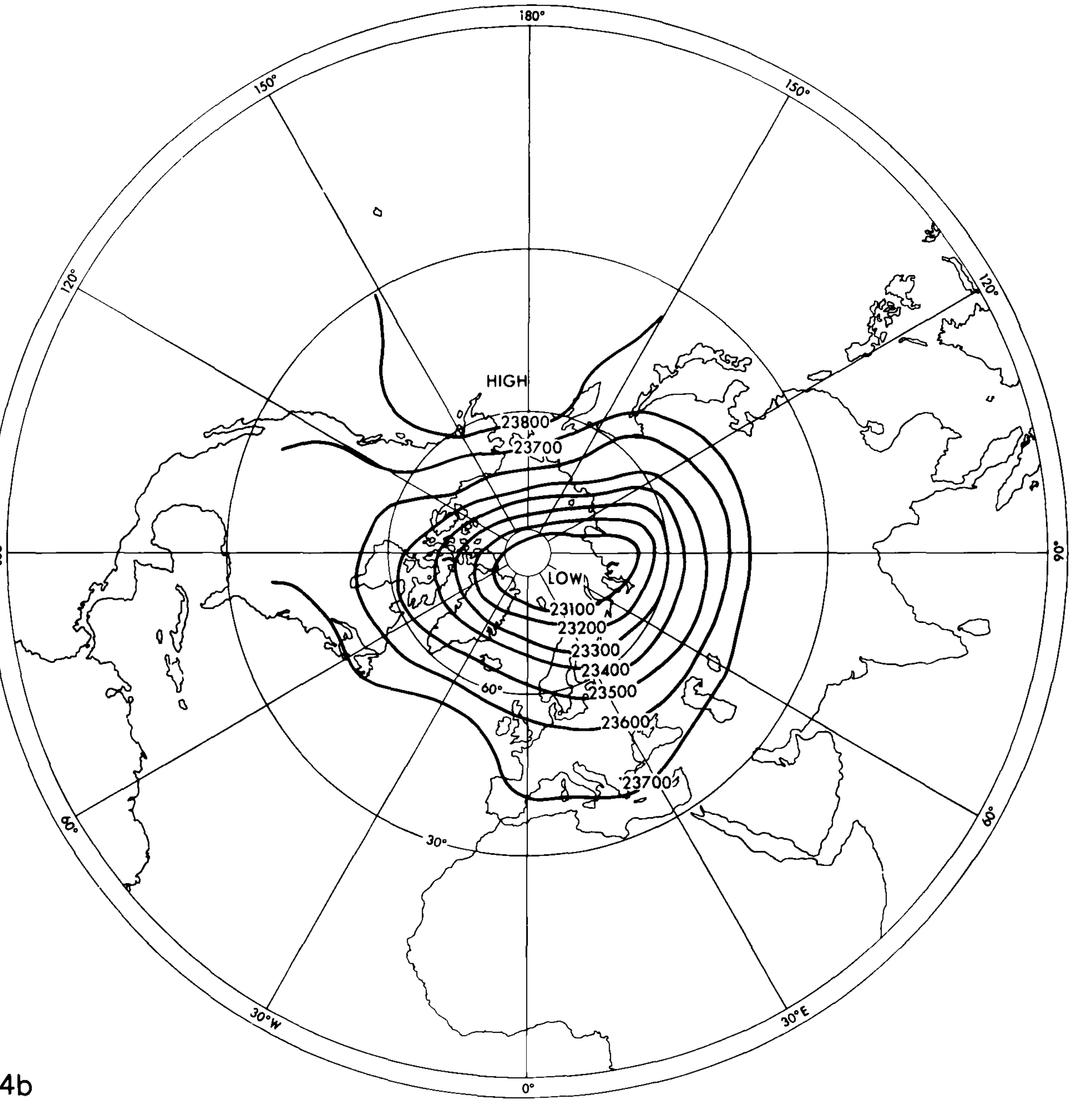
180°
150°
150°
120°
120°
90°
90°
60°
60°
30°W
30°E
0°
30°
60°
HIGH
LOW
23800
23700
23100
23200
23300
23400
23500
23600
23700

14b

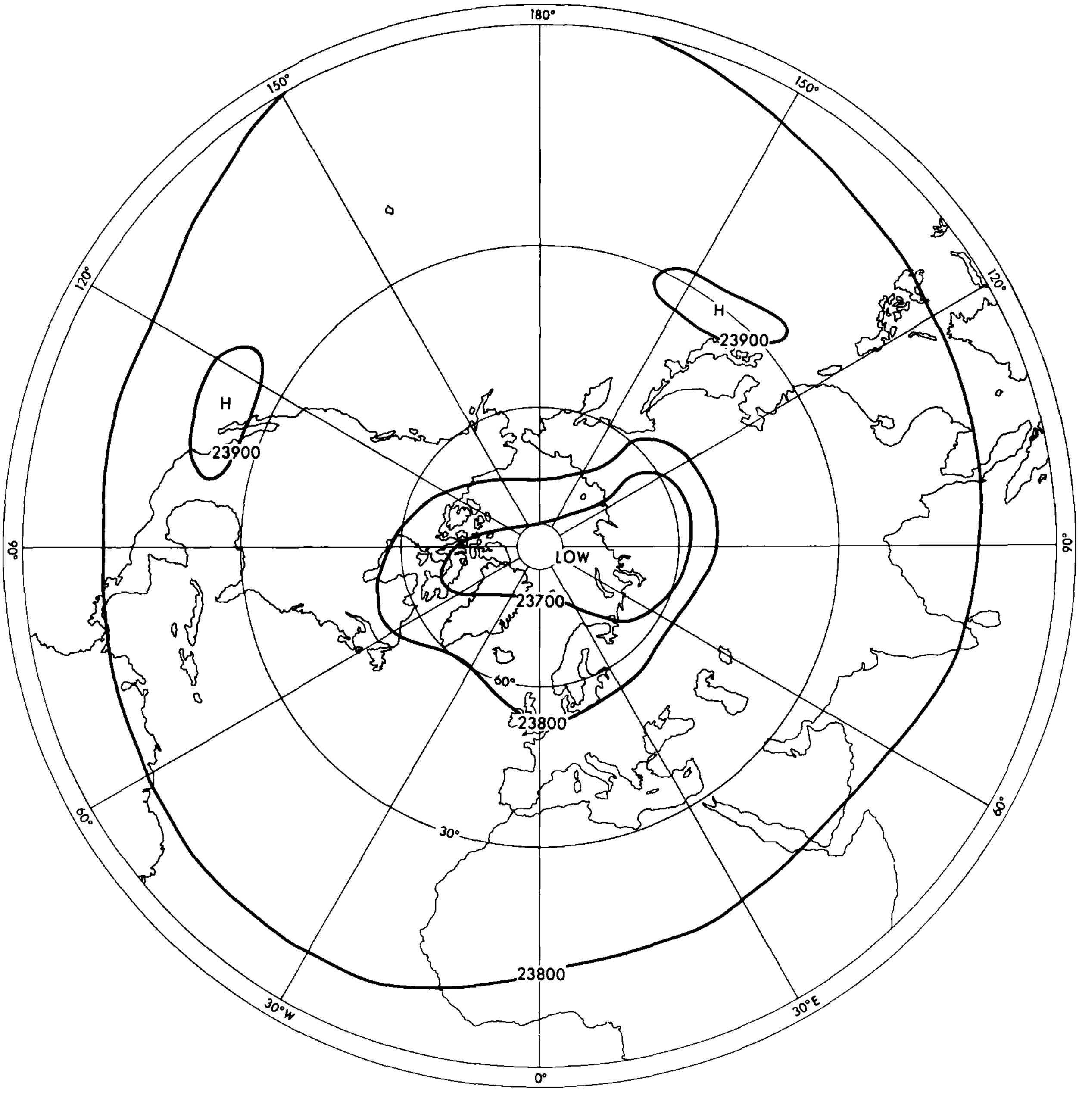

PLATE 15. AVERAGE CONTOUR HEIGHTS AT 30 MILLIBARS OVER THE NORTHERN HEMISPHERE IN APRIL, 1958–65

Heights are in geopotential metres.

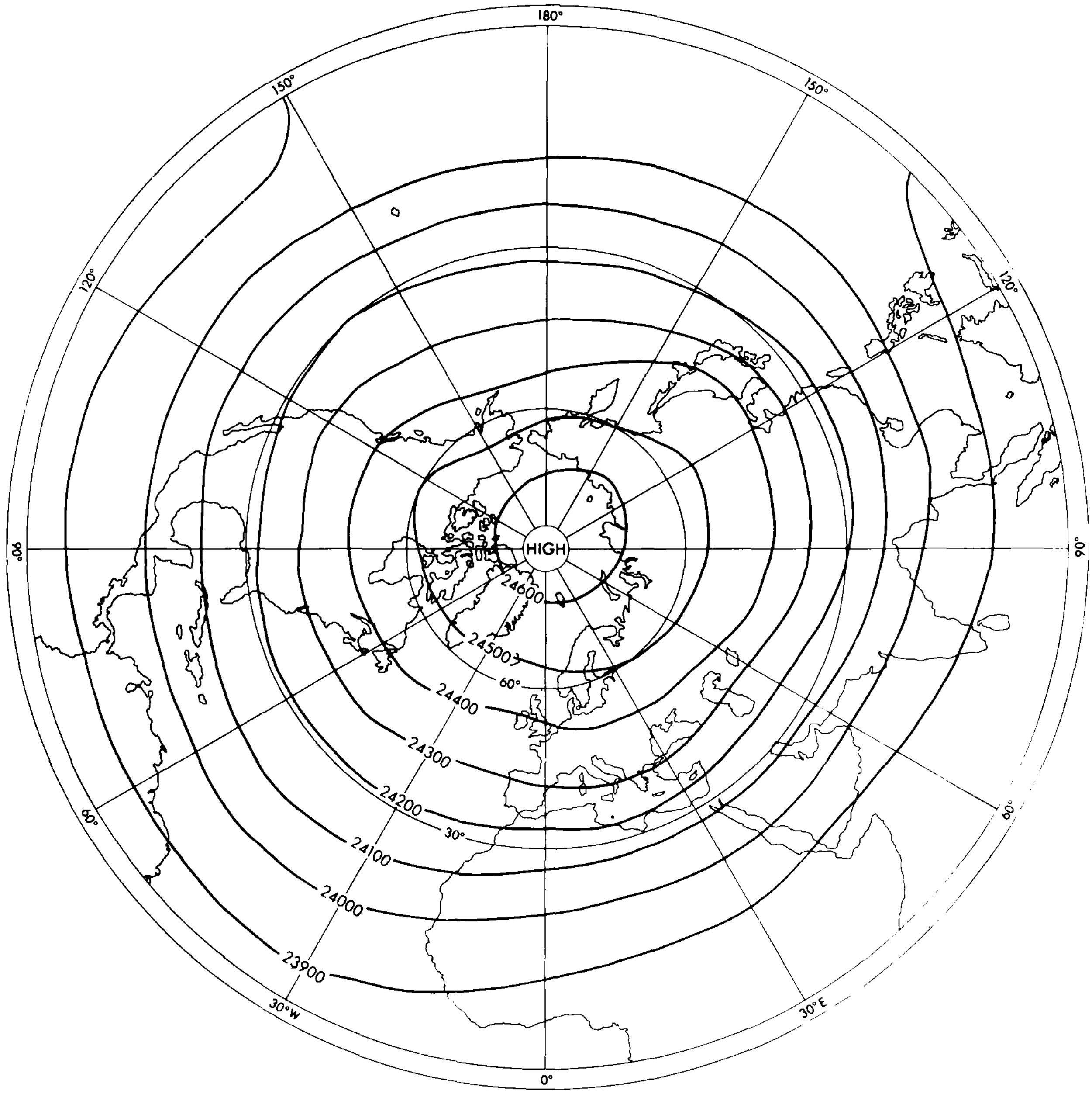

PLATE 16. AVERAGE CONTOUR HEIGHTS AT 30 MILLIBARS OVER THE NORTHERN HEMISPHERE IN JULY, 1957–64

Heights are in geopotential metres.

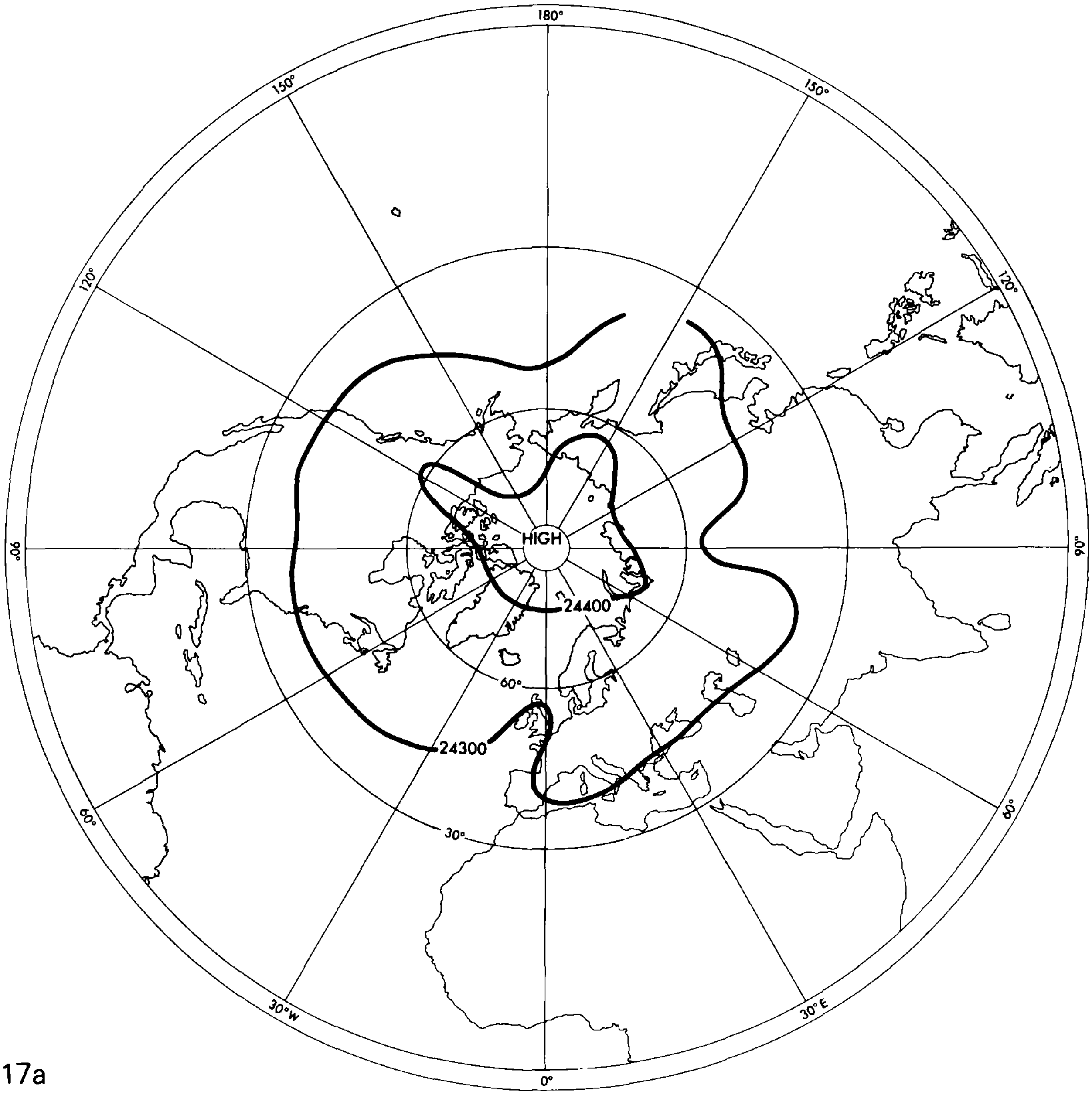

17a

PLATES 17a AND 17b. AVERAGE CONTOUR HEIGHTS AT 30 MILLIBARS OVER THE NORTHERN HEMISPHERE (NORTH OF LATITUDE 45°N) IN AUGUST (17a) AND SEPTEMBER (17b), 1957–64

Heights are in geopotential metres.

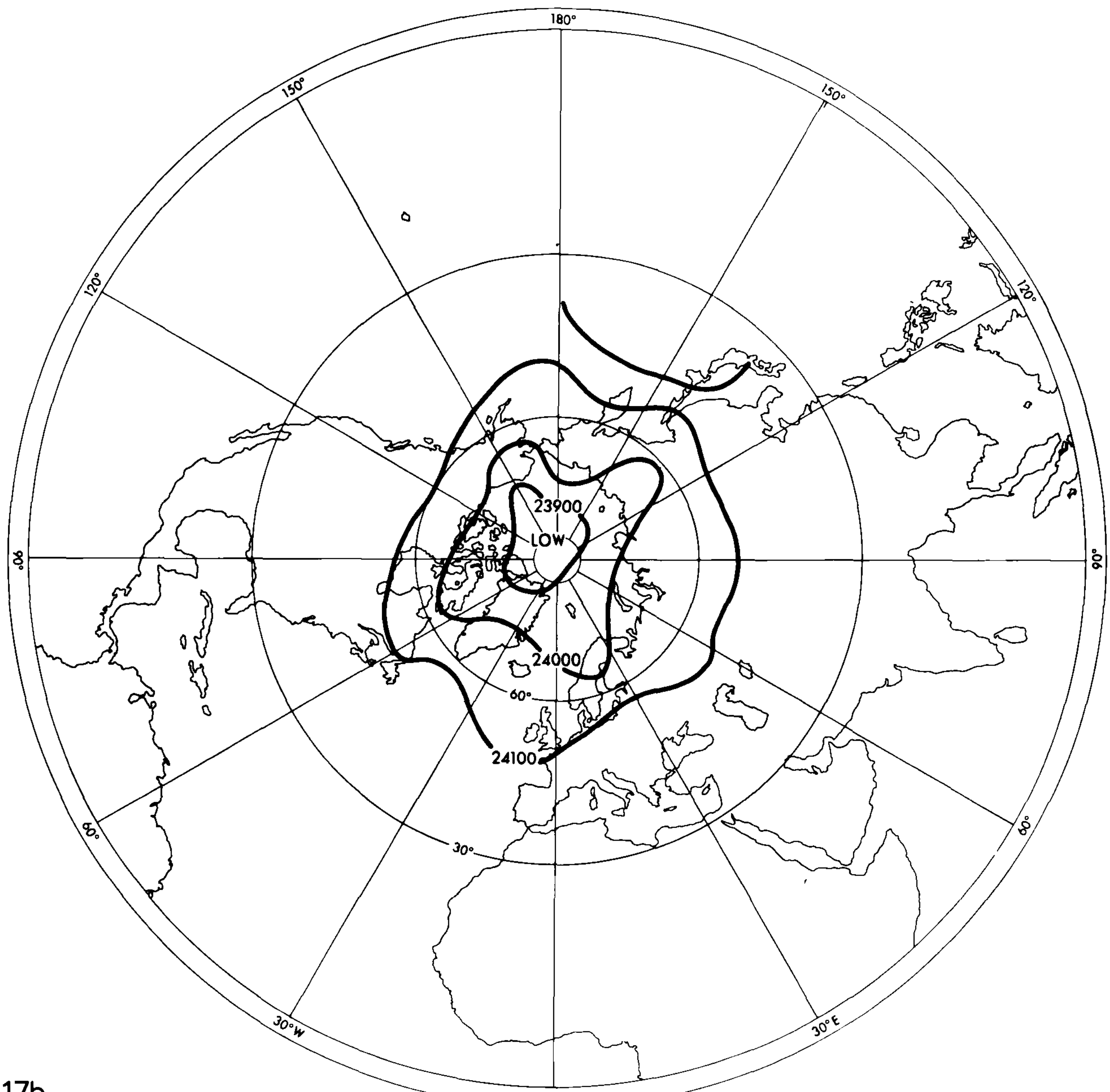
180°
150°
150°
120°
120°
90°
90°
60°
60°
30°W
30°E
0°
60°
30°
23900
LOW
24000
24100

17b

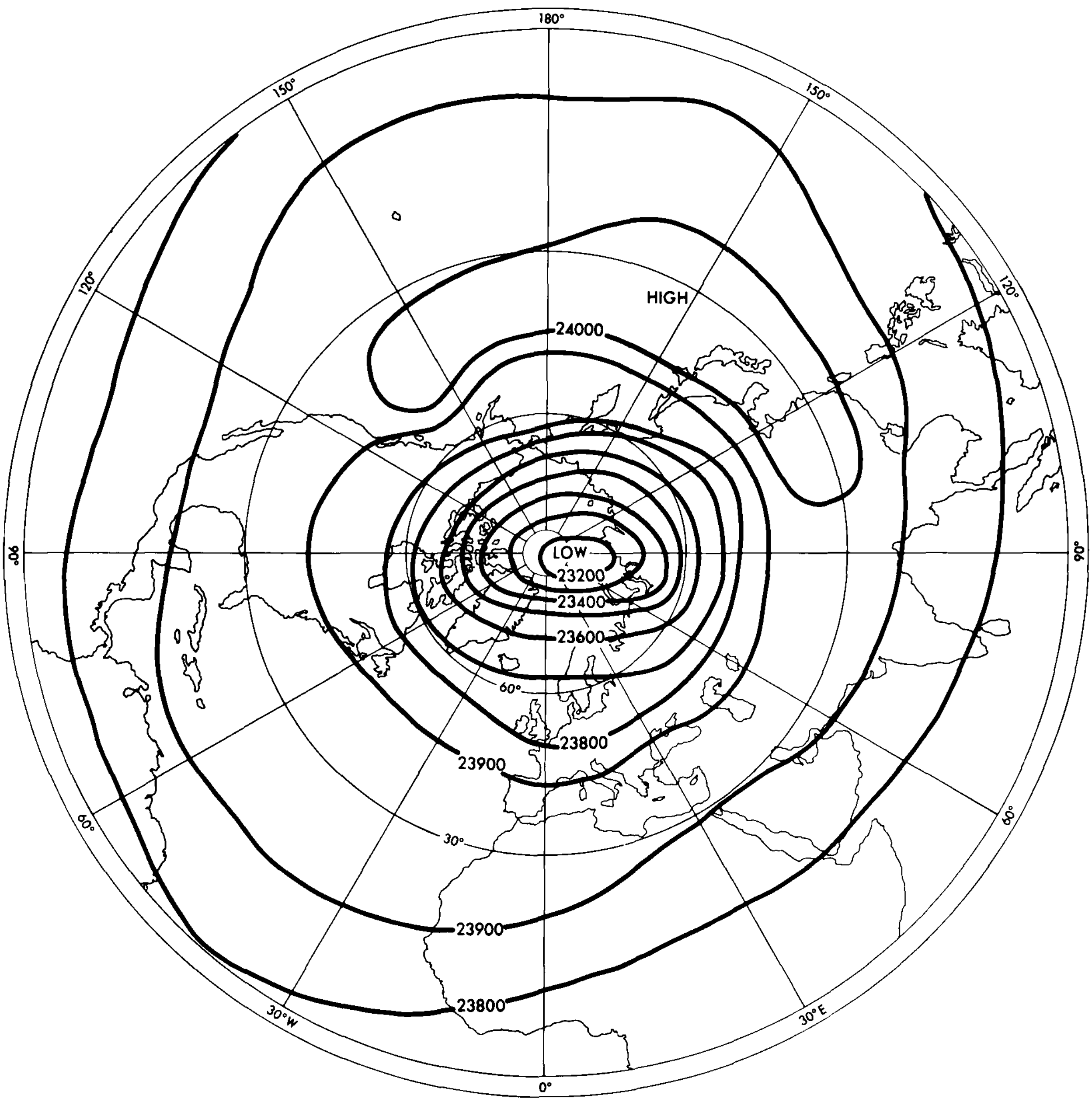

PLATE 18. AVERAGE CONTOUR HEIGHTS AT 30 MILLIBARS OVER THE NORTHERN HEMISPHERE IN OCTOBER, 1957–64

Heights are in geopotential metres.

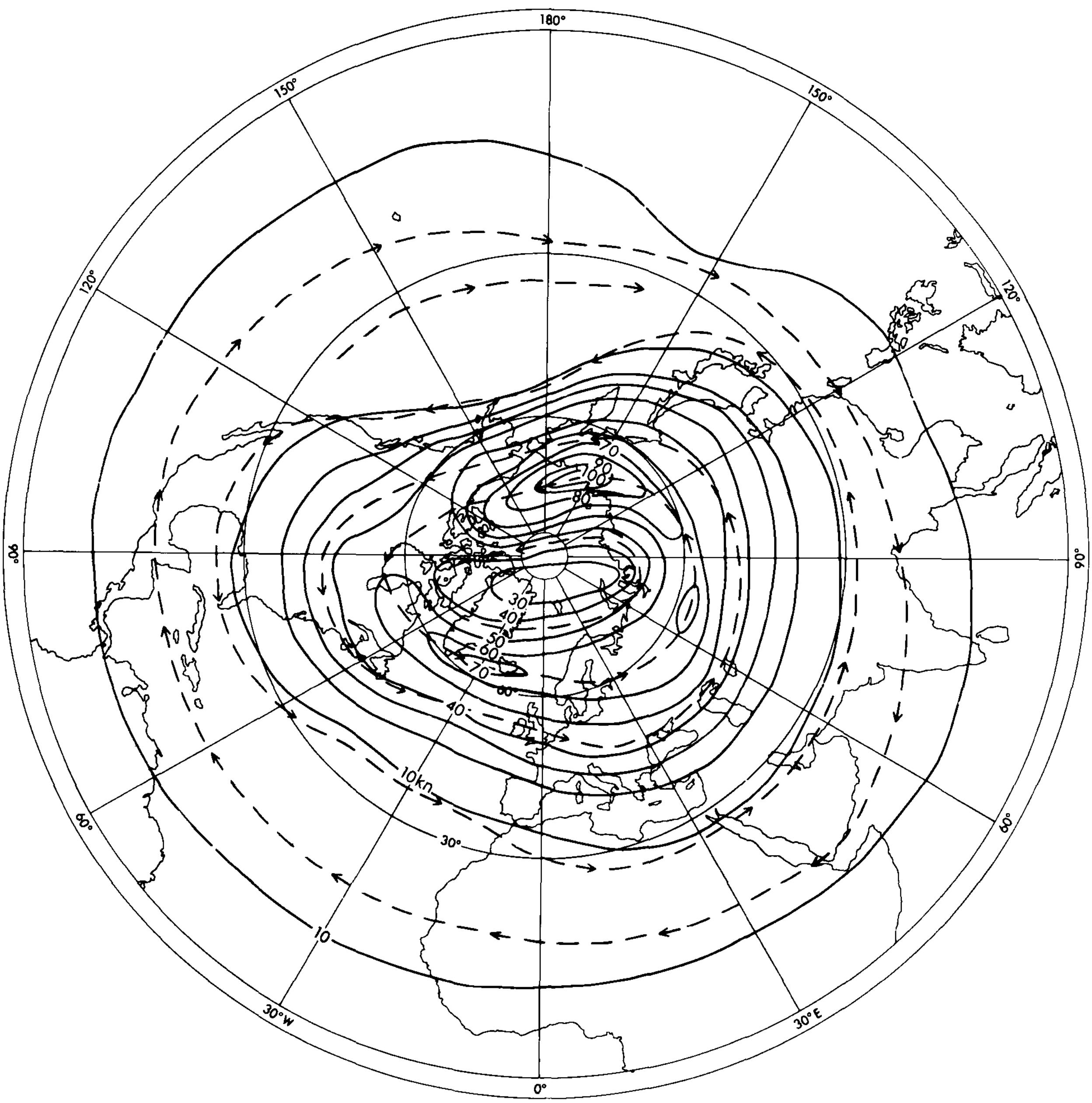

PLATE 19. AVERAGE WINDS AT 30 MILLIBARS OVER THE NORTHERN HEMISPHERE IN JANUARY, 1958–65

——— Isotachs (knots) - - - → - Streamlines

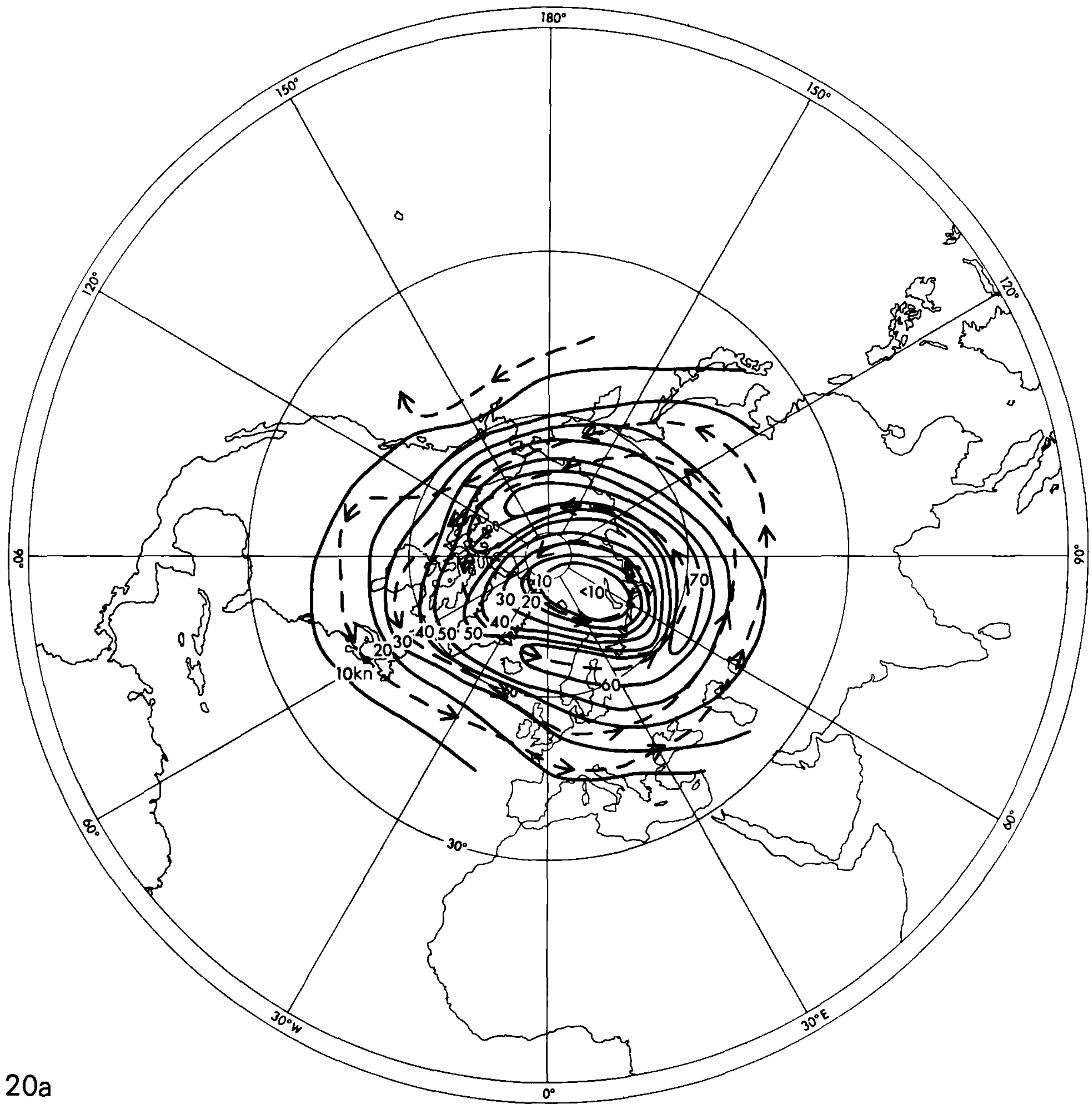

20a

PLATES 20a AND 20b. AVERAGE WINDS AT 30 MILLIBARS OVER THE NORTHERN HEMISPHERE (NORTH OF LATITUDE 45°N) IN FEBRUARY (20a) AND MARCH (20b), 1958–65

Isotachs (knots) Streamlines

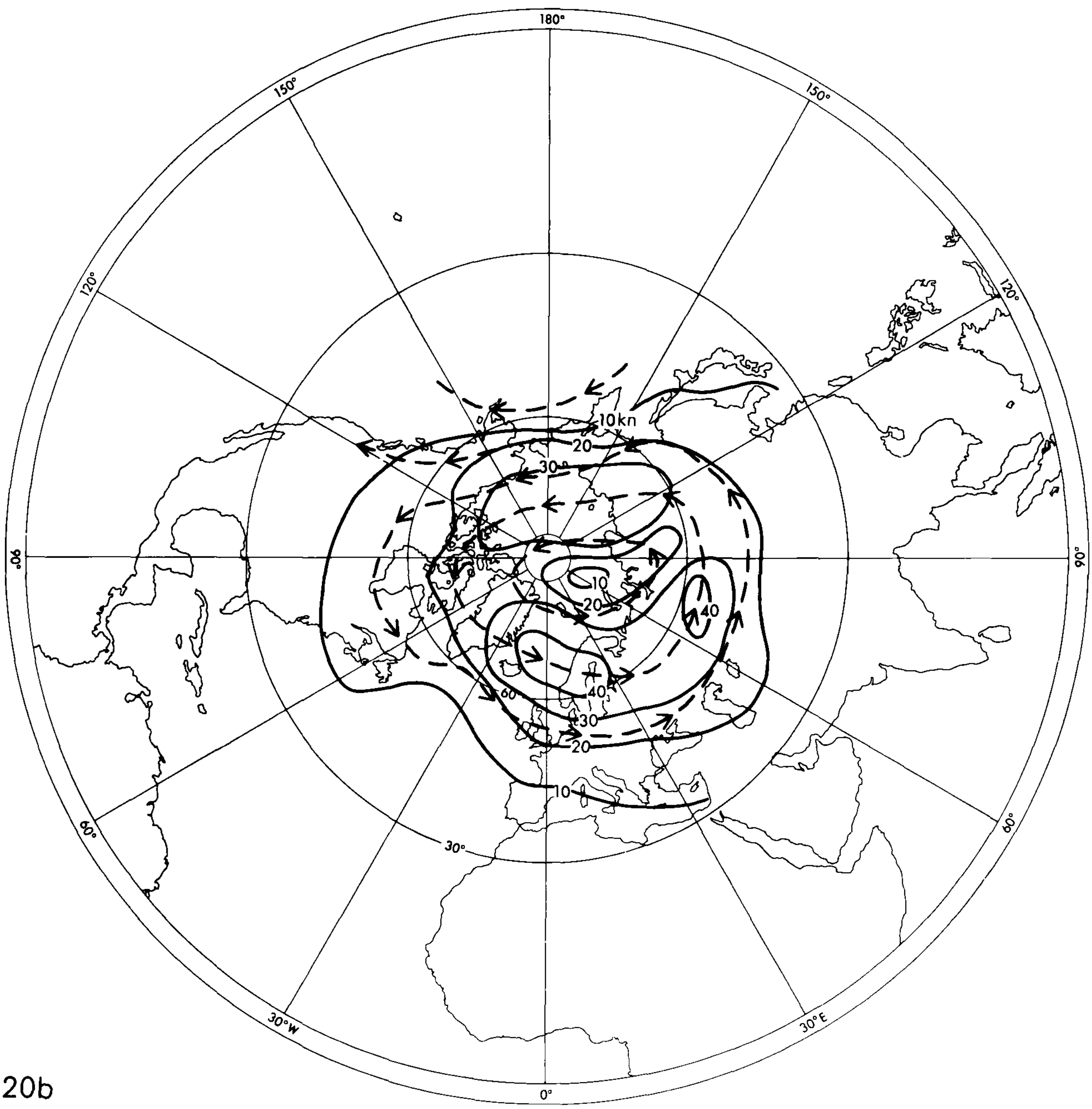
180°
150°
150°
120°
120°
90°
90°
60°
60°
30°W
30°E
0°
30°
10kn
20
30
40
40
30
20
10
60

20b

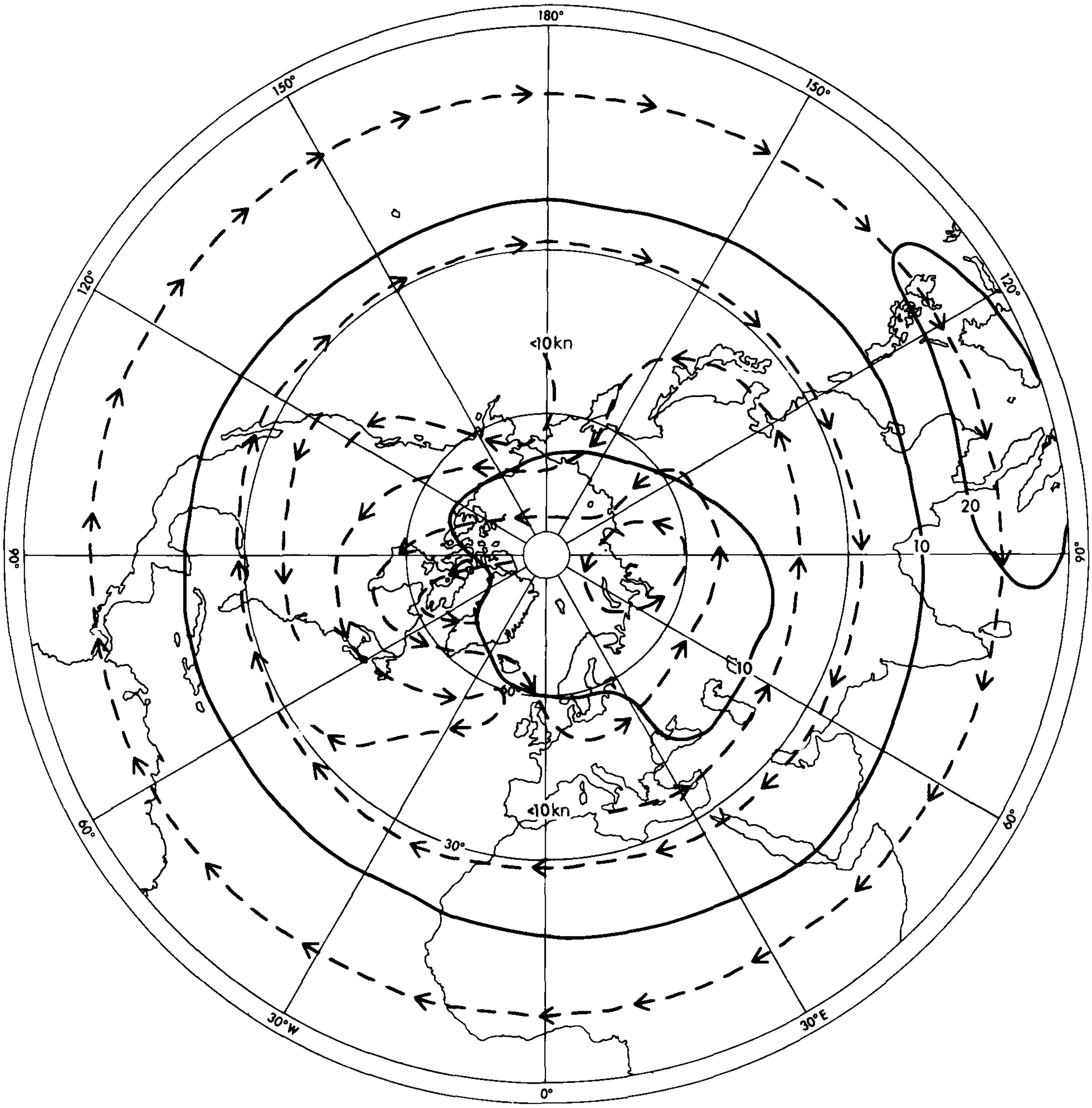

PLATE 21. AVERAGE WINDS AT 30 MILLIBARS OVER THE NORTHERN HEMISPHERE IN APRIL, 1958–65

——— Isotachs (kn) – – – → – Streamlines

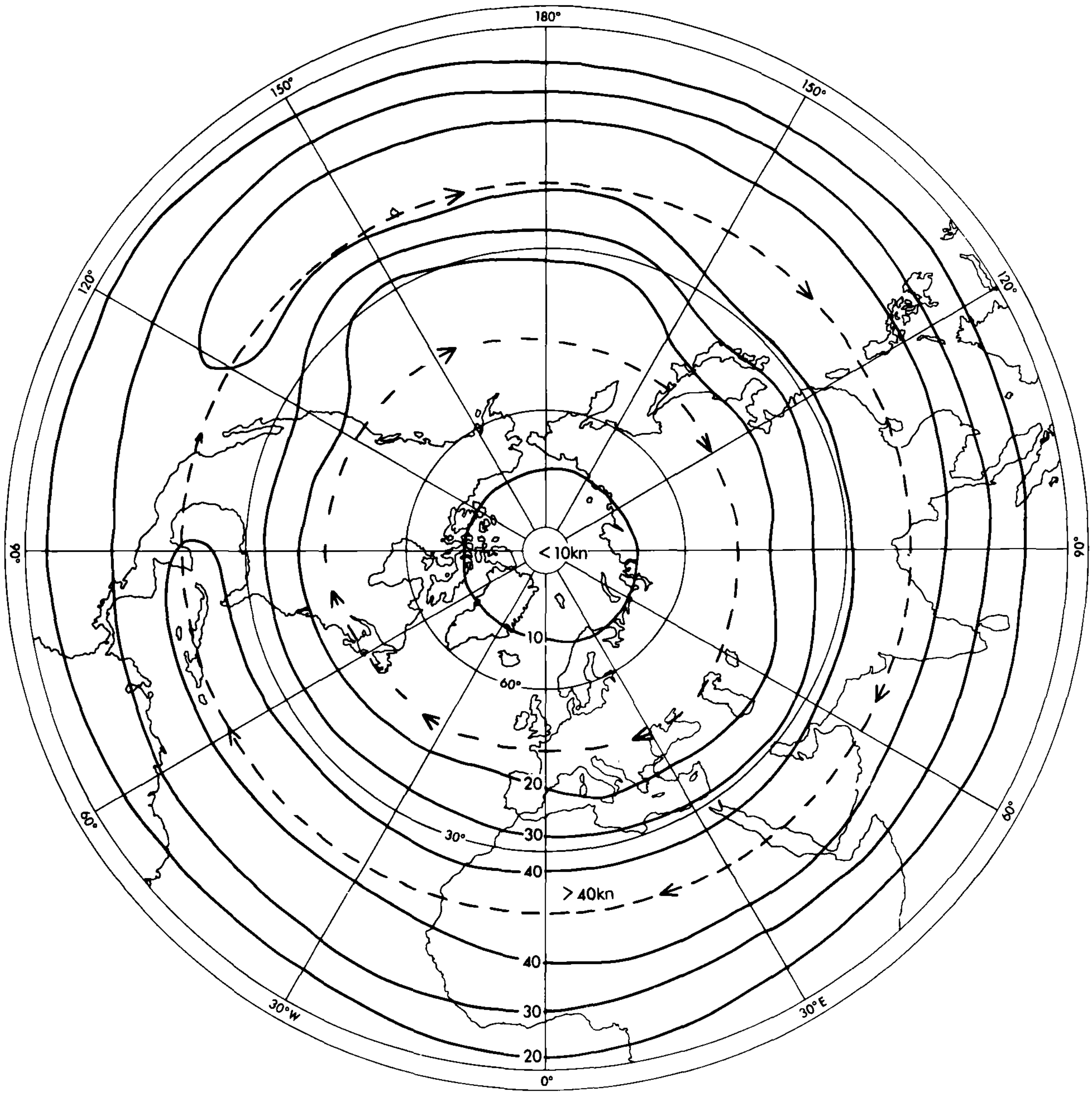

PLATE 22. AVERAGE WINDS AT 30 MILLIBARS OVER THE NORTHERN HEMISPHERE IN JULY, 1957–64

——— Isotachs(kn) - - - → - Streamlines

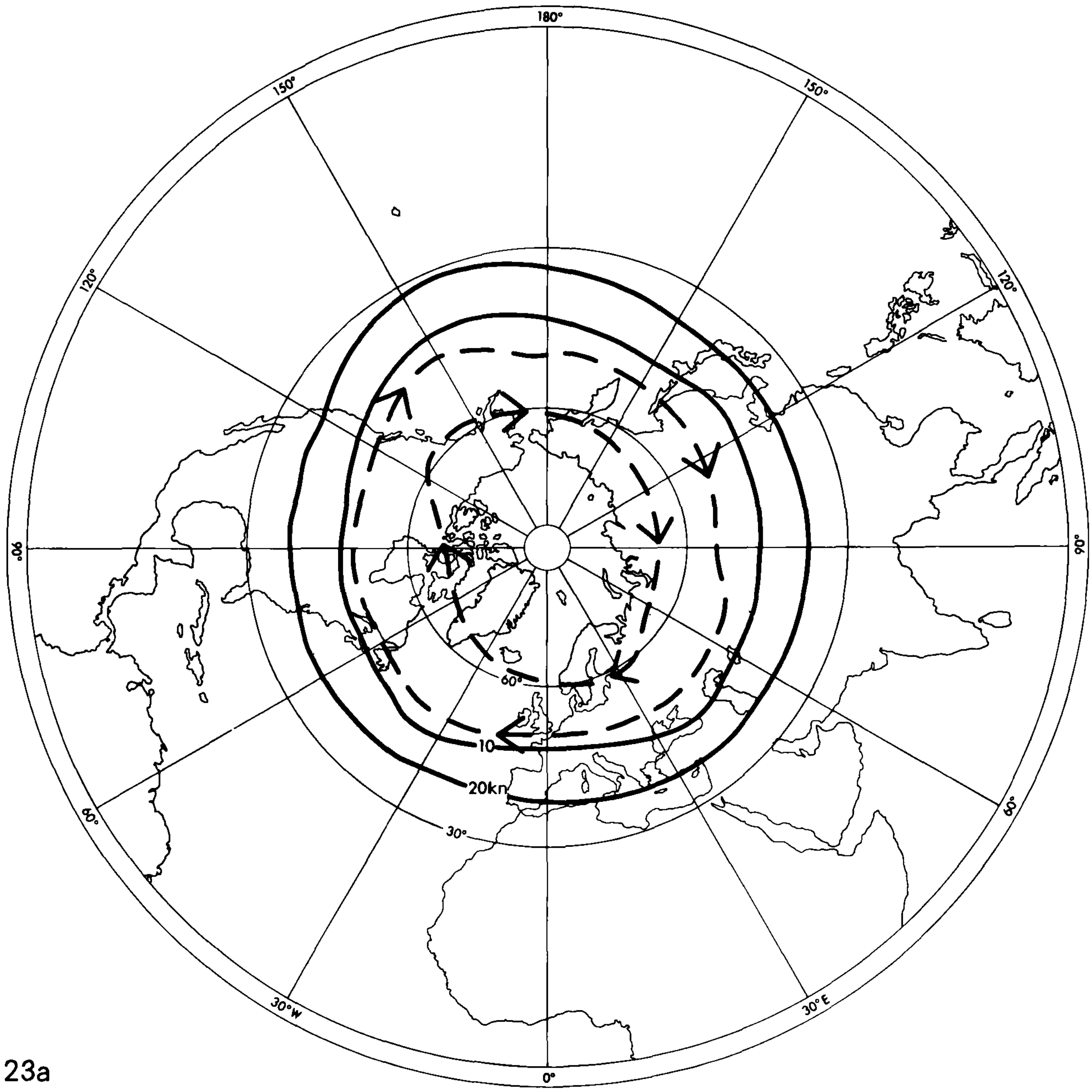

23a

PLATES 23a AND 23b. AVERAGE WINDS AT 30 MILLIBARS OVER THE NORTHERN HEMISPHERE (NORTH OF LATITUDE 45°N) IN AUGUST (23a) AND SEPTEMBER (23b), 1957–64

——— Isotachs (kn) – – – → – Streamlines

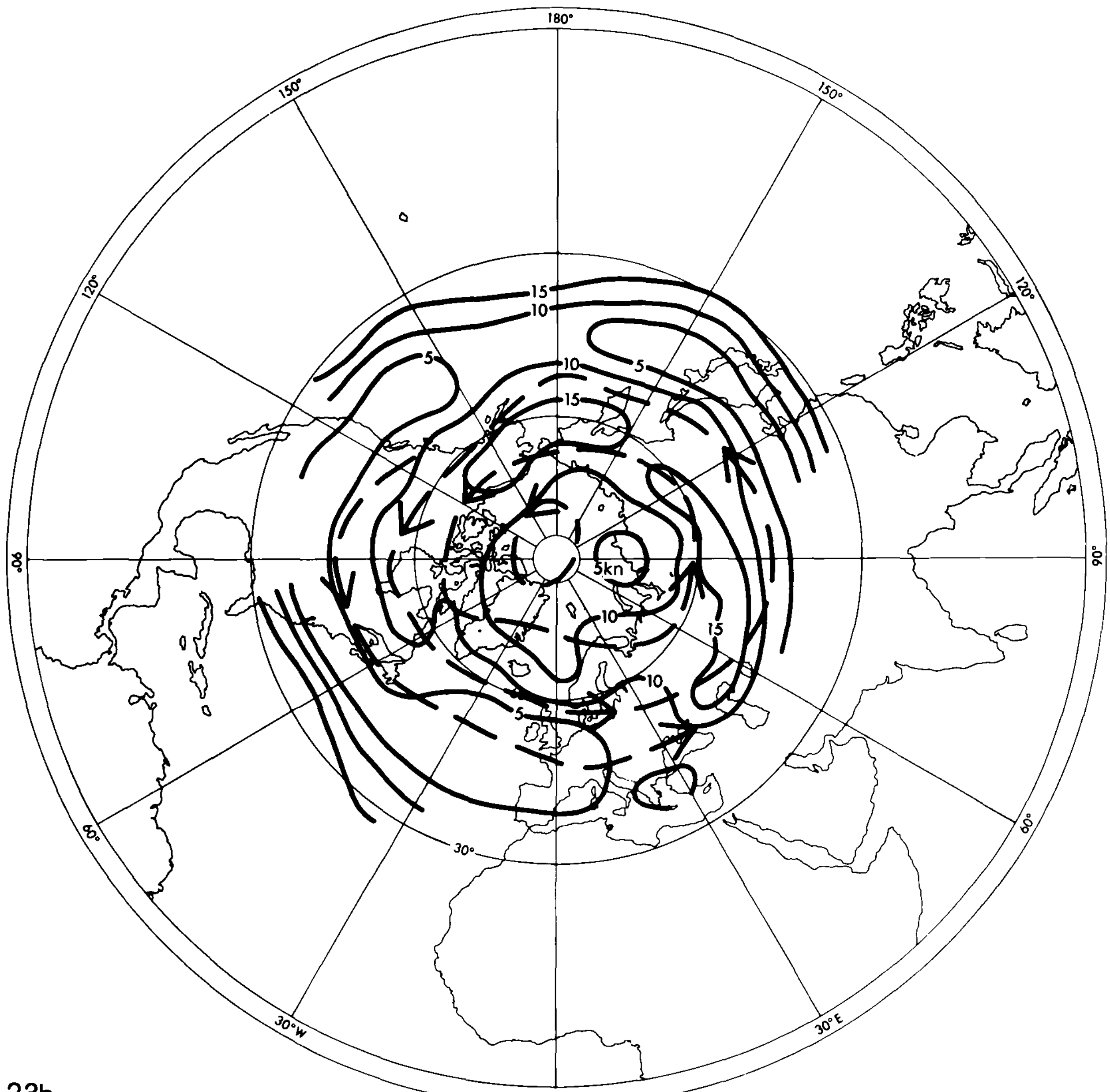
180°
150°
150°
120°
120°
90°
90°
60°
60°
30°W
30°E
30°
0°
15
10
5
10
5
15
5kn
10
15
10
5

23b

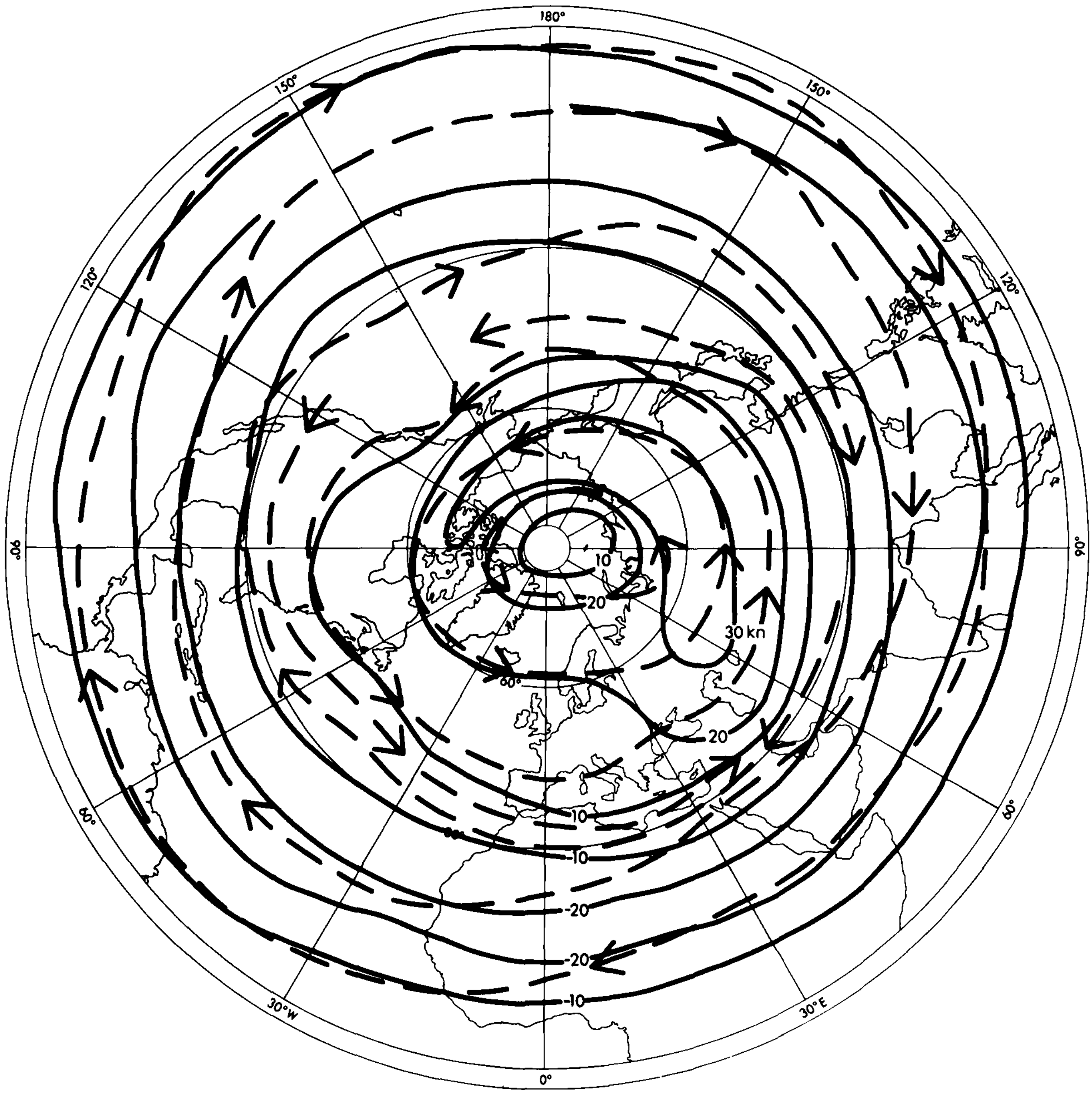

PLATE 24. AVERAGE WINDS AT 30 MILLIBARS OVER THE NORTHERN HEMISPHERE IN OCTOBER, 1957–64

——— Isotachs (kn) – – – → – Streamlines

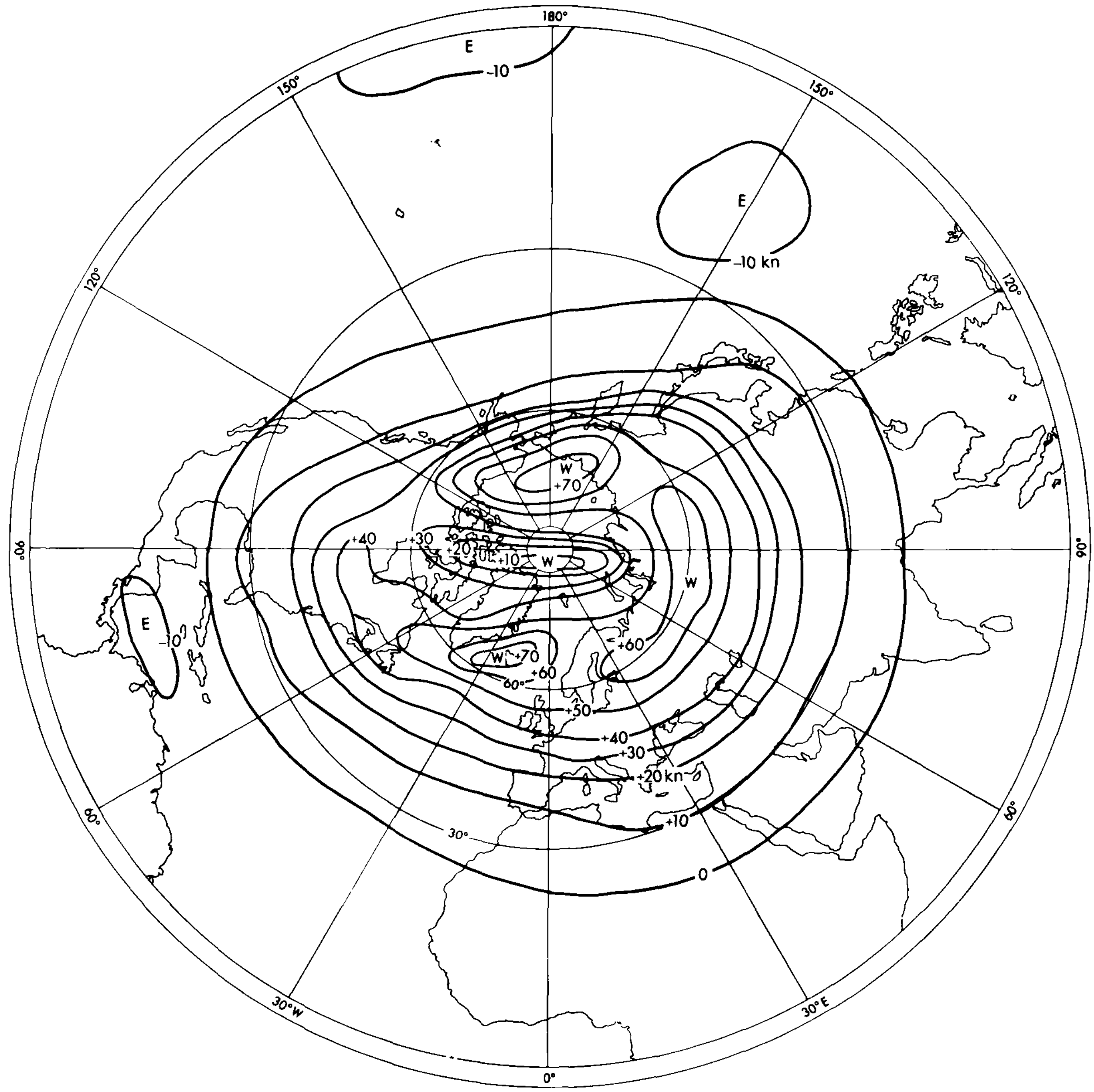

PLATE 25. AVERAGE ZONAL WIND COMPONENTS (KNOTS) AT 30 MILLIBARS OVER THE NORTHERN HEMISPHERE IN JANUARY, 1958–65

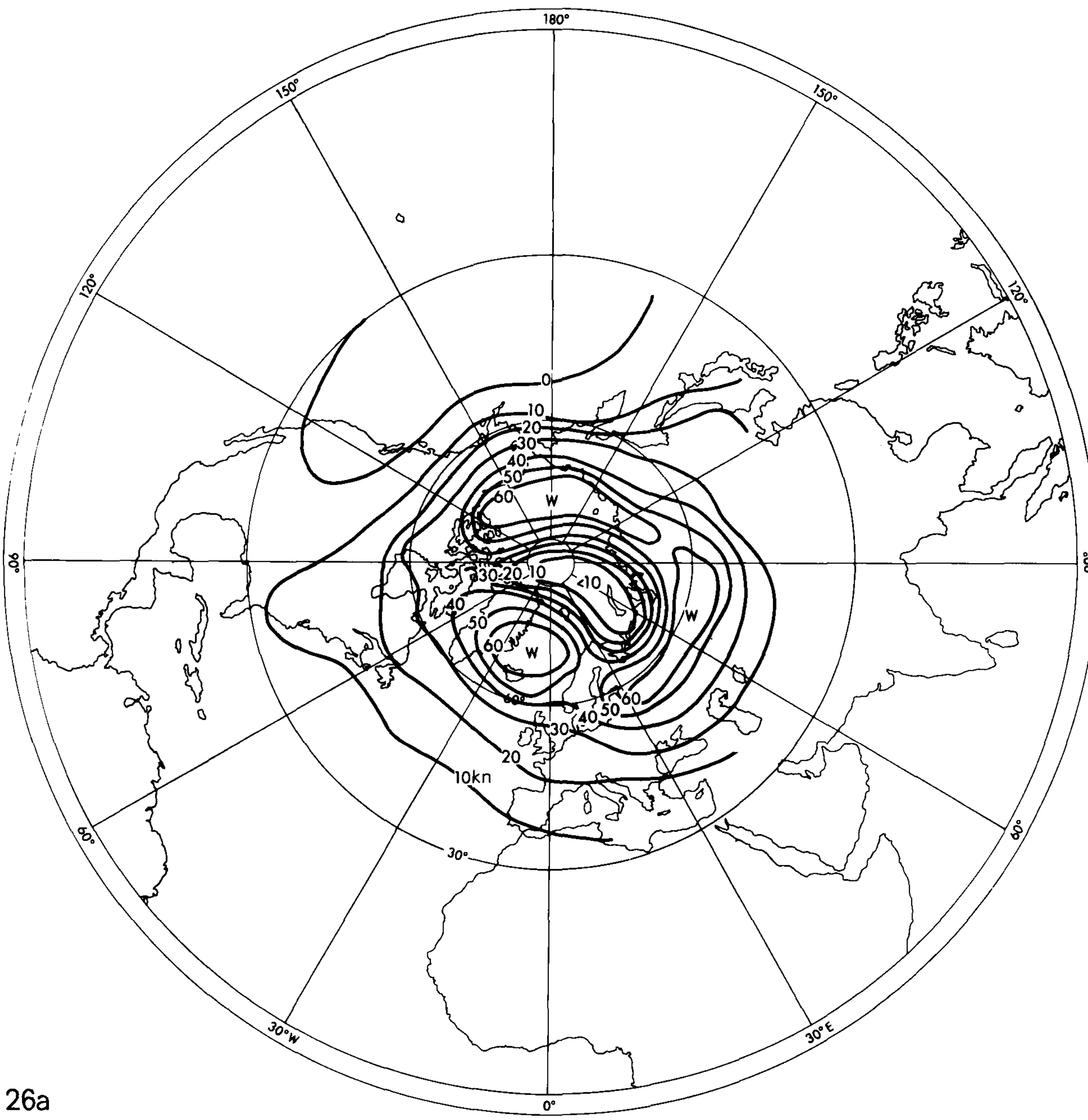

26a

PLATES 26a AND 26b. AVERAGE ZONAL WIND COMPONENTS (KNOTS) AT 30 MILLIBARS OVER THE NORTHERN HEMISPHERE (NORTH OF LATITUDE 45°N) IN FEBRUARY (26a) AND MARCH (26b), 1958–65

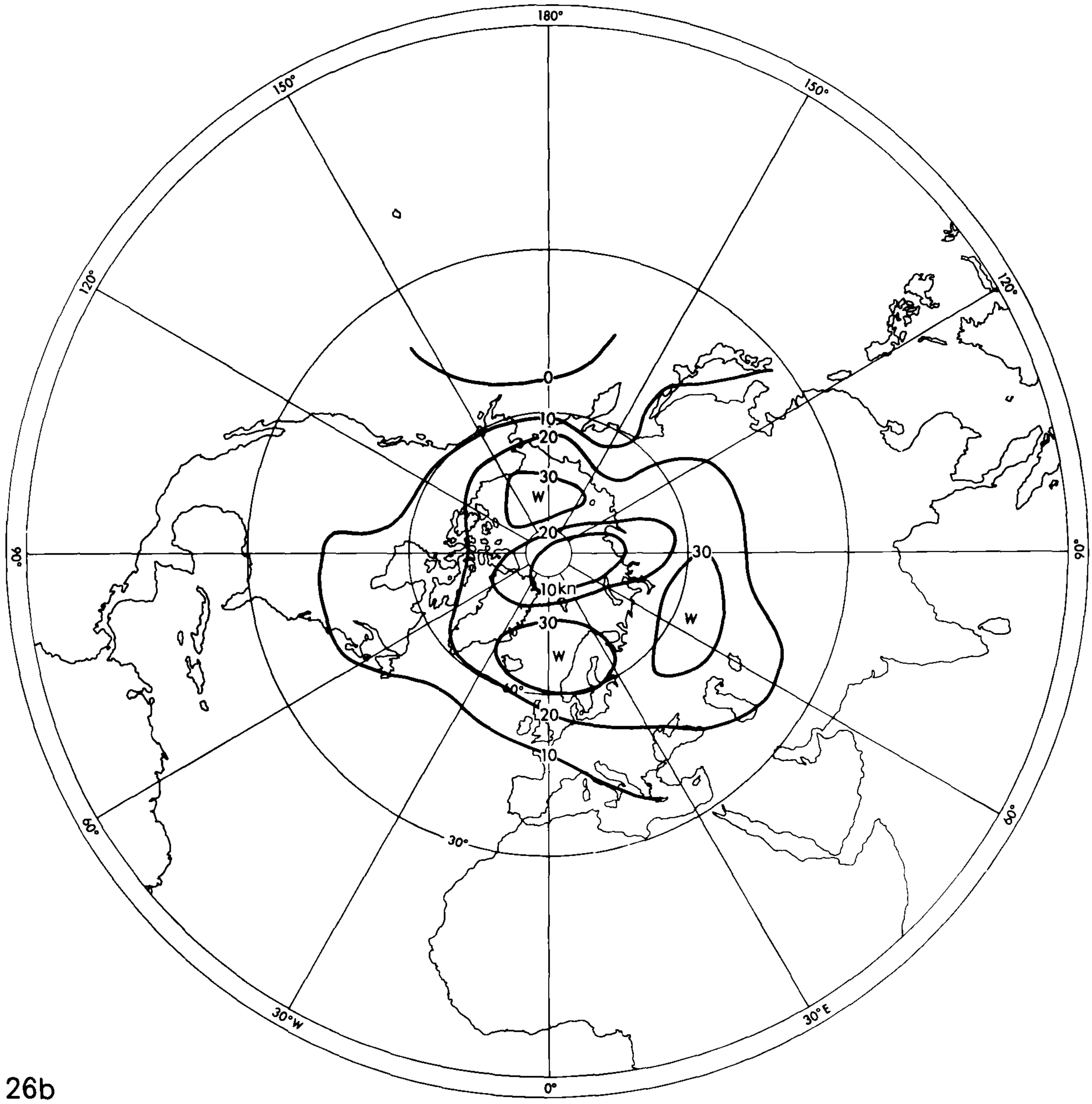
180°
150°
150°
120°
120°
90°
90°
60°
60°
30°W
30°E
0°
30°
0
10
20
30
W
20
10kn
30
30
W
W
40°
20
10

26b

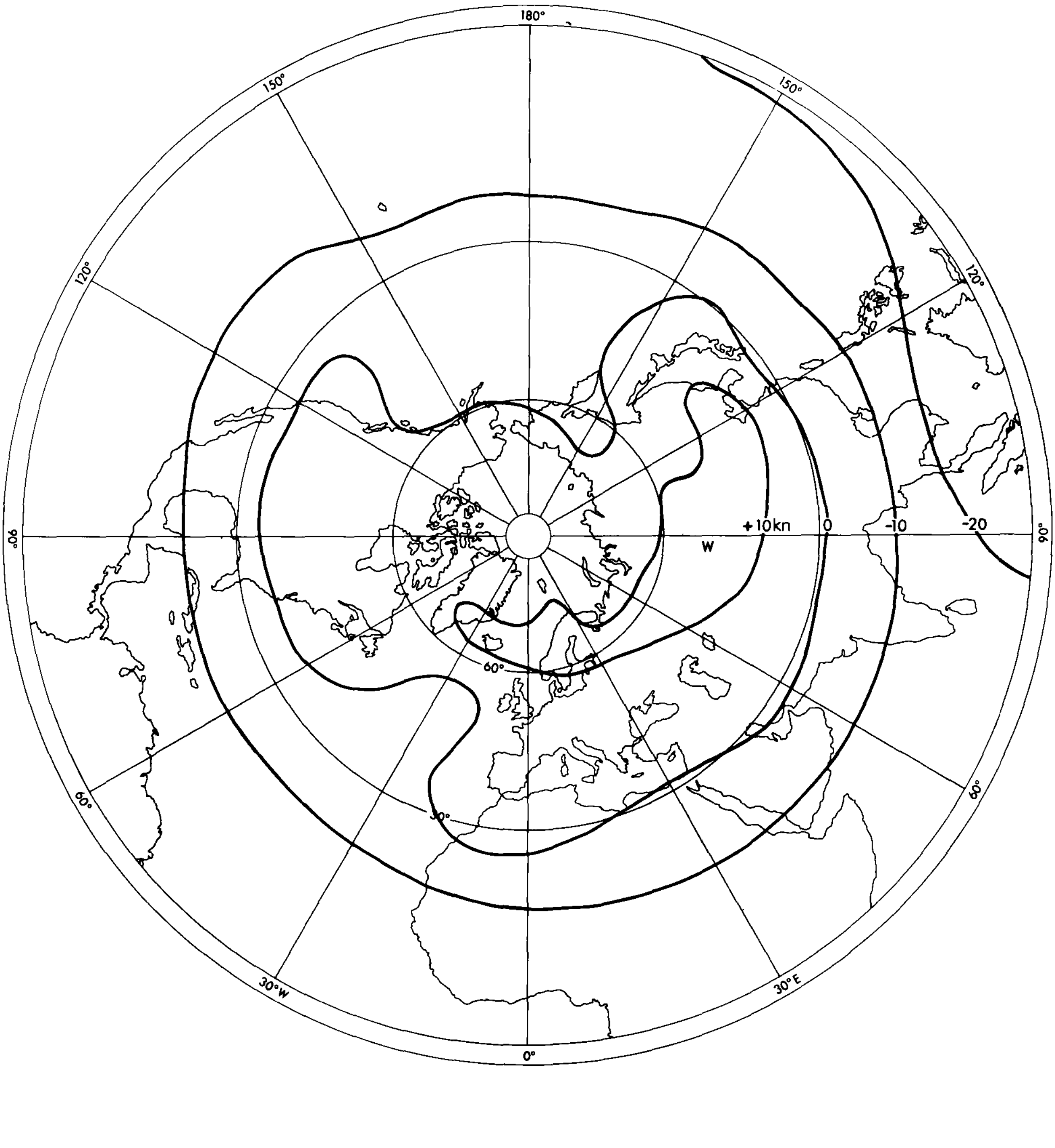

PLATE 27. AVERAGE ZONAL WIND COMPONENTS (KNOTS) AT 30 MILLIBARS OVER THE NORTHERN HEMISPHERE IN APRIL, 1958–65

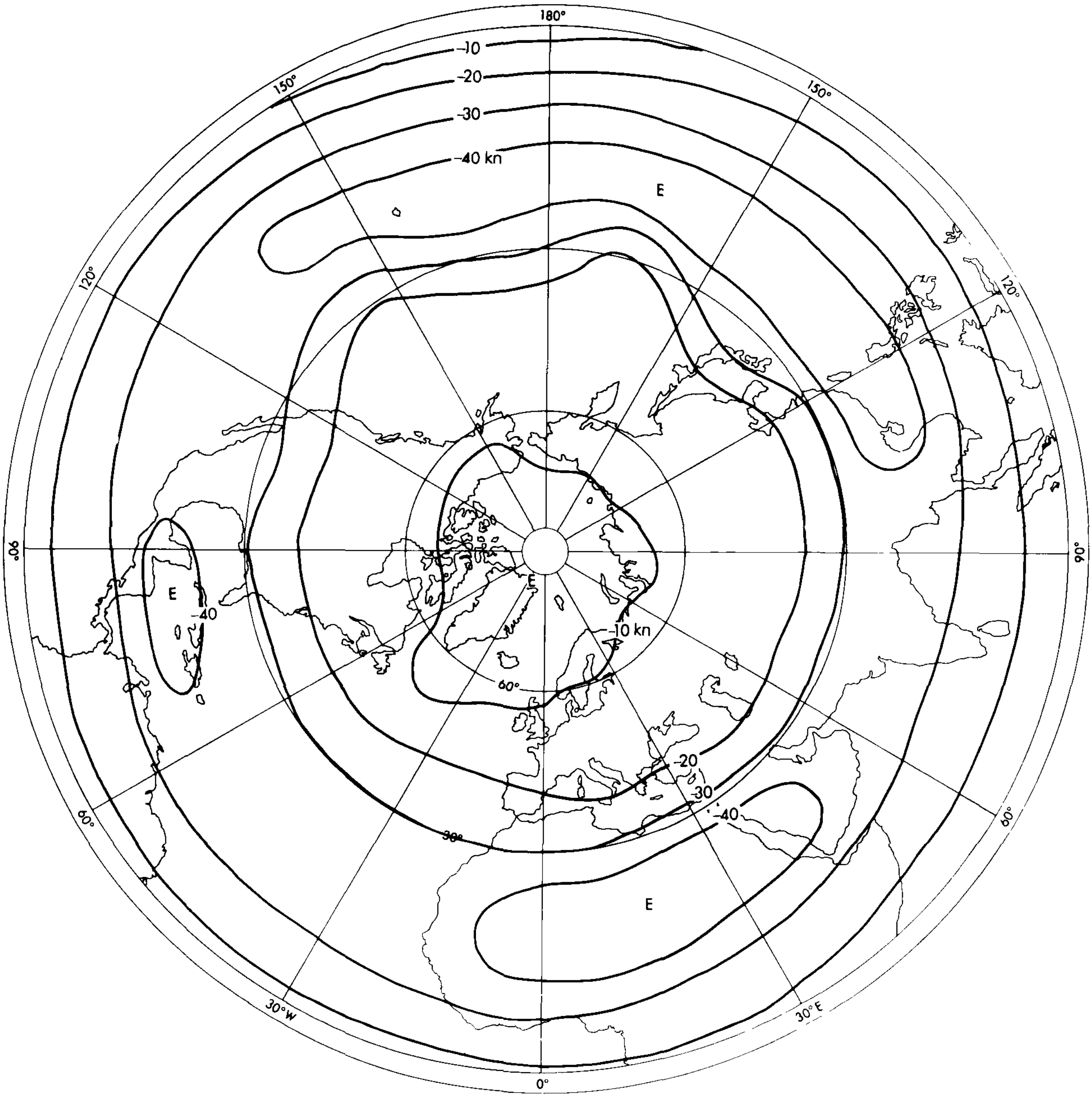

PLATE 28. AVERAGE ZONAL WIND COMPONENTS (KNOTS) AT 30 MILLIBARS OVER THE NORTHERN HEMISPHERE IN JULY, 1957–64

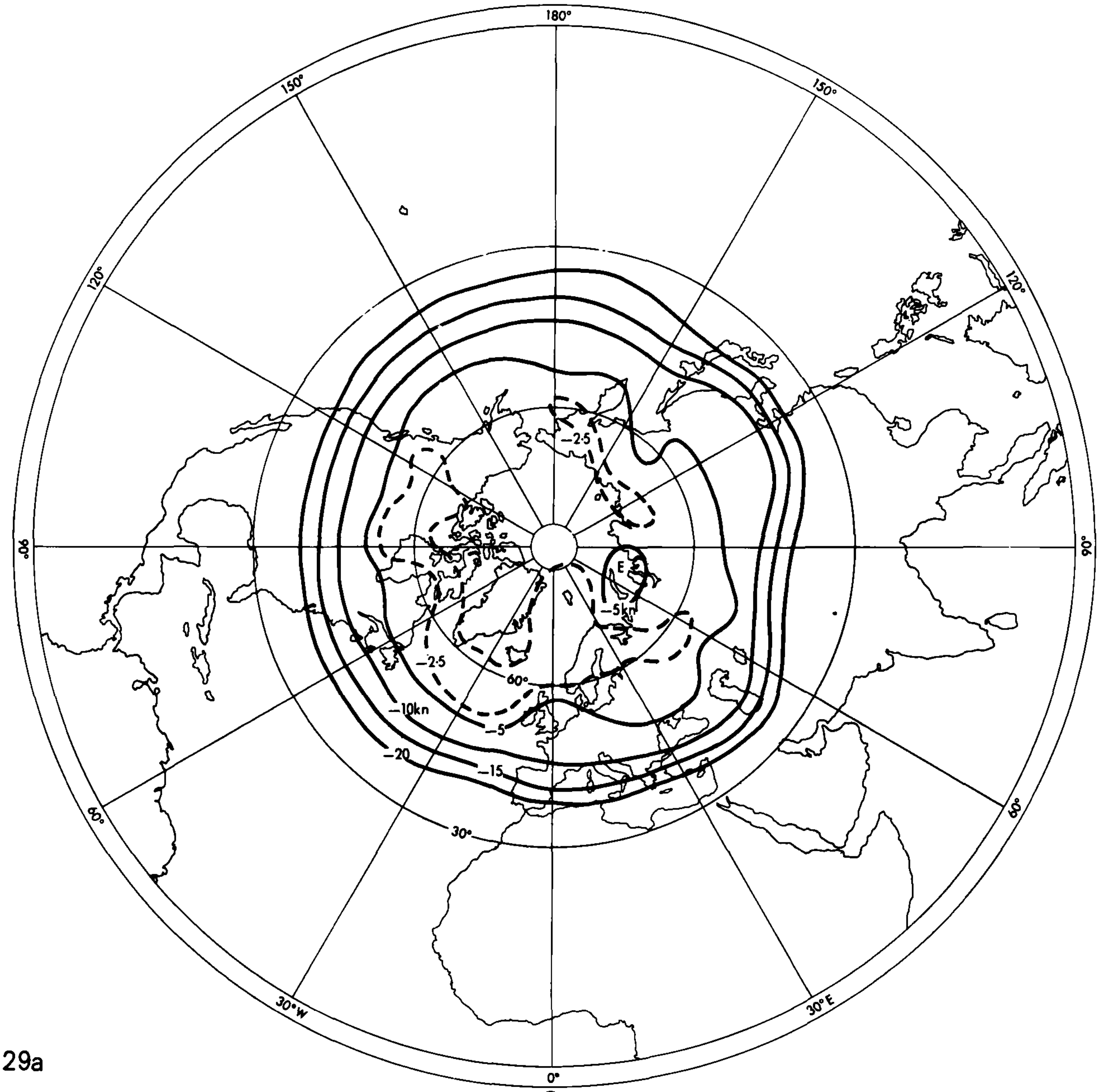

29a

PLATES 29a AND 29b. AVERAGE ZONAL WIND COMPONENTS (KNOTS) AT 30 MILLIBARS OVER THE NORTHERN HEMISPHERE (NORTH OF LATITUDE 45°N) IN AUGUST (29a) AND SEPTEMBER (29b), 1957–64

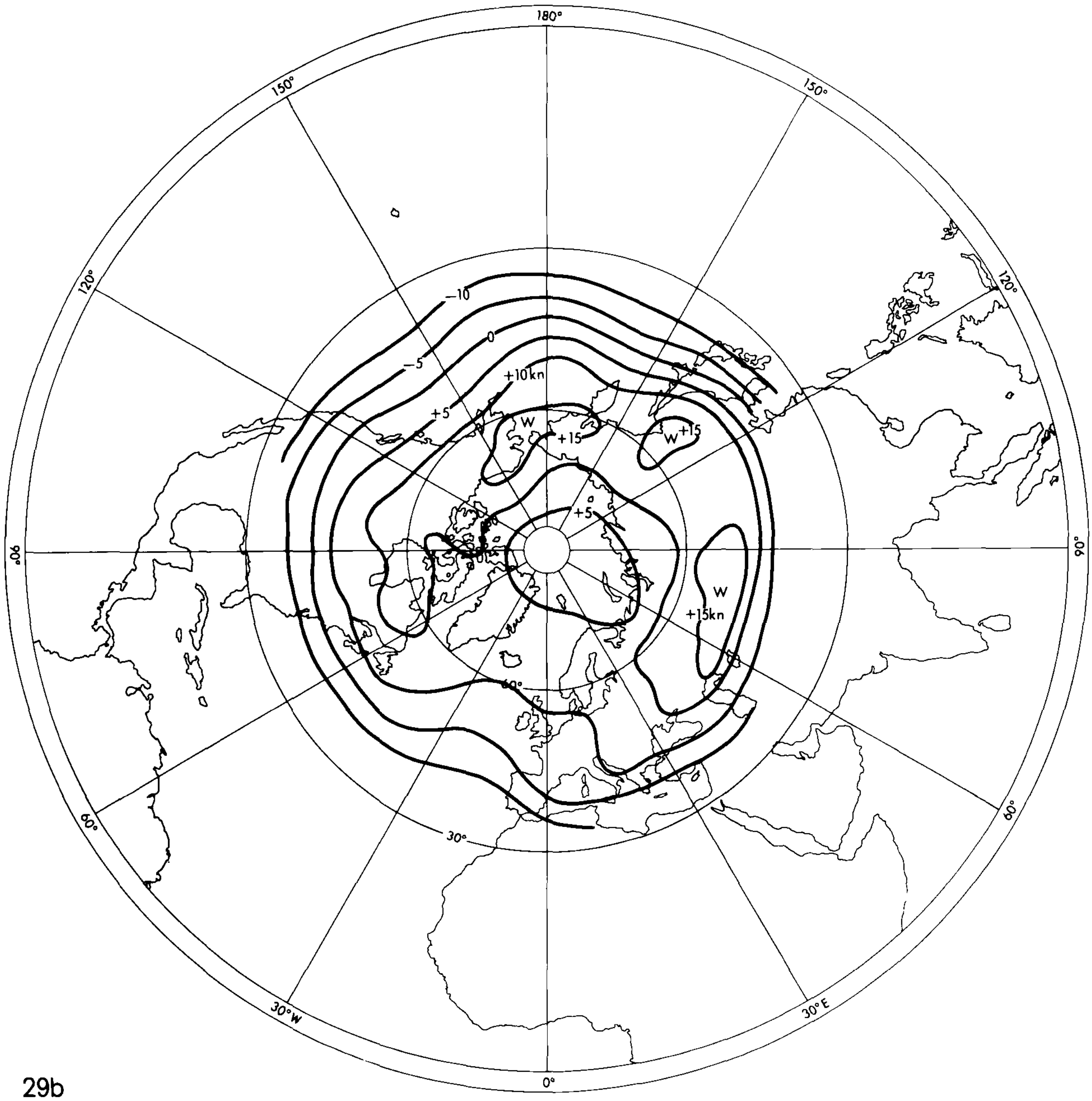
180°
150°
150°
120°
120°
90°
90°
60°
60°
30°W
30°E
0°
30°
60°
−10
0
−5
+10kn
+5
W
+15
W
+15
+5
W
+15kn

29b

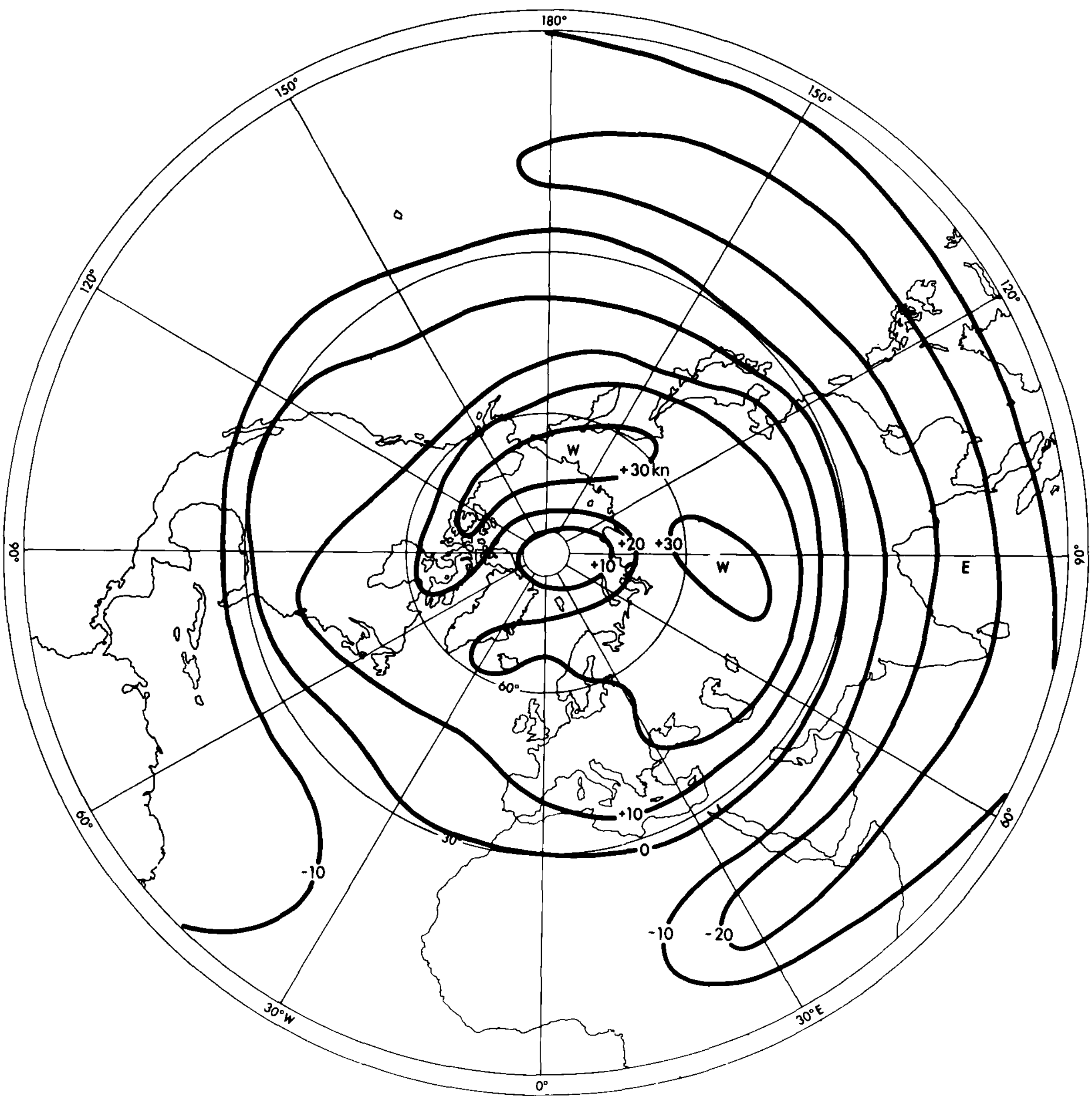

PLATE 30. AVERAGE ZONAL WIND COMPONENTS (KNOTS) AT 30 MILLIBARS OVER THE NORTHERN HEMISPHERE IN OCTOBER, 1957–64

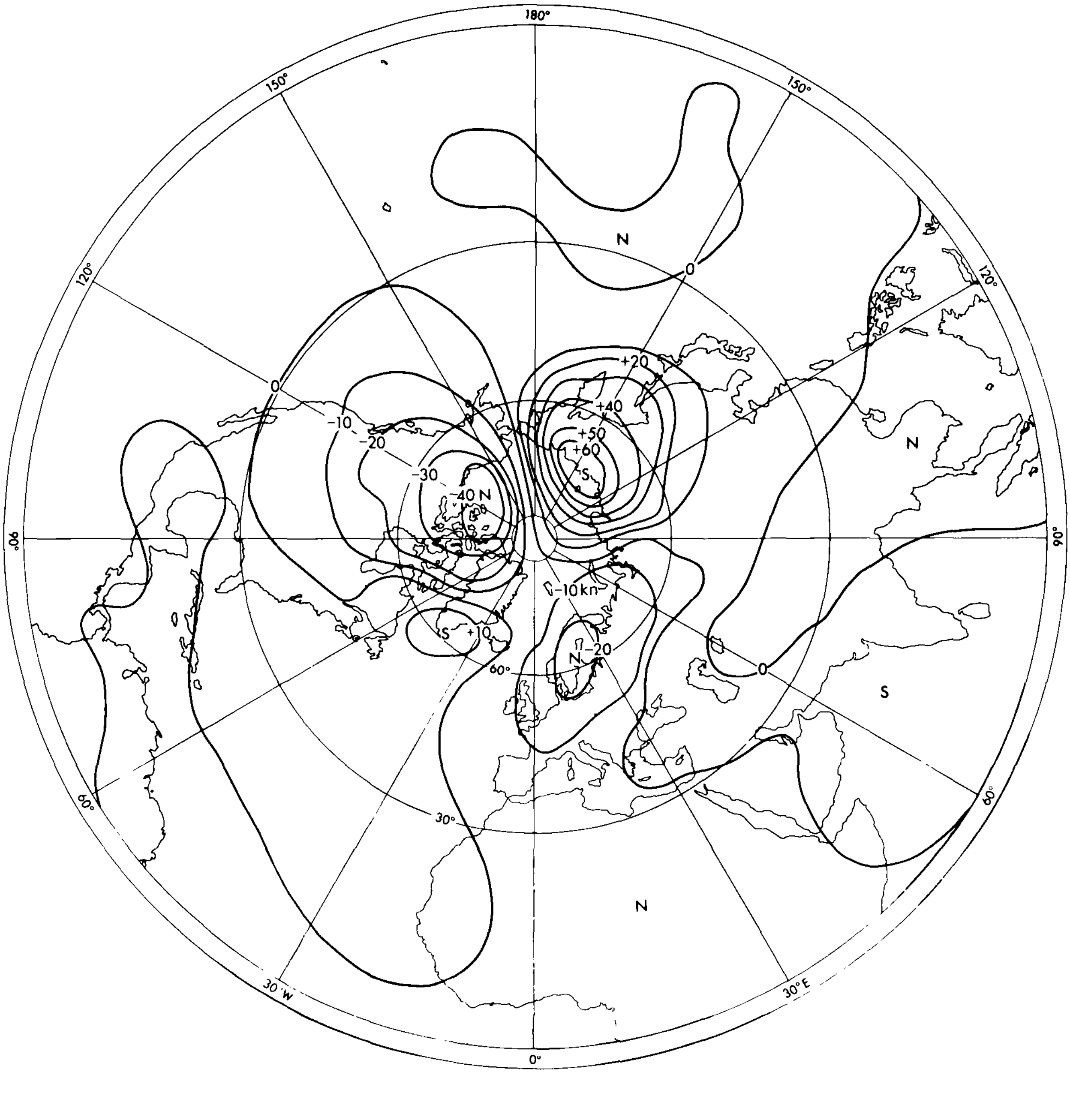

PLATE 31. AVERAGE MERIDIONAL WIND COMPONENTS (KNOTS) AT 30 MILLIBARS OVER THE NORTHERN HEMISPHERE IN JANUARY, 1958–65

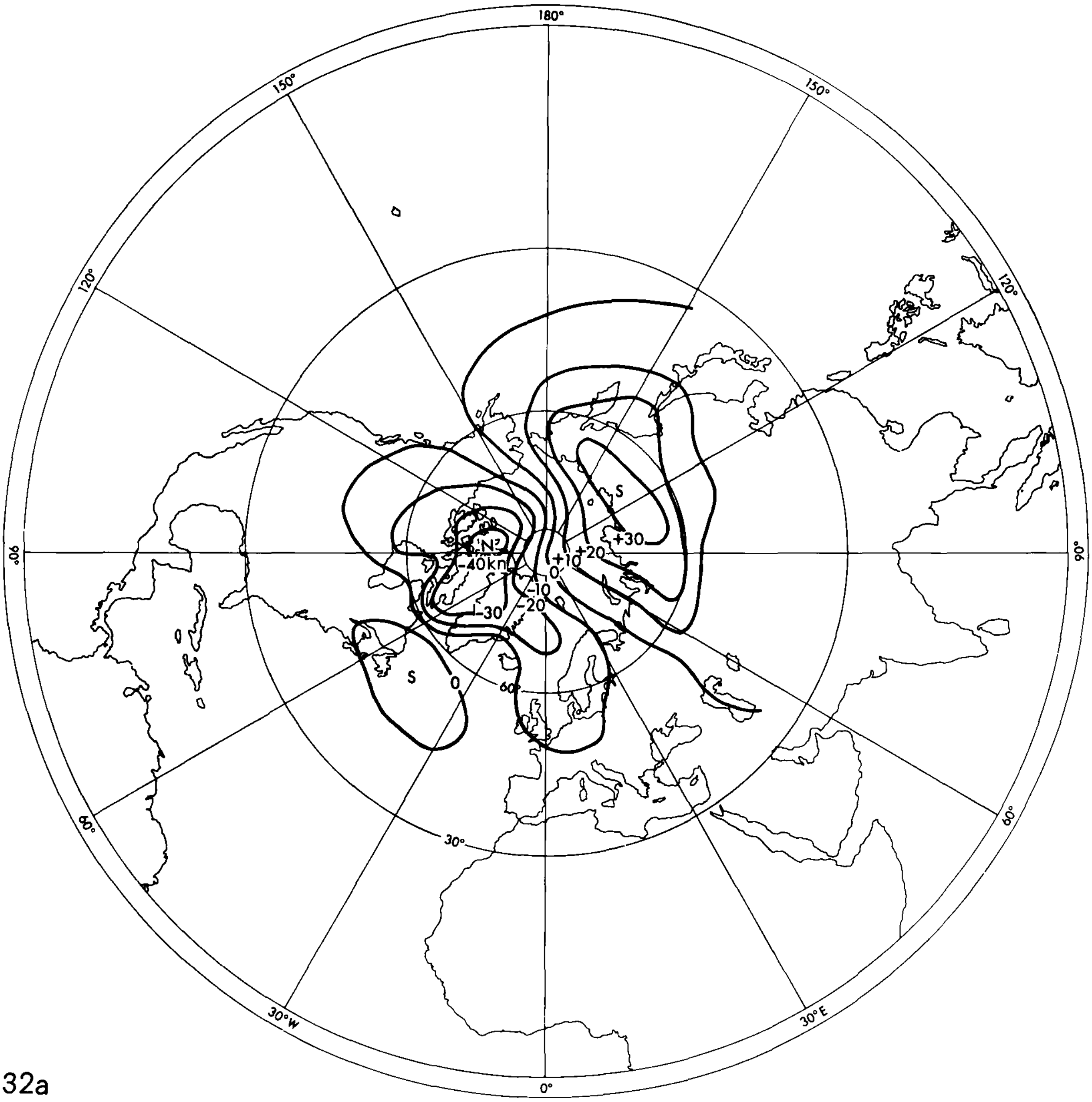

32a

PLATES 32a AND 32b. AVERAGE MERIDIONAL WIND COMPONENTS (KNOTS) AT 30 MILLIBARS OVER THE NORTHERN HEMISPHERE (NORTH OF LATITUDE 45°N) IN FEBRUARY (32a) AND MARCH (32b), 1958–65

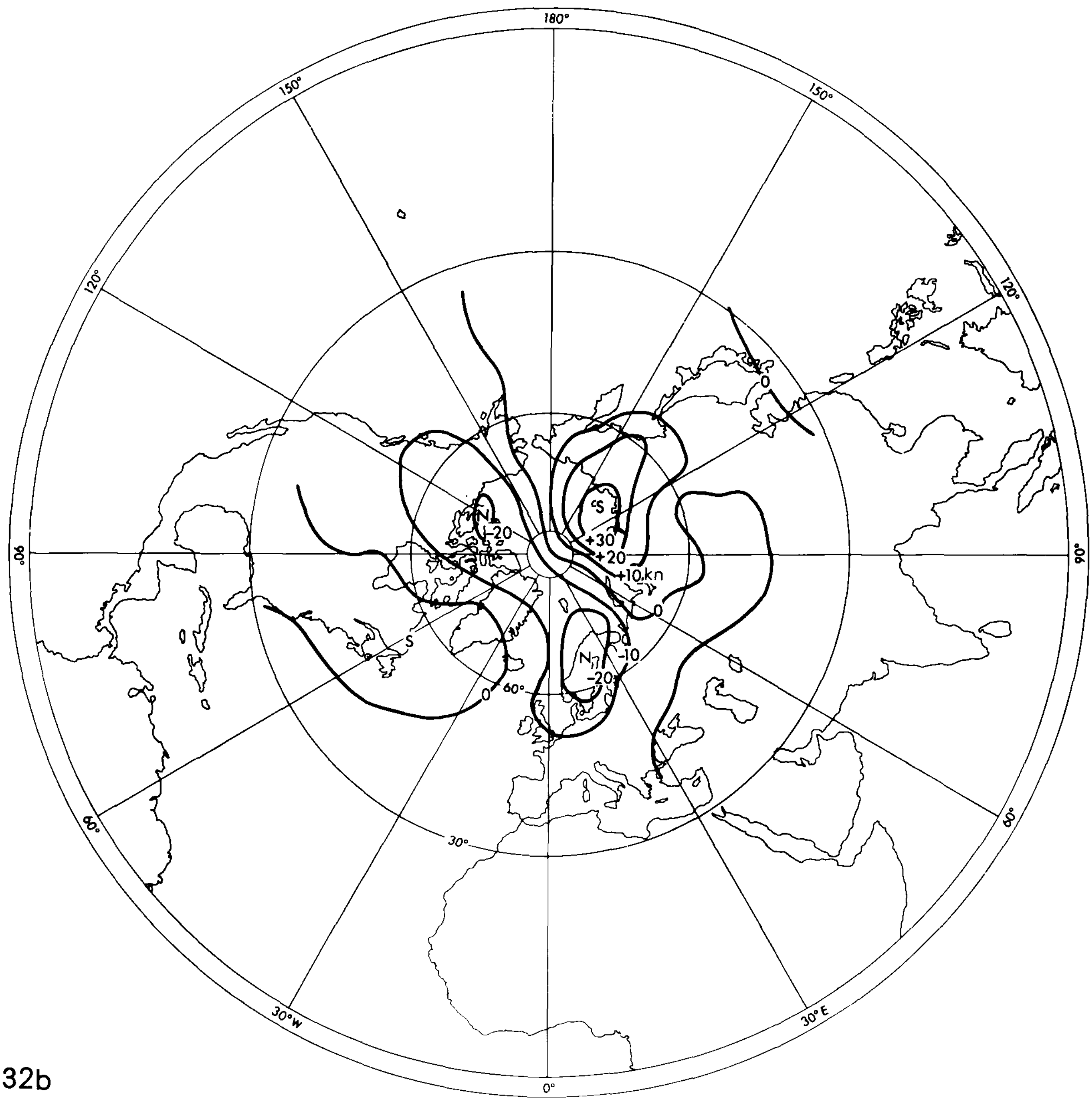
180°
150°
150°
120°
120°
90°
90°
60°
60°
30°W
30°E
0°
30°
60°
N
-20
S
+30
+20
+10 kn
0
-10
N
-20
0
S
0

32b

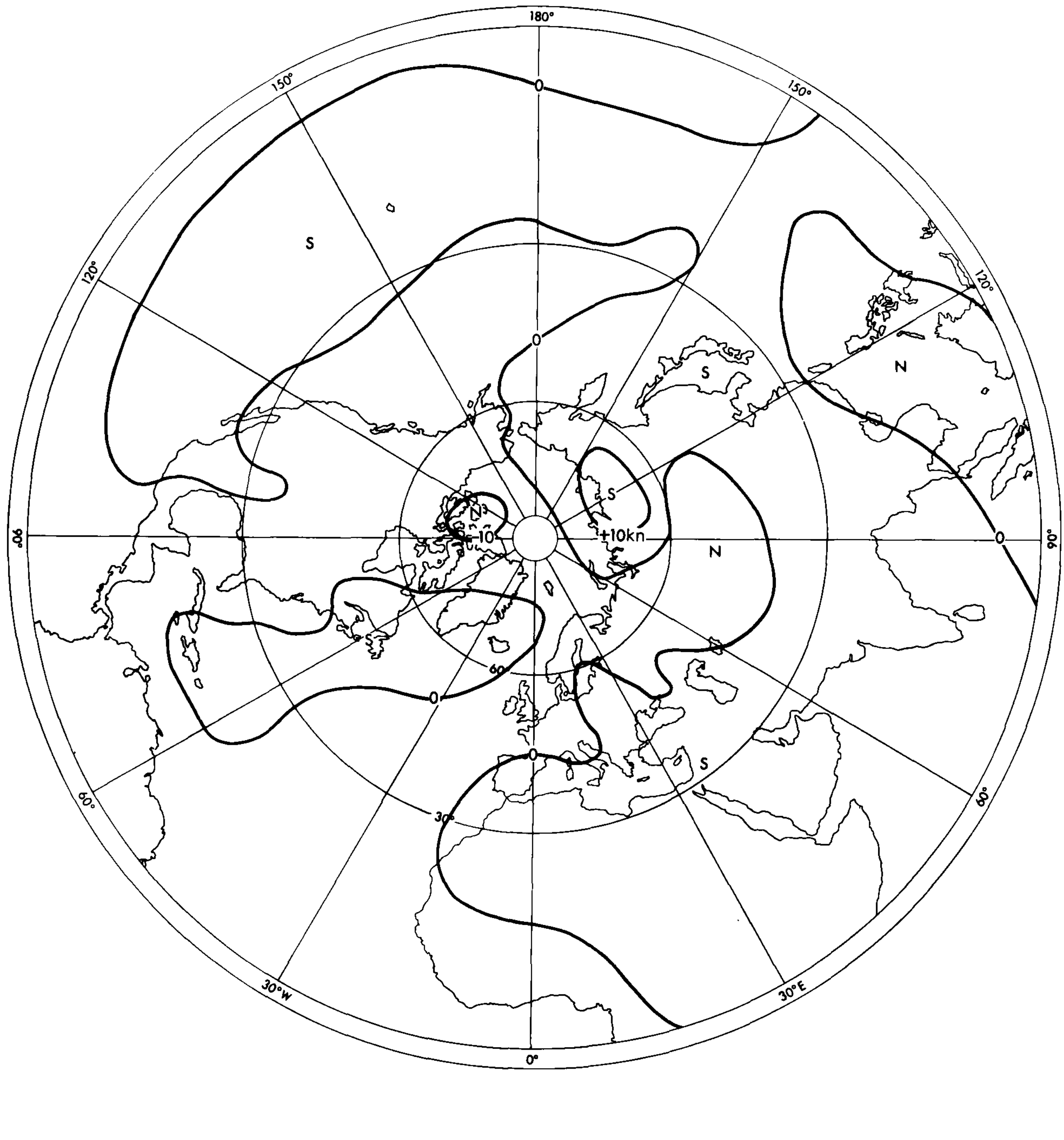

PLATE 33. AVERAGE MERIDIONAL WIND COMPONENTS (KNOTS) AT 30 MILLIBARS OVER THE NORTHERN HEMISPHERE IN APRIL, 1958–65

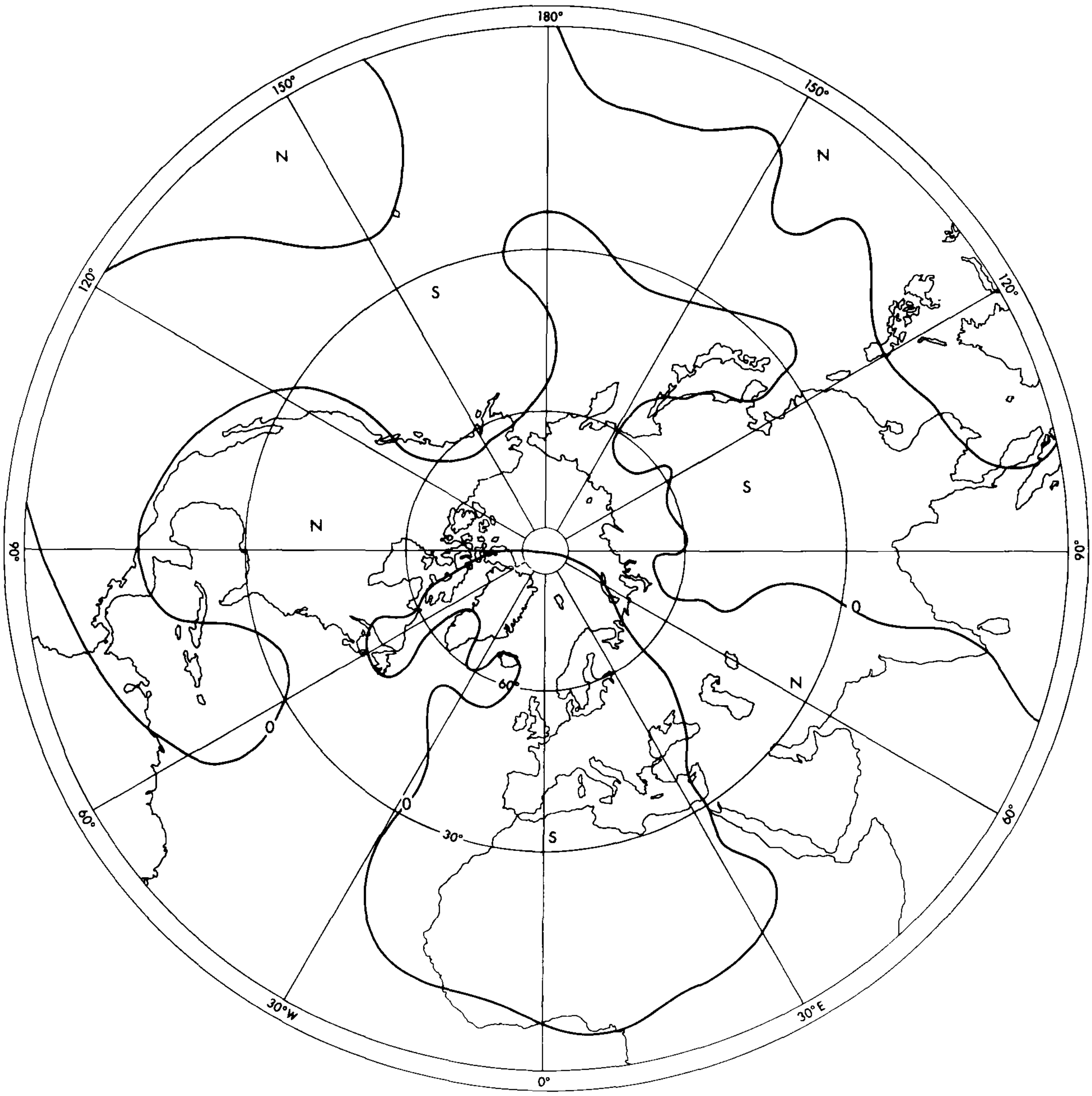

PLATE 34. AVERAGE MERIDIONAL WIND COMPONENTS (KNOTS) AT 30 MILLIBARS OVER THE NORTHERN HEMISPHERE IN JULY, 1957–64

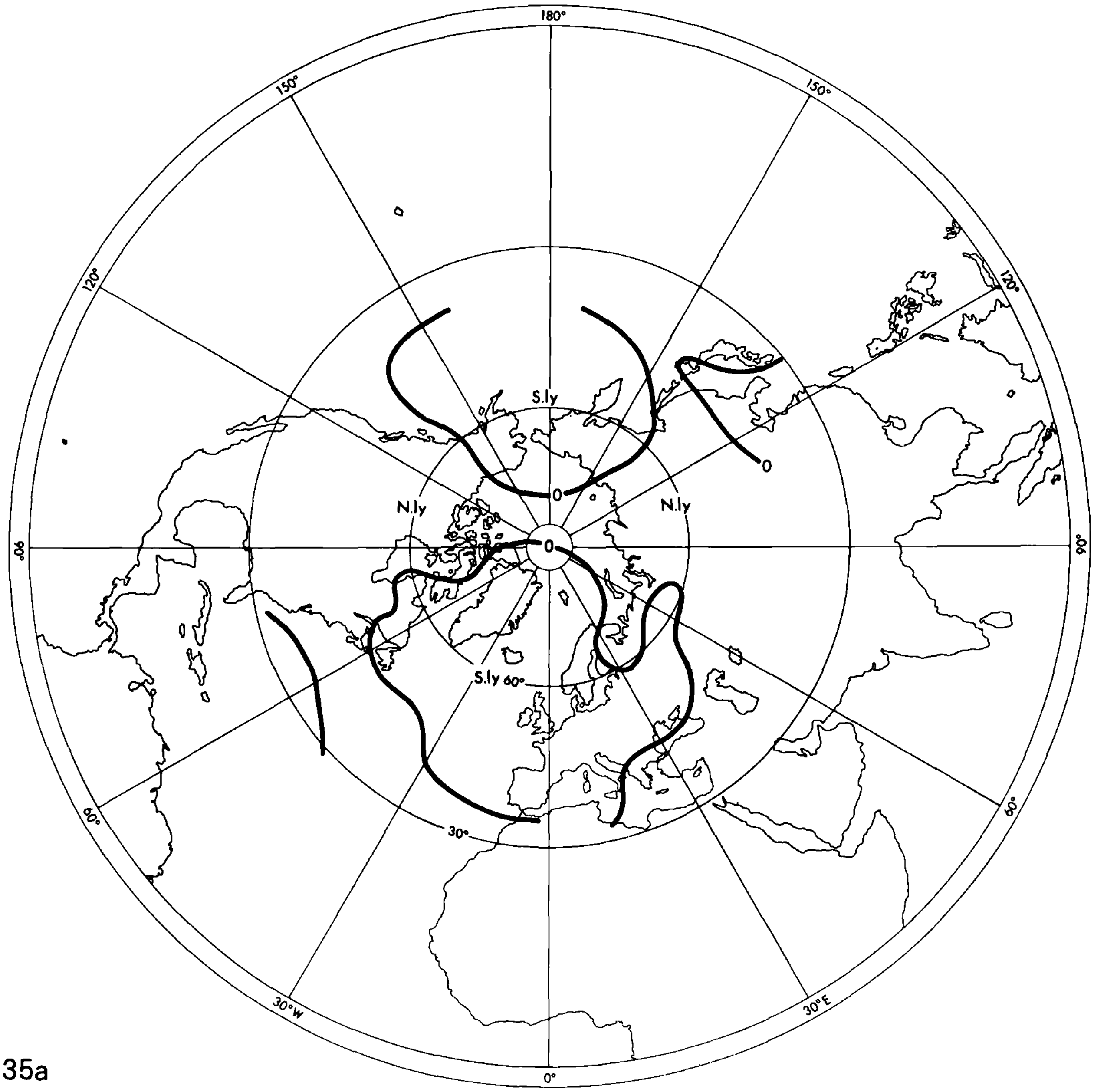

35a

PLATES 35a AND 35b. AVERAGE MERIDIONAL WIND COMPONENTS (KNOTS) AT 30 MILLIBARS OVER THE NORTHERN HEMISPHERE (NORTH OF LATITUDE 45°N) IN AUGUST (35a) AND SEPTEMBER (35b), 1957–64

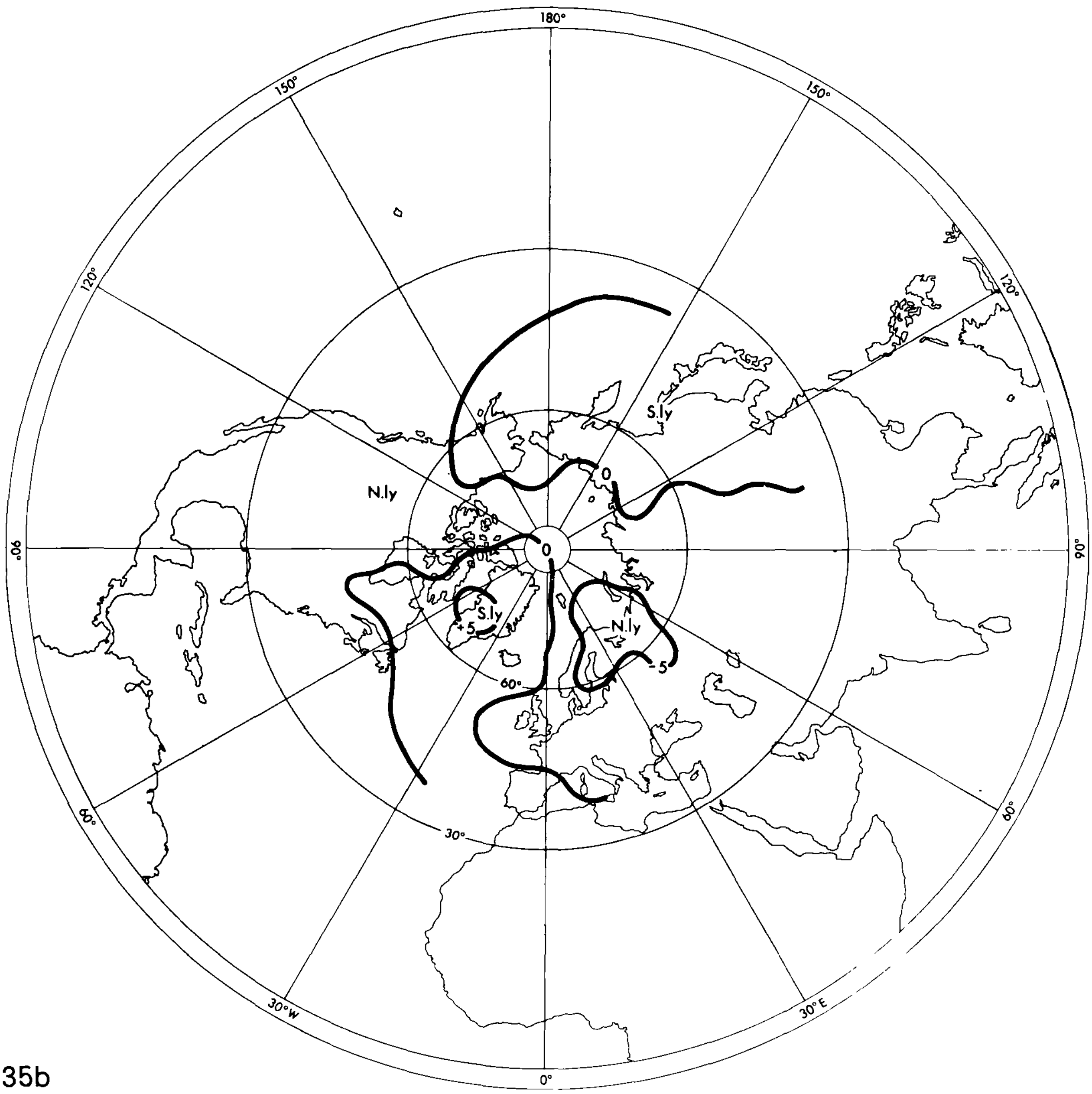
180°
150°
150°
120°
120°
90°
90°
60°
60°
30°W
30°E
0°
60°
30°
N.ly
S.ly
S.ly
N.ly
0
0
+5
-5

35b

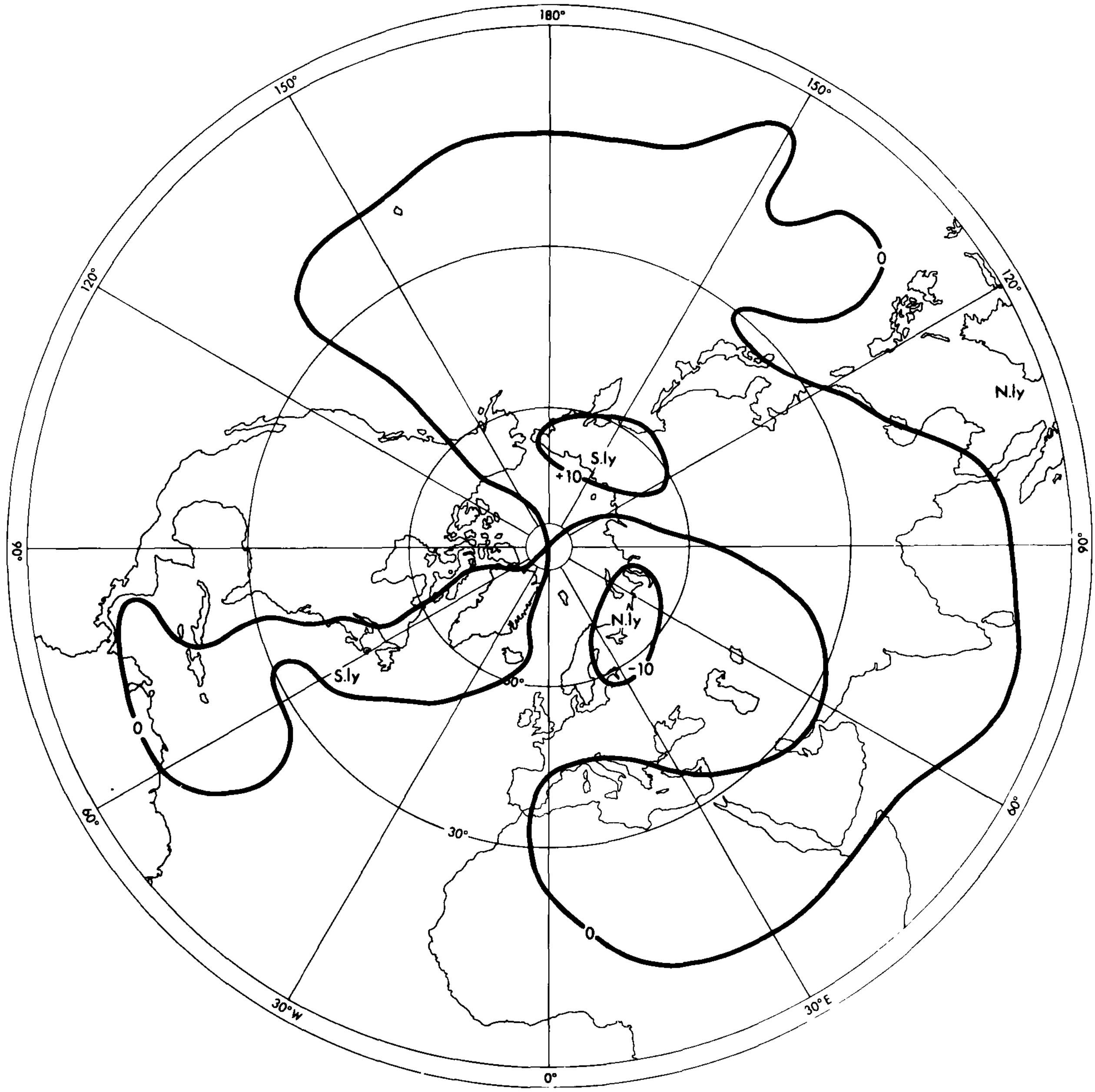

PLATE 36. AVERAGE MERIDIONAL WIND COMPONENTS (KNOTS) AT 30 MILLIBARS OVER THE NORTHERN HEMISPHERE IN OCTOBER, 1957–64

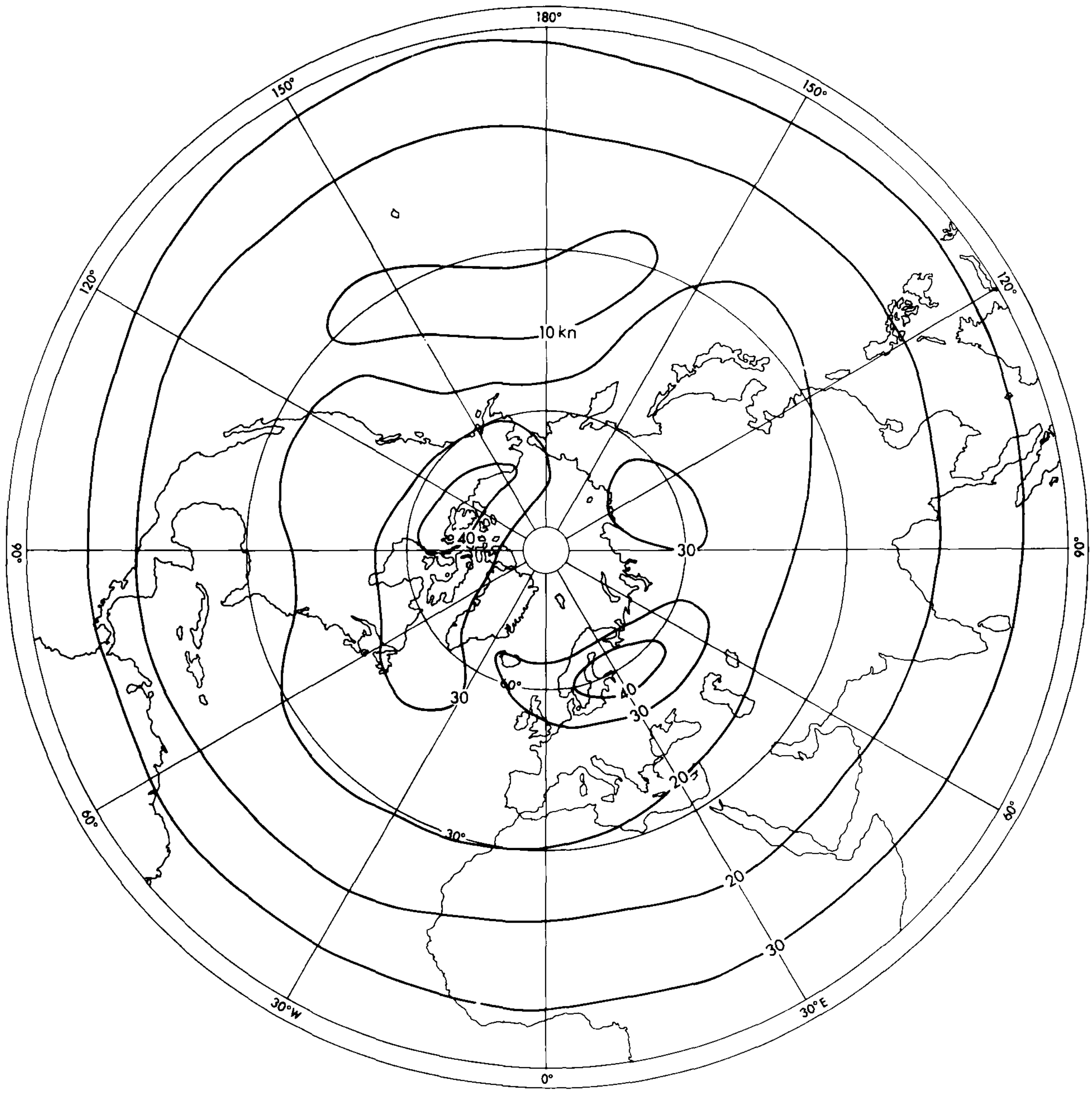

PLATE 37. STANDARD DEVIATION OF ZONAL WIND COMPONENTS (KNOTS) AT 30 MILLIBARS OVER THE NORTHERN HEMISPHERE IN JANUARY, 1958–65

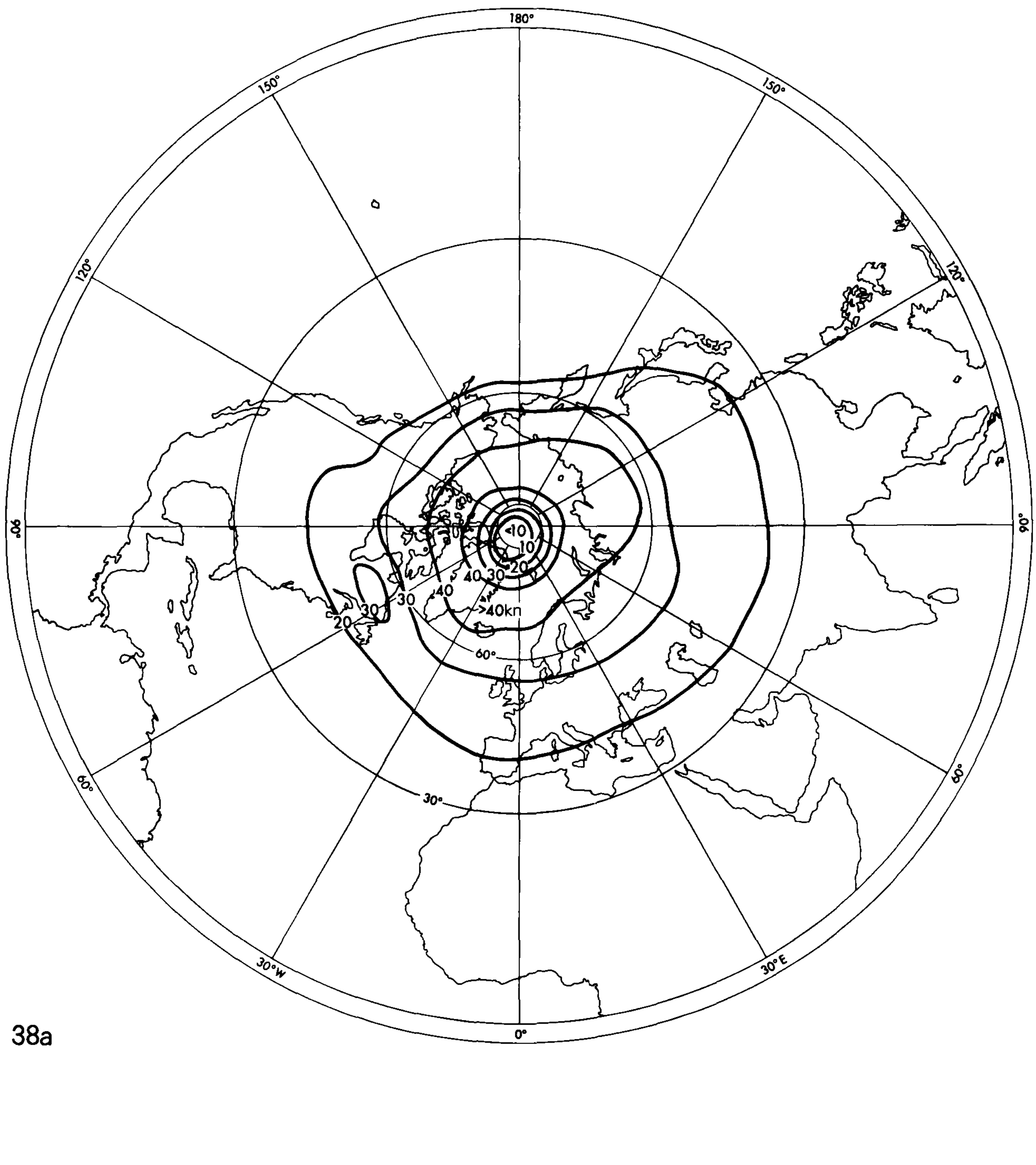

PLATES 38a AND 38b. STANDARD DEVIATION OF ZONAL WIND COMPONENTS (KNOTS) AT 30 MILLIBARS OVER THE NORTHERN HEMISPHERE (NORTH OF LATITUDE 45°N) IN FEBRUARY (38a) AND MARCH (38b), 1958–65

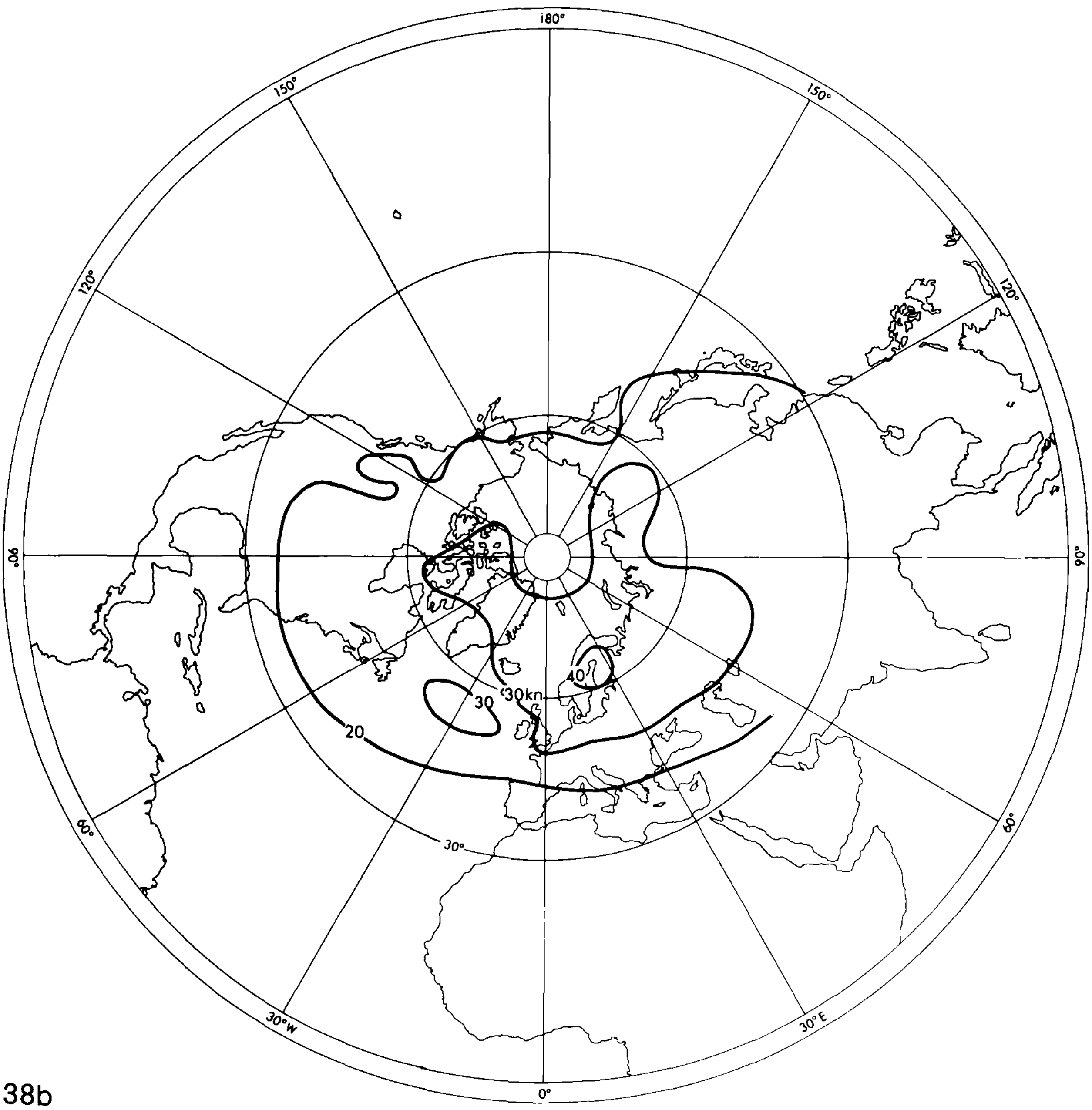

38b

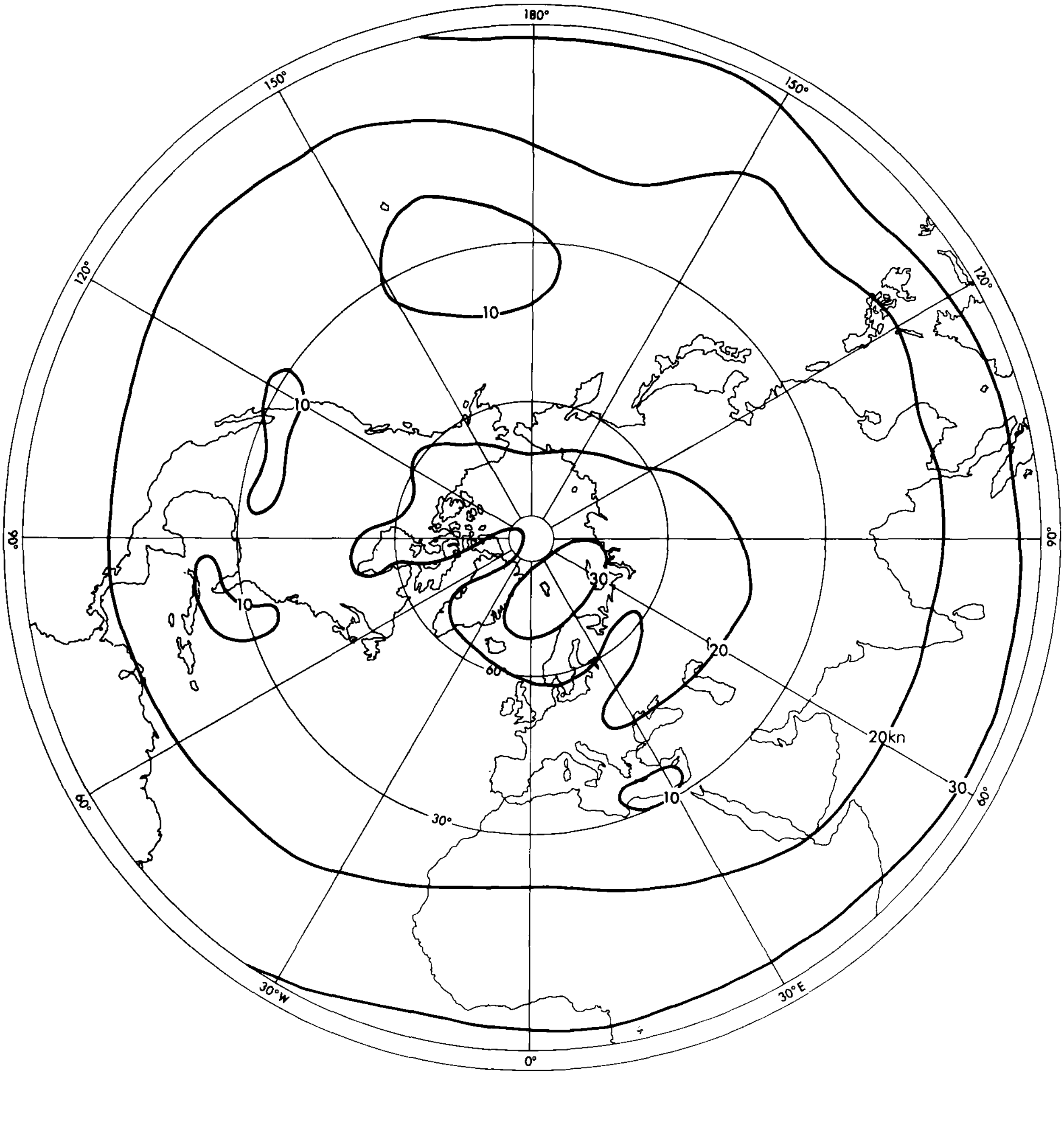

PLATE 39. STANDARD DEVIATION OF ZONAL WIND COMPONENTS (KNOTS) AT 30 MILLIBARS OVER THE NORTHERN HEMISPHERE IN APRIL, 1958–65

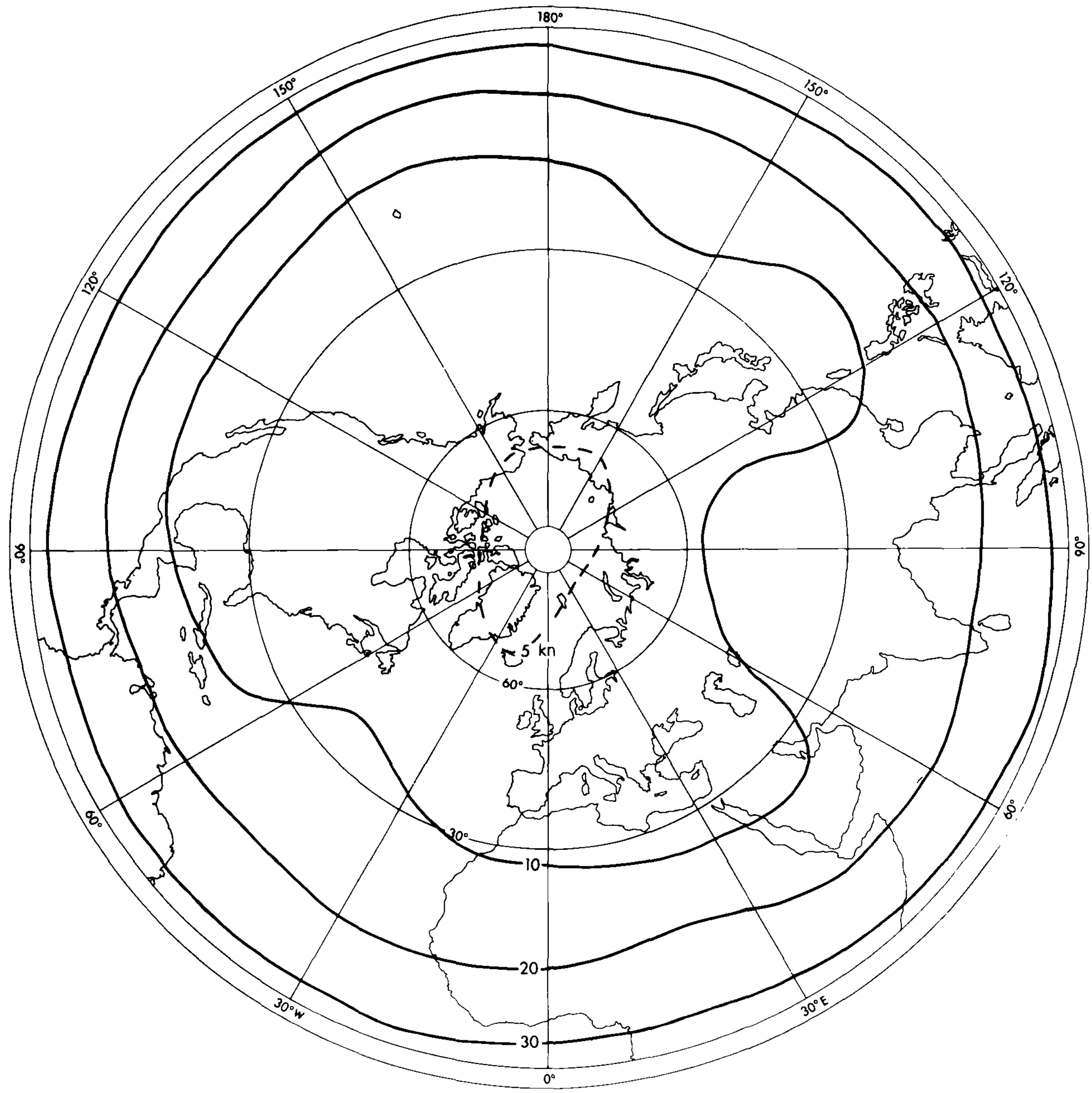

PLATE 40. STANDARD DEVIATION OF ZONAL WIND COMPONENTS (KNOTS) AT 30 MILLIBARS OVER THE NORTHERN HEMISPHERE IN JULY, 1957–64

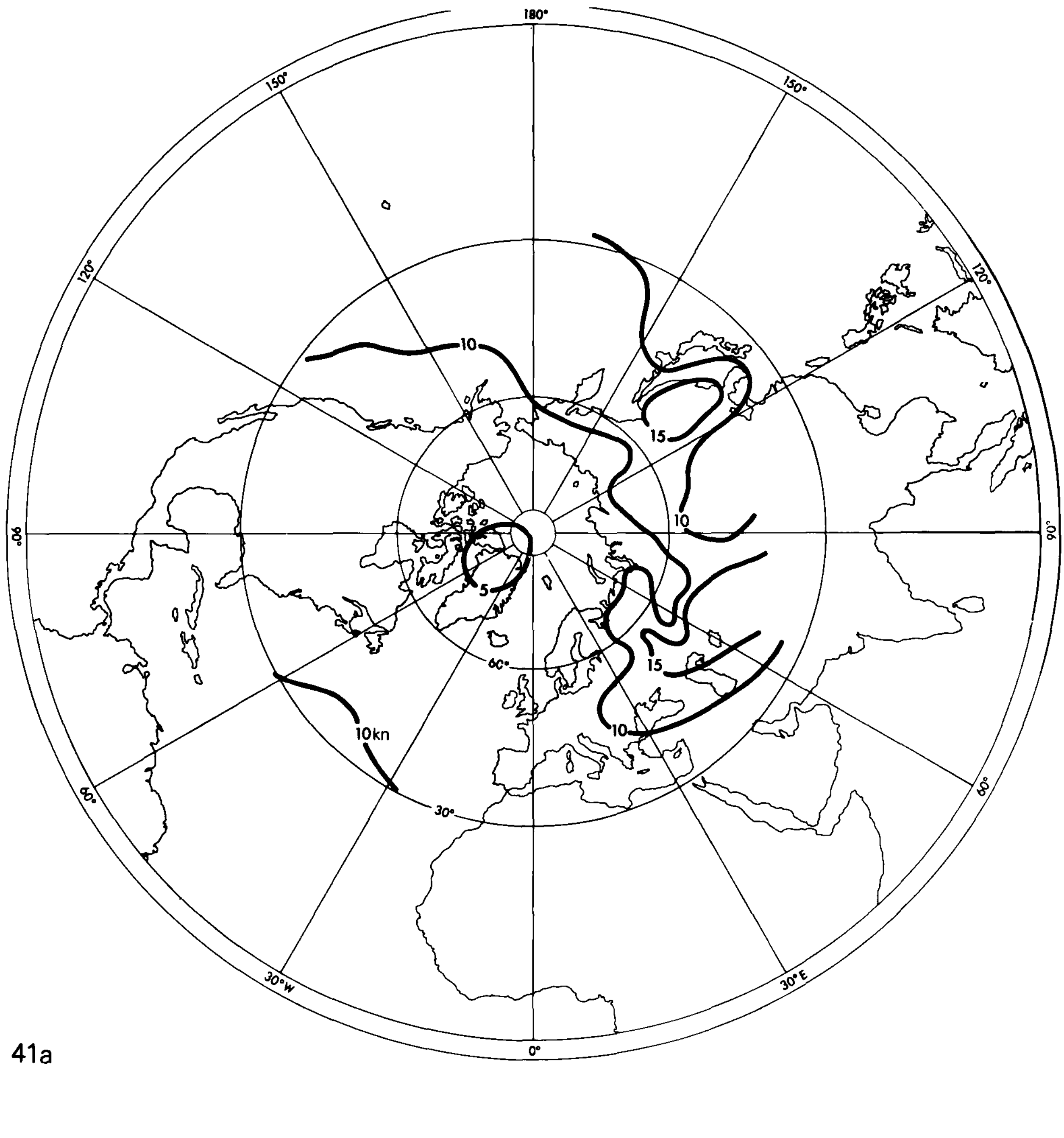

41a

PLATES 41a AND 41b. STANDARD DEVIATION OF ZONAL WIND COMPONENTS (KNOTS) AT 30 MILLIBARS OVER THE NORTHERN HEMISPHERE (NORTH OF LATITUDE 45°N) IN AUGUST (41a) AND SEPTEMBER (41b), 1957–64

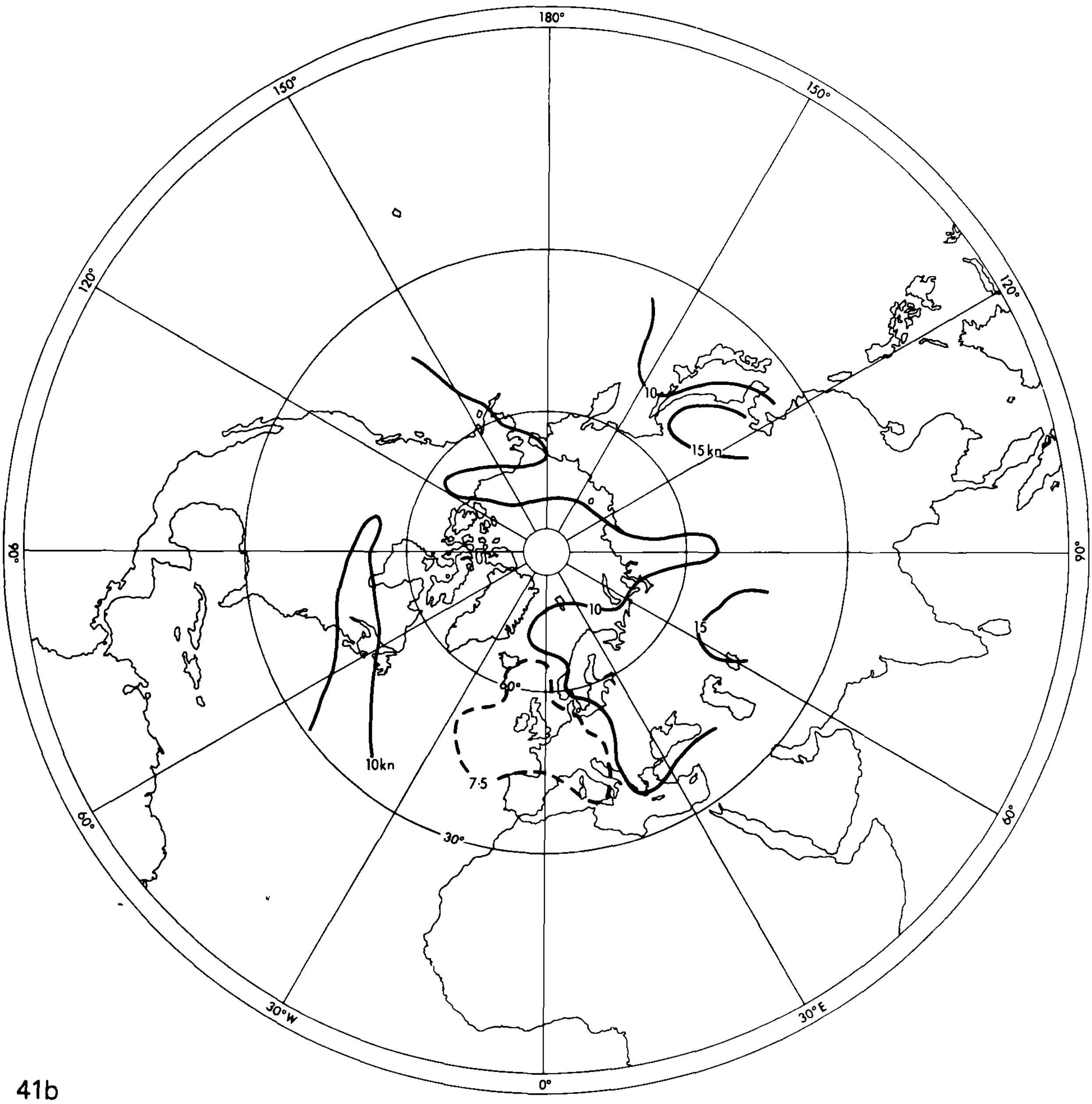
180°
150°
150°
120°
120°
90°
90°
60°
60°
30°W
30°E
0°
30°
60°
10kn
15kn
10
10
15
7·5

41b

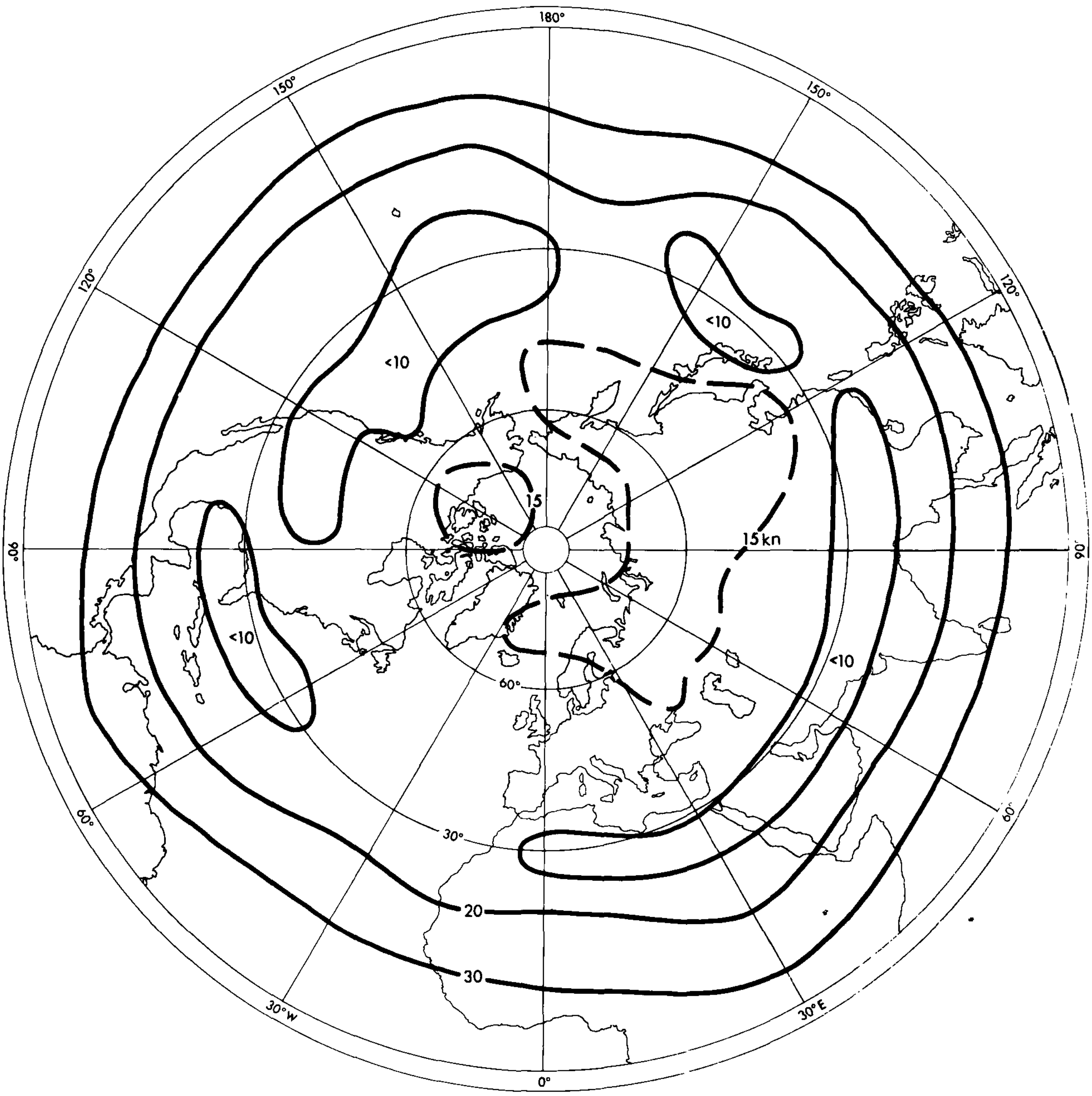

PLATE 42. STANDARD DEVIATION OF ZONAL WIND COMPONENTS (KNOTS) AT 30 MILLIBARS OVER THE NORTHERN HEMISPHERE IN OCTOBER, 1957–64

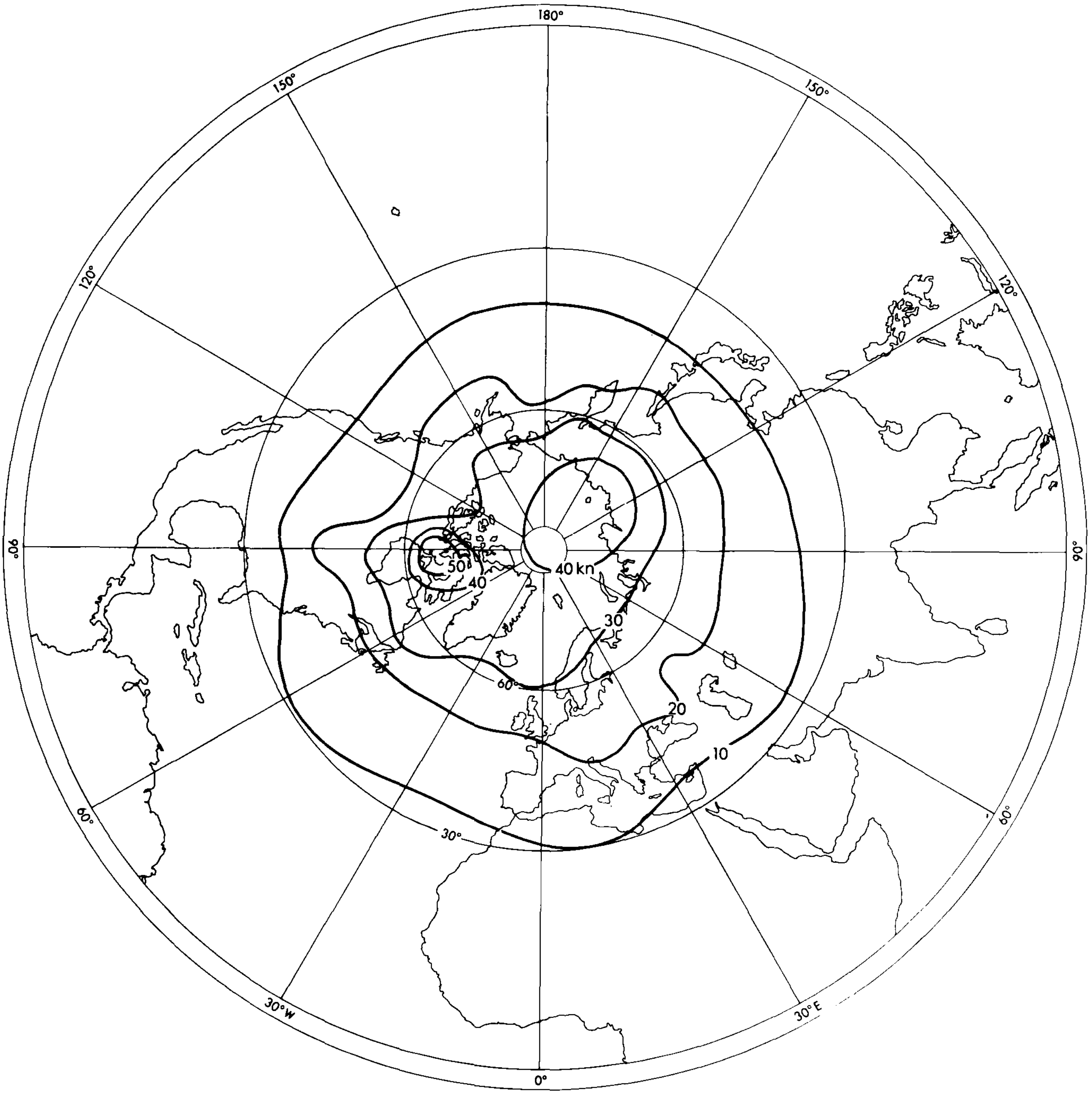

PLATE 43. STANDARD DEVIATION OF MERIDIONAL WIND COMPONENTS (KNOTS) AT 30 MILLIBARS OVER THE NORTHERN HEMISPHERE IN JANUARY, 1958–65

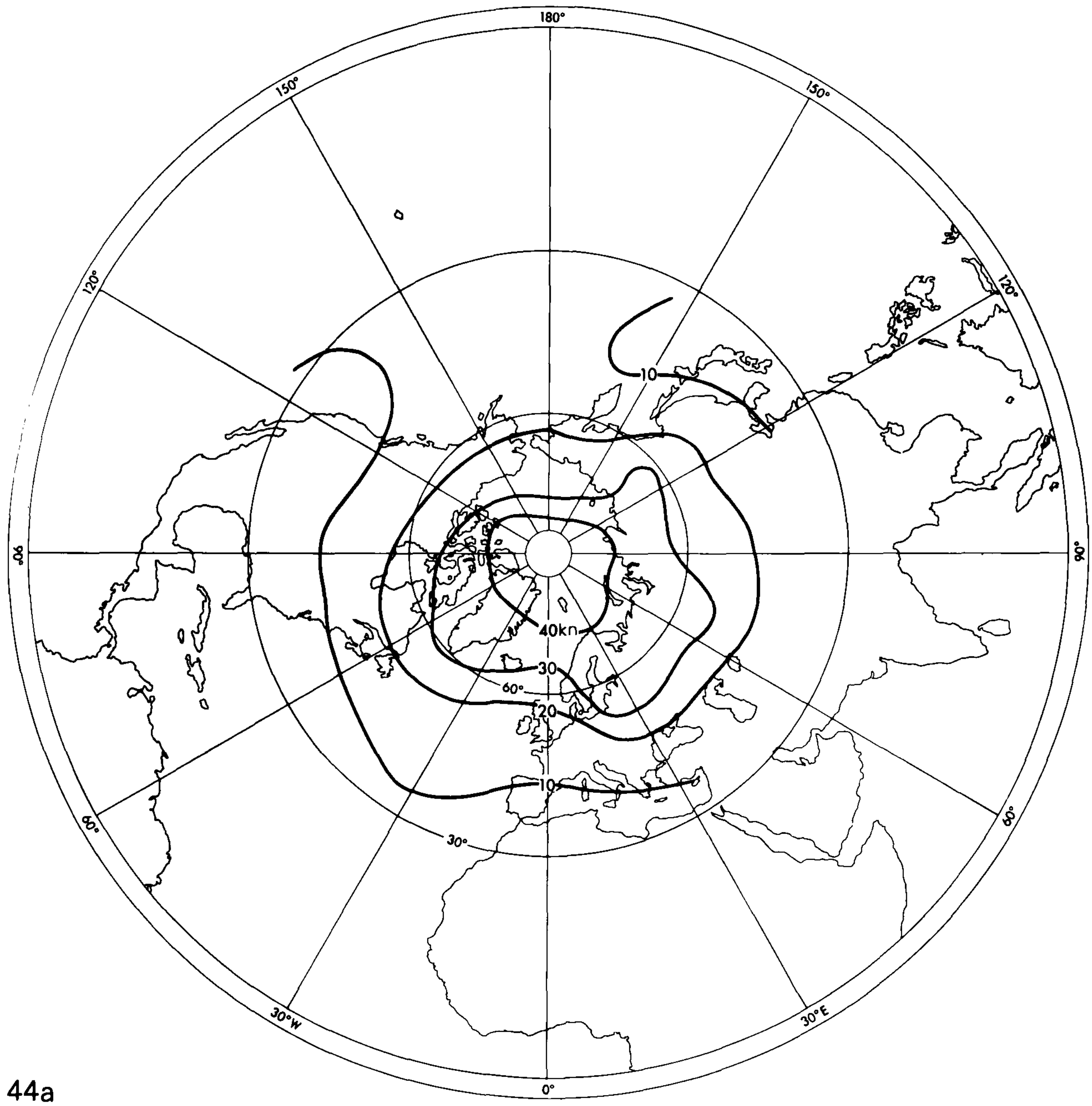

44a

PLATES 44a AND 44b. STANDARD DEVIATION OF MERIDIONAL WIND COMPONENTS (KNOTS) AT 30 MILLIBARS OVER THE NORTHERN HEMISPHERE (NORTH OF 45°N) IN FEBRUARY (44a) AND MARCH (44b), 1958–65

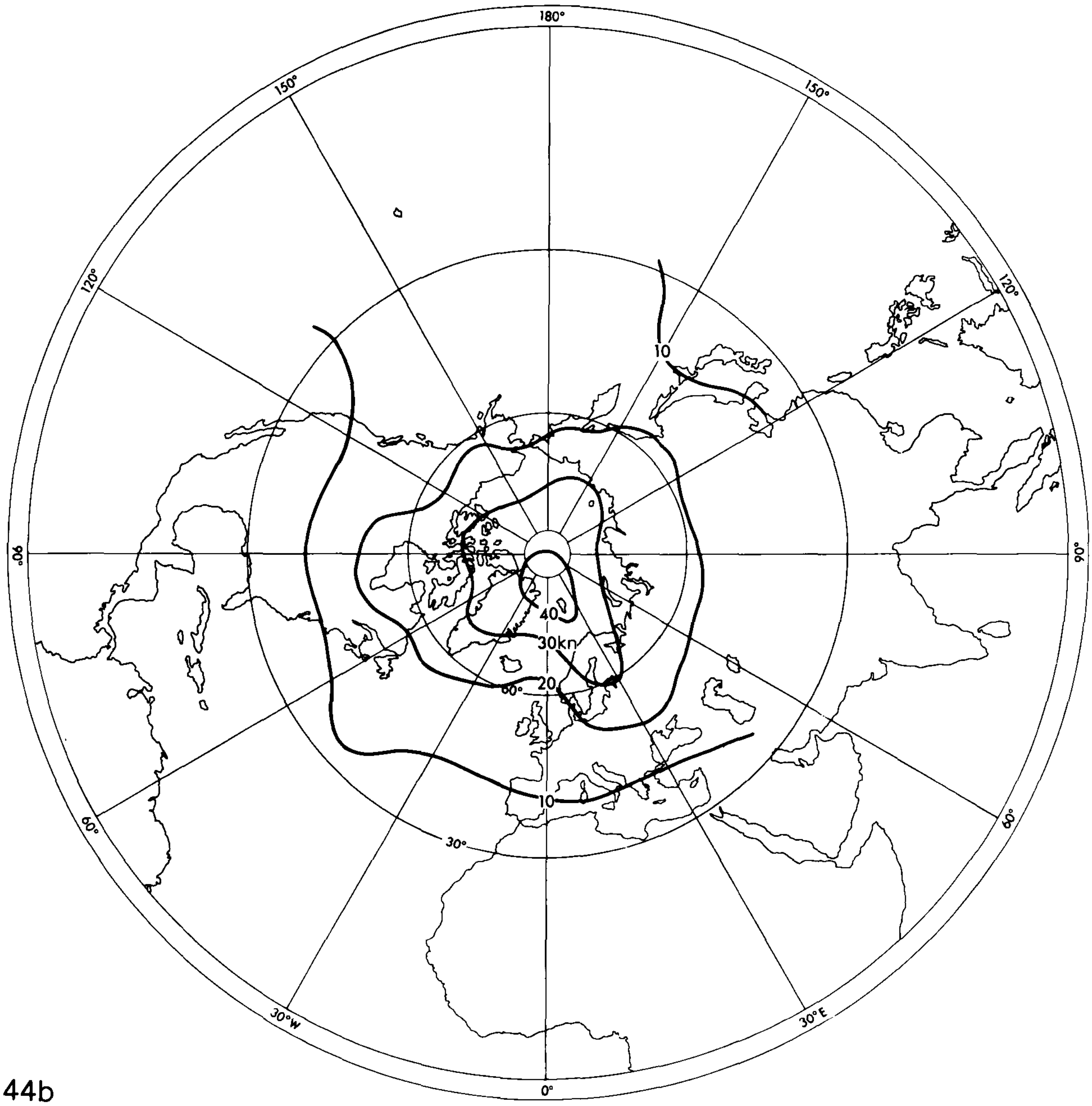

44b

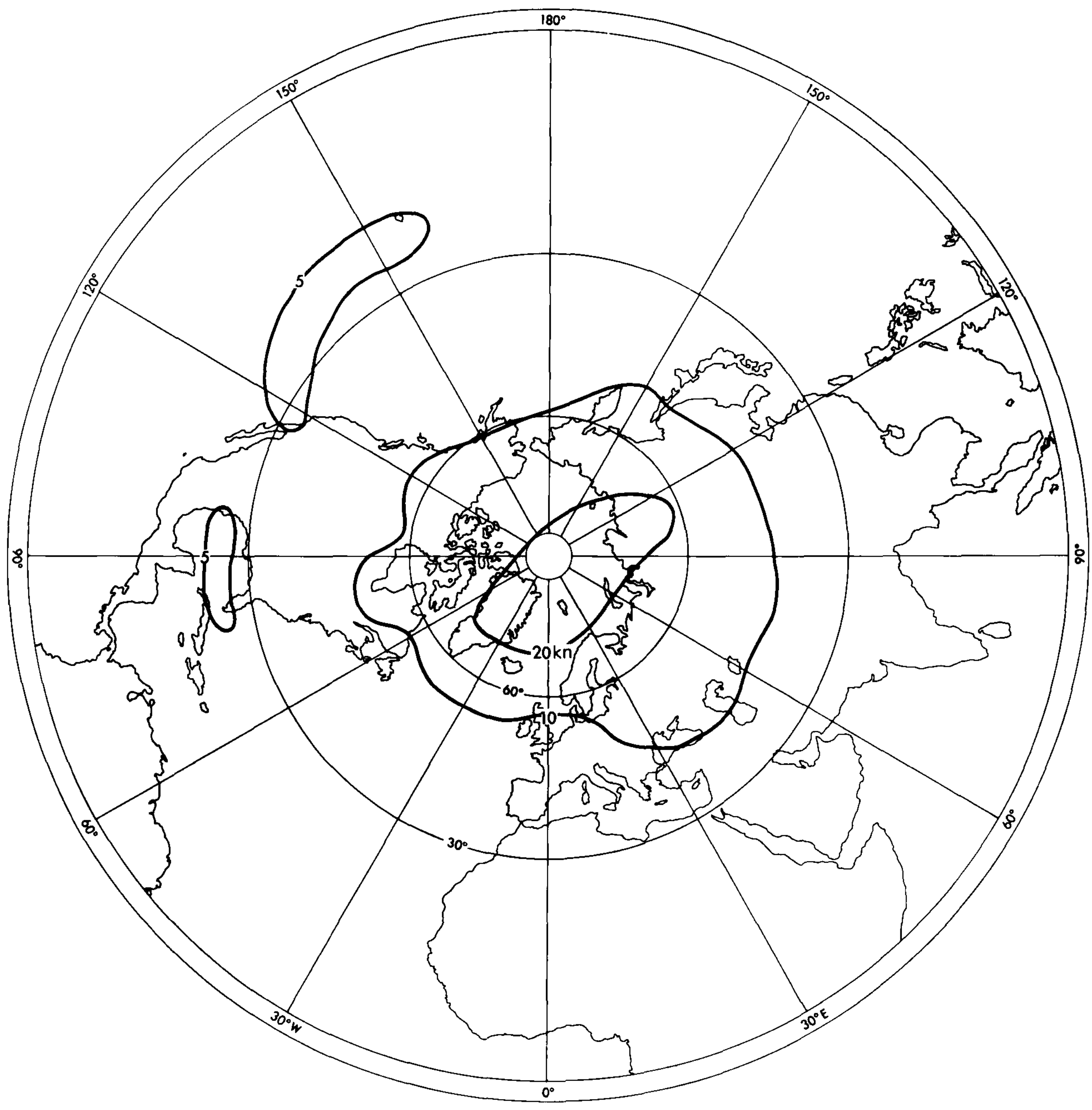

PLATE 45. STANDARD DEVIATION OF MERIDIONAL WIND COMPONENTS (KNOTS) AT 30 MILLIBARS OVER THE NORTHERN HEMISPHERE IN APRIL, 1958–65

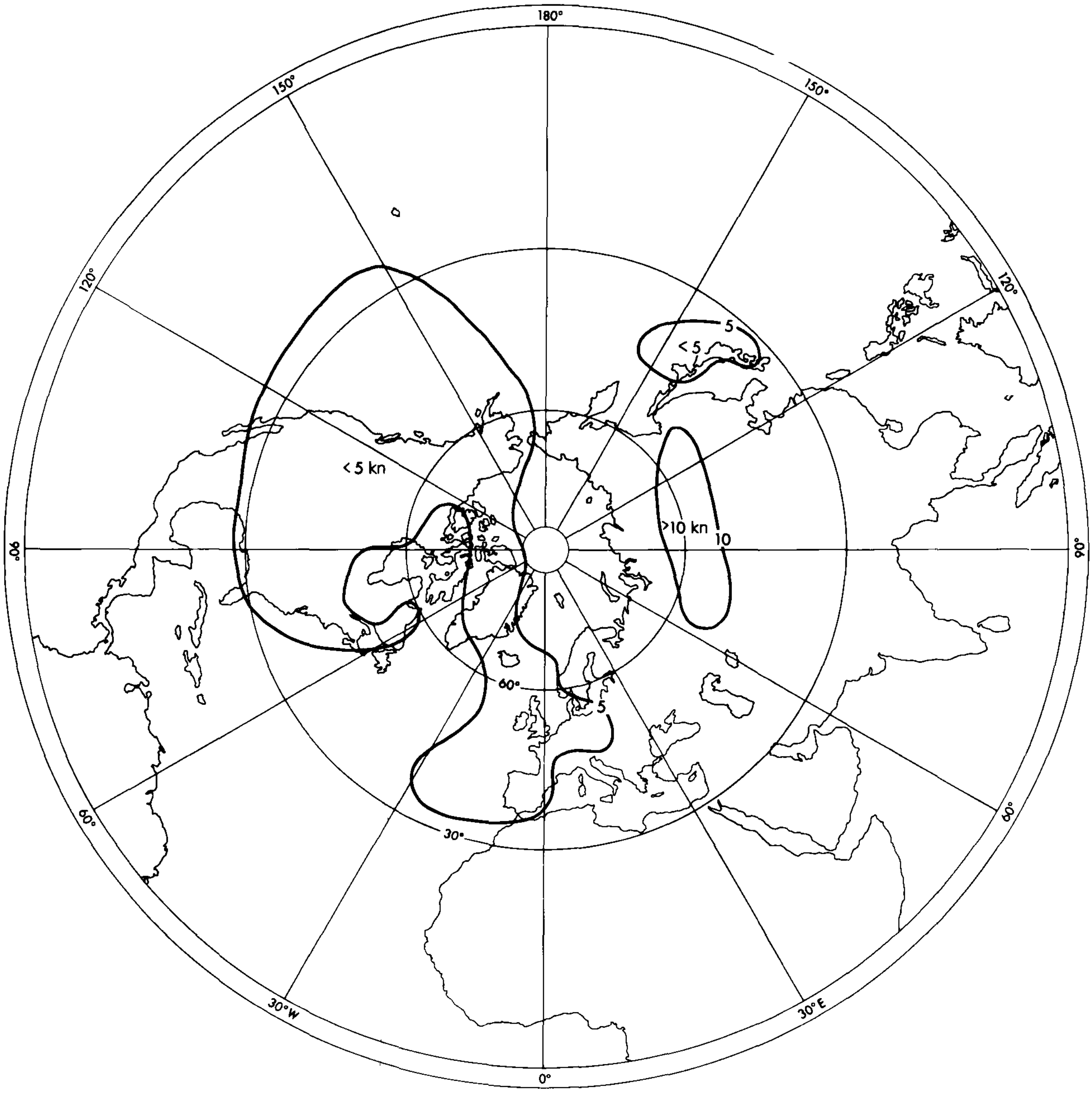

PLATE 46. STANDARD DEVIATION OF MERIDIONAL WIND COMPONENTS (KNOTS) AT 30 MILLIBARS OVER THE NORTHERN HEMISPHERE IN JULY, 1957–64

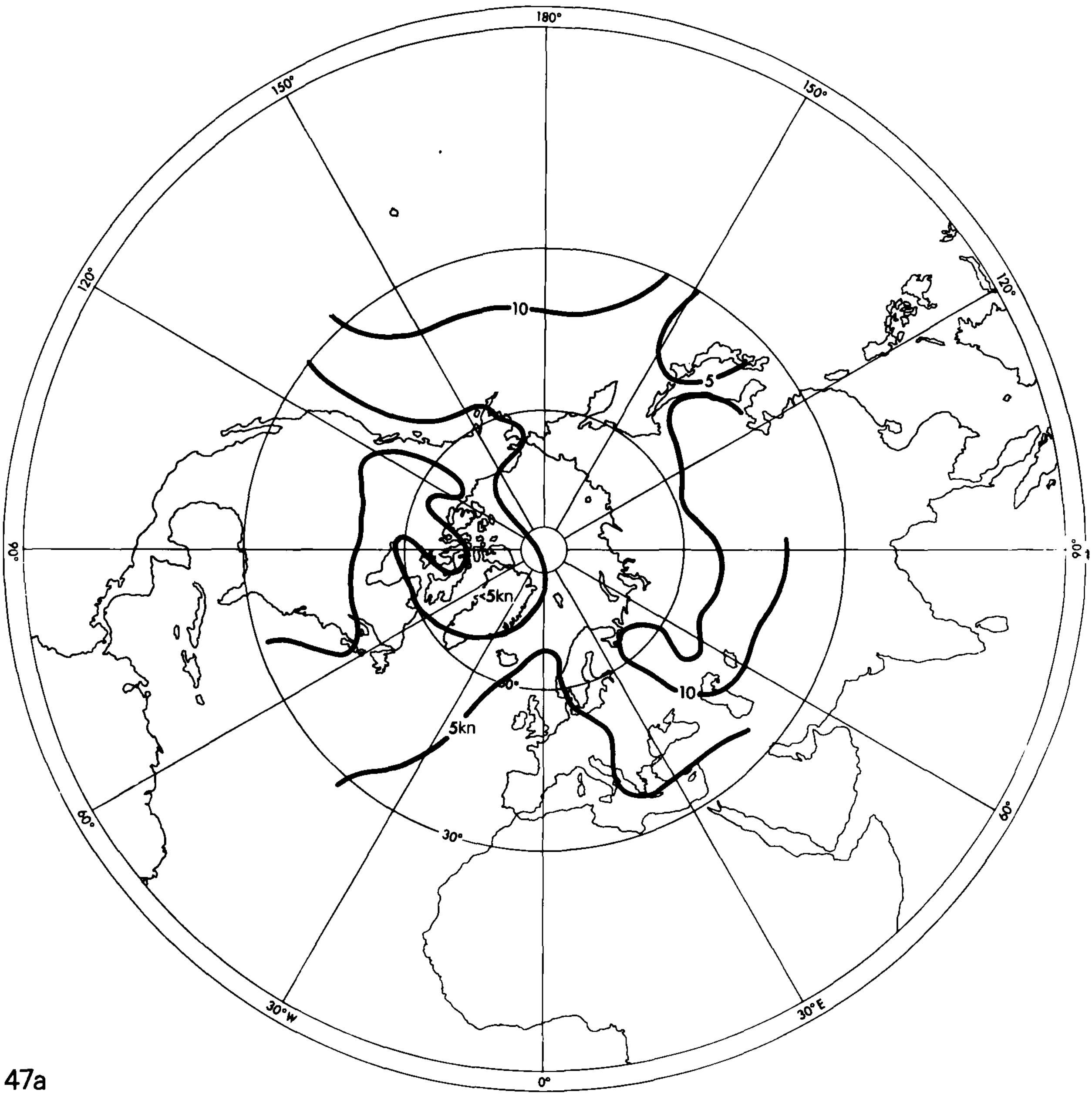

47a

PLATES 47a AND 47b. STANDARD DEVIATION OF MERIDIONAL WIND COMPONENTS (KNOTS) AT 30 MILLIBARS OVER THE NORTHERN HEMISPHERE (NORTH OF LATITUDE 45°N) IN AUGUST (47a) AND SEPTEMBER (47b), 1957–64

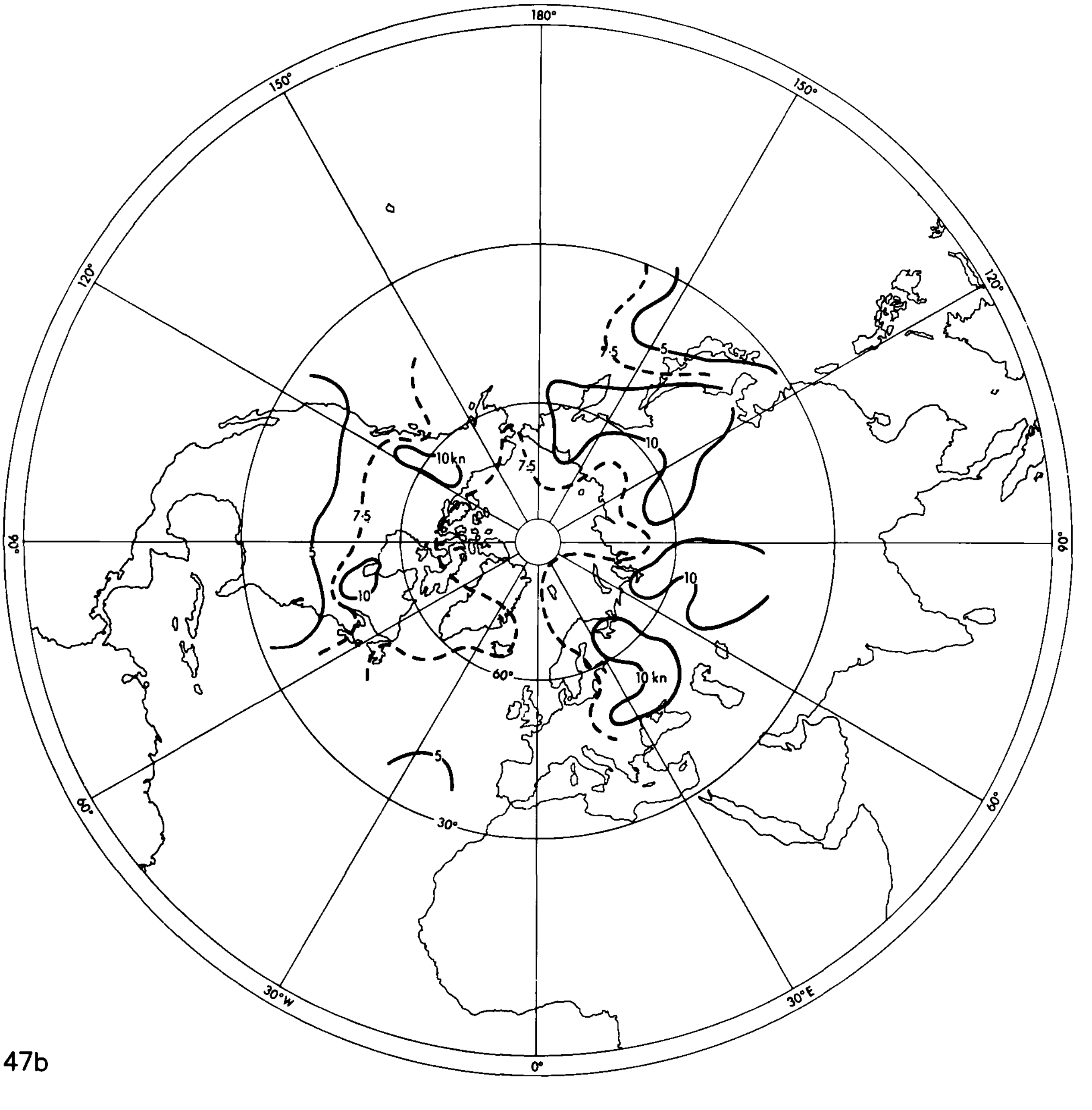
180°
150°
150°
120°
120°
90°
90°
60°
60°
30°W
30°E
0°
30°
60°
10kn
10 kn
10
10
10
7·5
7·5
7·5
5
5

47b

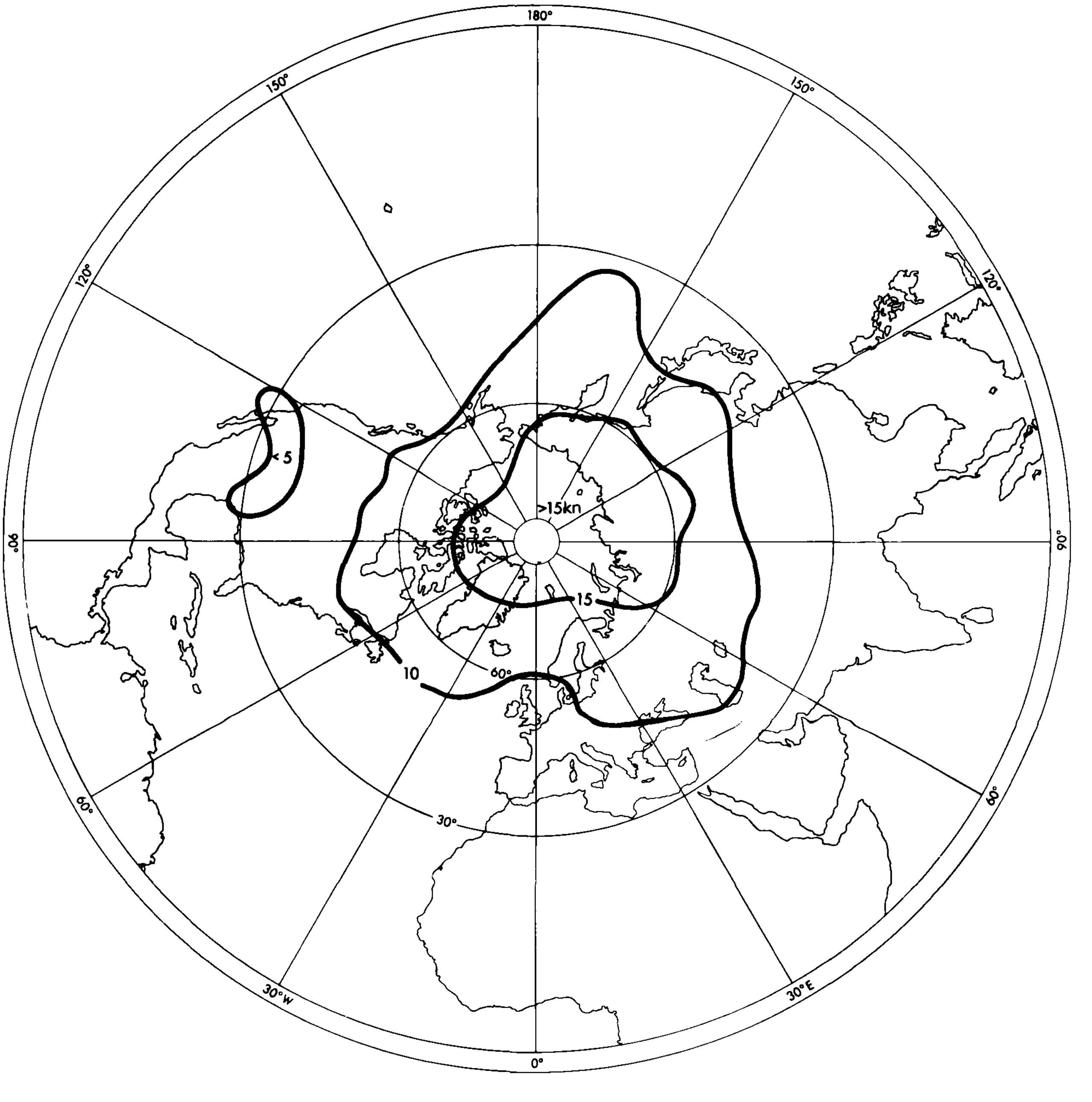

PLATE 48. STANDARD DEVIATION OF MERIDIONAL WIND COMPONENTS (KNOTS) AT 30 MILLIBARS OVER THE NORTHERN HEMISPHERE IN OCTOBER, 1957–64

Reproduced in England for Her Majesty's Stationery Office by Hobbs the Printers of Southampton
(1262) Dd586762 K7 8/77 G3927

First published 1977

HER MAJESTY'S STATIONERY OFFICE

Government Bookshops

49 High Holborn, London WC1V 6HB
13a Castle Street, Edinburgh EH2 3AR
41 The Hayes, Cardiff CF1 1JW
Brazennose Street, Manchester M60 8AS
Southey House, Wine Street, Bristol BS1 2BQ
258 Broad Street, Birmingham B1 2HE
80 Chichester Street, Belfast BT1 4JY

Government Publications are also available through booksellers

ISBN 0 11 400308 4*